Polydimethylsiloxane Tensile Mechanical Properties and Membrane Deflection Theory

Patrick A. Roman

A.A.S., State University of New York, College at Morrisville, 1993

B.T., State University of New York, College at Buffalo, 1995

A thesis submitted to the faculty of the
OGI School of Science and Engineering
at Oregon Health & Science University
in partial fulfillment of the
requirements for the degree
Master of Science in
Electrical and Computer Engineering

February, 2004

The dissertation "Polydimethylsiloxane Tensile Mechanical Properties and Membrane Deflection Theory" by Patrick A. Roman has been examined and approved by the following Examination Committee:

Sean Kirkpatrick
Associate Professor
Thesis Research Advisor

Jack McCarthy
Assistant Professor

Milt Scholl
Adjunct Faculty

Jody House
Adjunct Faculty

Dedication

To my wife Jessica, who is the joy of my life.

Acknowledgements

My gratitude goes to Oregon Graduate Institute and my thesis committee for giving me the opportunity to realize this work, and for patiently following me throughout its construction and completion.

I am most thankful to Dr. Jody House, whose friendship, generosity, and philanthropy planted the seeds that allowed me to embark on this journey. Thanks to Dr. Milt Scholl for revealing the world of MEMS, giving me interest and motivation for a fascinating field of science and engineering, and for being the best instructor I have ever had. These things enabled me to continue the journey. Many thanks to Dr. Jack McCarthy for many friendly discussions, advise, and for his undying interest in the research of things "small". This made the journey more enjoyable. Thanks to my advisor Dr. Sean Kirkpatrick for sharing his experience and knowledge of non-traditional materials analysis and for providing the necessary tools and equipment that made this work possible. I am most grateful for his patient yet relentless interest in following my progression, which helped me to complete this journey, to begin the next. Thank you all.

Many thanks to Dr. Simon McCarthy, for his interest and experience in polymer science, and for his professional guidance. Thanks are also due to Dr. Robert Hohlfelder, whose research and personal communications enabled the development of *The new spherical cap model*, a major part of this thesis.

Thanks to the instructors and staff of Oregon Graduate Institute for their willingness to help and share their expertise. To Andy Huffstutter and the machine shop, for his assistance in many projects related to this work.

Special thanks to Dr. Ken Gregory and the researchers of Oregon Medical Laser Center for giving me the opportunity to work with a great biomedical research group and to offer my contributions. My work there was of great engineering challenge and professional growth. Thanks to the crew at OMLC for keeping life interesting and giving much solace in our plight every Friday afternoon over a few good pints of IPA. To Dr. Scott Prahl for being patient, willing to listen, and always having a response that could etch steel, but mostly for keeping the faith. Thanks to Scott, Ted, Yin-Chu, and Paolo for many discussions over "great" meals, and for their friendship.

Sincere thanks to Dr. Guthrie Campbell, his family, and the team, for their inspiration, challenging me to improve, and tradition. These things have brought me a long way.

To my families; Mom, Dad, Rachael, Grandpa, Lella, Pietro, Matt, Eileene, Jim, Dray, and Brian, thank you for your love and support, and for setting me on my path.

Finally I must thank my wonderful wife, for without her this would have never been realized. *Grazie, e ti amo moltissimo, Bebé!*

Contents

List of Tables

List of Figures

Abstract

Polydimethylsiloxane Tensile Mechanical Properties and Membrane Deflection Theory

Patrick A. Roman
OGI School of Science and Engineering
Oregon Health and Science University

Supervising Professor: Dr. Sean Kirkpatrick, Ph.D.

Recent advances in Micro Electro Mechanical Systems (MEMS), semiconductor sensor and actuator chip based technology, have incorporated many non-standard silicon processing materials in their design. The use of materials such as polymers in conjunction with standard CMOS processing and materials has enabled many new MEMS sensors and actuators to be created. Even though the design enabling flexibility of polymers maybe very high, the processing and implementation of polymers for a given application is often more complex than what is encountered with standard engineering materials due to their ubiquitous qualities. The main focus of this thesis is to investigate both the tensile mechanical properties of Polydimethylsiloxane (PDMS), a material increasingly used in MEMS, and large deflection membrane theory in an effort to provide more accurate tensile mechanical material properties and analytical membrane models for

MEMS application design with PDMS. Batch material processing and the elastomer behavior of PDMS creates numerous mechanical testing issues, while its amorphous molecular structure requires that it be analyzed in a different manner than crystalline materials. This difference is primarily addressed through the use of true strain definitions. Fundamental works of membrane mechanical theory have focused on standard engineering materials due to the applications and available materials of the day, thus providing inadequate analytical models for elastomers. A new theory, *The new spherical cap model*, is developed for large deflection circular membranes made of elastomers, which incorporates an appropriate true strain definition using the membrane radius of curvature, accounting for large deflections. Experimental results suggest that this theory accurately predicts elastomer circular membrane behavior and may be used to simulate circular membranes made of crystalline materials as well. Static and dynamic stress-strain experiments and analysis are performed upon uniaxial tensile samples, and static load- deflected, or bulge tested, circular and square membrane experiments and analysis are performed; both to develop the material properties of PDMS unique to those tests. PDMS tan δ, Poisson's ratio, stress relaxation time, and stress deformation were also investigated. Methods for PDMS fabrication, uniaxial and biaxial testing, analysis and results are explained. The results show varied PDMS tensile elastic modulus values for static and dynamic uniaxial tensile and membrane deflection tests; E_{static} = 2.18 ±0.184MPa, $E_{dynamic}$ = 1.45 ±0.250Mpa, $E_{membrane}$ = 1.08 ±0.250Mpa, respectively. The PDMS loss factor, tan δ = 0.03, and Poisson's ratio ν = 0.47. These results display elastic constant strain rate dependence of varied PDMS tensile applications and agree with numerous published works on PDMS mechanical properties and MEMS elastomer membrane actuators.

Chapter 1
Introduction

Micro Electro Mechanical Systems (MEMS), or Micro Systems Technology (MST), has undergone vast development in the past decade [1,2]. As the computing and semiconductor industries matured over the past decade MEMS research grew, and the feasibility of varied and more complex on-chip micron scale sensor and actuator systems has become a reality [2]. Recent research contributions to MEMS advancement has been the development of non traditional semiconductor processes and materials. The combined application of these processes and materials has enabled the fabrication of MEMS sensors and actuators with previously unattainable performance from traditional silicon based semiconductor processes alone [2,3]. MEMS devices incorporating non traditional processes and or materials include: micro motors, micro gears, micro turbines, membrane actuators, microfluidics systems, micro optics, thermal and hygrometric sensors; nearly all new MEMS devices today [4,5,6]. MEMS design structures which have benefited significantly from the introduction of new materials and processes into MEMS design and fabrication include plates, membranes, and diaphragms [7-65]. A significant benefit to MEMS applications with these design structures comes from the use of low modulus ($\boldsymbol{E}\sim$1MPa) materials, such as Parylene, Polyethylene, and Polydimethylsiloxane (silicone rubber). These materials enable a greater range of structure mobility and design possibilities based on their material properties as compared to silicon and more standard engineering materials (metals). Polymeric materials have revolutionized MEMS microfluidic design and applications, in spite of limited fundamental research on the mechanical properties of these materials. However, there can be significant problems in the use of non-silicon polymer based processes and materials in MEMS design, fabrication, and use, due to their ubiquitous properties.

MEMS microfluidic systems and micro total analysis systems (uTAS) have developed to serve as "lab on a chip" chemical analysis and biochemical assay distribution systems [29,30]. These systems consist of micron sized flow channels and chambers, connected to pumping systems and check valves for flow control. Often the entire system may be fabricated from a single polymer [29]. However, it is the pumps and check valves of these systems that make use of the unique material properties of the polymer used. Most of the MEMS microfluidic pump and check valve systems employ plate and membrane mechanics as their operating physics. Polymers used in plate and membrane mechanics behave very differently from metals and other MEMS fabrication materials. In fact a microfluidic system fabricated of standard CMOS materials does not yield a practical solution for most microfluidics applications. Through the use of polymers, specifically in the pumping diaphragms and check valves, very large deflections are possible, which would otherwise be impossible employing standard fabrication materials. It is through these large membrane deflections that large amounts of fluid may be moved, and flow channels closed; controlling flows. The unique molecular structure of some polymers, specifically the elastomer group, enables extremely large tensile elongations, coupled with the ability to return to their original shape with little plastic deformation. Large deflections in membrane mechanics are dominated by tensile forces [66]. Through the great flexibility of polymers and their ability to withstand large tensile elongations, polymer membranes are able to achieve deflections which are not possible with other fabrication materials, thus increasing potential applications.

In this thesis, circular and square membranes of the elastomer polydimethylsiloxane (PDMS) were primarily investigated in connection with the tensile mechanical properties of PDMS and the resulting effects on large deflection membrane mechanical behavior, in an effort to reach a greater understanding of PDMS as an engineering material for MEMS applications.

1.1 Membranes

Plates, membranes, and diaphragms take many forms in society today. These forms can be force summing devices for low pressure applications [66] or balloon actuators for jet aircraft aerodynamic control [42]. Shapes and sizes can vary substantially, from the weatherproofing membrane of a building roof to a man hole sewer cover [68]. Thus, the theories used to describe plates and membranes vary greatly. In theory, plates and membranes may be analogous, while a diaphragm is considered a device employing plate theory for its function. Generally a plate has a thickness $1/20^{th}$ and greater of its smallest span, while a membrane is a thin plate that has a thickness $1/20^{th}$ and less of its smallest span [68]. Membranes typically undergo deflections many times larger than their original thickness, and when mounted horizontally cannot support their own weight without deflecting [66]. A membrane is a flat plate incapable of conveying bending moments or shear forces, thus unable to support a load without deflection. In this sense, a membrane may be thought of as a two-dimensional analog of a flexible string [66,84]. The main focus of this thesis is the load-deflection relationship of circular and square polymer membranes.

Plates, membranes, and diaphragms have been investigated in depth by many researchers since the original theory was developed by the French mathematician LaGrange in the 1800's [66]. The fundamental theory has been most notably covered by Timoshenko and Woinowsky-Krieger [69], and Roark and Young [67], who developed the fundamental theory to provide analytical solutions for numerous plate and membrane configurations for engineering use. The primary method for the application of plate and membrane theory developed is the energy method [69]. The energy method derives a solution for plate deflection behavior by first assuming the functional shape of a deflected plate by a load, and then calculating and minimizing the potential energy of the system to fit the initial assumption [69, 47]. The application of the energy method as described by

Timoshenko and Woinowsky-Krieger [69] for circular and square membranes will be discussed in 1.2.1, as it is relevant to this work. Further development upon the work of Roark and Young [67] and Timoshenko and Woinowsky-Krieger [69] was done by Di Giovanni [66], Ugural [68], Maier-Schneider *et al* [48], and Hohlfelder [70]. All of the authors discuss both theoretical and practical applications of plate and membrane theory for circular and square membranes, and how it may be used analytically, practically in experimental work, and in the design of diaphragm devices. Included in Di Giovanni [66] are experimental data and designs for corrugated plates, and computer methods for designing plates, membranes, and diaphragms. These works have proved invaluable throughout the production of this thesis.

1.2 MEMS Membranes

Membranes are used in numerous MEMS devices, primarily as actuators, but also as sensors [7-65]. MEMS plates and membranes have been used in pressure sensors [31-38], microphones [39-40], aerodynamic balloon actuators [41-45], in the material testing of thin films [46-52], as deformable mirrors [53-62], as mass flow meters, and as thermal and hygrometric sensors [63-65]. The most prolific application of MEMS membranes are as the functional components of microfluidic valves and pumps [7-30]. These MEMS devices serve in many new applications throughout a number of different industries, facilitated by their small size, and relatively low cost due to semiconductor batch fabrication. Plate and membrane based MEMS devices have been used as blood pressure sensors for a single blood vessel [33], microfluidic channel pressure and flow sensors [32], as deformable mirrors for optical correction [54-57], mirrors for fiber optic network switching [62], and manifold air pressure (MAP) sensors for automobile air/fuel mixture control systems [1], as aerodynamic controls for fighter jet aircraft [42], and as check valves and pump actuators in micro total analysis systems (uTAS), lab on a chip based chemical analysis and biochemical assay distribution systems [29,30]. Due to the nature of planar semiconductor processing, which incorporates thin film deposition, plates and membranes are a logical design platform for MEMS, facilitating the previously mentioned devices.

Of particular interest to this work are MEMS microfluidics and the investigation of the mechanical properties of thin films by way of load–deflection testing of MEMS membranes [46-51]. The microfluidic membrane pumps and valves developed by Yang *et al* [7-12] and Sim *et al* [13,14] are most similar to the research presented herein. The thin film mechanical property membrane tests of Tabata *et al* [47], Maier-Schneider *et al et al* [48], Pan *et al* [49], Lin and Hohlfelder [70], and Vlassak [71], are also of significant interest. The research conducted by the groups applying membrane load–deflection theory to circular and square plates having large deflections and very small thickness is applied herein to elastomer membranes, which are common microfluidic design structures and the subject of this work.

1.2.1 Mechanics

Membrane behavior is very different from plate behavior for circular and square structures uniformly loaded and rigidly fixed at the edges. Unlike plates, membranes develop negligible bending stress when exposed to a uniform external load, with the resistance to loading developing with the cube of the deflection of the membrane, see Fig. 1.1 and equation 1.1. Plates are dominated by a linear relation of load–deflection for small displacements, generally the maximum deflection being half the plate thickness [67,68,69]. The purpose for the development of membrane mechanics is to obtain analytical models that very accurately describe the load–deflection behavior of bulk and thin film membranes. These models also enable the determination of thin film mechanical properties and residual stress inherent in manufacturing and testing. Membrane load–deflection theory is the foundation for bulge testing, which has proven to be a successful method used to test semiconductor and MEMS material properties [70]. Equation 1.1 is a generalized bulge equation that may be applied to any membrane geometry, where c_1 and c_2 are constants that account for membrane shape and Poisson's ratio [70].

$$P = c_1 \sigma_0 t \frac{h}{a^2} + c_2 M t \frac{h^3}{a^4} \tag{1.1}$$

Much of the membrane deflection theory literature was developed assuming the application of standard engineering materials, such as metals, having Poisson's ratio values of 0.25 to 0.35, resulting in inadequate approximations for non-traditional materials, such as elastomers with higher values of Poisson's ratio, from 0.4 and higher. Presently more accurate or exact theoretical models allow the selection of Poisson's ratio values, hence improving analytical approximations.

Andreeva [66] developed a general solution to model the load–deflection relationship of circular membranes. This solution expresses the membrane shape and Poisson's ratio as a constant determined analytically, while other general solutions assume a value for this constant based on an assumed Poisson's ratio value. Hohlfelder [70] developed a general solution for circular membrane load–deflection based on Hencky [70] and Timoshenko's work, as well as incorporating residual stress into the solution [70]. This solution expresses the membrane shape and Poisson's ratio as analytically determined constants. These membrane shape constants, c_1 and c_2, are of considerable interest relative to the load–deflection theory, as a common application is the "bulge test", which is used to determine the tensile mechanical properties of micron scale thin film materials [47,48,49,70,71]. These constants vary according to membrane shape and Poisson's ratio and may have a significant effect upon the accuracy of the analytical model. Among the different groups cited various membrane theory derivation methods are used, producing different results for these constants, see table 1.1 [70]. This thesis outlines the most suitable circular and square membrane theories for PDMS based on the literature review, theoretical, and experimental investigation.

Table 1.1.: Constants for the generalized bulge equation [70]

Geometry	Model	c_1	c_2
Circular	Spherical cap	4	8/3
Circular	Energy minimization (Lin)[70]	4	(7-ν)/3
Circular	Finite element (Pan)[49]	4	8/3 • (0.974-0.233ν)
Circular	Finite element (Hohlfelder)[70]	4	$c_2(\nu)=\frac{\frac{8}{3}(1.015-0.247\nu)}{(1-\nu)}$
Square	Analytical+energy minimization (Vlassak/Timoshenko)[71]	3.393	1.996-0.613ν
Square	Finite element (Pan)[49]	3.41	1.981-0.585ν
Square	Finite element+energy minimization (Maier-Schneider *et al*)[48]	3.45	$c_2(\nu)=\frac{1.994(1-0.247\nu)}{(1-\nu)}$

Many groups have investigated circular and square membrane theory and its application in the determination of material properties and membrane large deflection behavior. Tabata *et al* [47] performed membrane load–deflection tests of square MEMS membranes to determine the mechanical properties of LPCVD silicon nitride and found good agreement between the analytical and experimental results. They were investigating the quantification of the residual stress and Young's modulus of thin film membranes from silicon planar processing. Substantial amounts of residual stress can be introduced by the planar processing of MEMS and thin film depositions. The membrane theory of Tabata *et al* [47] was based upon the work of Timoshenko *et al* [69].

Yang *et al* [7-12] performed membrane load–deflection testing using square silicone rubber membranes and applied the membrane theory of Timoshenko *et al* [69]. They found good initial agreement for plots of load versus deflection with some experimental data points lying outside of the theoretical curve at the highest load versus deflection levels. Yang's group attributed this to plastic deformation of the silicone rubber membrane material.

Pan *et al* [49] did a similar study of circular and square polyamide membranes, which included finite element model (FEM) correction of the analytical model membrane shape constants. Their study resulted in a more accurate analytical model, providing this group with a more reliable load-deflection test for determining material properties. Maier-Schneider *et al* [48] performed an analytical study of the Pan *et al* [49] and Tabata *et al* [47] experiment and FEM analysis. This study included the development of a new and expanded analytical solution of Timoshenko *et al* [69] square membrane theory, further expressing the membrane shape constants c_1 and c_2 as a function of Poisson's ratio, and compared the results to the two groups. This analysis resulted in a ~ 1% error between Pan *et al* [49] and the Maier-Schneider et al [48] new analytical solution, and excellent agreement with experimental results. The Maier-Schneider *et al* [48] new analytical solution claims to be a more accurate solution for square membrane deflection than the original Timoshenko *et al* [69] theory for a Poisson's ratio of 0.25. This solution more accurately represents true membrane shape, and is the analytical model used for square membranes in this thesis.

Hohlfelder's aluminum circular membrane experimental results yielded values of 1.5% error in comparison to his approximate circular membrane theory derived from Hencky [70] and Timoshenko *et al* [69]. Thus providing the Nix *et al* [70, 72] group with a more tractable and accurate circular membrane solution. Further development of the circular bulge equation, through investigation and personal communications with Hohlfelder [70], provides a more accurate large deflection analytical model, which is explained herein.

These new load–deflection analytical models for circular and square membranes result in a more accurate calculation of the residual stress and Young's modulus of material films, as well as in the prediction of membrane load–deflection behavior. These solutions also show their practical limitations when compared to experimental results, making clear which theoretical models are most applicable to what materials.

The original plate and membrane theories of Timoshenko and Woinowsky-Krieger [69] have been expanded and developed for circular and square geometries by

Pan *et al* [49], Maier-Schneider *et al* [48], Hencky and Hohlfelder [70], and in this work. The new analytical solutions for circular and square membranes by Hohlfelder [70] and Maier-Schneider *et al* [48] respectively, are developed and discussed herein. These new solutions are used to analytically define membrane load–deflection behavior in this thesis for the determination of elastomer membrane elastic modulus and residual stress. A new theory for large deflections of circular elastomer membranes based on a pressurized sphere is also proposed.

1.2.1.1 Membrane load-deflection nomenclature

Table 1.2 below lists relevant nomenclature for working with membrane load-deflection mechanics.

Table 1.2: Membrane mechanics nomenclature

E	Young's modulus
M	Biaxial modulus = $E/(1-\nu)$
σ_{xx}	Biaxial stress $\sigma_{xx} = \sigma_{yy} = \sigma$
ε_{xx}	Biaxial strain $\varepsilon_{xx} = \varepsilon_{yy} = \varepsilon$
ν	Poisson's ratio
c_1,c_2	Membrane shape constants
h	Membrane deflection
t	Film thickness
a	Membrane radius
R	Membrane radius of curvature
P	Pressure
σ_o	Membrane residual stress

1.2.1.2 Circular membrane mechanics

Circular membrane load–deflection theory was most accurately described by Hencky, and practically developed for the bulge test by Beams *et al* [70]. Both models similarly describe the system, the bulge test being the more simple of the two models. The Nix group [70, 71,72] further developed Henky's theory for application to the bulge test for thin film material property and residual stress investigation.

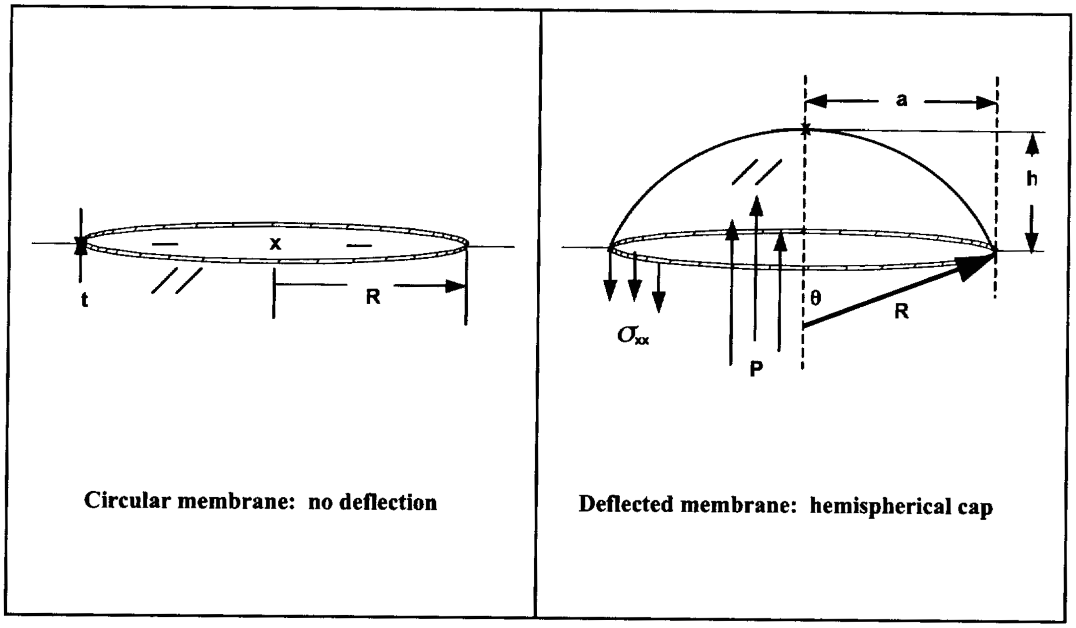

Fig. 1.1. – Circular membrane schematic

The bulge test is based on the derivation of the stress in a pressurized thin-walled sphere. This problem is found in most engineering mechanics texts and provides the foundation for the bulge test as a spherical cap, see Fig. 1.1, for approximating the load deflection of circular membranes [70]. Given that the model is a sphere, equi-biaxial stress is considered ($\sigma_{xx} = \sigma_{yy}$), and a balance of forces is applied. The Nix group derivation is as follows [72]:

$$P\left(\pi R^2\right) = \sigma(2\pi R)t \tag{1.2}$$

resulting in,

$$\sigma = \frac{PR}{2t} \tag{1.3}$$

By definition a membrane has no bending stress. This is due to the thin film thickness being much smaller than the deflection of the membrane ($t \ll h$), which agrees well with the theory of the spherical cap model, which assumes that the membrane has only equi-biaxial tension. Observing Fig. 1.1 it is assumed that when pressurized, the cap is under uniform load, equi-biaxial stress, and of equal radius [70]. Once pressurized the membrane is deflected to a height h, which is used to determine R, the membrane radius of curvature, which is calculated by using Pythagorean's theorem.

$$(R-h)^2 + a^2 = R^2 \tag{1.4}$$

Rearranging,

$$R = \frac{h}{2} + \frac{a^2}{2h} \tag{1.5}$$

For deflections h is much smaller than the membrane radius a, which is typical for linear elastic materials.

$$R \approx \frac{a^2}{2h} \tag{1.6}$$

Substituting equation (1.5) into (1.2) gives:

$$\sigma = \frac{Pa^2}{4ht} \tag{1.7}$$

Equation (1.5) defines the biaxial stress of the spherical cap model.

Defining the strain of the membrane as a function of the radius of curvature using a linear elastic engineering strain definition yields:

$$\varepsilon = \frac{\Delta l}{l_o} = \frac{R\theta - a}{a} = \frac{R\theta}{a} - 1 \tag{1.8}$$

The angle θ below the membrane is given by:

$$\sin\theta = \frac{a}{R} \approx \theta - \frac{\theta^3}{6} \tag{1.9}$$

Substituting (1.9) into (1.8) we arrive at:

$$\varepsilon = \frac{R\theta}{R\theta\left(\frac{1-\theta^2}{6}\right)} - 1 = \frac{\theta^2}{6} \tag{1.10}$$

Approximating that $\theta \approx a / R$ and substituting for R, the strain definition becomes:

$$\varepsilon = \frac{a^2}{6R^2} = \frac{2h^2}{3a^2} \tag{1.11}$$

Given the stress-strain relationship of a membrane in biaxial tension,

$$\sigma = M\varepsilon \tag{1.12}$$

Substituting equations (1.7) and (1.11) into the above equation and solving for pressure:

$$P = \frac{8}{3}Mt\frac{h^3}{a^4} \tag{1.13}$$

Equation (1.13) is the spherical cap bulge equation for a membrane in tension without residual stress. Residual stress may be accounted for by modifying (1.12),

$$\sigma = M\varepsilon + \sigma_0 \tag{1.14}$$

Inserting equatons (1.7) and (1.11) into (1.14) and again solving for pressure yields:

$$P = 4\sigma_0 t \frac{h}{a^2} + \frac{8}{3} Mt \frac{h^3}{a^4} \tag{1.15}$$

This is the spherical cap bulge equation for a circular membrane [70]. Although this model maybe greatly simplified in comparison to exact solutions, it is a reasonable approximation for load-deflection behavior of a circular membrane system with residual stress [70]. A more exact solution by Timoshenko [69] develops the differential equations describing this problem at length, and Hencky [70] derived an exact solution very similar to the common shell solution found in many texts. However, the Hencky [70] model applies boundary conditions about the outer edge to limit transverse strain in order to more accurately describe membrane behavior, and neither model readily accounts for residual stress which is present in experimental tests. Based on the work of Hencky and Vlassak [70.71], Hohlfelder developed a general solution by describing two cases; the modulus dominated regime and the residual stress dominated regime.

For a circular membrane the modulus dominated regime assumes no residual stress in the thin film, therefore the mechanics are dominated by membrane elasticity. This yields a general case modulus dominated solution of [70]:

$$P = \frac{c_2(v)Mth^3}{a^4} \tag{1.16}$$

where,

$$c_2(v) = \frac{\frac{8}{3}(1.015 - 0.247v)}{(1 - v)} \tag{1.17}$$

Equation (1.17) is a relation describing the membrane shape constant and how it varies with (v).

Considering the residual stress dominated case, membrane behavior is governed to residual strains in the thin film. The general case solution of a residual stress dominated membrane is [70]:

$$P = 4\frac{\sigma_0 t}{a^2}h \tag{1.18}$$

A general case solution may be developed in which residual stress in the membrane is neither dominant nor negligible. This is done by superposing the two solutions to the limiting cases. This gives the solution for the general case circular membrane load–deflection analytical model resulting in, *The bulge equation for a circular window* [70]:

$$P = 4\frac{\sigma_0 t}{a^2}h + c_2(\nu)\frac{Eth^3}{a^4} \tag{1.19}$$

where,

$$c_2(\nu) = \frac{\frac{8}{3}(1.015 - 0.247\nu)}{(1-\nu)} \tag{1.20}$$

Although this is not an exact solution, it was found to be within 1.5% of Hencky's solution for a circular aluminum membrane [70].

The bulge equation for a circular window by Hohlfelder [70] accurately describes the physical system for linear elastic materials within the elastic stress-strain region, and enables the determination of thin film material properties and residual stress, which is present when working with membranes. The above theory is one of the models used herein for approximating circular membrane performance.

Considering the derivation of the spherical cap model and its close approximation to exact solutions for circular membrane behavior as applied to linear elastic materials, an investigation into its application to non-linear elastic materials has been pursued. As can be found in most strength of materials texts, tensile strain definitions can have a significant impact upon material property characterization [73,74]. Based on this premise, a suitable tensile strain definition must be chosen to approximate any given material performance. Each material behaves in a different manner under the same loading conditions due to material composition and molecular structure. Numerous strain definitions have been developed by using different strain or stretch ratios to provide accurate elongation approximations for all materials [73,74,103]. Most engineering materials use the engineering strain definition:

$$\varepsilon = \frac{\Delta l}{l_o} \tag{1.21}$$

While (1.21) describes engineering materials very well, and is the definition used in the spherical cap method, assuming h is small so equation (1.6) is assumed, its ability to describe elastomers is poor. This is due to the model being tailored to engineering material or small strain analysis, and the ability of elastomers to elongate up to 600% of their original length before failure. To date only the standard engineering strain definition has been applied to the spherical cap model, limiting R to the form shown in equation (1.6) [75]. Therefore, an investigation assuming the exact form of R in equation (1.5) and applying it to the engineering strain definition, and true strain definitions was performed to better approximate the load-deflection behavior of elastomer membranes [74,75]. Applying equation (1.5) to the engineering strain definition from equation (1.8), as defined by Cauchy infinitesimal [74,75], yields:

$$\varepsilon_E = \left(\frac{R \sin^{-1} \frac{a}{R}}{a} \right) - 1 \tag{1.22}$$

This is the engineering strain definition as a function of R [75].

True strain, as defined by Cauchy [74,75,103], is:

$$\varepsilon_T = \frac{\Delta l}{l_o + \Delta l} \tag{1.23}$$

Applying the true strain definition to the spherical cap model. From equation (1.8):

$$\Delta l = R\theta - a \tag{1.24}$$

and

$$l_0 = a \tag{1.25}$$

Substituting (1.24) and (1.25) into (1.23) yields:

$$\varepsilon_t = \frac{R\theta - a}{R\theta} = 1 - \frac{a}{R\theta} \tag{1.26}$$

From equation (1.9), solving for θ,

$$\theta = \sin^{-1}\frac{a}{R} \tag{1.27}$$

Substituting (1.27) into (1.26) yields:

$$\varepsilon_T = 1 - \left(\frac{a}{R\sin^{-1}\frac{a}{R}} \right) \tag{1.28}$$

This is the true strain definition applied to the spherical cap model.

The Almansi true strain definition is [74,103]:

$$\varepsilon_A = \frac{(\Delta l + l_o)^2 - l_o^2}{2(\Delta l + l_o)^2} \tag{1.29}$$

Applying the Almansi true strain definition to the spherical cap model by inserting (1.24) and (1.25) into (1.29) yields,

$$\varepsilon_A = \frac{\left[\left(R\sin^{-1}\frac{a}{R}\right)^2 - a^2\right]}{2\left(R\sin^{-1}\frac{a}{R}\right)^2} \tag{1.30}$$

This is the Almansi true strain definition for the spherical cap model.

Now the new engineering and true strain definitions are applied to the spherical cap model following Nix [72]. Given the biaxial modulus:

$$M = \frac{E}{(1-v)} \tag{1.31}$$

By inserting equations (1.3), (1.31), and (1.22) into equation (1.14):

$$\frac{PR}{2t} = \frac{E}{1-v}\left(\frac{R\sin^{-1}\frac{a}{R}}{a} - 1\right) + \sigma_0$$

Solving for pressure:

$$P=\frac{\left[\frac{E}{1-\nu}\left(\frac{R\sin^{-1}\frac{a}{R}}{a}-1\right)+\sigma_0\right]2t}{R} \tag{1.32}$$

This is the spherical cap model with engineering strain as a function of R [75].

The true strain spherical cap model is determined by inserting equations (1.3), (1.31), and (1.28) into equation (1.14) yielding:

$$\frac{PR}{2t}=\frac{E}{1-\nu}\left(1-\frac{a}{R\sin^{-1}\frac{a}{R}}\right)+\sigma_0$$

Rearranging to solve for pressure:

$$P=\frac{\left[\frac{E}{1-\nu}\left(1-\frac{a}{R\sin^{-1}\frac{a}{R}}\right)+\sigma_0\right]2t}{R} \tag{1.33}$$

This is the Cauchy true strain spherical cap model.

The Almansi true strain spherical cap model is determined by inserting equations (1.3), (1.31), and (1.30) into (1.14) yielding:

$$\frac{PR}{2t} = \frac{E}{1-v}\left(\frac{\left(R\sin^{-1}\frac{a}{R}\right)^2 - a^2}{2\left(R\sin^{-1}\frac{a}{R}\right)^2}\right) + \sigma_0$$

Rearranging to solve for pressure:

$$P = \frac{\left[\frac{E}{1-v}\left(\frac{\left(R\sin^{-1}\frac{a}{R}\right)^2 - a^2}{2\left(R\sin^{-1}\frac{a}{R}\right)^2}\right) + \sigma_0\right]2t}{R} \tag{1.34}$$

This is *The new spherical cap model.*

Equations (1.32), (1.33), and (1.34) are the new analytical models for circular membrane large deflection. Figure 1.2 below is a plot of a PDMS circular membrane bulge test experimental data and compares the different analytical models previously outlined. This plot demonstrates the difference between the various analytical models and their ability to accurately approximate the experimental data.

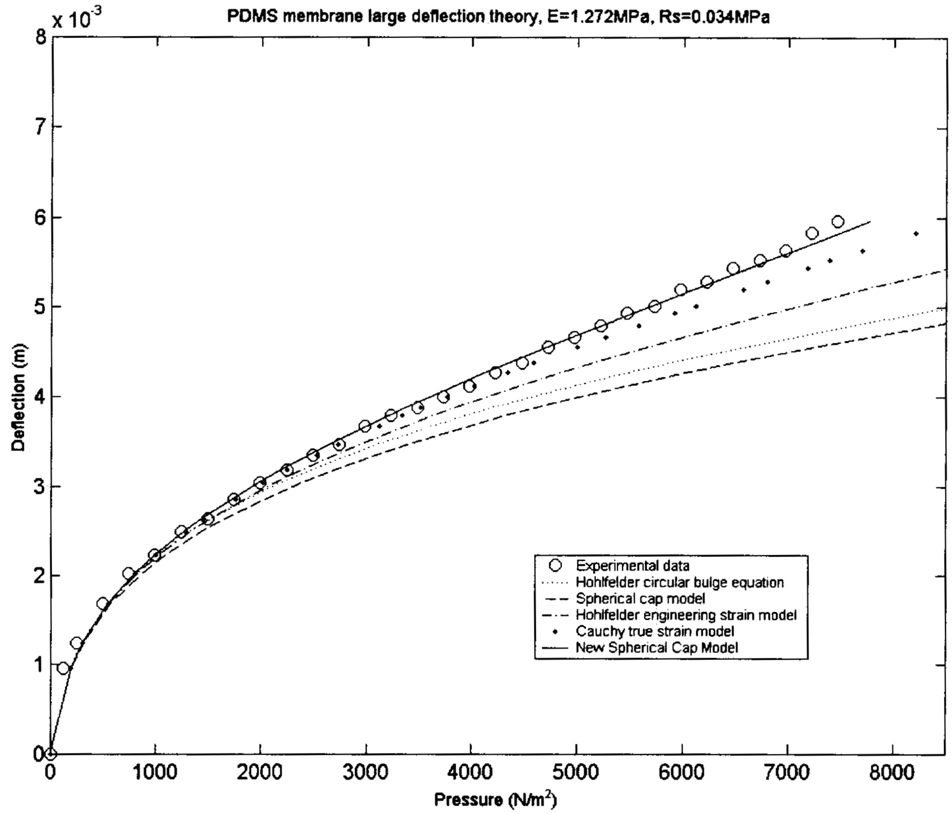

Fig 1.2. - Plots of circular membrane theory

1.2.1.3 Square Membrane Mechanics

Square membranes are different from circular, assuming the same radius and thickness, square membranes have 21% more material, see Fig. 1.3. This is significant in that the predominant force acting on a membrane is tension, therefore there is more strain for a given pressure as compared to a circular membrane [68]. The stress-strain field is also very different from a circular membrane, as equibiaxial stress and strain can no longer be assumed. When pressurized, square membranes develop a circular bulge, going from their initial square shape and becoming more circular in the center, while the perimeter and corners assume a different shape [68]. This is especially evident for elastomer membranes, as seen in Fig. 1.3 and 2.11. The theory describing the physical system of square membrane load-deflection is not as simple as the spherical cap model for circular membranes. Most solutions were developed using differential equations and focus on membranes made of linear elastic materials, under small deflections. The complexity of square membrane theory and an analytical model that accurately approximates elastomer membrane load-deflection performance is further compounded by the large deflections achieved by elastomer materials, and has yet to developed. Therefore, the most accurate square membrane solution from the literature search is used herein.

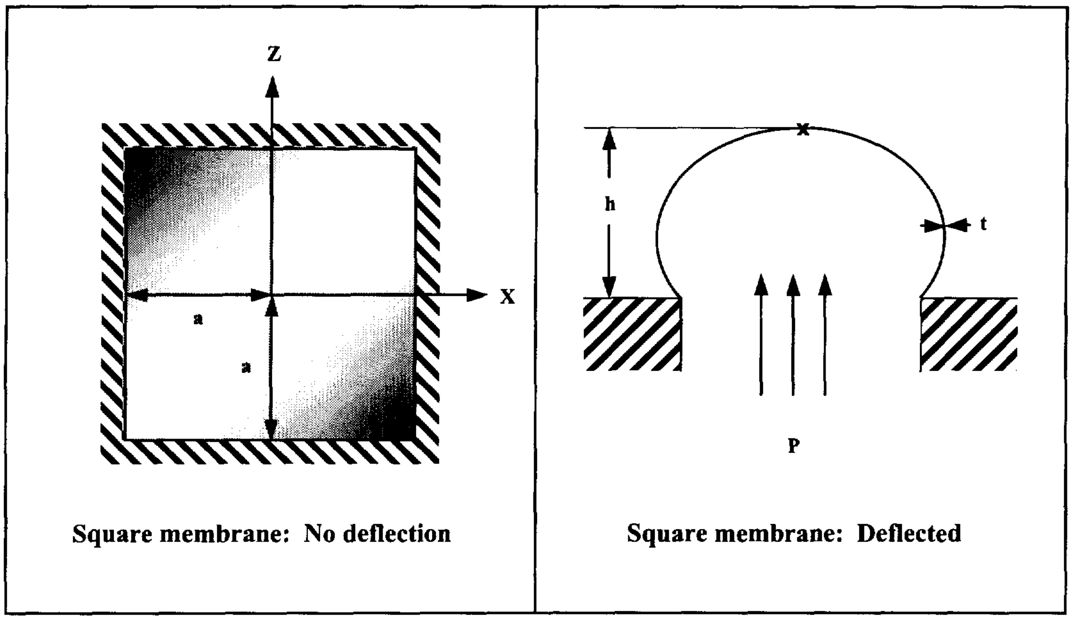

Fig. 1.3. - Square membrane schematic

Square and rectangular membrane load-deflection theory was originally described by Timoshenko *et al* [69] employing the energy method [48]. The energy method derives a solution for plate deflection behavior by first assuming the functional shape of a deflected plate by a load, and then calculating and minimizing the potential energy of the system to fit the initial assumption [69, 47]. Unfortunately, early assumptions for the functional shape of a plate deflected by a load, a square plate to spherical cap, were inaccurate. The inaccuracy was due to mathematical simplification of the problem to facilitate ease of computation at the expense of accuracy [49] . However, with the interest of determining the residual stress of thin films and their material properties, very accurate analytical models are desired. Maier-Schneider *et al* further developed the energy method theory of Timoshenko *et al* [49,69] for linear elastic materials by expanding the functional shapes of square plate load–deflection, thus improving the accuracy of the model. Maier-Schneider *et al* [48] developed this improved analytical solution using the computational software program MATHEMATICA, and is within 1.2% error with FEM solutions developed by Pan *et al* [49]. The new analytical solution for square membrane load–deflection developed by Maier-Schneider *et al* is:

$$P = c_1 \frac{t\sigma}{a^2}(h) + c_2(v)\frac{tE}{a^4}(h^3) \tag{1.35}$$

where c_1=3.45 and

$$c_2(v) = \frac{1.994[1 - 0.247(v)]}{(1 - v)} \tag{1.36}$$

This solution for square membrane mechanics enables the determination of thin film material properties and residual stress, it is the most accurate solution known to date, and is the theory used herein to approximate square membrane load–deflection behavior.

1.3 MEMS Materials

Materials used for MEMS fabrication vary widely and are steadily increasing in number. This is due to new applications of MEMS with existing materials and new materials. Due to the application of MEMS as “chip level sensors and actuators” integrated into ICs, fabrication is done primarily employing bulk CMOS IC planar processing. The fabrication techniques used for MEMS employ standard CMOS processing as well as new MEMS processing techniques, such as LIGA, SCREAM, and

MOSIS, used to facilitate more complex MEMS structures and devices. In standard CMOS fabrication and specific MEMS processing techniques the process usually begins with a bulk substrate. The most common materials used are silicon, bulk metals, polymers, and ceramics [77] Planar processing uses two dimensional lithographic techniques for patterning and incorporates layering and removal of materials for the third dimension. Materials used for layering are silicon dioxide, metal films, polymers, and ceramics. Many of these materials are well suited for MEMS applications, are standard processing materials, and have well known material properties. However, some materials have non-typical material properties which can offer enhanced performance, or enable particular MEMS sensory and actuation applications previously unavailable using standard processing materials, this is the case for PDMS MEMS membranes.

1.3.1 Metals

The use of metals in MEMS fabrication is vast. The ability to deposit thin metal films by electro-plating or thermal evaporation, is particularly suited for the fabrication of MEMS membranes. Plate and membrane mechanics were developed for practical use assuming metal as the material of choice. Metals are crystalline solids whose forms consist of a crystal lattice molecular structure, where each metal atom occupies its ordered space within the structural array forming a three dimensional material [77,78]. Metals crystallize in different structures and unit cells of atoms are formed, the most common being face-centered cubic, body-centered cubic, and close-packed hexagonal. When the unit cell is repeated in all directions a crystal lattice is formed. Fig. 1.4 displays a body-centered cubic unit cell and crystal lattice. It is the atomic make up and resulting crystalline structure that give metals their individual material properties [80].

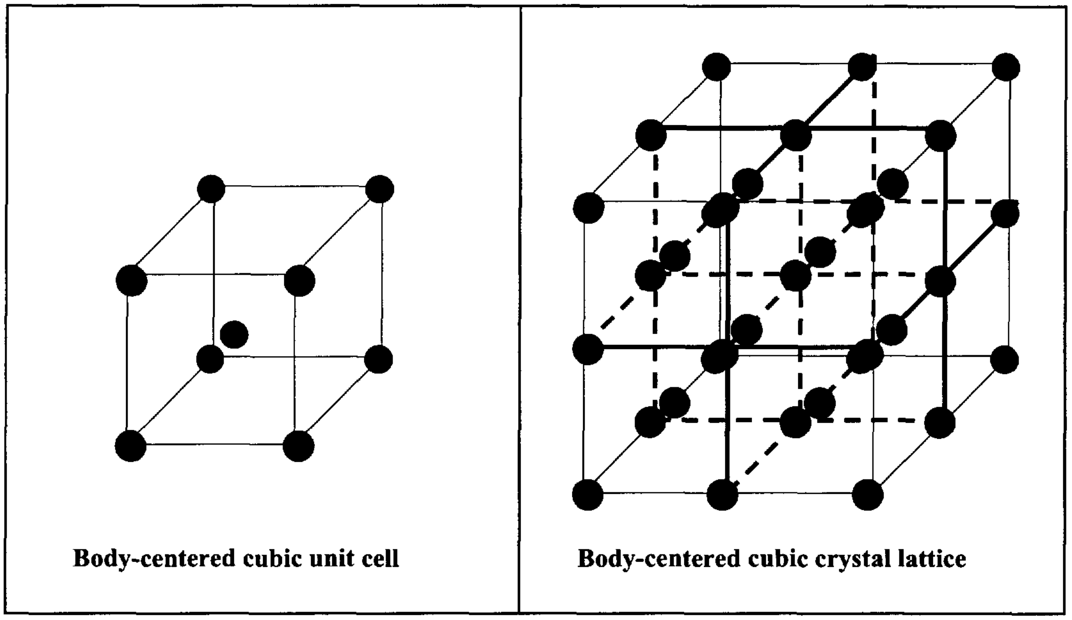

Fig. 1.4. - Metallic body-centered cubic crystalline solid structures

Plate and membrane theory developed by Timoshenko *et al* [69], Hencky, Di Giovanni, and others assumes the use of materials having a Poisson's ratio of $v = 0.25$ to $v = 0.35$, these values of Poisson's ratio are typical for most metals [67,72,75]. Given that the theory was developed assuming material properties of common metals, the analytical solutions perform well for those materials. Metal films perform in a specific manner as plates and membranes, as governed by their material properties. The mechanical response, load-deflection, of a metal plate clamped at the edges and subject to a uniform load have been well documented [67, 68,69]. Plate deflection is linear up to ~ 30% of the plate thickness as dominated by pure bending theory, which dictates that an inflection circle of the plate be located at 57.73% of the plate radius [66]. Non-linearity is introduced when plate deflections greater than ~ 30% of the thickness are present, resulting in the inflection circle being pushed to the perimeter of the plate [66]. The result is a plate that is now governed by membrane load–deflection theory, the degree of which may introduce large amounts of hysteresis and plastic deformation. Metal plates and membranes are most often used as force summing devices or pressure sensors, due to their crystalline structure, linear elastic behavior, low hysteresis, ease of fabrication, and resistance to vibration [66]. Metal plates used as pressure sensors produce highly linear and reproducible response for their design range, deflection ~ 30% of the plate thickness.

1.3.2 Polymers

Polymers have had an enormous impact upon MEMS research and the emerging MEMS industry. The use of polymers has made particular MEMS applications and devices a reality. Many of the MEMS applications to benefit from polymer use are microfluidics systems, hygrometers, accelerometers, and aerodynamic controllers [7-30, 64,99,42]. Many of these applications would otherwise be impossible implementing standard CMOS fabrication materials and processes. The benefits of polymer use for MEMS applications are numerous. Polymers are used both as substrates and layering materials in MEMS fabrication. There is a vast selection of polymers in industry today yielding a wide range of material property selection. Elastic modulus values for polymers can vary from ~ 1 MPa for synthetic rubbers to ~ 4 GPa for polyamide nylon. Polymers with soft amorphous elastomer structures are favorable for MEMS applications due to their ability to withstand large deformations with low stress, which match favorably with low power MEMS actuation techniques [1,4,5]. Elastomers are polymers which exhibit large deformation at room temperature with non-plastic deformation when loading is released [3]. At room temperature typical elastomeric polymers, such as natural rubber and PDMS, have elastic modulus values of ~ 10^6 N/m^2, while glassy and crystalline polymers have elastic modulus values which are three orders of magnitude higher, ~ 10^9 N/m^2 [2]. This difference is due to the molecular structure and respective glass transition temperature (*Tg*) of the different polymers [2,3].

Cured polymers consist of long chain polymer molecules which are cross-linked. Glassy and crystalline polymers may have a molecular structure somewhat similar to the structure of crystalline metals in Fig. 1.4, while elastomers consist of amorphous cross-linked structures as shown in Fig. 1.5. Semi-crystalline polymers are composed of both amorphous and crystalline molecular structures, to lesser and greater degrees, depending upon the material in question. Both amorphous and semi-crystalline polymers are considered visco-elastic materials due to their ability to behave like viscous fluid like gels and crystalline materials, with each molecular structure contributing its unique relationship to a given material's stress-strain curve [94]. Under relaxed conditions elastomer molecular structure is amorphous, making it an ubiquitous material which is difficult to characterize. When loaded the long chains disentangle and orient in the direction of the load, this is called strain crystallization, and is the typical elastic response of elastomer materials [80]. Semi-crystalline polymers have both an amorphous and crystalline elastic response to loading, which varies depending on the material. Semi-crystalline polymers are generally more rigid in stress-strain tests compared to elastomers, given their partial crystalline molecular structure. Standard tensile tests of typical crystalline polymers have a linear elastic stress-strain curve, without deforming, due to their ordered molecular structure, acting much like metals. This behavior is linear in the sense that the stress-strain relationship is a straight line until the yield point, where the material starts to deform, deviating from the straight line in a non-linear fashion. Elastomers and semi-crystalline polymers may have a similar linear stress-strain curve in standard tensile tests, depending on the material. The elastomer amorphous molecular structure having a linear elastic stress-strain curve until strain crystallization begins, thus changing to a non-linear stress-strain curve. Assuming that the breaking point is not reached, elastomers return to their original shape once loading is released and without substantial deformation, unlike semi-crystalline materials. Elastomers are unique in this behavior. These fundamental material properties of elastomers may be manipulated by varying the cross-link density of the polymer molecules [80,84].

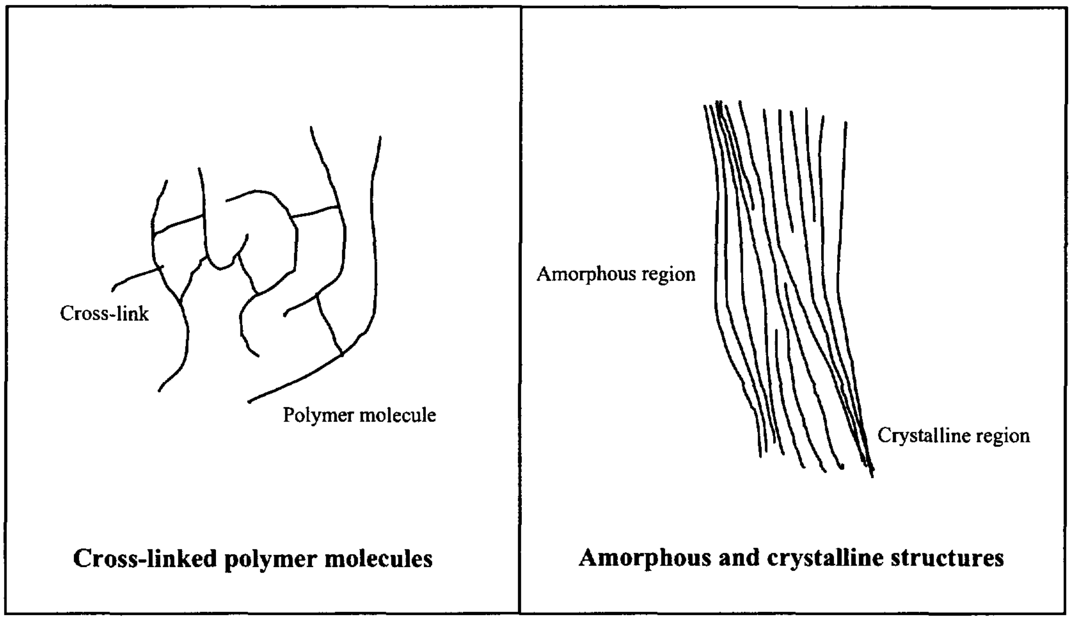

Fig. 1.5. - Polymer molecular structures

Elastomers are gel like and amorphous due to their respective glass transition temperature. The glass transition temperature of a polymer may be considered analogous to the freezing point of a liquid. As the temperature is reduced, the amount of free volume in the polymer is also reduced, thus restricting molecular motion. Elastomers have glass transition temperatures well below room temperature, PDMS has a $Tg \sim -127^{\circ}$ C [2,3,17,18]. Due to the intrinsic molecular structure, molecules of elastomeric polymers readily slide past each other when subjected to an external load, generating heat. This may result in significant energy loss when materials are dynamically loaded, creating a mechanical hysteresis loop. The hysteresis is due to stress relaxation, molecules sliding past each other in the polymer, and is more evident at slow strain rates, due to the molecules having more time to disentangle. The measure of the energy lost is defined as tan δ, or "loss factor". The tan δ of a material is a representation of energy loss due to mechanical hysteresis and stress softening [88]. For elastomers, this energy loss is often in the form of heat, which may have a cumulative effect on the given application and therefore is an important material property to be included in material selection data [11,17].

Amorphous elastomers are capable of very large elongations, up to 600% or more of the original sample length, with a corresponding reduction in cross section, [14,17]. Poisson's ratio is the lateral strain over the longitudinal strain for a material subjected to an axial load with resulting elongation, and is an important mechanical property to be included in simulation models. Poisson's ratio is typically from 0.25 to 0.35 for most metals, and is well above 0.35 for most amorphous elastomers [12,17]. Many polymers may be made to suit a wide range of material property requirements and MEMS processing needs. Once a polymer is chosen for a particular application often the material properties and processing technique are tailored to optimize the application requirements. Most other fabrication materials do not have such a dynamic range of material property manipulation.

1.3.2.1 Polyethylene

Polyethylene, a polyolefin plastic discovered in 1933 by E. Fawcett and R. Gibson of the Imperial Chemical Industries Laboratories (England), was the first synthetic polymer. Over the last seventy years polyethylene has been improved, costs less to manufacture, and is used in nearly every industry and consumer product today. Polyethylene is made in three primary methods; gas-phase, solution, and slurry (liquid-phase), through addition reactions of ethylene [94]. Generally these reactions consist of ethylene monomer molecules being polymerized in a pressurized environment containing ethylene, and a catalyst. Varying the pressure and temperature of the process environment yields different grades of polyethylene, each with different material properties, such as LDPE, MDPE, and HDPE; corresponding to low, medium, and high polymerization densities. LDPE polymerization processes result in producing polyethylene molecules with many long chain side branches off of the main polymer chain molecule. Processes that produce MDPE and HDPE yield polyethylene with reduced side branches. It is these side branches that affect the ability of the polymer molecules to pack closely together and the resulting bulk density of the material. Recently LLDPE (linear low density polyethylene) has been produced using a low pressure process. This is different from LDPE in that it has many short chain side branches and fewer long chain branches off the main polymer chain molecule. The low pressure process is more economical and is used as a standard process for most LDPE applications, such as food service films and plastic bags, today. Polyethylene is a material that has amorphous and crystalline regions. The crystalline regions consist of portions of the polymer chains aligning in ordered microscopic polyhedral-shaped spherulite crystals. While the amorphous regions are in no particular molecular order. HDPE may consist of up to ~ 90% crystalline regions, as compared to LDPE with up to ~ 40% crystalline regions. It is the close packing of the polymer molecules in the crystalline regions that give an increased density to the material, where the amorphous regions have a reduced structural order and density. Due to the coexistence of the amorphous and crystalline molecular packing regions, polyethylene is considered a semi-crystalline material, as shown in Fig. 1.5. Tensile stress–strain response is typically a short curvilinear elastic region with a lengthily cold draw region, due to the amorphous and crystalline packed molecular structure undergoing strain crystallization [94]. Polyethylene may be manufactured as a film for food service and packaging applications, pellets for raw material, and stock extrusions for industry. Typically it is injection molded, spin or blow molded, and extruded to form milk containers, fleece pullovers, kayaks, writing instruments, electrical wire insulation, automobile interior and exterior components, and innumerable packaging and industrial applications. Polyethylene may also be reused and recycled for remanufacture in new products [81,94].

Polyethylene film was of particular interest as a reference material for this thesis. Linear low density polyethylene (LLDPE) film, manufactured by GLAD, was used to provide a known material for comparison to PDMS. LLDPE is an amorphous semi-crystalline plastic made from a low pressure polymerization process, having range of elastic modulus values E = 50-300 MPa for all Polyethylenes, and a Poisson's ratio ν = 0.4 [94,104]. Static uniaxial tensile specimens and membranes were made from the LLDPE film; GLAD wrap. The uniaxial tensile specimens were used to determine the elastic modulus of LLDPE and the membranes were used to produce load-deflection data.

Both sets of specimens were used to verify the test setups and to give a known material reference for PDMS material property tests.

1.3.2.2 Polydimethylsiloxane (PDMS)

Polydimethylsiloxane is an elastomeric polymer or synthetic rubber, and the material of investigation for this thesis. PDMS was developed in the mid twentieth century as a replacement for natural rubber and is the most common elastomer in use today. PDMS or silicone rubber is different from other elastomers in that it consists of silicon and oxygen in the form of siloxane to form its main flexible backbone polymer molecules [80,82]. It is the structure and combination of these molecules that gives the flexible elastomeric nature of PDMS and its non-standard mechanical properties. Elastomer molecular structure when strained goes from an amorphous gel like state to a more crystalline state. This is called strain crystallization. Due to the change in molecular structure, large elongations result. Elastomers are capable of great elongations while strained, and are able to return to their initial state with little or no plastic deformation when the strain is released. Therefore, PDMS stress-strain behavior is linear to non-linear or varies as a function of the strain, thus the elastic modulus varies as a function of the strain. These phenomenon also have a significant effect upon the Poisson's ratio of PDMS.

Vulcanization of PDMS is most commonly done by room temperature vulcanization (RTV). PDMS may come in the one-component form, where the cross linking component is manufactured into the base compound and vulcanization occurs upon use with exposure to atmospheric moisture. In this case, curing occurs from the outside-in with time, and is the form that most silicone sealants are found today. Another common type of RTV of PDMS is the two-component system, where the cross linking component is added to the base compound just before use, giving uniform curing throughout [80]. Variations in the mixing ratio and curing process of the two-component system have a significant impact upon the PDMS mechanical properties. Upon polymerization PDMS is inert, taste and odorless, resistant to biological and ultra-violet degradation, stable over a temperature range of -60° C to 300° C in air, and non reactive with most materials [80]. Applications of PDMS silicone rubber include, automobile ignition cables, gaskets, sealants, o-rings, static seals, food and medical grade tubing, human prosthesis implants and augmentation, contact lenses, electrical component insulators, and as a MEMS fabrication material. PDMS is a very common and economical industrial material, which is stable after processing, has a vast range of applications and flexible processing capabilities. It is these characteristics along with its mechanical properties that make it a popular choice for many MEMS applications.

1.4 Motivation

Plate and membrane mechanics have been investigated for numerous ends, and for a number of different geometries and materials in MEMS research. However, the load-deflection mechanical response of circular and square PDMS membranes, with accurately defined material properties, has yet to be fully characterized. These are investigated herein to provide more accurate large deflection elastomer mechanical models for MEMS design applications of elastomer membranes and PDMS in varying applications.

Chapter 2
Experimental procedures and techniques

To investigate the tensile mechanical properties and membrane load-deflection mechanical response of PDMS a number of experiments and modeling was conducted. Dynamic and static uniaxial tension tests were performed to determine tensile mechanical properties. Static membrane bulge tests were conducted to determine the mechanical response of circular and square membranes under static uniform load, and to derive the membrane biaxial modulus. The results of these tests provided accurate tensile mechanical property data for PDMS in varied tensile applications, which was used in analytical membrane deflection models to simulate membrane deflection experiments.

2.1 Mechanical testing

Mechanical testing consisted of static and dynamic uniaxial tensile tests as well as circular and square membrane testing. The purpose of the tensile testing was to characterize the tensile mechanical properties of the polymers investigated; PDMS and LLDPE. The mechanical properties of particular interest are the elastic modulus (E), loss factor (Tan δ), Poisson's ratio (ν), and stress relaxation (τ). For obtaining tensile test data three types of tests were conducted; static uniaxial tension, dynamic uniaxial tension, and video dimensional analysis (VDA) for determining Poisson's ratio. Stress relaxation and deformation tests of PDMS tensile samples were conducted to verify PDMS relaxation time and the feasibility of the membrane testing technique, as well as to determine relative amounts of plastic deformation at a particular stress level. The purpose of the membrane testing was to characterize the specific load-deflection response of PDMS and LLDPE for circular and square geometries. These tests also provide residual stress (σ_0) and biaxial modulus (M) material properties. Membrane testing experimental results also serve to validate membrane analytical models. All mechanical tests were performed on a Materials Testing Systems, Eden Prarie, Mn USA, (MTS) Tytron servo-pneumatic tensile testing machine, Fig. 2.1.

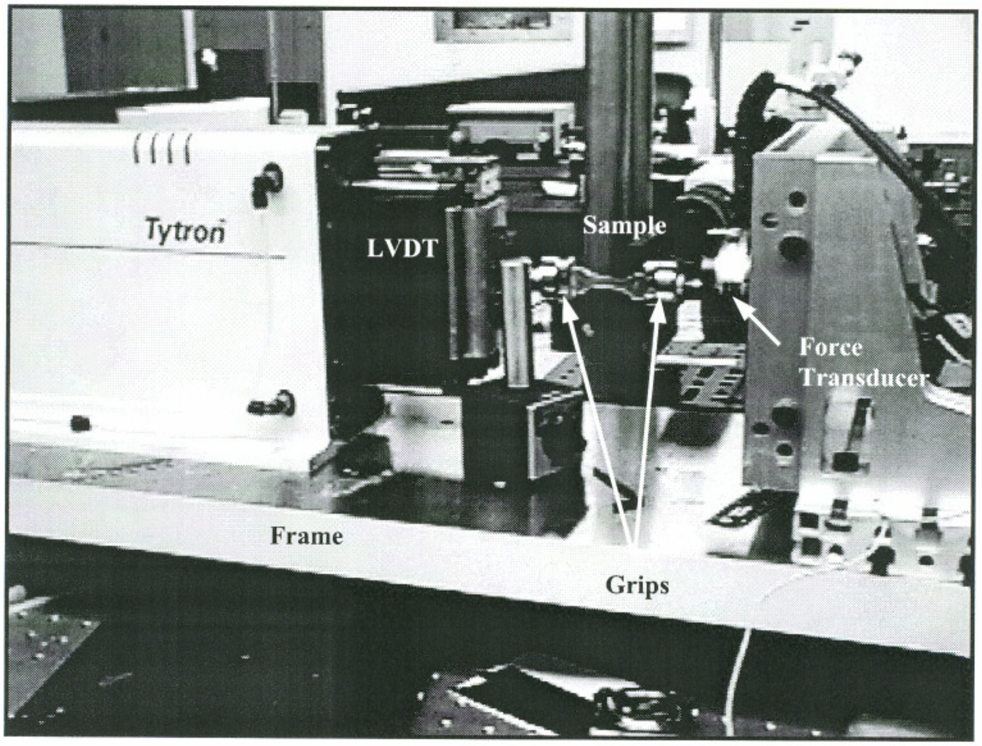

Fig. 2.1. - MTS Tytron mechanical tester

2.1.1 PDMS material processing

Industrial grade polydimethylsiloxane, manufactured by Silicones, Inc., of High point, North Carolina USA, [P-125, RTV-2 PDMS silicone rubber], was used to fabricate all PDMS films and test samples [83]. PDMS [P-125, RTV-2] is a common industrial grade, two part (base and activator) silicone rubber. A curing agent (activator), or polymerization catalyst, is added to the (base) polymer to form the final material. Varying the mixture ratio of base to activator varies the degree of base polymerization and the resulting final material properties of the PDMS [84]. Various curing techniques may also be added to the material processing, such as degassing the mixture and or heat curing, to further drive the polymerization reaction to completion. A common manufacturer recommend mixture and curing process was used to fabricate all samples.

2.1.2 Polyethylene (LLDPE) film

Polyethylene (LLDPE) film was used for the fabrication of tensile samples to provide a tensile test reference for the experimental test setup. This film was chosen for its similar mechanical properties to PDMS, film uniformity (~ 0.0254e-3 m thick), availability, and low cost. The LLDPE film used is commercially known as GLAD wrap, a film invented in 1966 by GLAD Products of Australia for food packaging [85]. Glad wrap is made from hard polyethylene resin with a cast film extrusion machine, and is commercially available at most food stores in the USA [85]. The tensile specimens were punched from LLDPE film sheet.

2.1.3 Tensile specimen fabrication

Tensile specimens were fabricated from PDMS and LLDPE film sheets. Three sizes of PDMS tensile samples were prepared for the tensile tests, Fig. 2.2. *A* size samples were used for dynamic uniaxial tensile testing, *B* size samples were used for static uniaxial tensile testing, and *C* size samples were used for Poisson's ratio testing.

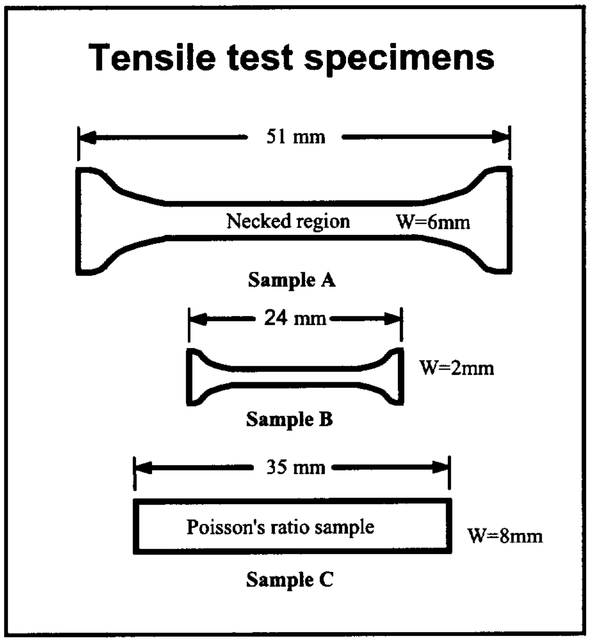

Fig. 2.2. - Tensile specimens

For the *A* samples the PDMS was prepared by thoroughly mixing 10 parts base to 1 part activator by weight. Air bubbles were removed twice, sequentially in a vacuum chamber, and the PDMS allowed to cure in flat molds (2-mm thick) at room temperature for 24 hours. Rectangular *C* samples of this material batch were used in determining Poisson's ratio. The *B* samples were made with the same PDMS mixture ratio by weight, but spread to form very thin sheets and cured at room temperature for 24 hours without exposure to a vacuum. A special jig was constructed using a variable height silk screening squeegee, Parafilm, and shim material. Parafilm was taped to a very flat work surface and a layer of PDMS, ~ 0.1016e-3 m thick, was squeegeed on the Parafilm. Parafilm is a wax type standard laboratory film used to seal test tubes and etc. It was used as a base for the PDMS film due to its non-adhesion to PDMS, and it could be rolled up and stored for later use. Once the PDMS batches were fully cured, after 24 hours or more, *A*, and *B* size tensile specimens were then fabricated with their respective punch, Fig. 2.3, to provide a necked region in accordance with industry uniaxial tensile testing standard (ASTM D 412-98a) for elastomer polymers [86]. LLDPE *B* size samples were also punched. Rectangular *C* samples were cut to size Fig. 2.2. Testing standard (ASTM D 412-98a) dictates that dumbbell specimens be punched from thin sheets of the material to be tested. Two different punches were used to fabricate the *A* and *B* size dumbbell specimens, (Fig. 2.3). Each test sample was of uniform shape and thickness.

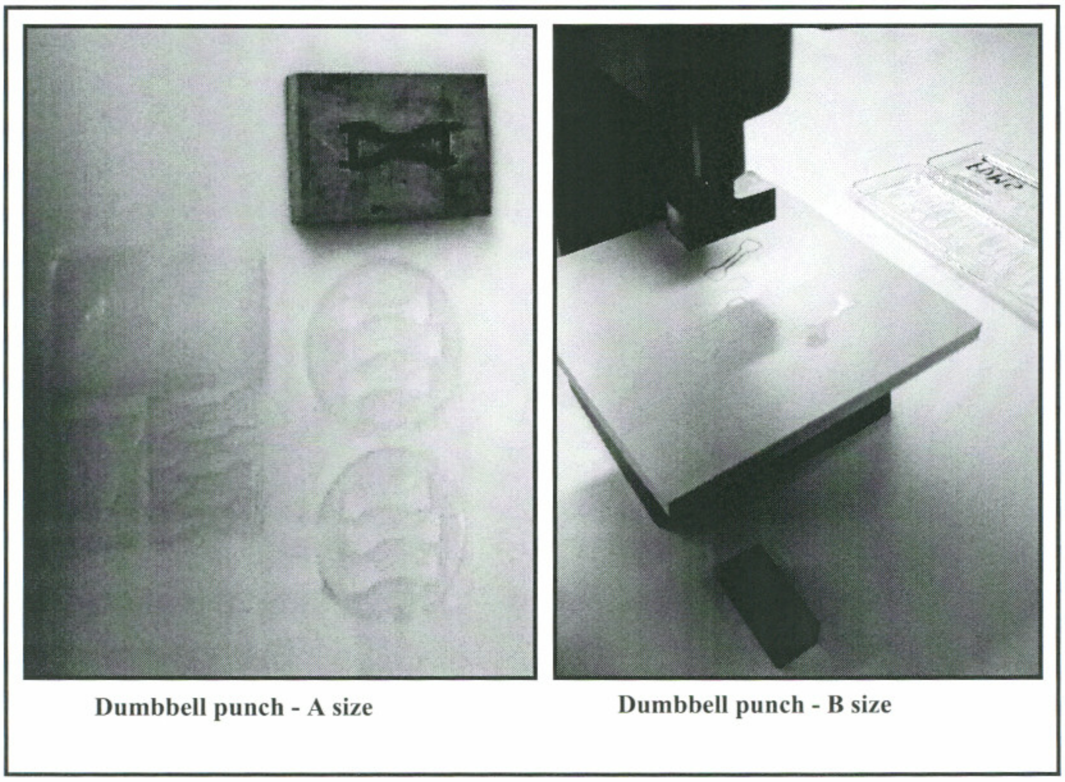

Fig. 2.3. - Tensile specimen punches

2.1.4 Membrane fabrication PDMS and LLDPE

Membrane fabrication was achieved through the use of fabricated PDMS and LLDPE films previously noted in section 2.1.1 and 2.1.2, in conjunction with the membrane block Fig. 2.4. The film to be tested was placed between the two disassembled sections of the membrane block, with a small amount of membrane pre-tension to eliminate sag. The two sections were then fastened together, resulting in clamped edge circular and square film membranes with an air tight seal, Fig. 2.4. Any remaining film extending from the edges of the membrane block was trimmed away. The membrane block was designed to create clamped edge circular and square membranes of the same radius, $r = 9.525$mm, from the film sheets. These sheets are readily changed to facilitate ease of testing. For deflection measurement purposes, each membrane was marked with a black dot in the center to aid in aligning the probe to the membrane.

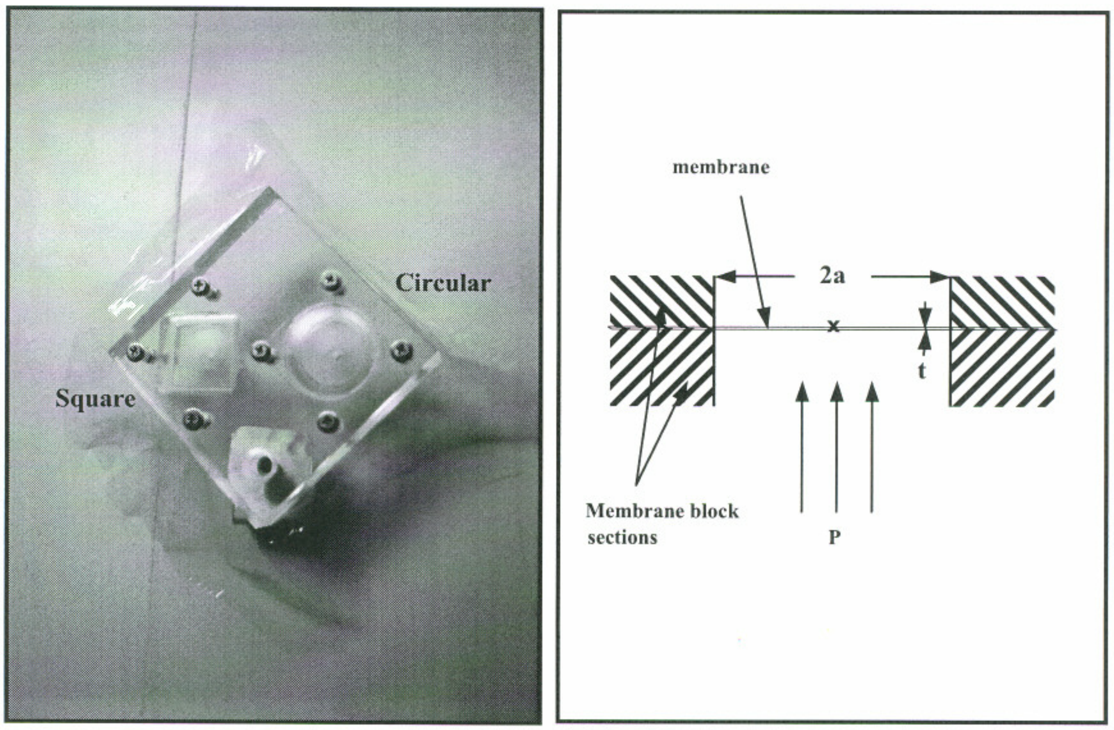

Membrane block with new membranes | **Clamped edge membrane**

Fig. 2.4. - Membrane block and membranes

2.1.5 Tensile test procedures

Three types of tensile tests were performed to determine the tensile mechanical properties of PDMS using an MTS Tytron servo-pneumatic uniaxial tensile testing machine. These tests are; static uniaxial tension, dynamic uniaxial tension, and video dimensional analysis (VDA) for determining Poisson's ratio. LLDPE was tested in static uniaxial tension only. The static and dynamic tension tests performed were at particular rates of strain, and measurements were recorded in real time. The static uniaxial tests were performed at $\dot{\varepsilon} = 0.741$/sec, while the dynamic uniaxial tests were tested over a strain rate range of $\dot{\varepsilon} = 0.033$/sec to $\dot{\varepsilon} = 0.256$/sec for the A samples, and $\dot{\varepsilon} = 0.317$/sec to $\dot{\varepsilon} = 0.823$/sec for the B samples.

The PDMS specimens did not reach the breaking point due to elastomer elongation capability ~ 600%, and the limited displacement range of the MTS tester. When the samples were returned to their original gauge length, minimal deformation was observed, which may have been due to sample to grip slippage and/or plastic deformation in the samples. There is an element of strain rate dependence in the results obtained, which is typically encountered in elastomer polymer testing due to their viscoelastic nature and amorphous molecular structure. This is less significant in LLDPE due to testing the specimens solely in static uniaxial tension. However, the breaking point was reached for the LLDPE samples, given the more crystalline LLDPE material molecular structure.

2.1.5.1 Equipment description

Tensile testing was performed with an MTS Tytron servo pneumatic tensile testing machine. The MTS Tytron is a specialized tensile testing machine which incorporates a horizontal air bearing uniaxial test frame, a linearly variable displacement transducer (LVDT) actuator, an array of force transducers, computer software control, and data acquisition capability. The MTS Tytron was configured to have a working

LVDT displacement of ~ 70 ±0.1mm with a set of compression clamps, one on the LVDT and the other on the force transducer, to hold tensile samples at either end, Figs. 2.1,2.5. Testing may be done using the machine in manual control mode or computer controlled. Test recipes may be programmed to execute testing and data acquisition. The MTS Tytron is primarily used with very small test samples for sensitive or non-destructive tests. The entire system operates on an isolated air cushion table. The MTS Tytron is a sophisticated and accurate tensile testing machine, which made the work of this investigation possible.

2.1.5.2 Static uniaxial tension test procedure

The static uniaxial tensile test resembled the standard industry tensile test (ASTM D 412-98a) used for determining the stress-strain behavior of elastomers in tension [86]. However, due to the lack of a suitable extensometer, displacement measurements were taken from the LVDT grip actuator movement. With the force transducer zeroed, fabricated standard tensile specimens, *B* type, Fig. 2.2, were loaded into the grips of the MTS Tytron tester, and slack was removed. At a measured gauge length of 18.1 mm with a force of 0 N, the specimens were uniaxially displaced 50 mm in 1s, yielding a strain rate of, $\dot{\varepsilon} = 0.741/\text{sec}$, Fig. 2.5. Time, displacement, and force were recorded. Difficulties encountered in testing elastomers in this manner were; grip slippage, specimen tearing at grips, large deformation of specimen at grip section, and premature failure due to sample imperfections. These are common occurrences in elastomer tensile testing [87]. Successful test results were obtained through technique and patience. In total, 10 satisfactory static uniaxial tensile tests of each material were performed to determine the static uniaxial elastic modulus of PDMS and LLDPE.

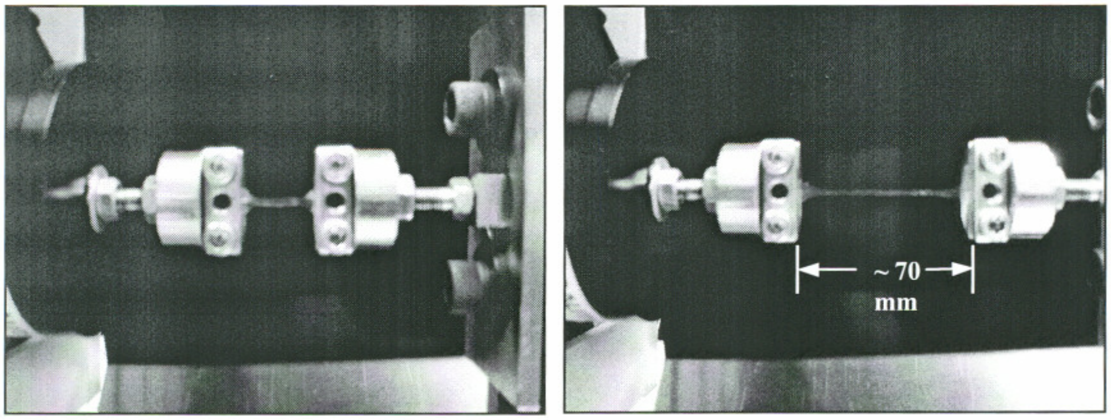

B sample loaded in tester B sample elongated ~ 50 mm

Fig. 2.5. - Displaced uniaxial PDMS tensile specimen

2.1.5.3 Dynamic uniaxial tension test procedure

Dynamic tensile testing consisted of the initial specimen loading technique, a very small pre-straining, $\varepsilon = 0.17$, of the specimen to eliminate slack, with corresponding oscillation about that pre-strain at a set displacement and frequency. Testing in this manner yields data that enables the determination of the tan δ as a function of frequency for the material. This is important data in the selection of dynamic design applications, which may have a cumulative effect upon a given design. PDMS was the only material tested in this manner. Dynamic testing was performed on two sizes of PDMS specimens, *A* and *B* Fig. 2.2, to observe the effects of film thickness upon the mechanical properties. Fifty samples were tested in total at frequencies ranging of 0.5Hz, 1.0Hz, 2.0Hz, 3.0Hz, 4.0Hz, and 5.0Hz. The *A* samples had a dynamic stress range from 1.4e5 to 2.1e5 Pa and a strain range of 0.155 to 0.185, while the *B* samples dynamic stress range of 0.3e6 to 1.6e6 Pa and a strain range of 0.230 to 0.470. Five samples were tested at each frequency.

2.1.1.4 Poisson's ratio (VDA) test procedure

Poisson's ratio was determined using video dimensional analysis (VDA), using three rectangular type *C* samples, Fig. 2.2. Each sample was loaded in the MTS Tytron grips and subjected to axial tension in 2mm increments from 0 to 48 mm. VDA was used to determine the axial and lateral change in the sample by measuring the sample at each increment. The VDA system was calibrated with a standard metric scale. Force and displacement (axial and lateral) were recorded.

2.1.1.5 PDMS stress relaxation and deformation test procedure

Stress relaxation of PDMS was done using *B* samples loaded into the MTS tester and strained, while recording time and load. Two groups of three samples strained to 0.3 and 0.6 in 1s, yielding strain rates of $\dot{\varepsilon}$ = 0.3/sec and $\dot{\varepsilon}$ = 0.6/sec, respectively, and then held at that strain for 60s. This data enables the determination of a relaxation time for the two strain levels, accounting for the viscous portion of the viscoelastic material characteristics, 0.3 true strain being in the linear region of the PDMS stress-strain curve, and 0.6 true strain in the non-linear region, from Fig. 3.1. The relaxation time for PDMS at a given strain level allows the determination of the amount of time that is required to reach static equilibrium for a given loading scenario. This was important to know to validate membrane deflection measurements.

Deformation of the samples tested at a true strain of 0.6 was quantified by measuring the overall length of the samples with calipers immediately after they were removed from the test grips, and consecutively over a period of one week. This was done to observe the total plastic deformation of the samples and their ability to recover from the test. Twelve *B* samples were tested in total.

2.1.6 Membrane testing

Membrane testing, or bulge testing, was performed to determine the load–deflection mechanical response of PDMS and LLDPE circular and square film membranes. Membrane testing of this type is typically achieved using an apparatus similar to what is shown in the schematic of Fig. 2.6. A flat membrane is pressurized with air from the back side with a syringe. The syringe enables the control of the applied pressure, which is monitored by the pressure sensor. Once a membrane is pressurized it deflects, enabling measurement of the deflection at the center of the membrane.

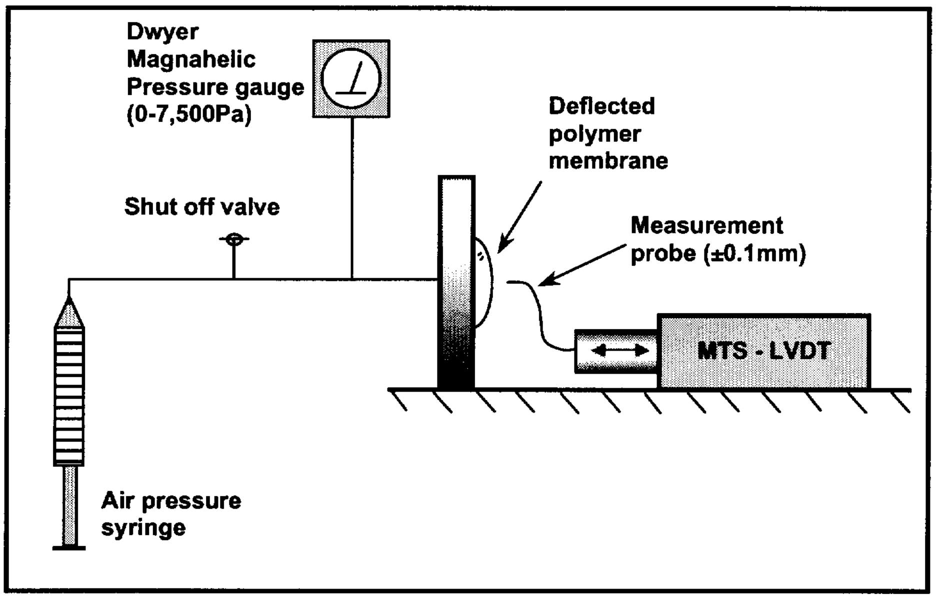

Membrane bulge test schematic

Fig. 2.6. – Membrane bulge test schematic

Membrane testing was done using the MTS Tytron tester in conjunction with a special test apparatus constructed for load-deflection testing of films; the membrane block Fig. 2.8. The membrane block creates clamped edge circular and square membranes of the same radius, $r = 9.525$mm, from film sheets. The test consists of pressurizing the backside of a membrane and measuring the resulting membrane center deflection. Bulge test data not only provides characteristic membrane load-deflection mechanical response, but through analysis, membrane residual stress (σ_0), material biaxial modulus (M) and the elastic modulus (E) may be determined.

2.1.1.1 Equipment description

For membrane testing a special test apparatus (the membrane block) was constructed and mounted to the MTS Tytron tester. The membrane block in conjunction with the LVDT of the tester produces the loading and deflection measurement of the membrane, Fig. 2.7. By mounting a film layer between the two sections of the membrane block, clamped edge circular and square film membranes from simple films are produced, Fig. 2.8. An air pressurization system of a syringe, pressure gauge (0 – 30 in.w.g. = 7,472.6 Pa), tubes, and valves enables pressurization of the membranes, individually or simultaneously, Fig. 2.9. The MTS tester had a special vibrating tip attached to the LDVT which facilitates membrane deflection measurement, Fig. 2.7.

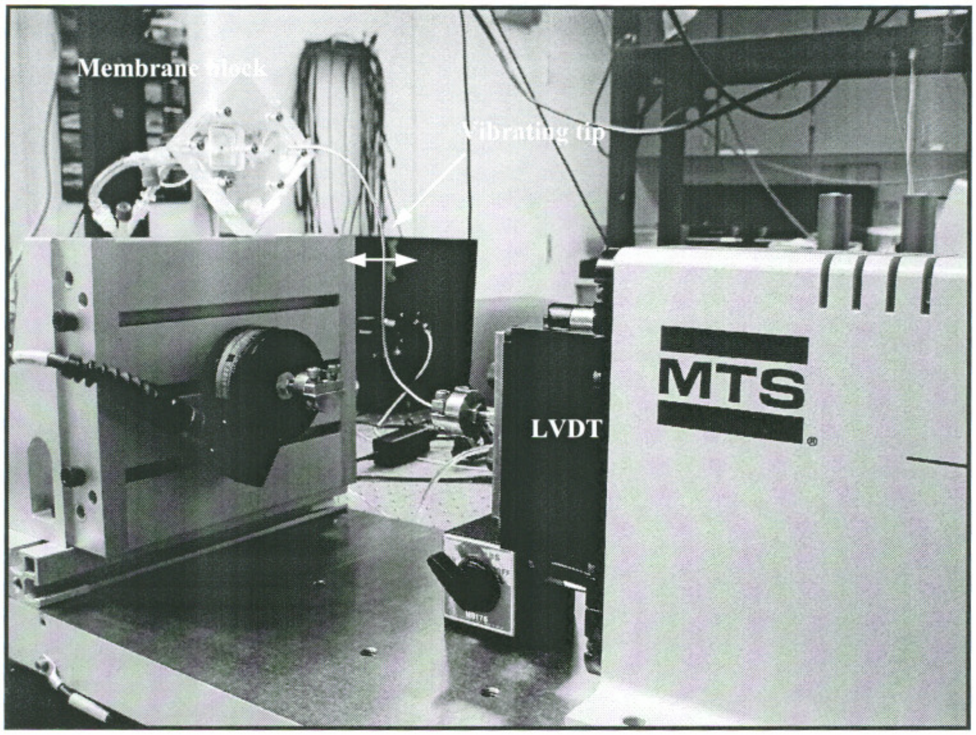

Fig. 2.7. - Membrane testing apparatus

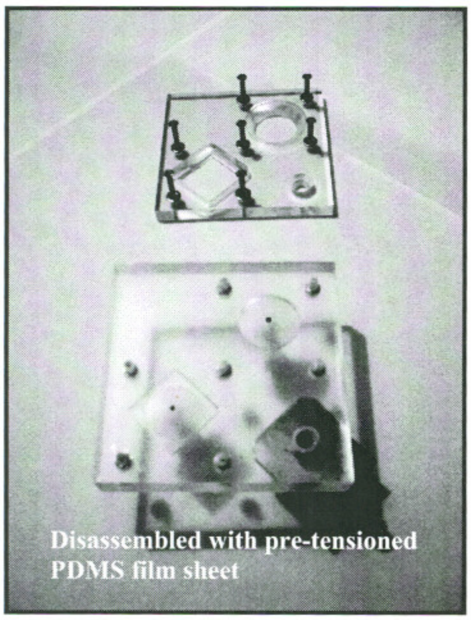

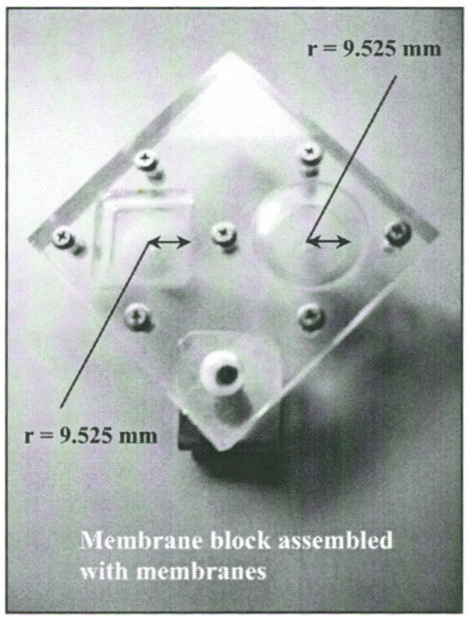

Fig. 2.8. - Membrane block

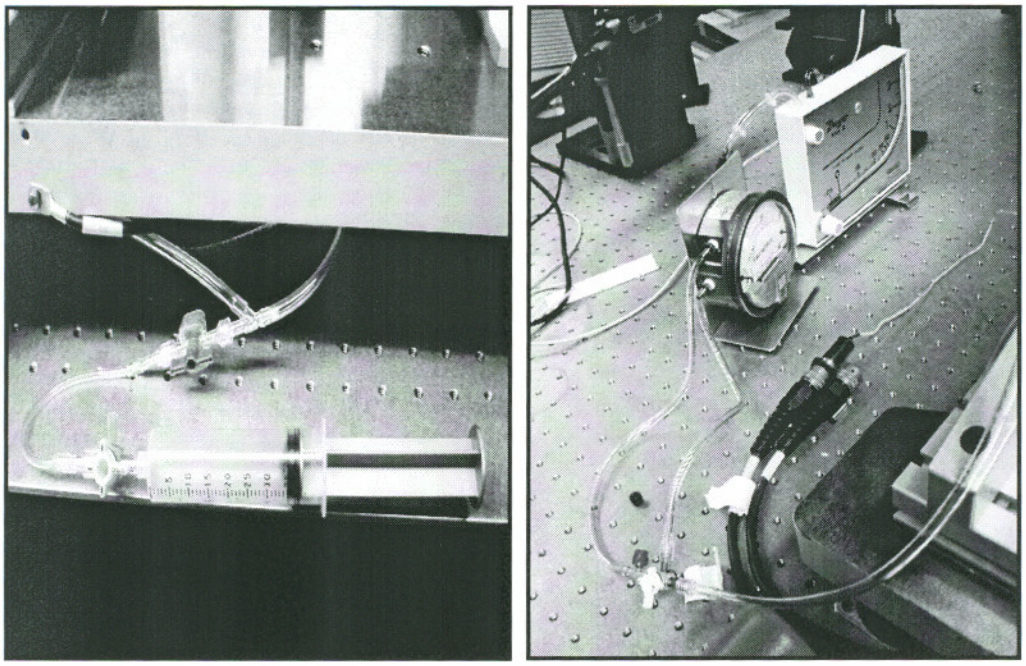

Pressurization syringe, metering valves **Pressurization meters, valves, and tubing**

Fig. 2.9. - Membrane block pressurization system

2.1.1.2 Membrane test procedure

Membrane testing was performed by first assembling the membrane block with a PDMS or LLDPE film, Fig. 2.8. The membrane block assembly was then mounted to the MTS tester as shown in Fig. 2.7. Next the pneumatics were connected to the membrane block and the membranes pressurized. Deflection was measured with the vibrating tip attached to the LVDT. The tip was gently set into motion and slowly advanced toward the center of the membrane with the LVDT. Tip vibration stopped as the tip advanced and contacted the center of the deflected membrane. An averaged value of three deflection readings was recorded for each data point, afterwards the membrane pressure was released to zero. This was repeated for the entire pressure range of the membranes, from 0 ~ 7,500 Pa. This measurement technique was found to be convenient and successful given the relative scale of the experiment and components. The PDMS membranes were tested at 250 Pa per datum, while the LLDPE membranes were tested at 500 Pa per datum. This was due to the lower deflections of LLDPE as compared to PDMS. Fig. 2.10 and 2.11 show circular and square PDMS membrane deflection.

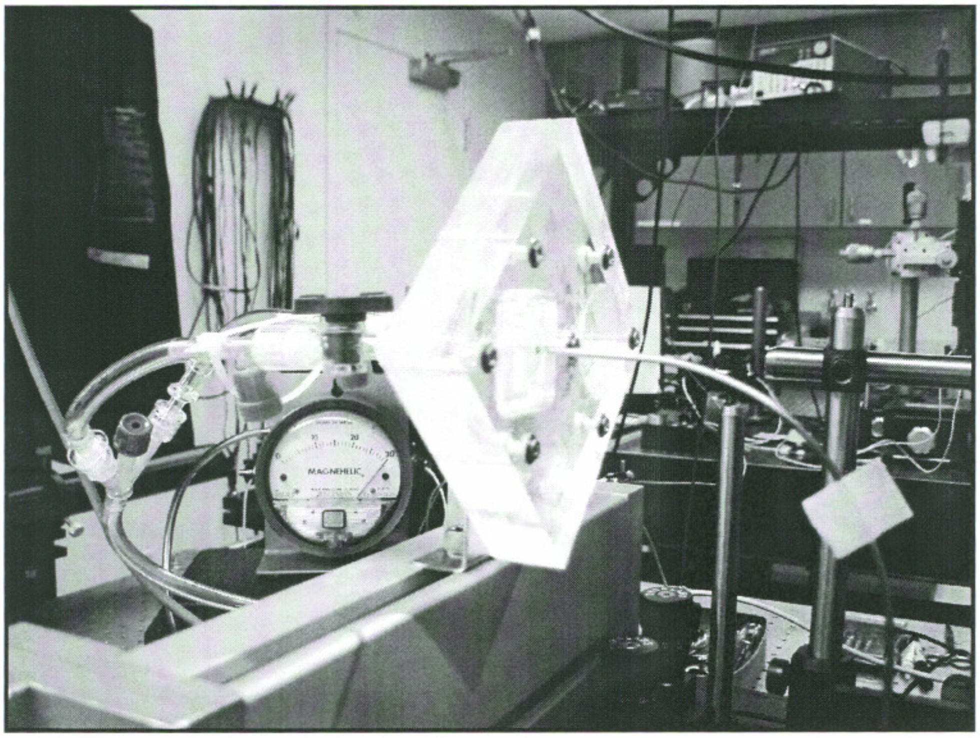

Fig. 2.10. - Membrane block and deflected membrane

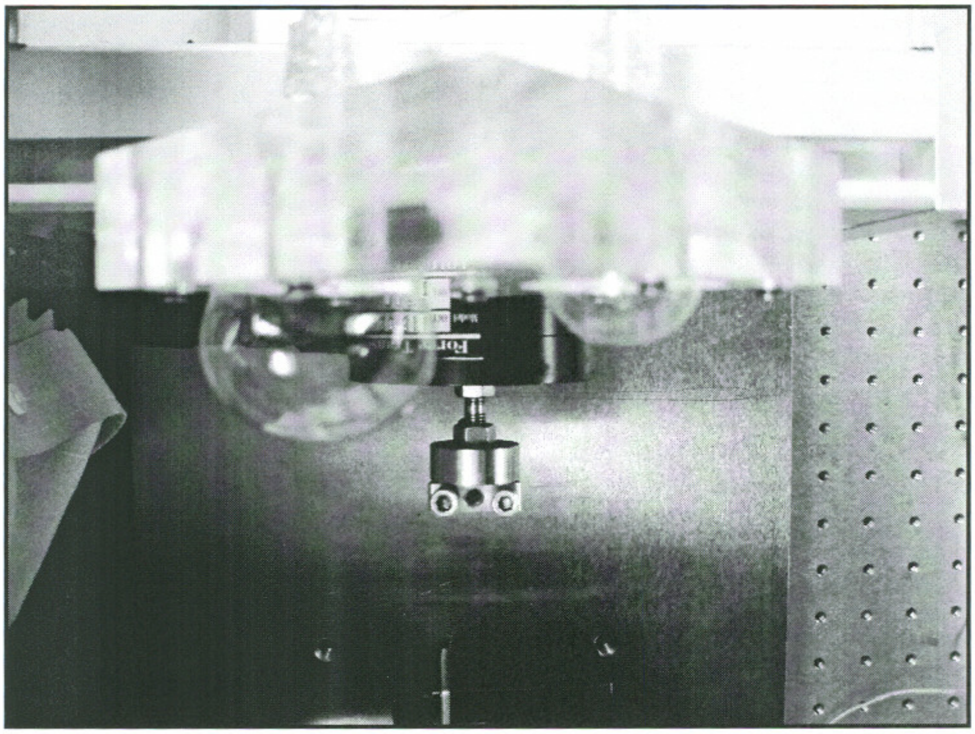

Fig. 2.11. - Square and circular deflected membranes at equal pressure, respectively.

2.2 Analytical methods and Modeling

Analytical methods were used to analyze the tensile specimen and membrane experimental data. Methods were chosen based on the literature search, and further developed into analytical models to approximate the experimental tensile specimen stress-strain and membrane bulge test physical systems.

2.2.1 Description of analytical software and techniques

Tensile specimen and membrane mechanical response data from all experiments were analyzed with analytical methods and models built in Matlab. Matlab is a high-performance programming language for technical computing. Matlab utilizes data and computation arrays which enable the building of sophisticated analysis models in familiar mathematical notation [88]. Experimental data may be imported to analysis programs from text data files, entered by user input, or incorporated as a part of a program. Tensile specimen data were imported from specimen test files created during experimentation, while membrane data were made a part of the analysis programs. Matlab programs provide a comprehensive view of experimental data range analysis through the plotting of analysis results. Plots with curve fitting capabilities and equations aid in further defining the results.

2.2.2 Tensile specimen analytical methods

Tensile specimen data was analyzed with the following stress-strain method for PDMS and LLDPE.

Stress calculation, as defined by Euler [74,103]. Assumes constant volume and strains $\varepsilon_{yy}/\varepsilon_{xx}=\varepsilon_{zz}/\varepsilon_{xx}$.

$$\sigma_E = \left(\frac{F}{A}\right)\lambda \tag{2.1}$$

where lambda is the stretch ratio [103].

$$\lambda = \left(\frac{L_o + \Delta L}{L_o}\right) \tag{2.2}$$

True strain calculation, as defined by Cauchy.

$$\varepsilon_c = \frac{L - L_o}{L} = \frac{\Delta L}{L_o + \Delta L} \tag{2.3}$$

For materials which exhibit large elastic strains, such as PDMS, true stress, (σ_E), and true strain, (ε_C), in the sense of Euler and Cauchy respectively, are typically used to develop a more accurate stress-strain behavior model [73,74,89,102,103]. Assuming constant volume in the true stress relation and using the true strain definition gives an accurate representation of the stress-strain relationship to loading for the large deformations of elastomers. This method was used to determine static uniaxial tension and dynamic elastic modulus values, and tan δ values. Tables 2.1 and 2.2 below summarize the results from the static and dynamic uniaxial tension tests.

Table 2.1 - PDMS and LLDPE elastic modulus – static uniaxial test results

Test	σ_{max}	ε_{max}	Linear elastic modulus
Static uniaxial PDMS	1.26 ±0.16 Mpa	0.342 ±0.026	2.18 ±0.184 MPa
Static uniaxial LLDPE	3.33 ±0.22 MPa	0.020 ±0.000	166 ±6.270 MPa

Table 2.2: PDMS dynamic elastic modulus – dynamic uniaxial test results

Test	σ_{max}	ε_{max}	Dynamic linear elastic modulus	Average dynamic modulus
Dynamic *A*	0.27± 0.05 MPa	0.18 ±0.015	1.49 ±0.143 Mpa	1.45 ±0.250 MPa
Dynamic *B*	0.42± 0.10 MPa	0.30 ±0.002	1.39 ±0.381 Mpa	

2.1.3 Poisson's ratio analytical method

Poisson's ratio is defined as lateral strain over longitudinal strain for a material subjected to an axial load with resulting elongation [73,89]. The method used to calculate Poisson's ratio utilized true strain definitions from equation (2.3) to best approximate the elastomer behavior of PDMS as shown below. Poisson's ratio of LLDPE was obtained from the literature search, and has a value of, $v = 0.4$.

Poisson's ratio for elastomers:

$$v = \frac{\varepsilon_{lateral}}{\varepsilon_{longitudinal}} = \frac{\left(\frac{\Delta L}{L_o + \Delta L}\right)}{\left(\frac{\Delta L}{L_o + \Delta L}\right)} \qquad (2.4)$$

The average Poisson's ratio of PDMS was 0.47 ±0.028, for the entire range of axial true strain.

2.1.4 Stress relaxation analytical method

Stress relaxation was quantified for PDMS uniaxial tensile specimens with The following analytical method:

Stress relaxation time:

$$\tau = \frac{t}{\log\left(\frac{\sigma_0}{\sigma}\right)} \qquad (2.5)$$

Where t is the specimen loading time (sec) to initial stress σ_0, and σ is the selected stress test level [77]. Tests where σ_0 and σ are the same value is characteristic of materials with long relaxation times; linear elastic materials and the elastomer linear elastic stress-strain region. Table 2.3 displays the results for the two tests below.

Table 2.3: PDMS stress relaxation results

Test	ε_{max}	Test time (s)	σ_0	σ	Relaxation time (s)
Stress Relaxation A	0.30	60 s	1.0 MPa	1.0 MPa	0.0s
Stress Relaxation B	0.60	60 s	5.1 Mpa	3.8 MPa	7.82 s

2.1.5 Tan δ analytical method

The tan δ or loss factor for dynamic tensile specimens was analyzed by the following method [77].

The loss factor given by the equation below [101]:

$$\tan\delta = \frac{1}{\omega t} = \frac{E'}{E^*} \tag{2.6}$$

Where E' is the real modulus, or storage modulus, in-phase with the stress and defined as:

$$E' = \frac{\omega^2\tau^2 E^*}{(1+\omega^2\tau^2)} \tag{2.7}$$

and E'' is the imaginary modulus, or the out-of-phase strain component, defined as:

$$E'' = \frac{\omega\tau E^*}{(1+\omega^2\tau^2)} \tag{2.8}$$

E^* is the complex or dynamic modulus.

Due to the amorphous structure, molecules of elastomer polymers readily slide past each other, resulting in energy loss when these materials are dynamically loaded. This effect creates a mechanical hysteresis loop. The measure of the energy lost is defined as the tan δ or loss factor [90]. The amount of energy lost may also be a function of the amount of strain for these materials, given their strain crystallization behavior [80,90]. The tan δ as a function of frequency for PDMS was (tan δ = 0.03 ±0.015) for the frequency range of 0.5 to 5 Hz.

2.1.6 Membrane analytical methods and models

Circular and square membrane data was analyzed with the following analytical methods and models. Biaxial stress and strain definitions from the equations of large deflection circular membrane theory discussed in section 1.2.1.2 were used to analyze membrane experimental data. The Almansi true strain definition as applied to membrane deflection theory in conjunction with spherical cap stress were used due to their accurate approximation of the experimental systems, and are defined below:

Circular membrane biaxial stress:

$$\sigma_{xx} = \sigma_{yy} = \frac{PR}{2t} \tag{1.3}$$

Circular membrane Almansi biaxial true strain:

$$\varepsilon_{xx} = \varepsilon_{yy} = \frac{\left[\left(R\sin^{-1}\frac{a}{R}\right)^2 - a^2\right]}{2\left(R\sin^{-1}\frac{a}{R}\right)^2} \tag{1.30}$$

Applying the new Almansi biaxial true strain definition and biaxial stress, allows the determination of the membrane biaxial modulus (*M*) and residual stress (σ_0). The residual stress is due to membrane pre tensioning to eliminate sag during testing, and appears as an offset in the biaxial stress-strain plots, where the slope of the plot is the biaxial modulus [91]. The membrane elastic modulus may then be calculated from the following equation [92]:

Membrane biaxial modulus: $M = \dfrac{E}{(1-\nu)}$ (1.31)

rearranging for *E* we get: $E = (1-\nu)M$ (2.9)

Where *E* is the membrane elastic modulus.

Once the membrane elastic modulus and residual stress are determined, they may be used in the circular and square analytical models. The models used to simulate the experimental data of PDMS and LLDPE were as follows.
New circular membrane analytical model:

The new spherical cap model

$$P = \frac{\left[\dfrac{E}{1-\nu}\left(\dfrac{\left(R\sin^{-1}\dfrac{a}{R}\right)^2 - a^2}{2\left(R\sin^{-1}\dfrac{a}{R}\right)^2}\right) + \sigma_0\right]2t}{R} \tag{1.34}$$

where,

$$R = \frac{h}{2} + \frac{a^2}{2h} \tag{1.35}$$

Maier-Schneider *et al* square membrane analytical model:

$$P = c_1 \frac{t\sigma}{a^2}(h) + c_2(v)\frac{tE}{a^4}(h^3) \tag{1.36}$$

where $c_1 = 3.45$ and

$$c_2(v) = \frac{1.994[1 - 0.247(v)]}{(1 - v)} \tag{1.37}$$

The development of *The new spherical cap model* for circular membranes, as shown in equation (1.34) and discussed in section 1.2.1.2, represents membrane deflection as a function of membrane radius of curvature, and was used to simulate PDMS and LLDPE circular membrane load-deflection experiments. Equation (1.36) by Maier-Schneider *et al* is the analytical model used for square membrane experiment simulation. Table 2.4 below displays the results from the circular membrane tests.

Table 2.4: Circular membrane biaxial stress-strain and modulus results

Material	σ_{xxMax}	ε_{xxMax}	M	E	σ_0
PDMS	0.427 MPa	0.21	2.03 MPa	1.08 ±0.250 MPa	0.038 Mpa
LLDPE	2.75 MPa	0.020	127 MPa	76.0 ±6.110 MPa	0.427 MPa

Chapter 3
Results

3.1 Tensile tests

3.1.1 Static uniaxial testing of PDMS and LLDPE

Data from the *B* sample static uniaxial tests, analyzed using Euler and Cauchy true stress and true strain for PDMS and LLDPE, yielded an elastic modulus of 2.18 ±0.184 MPa, up to a strain of 0.375 for PDMS, and an elastic modulus of 166 ±6.270 MPa for LLDPE. The behavior of the stress-strain curve shown in Fig. 3.1 for PDMS, is nearly linear for low stress values at or below 1.25 MPa, representing the elastic stress-strain region. This behavior agrees with published results for elastomeric polymers [82,90,93,98,100]. A fifth order approximation of the non-linear performance of PDMS in uniaxial tension is also given in Fig. 3.1, and was chosen as a best fit approximation. The stress–strain curve of LLDPE in Fig. 3.2 depicts typical polyolefin plastic behavior. There is not a straight line for the initial section of the curve, therefore as a standard linear approximation, a secant is drawn from the origin to where the curve intersects 2% strain to obtain an elastic modulus value [81,94]. The elastic tensile modulus also falls within the range of tensile modulus values of 50 – 300 MPa for LLDPE, giving confidence in both PDMS and LLDPE experimental test procedures and results [94,104].

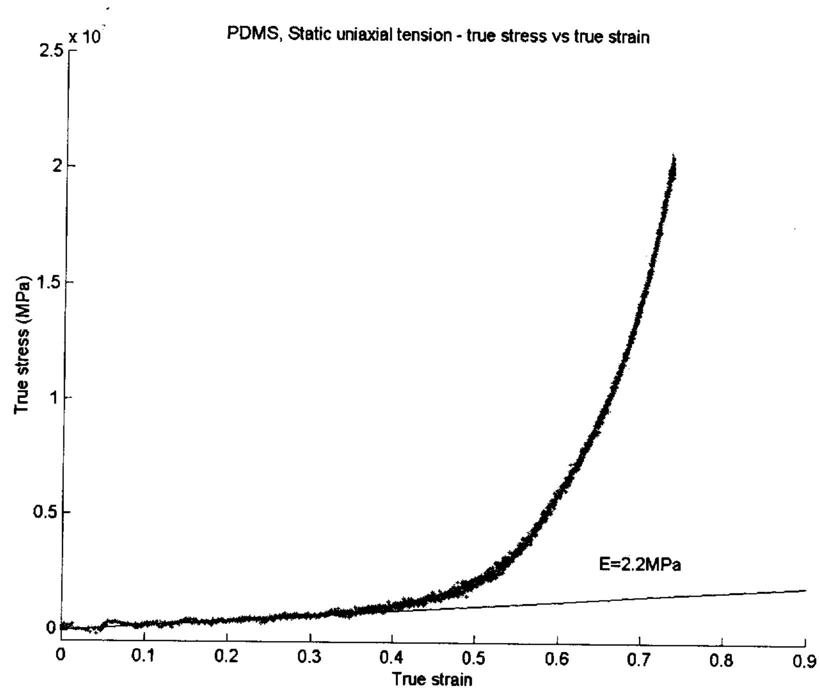

Fig. 3.1. - Stress-strain curve (true strain), and elastic modulus for PDMS tested in static uniaxial tension. Non-linear curve fit: $Y = 5.1e8x^5-5.8e8x^4+2.6e8x^3-5.3e7x^2+5.7e6x+6.7e2$

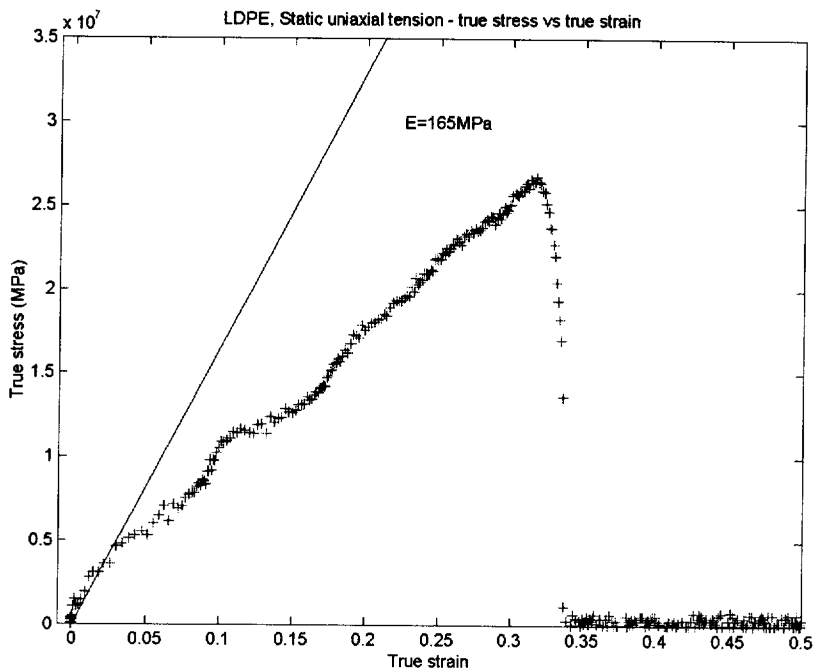

Fig. 3.2 - Stress-strain curve (true strain), and elastic modulus for LLDPE tested in static uniaxial tension.

Table 3.1 below gives a summary of the PDMS and LLDPE elastic modulus values. Non-linear approximations of PDMS stress-strain may be made utilizing the fifth order equation in Fig. 3.1.

Table 3.1.: PDMS and LLDPE elastic modulus – static uniaxial test results

Test	σ_{max}	ε_{max}	**Linear elastic modulus**
Static uniaxial PDMS	1.26 ±0.16 Mpa	0.342 ±0.026	2.18 ±0.184 MPa
Static uniaxial LLDPE	3.33 ±0.22 MPa	0.02 ±0.000	166 ±6.270 MPa

3.1.2 Dynamic uniaxial testing of PDMS

Dynamic testing of samples *A* and *B* was done in two groups respectively, to observe the effects of varying sample size and initial strain on the mechanical properties. A *Students t-test* was performed on the two groups and yielded an α = 0.0763, which determined that the elastic modulus of the two groups were not statistically different. Fig. 3.3 shows a typical plot of stress versus strain for the dynamic tests, where an *A* sample was cycled sinusoidally between true strains of 0.155 and 0.185 at 1.0 Hz. The shape of the plots depicts mechanical hysteresis loops for the *A* samples, with the open center areas in the plots representing the amount of energy lost, per volume of material, during cyclic loading [82]. The size of the hysteresis loop is a visual representation of the magnitude of the loss factor or tan δ. The two plots correspond to true and engineering strain as defined by Cauchy and Green respectively, and display the differences that may be encountered analyzing non-Hookian materials [74].

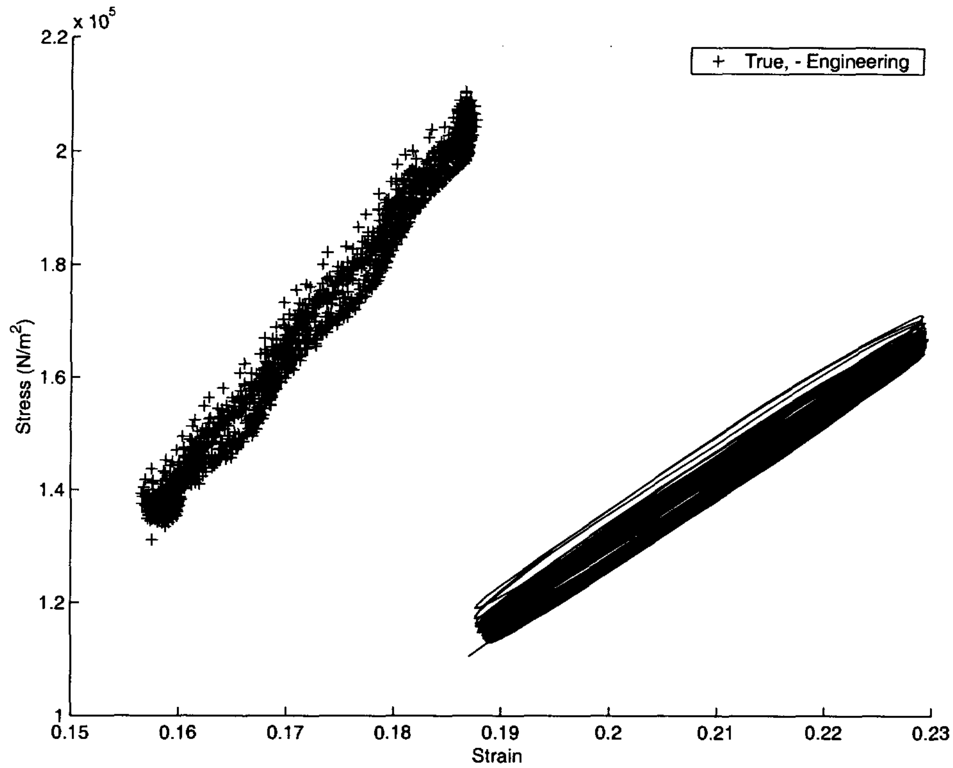

Fig. 3.3 - Dynamic testing stress-strain plot

Dynamic testing of the *A* samples was done at an initial strain of 0.17 oscillating ±1mm of displacement about that point at frequencies from 0.5Hz to 5Hz, yielding strain rates of $\dot{\varepsilon}$ = 0.086/sec to 0.86/sec, and an elastic modulus of 1.49 ±0.143 MPa. Testing of the *B* type samples was performed at an initial strain of 0.37 oscillating ±5mm of displacement about that point at frequencies from 0.5Hz to 5Hz, yielding strain rates of $\dot{\varepsilon}$ = 0.115/sec to 1.16/sec, yielding an elastic modulus of 1.39 ±0.381 MPa for the smaller PDMS dynamic test samples. Fig. 3.4 displays the elastic modulus for both dynamic tests versus frequency. An average elastic modulus of 1.45 MPa ±0.250 MPa was obtained. Over the strain rates tested, the modulus of PDMS appears to be independent of strain rate for the given strain range and test frequencies. Table 3.2 below summarizes the dynamic modulus results between the *A* and *B* samples for PDMS tested in the linear elastic region.

Table 3.2.: PDMS dynamic elastic modulus – dynamic uniaxial test results

Test	σ_{max}	ε_{max}	Dynamic linear elastic modulus	Average dynamic modulus
Dynamic *A*	0.27± 0.11 MPa	0.18 ±0.003	1.49 ±0.143 Mpa	1.45 ±0.250 MPa
Dynamic *B*	0.42± 0.11 MPa	0.30 ±0.0006	1.39 ±0.381 Mpa	

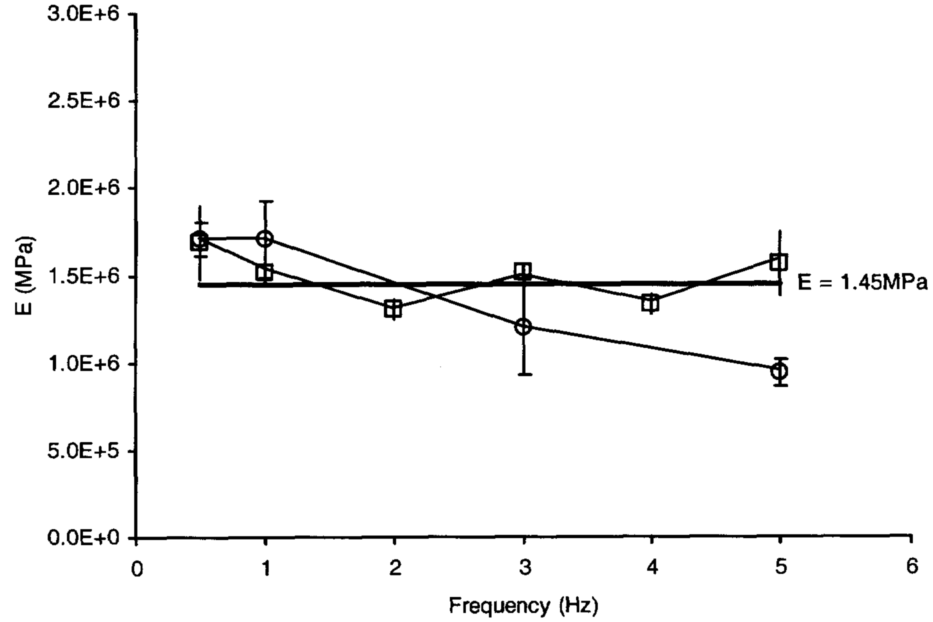

Fig. 3.4. - Elastic modulus versus Frequency for PDMS *A* (□) and *B* (O) samples (E = 1.45 ±0.250 MPa)

Fig. 3.5 displays the tan δ of the PDMS *A* samples versus frequency as (tan δ = 0.03 ±0.015) for the frequency range of 0.5 to 5 Hz. This result agrees with published tan δ results for elastomers at room temperature [96].

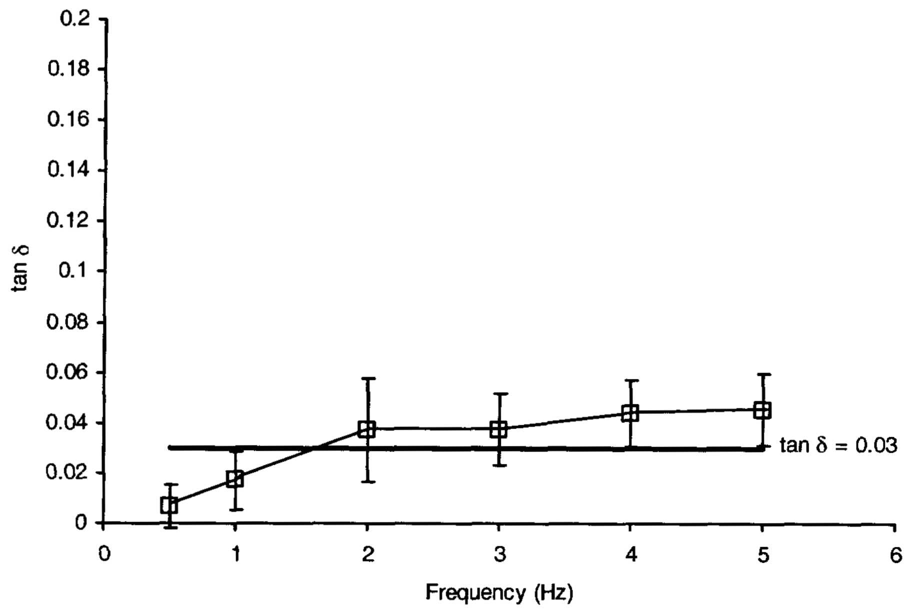

Fig. 3.5. - tan δ versus Frequency for PDMS *A* samples (tan δ = 0.03 ±0.015)

3.1.3 PDMS Poisson's ratio (ν)

Axial and lateral displacement data from Poisson's ratio testing was analyzed using true strain. Fig. 3.6 shows the Poisson's ratio of PDMS to be a constant value of 0.47 ±0.028, for the entire range of axial strain. This value is well above the Poisson's ratio for most metals and agrees with Poisson's ratio values for elastomers [82,96].

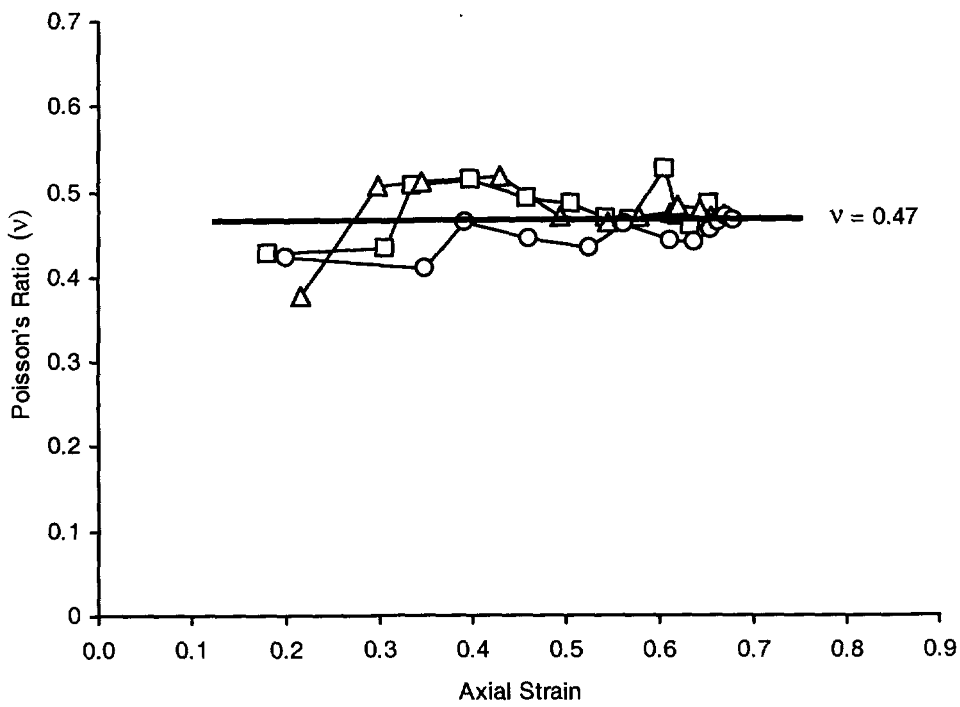

Fig. 3.6. - Plot of PDMS Poisson's ratio versus Axial strain ($\nu = 0.47 \pm 0.028$)

3.1.4 Stress relaxation and deformation of PDMS

Stress relaxation and deformation tests of *B* type tensile specimens of PDMS were performed. This was done to observe the initial stress relaxation in specimens strained to 30%, $\dot{\varepsilon}$ = 0.3/sec and 60%, $\dot{\varepsilon}$ = 0.6/sec true strain, to aid in confirming the validity of the test setup for membrane deflection measurement; stepped static pressurization with deflection measurement. Average stress relaxation times were determined for strain levels of 30% and 60%, inside and outside the linear regions of the stress-strain curve for PDMS, respectively. Full stress relaxation times were not determined due to the sample testing time being limited to 60 seconds. Samples strained to 30% with a testing stress of 1.0 MPa had no detectible difference between the initial stress and the test stress for the 60 second test, Fig. 3.7, see table 3.3 [77,90]. This suggests that there is minimal molecular motion in the samples, resulting in a long relaxation time for PDMS at this strain level. For samples strained to 60% true strain the initial stress was much higher than the testing stress, thus yielding an relaxation time of 7.82 seconds with no noticeable change thereafter, Fig. 3.8, which suggests a long relaxation time for PDMS at 60% strain as well. The apparent long relaxation time for PDMS at the tested stress and strain levels suggest that the static pressurization and deflection method used for membrane testing is valid, as the resulting strain for those tests was ~ 20% true strain for the membranes tested. Complete stress relaxation values for PDMS under these test conditions would have required the tests to be carried out over a much longer period of time to achieved accurate stress relaxation values. However, this test provides sufficient information to validate the membrane deflection measurement method. Figure 3.9 displays a decaying exponential fit for the stress relaxation curve at a true strain of 0.6, which enables the extrapolation of longer relaxation times if desired. Table 3.3 summarizes the stress relaxation results.

Stress deformation was investigated for the samples tested at a true strain of 0.6 only, due to the large strain level and difference in the testing and relaxing stresses. This was done to determine the relative amount of permanent plastic deformation in the samples from the test and the ability of the samples to recover over time. The average total plastic deformation of the 24mm *B* samples tested was 0.135mm ±0.022mm, which is approximately 0.5% total elongation. Figure 3.10 displays the plasic deformation in relation to the sample initial length of 24mm. A decaying exponential fit is also shown in Fig. 3.10, which enables the determination of selected time or deformation values. The large standard deviations in Fig. 3.10 are due to the inaccuracy of measuring sample total length with manual calipers. Some error may have also been introduced to sample total length by the gripping technique compressing the ends of the samples during testing.

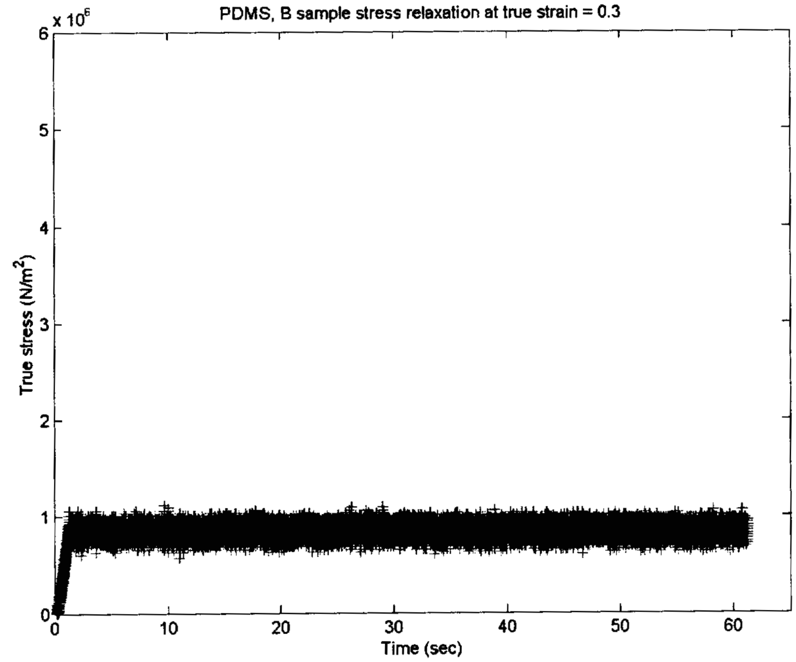

Fig. 3.7. - Plot of PDMS stress relaxation at true strain = 30%

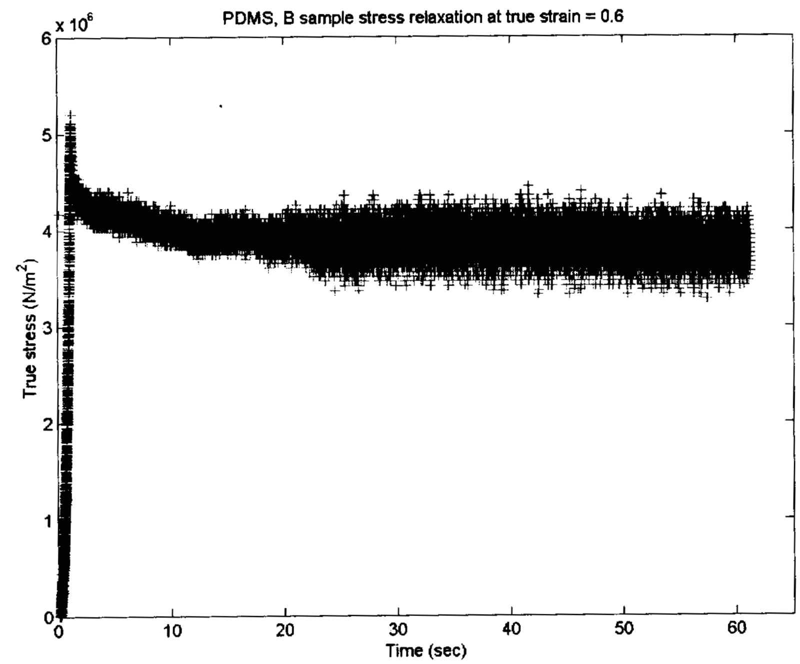

Fig. 3.8. - Plot of PDMS stress relaxation at true strain = 60%

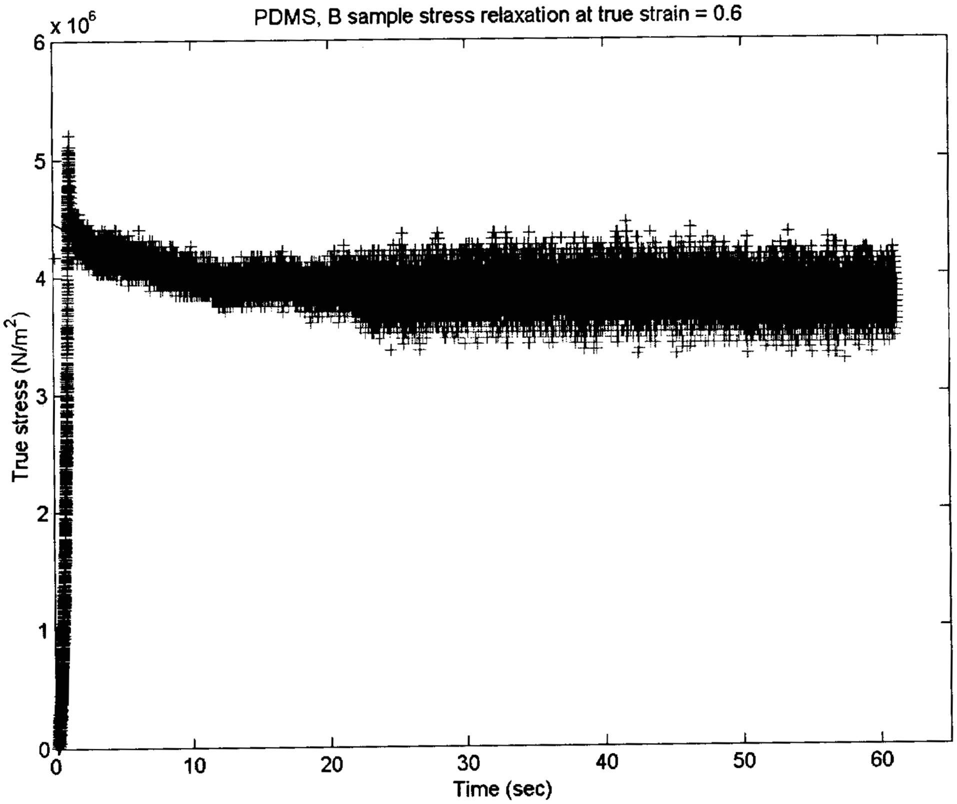

Fig. 3.9 - Plot of PDMS stress relaxation at true strain = 60%

Decaying exponential curve fit: $\sigma = \sigma_0 \exp(-t/\tau)$, where τ = 7.82 seconds

Table 3.3.: PDMS stress relaxation results

Test	ε_{max}	**Test time (s)**	σ_0	σ	**Relaxation time τ (s)**
Stress Relaxation A	0.30	60 s	1.0 Mpa	1.0 Mpa	0.0s
Stress Relaxation B	0.60	60 s	5.1 Mpa	3.8 Mpa	7.82 s

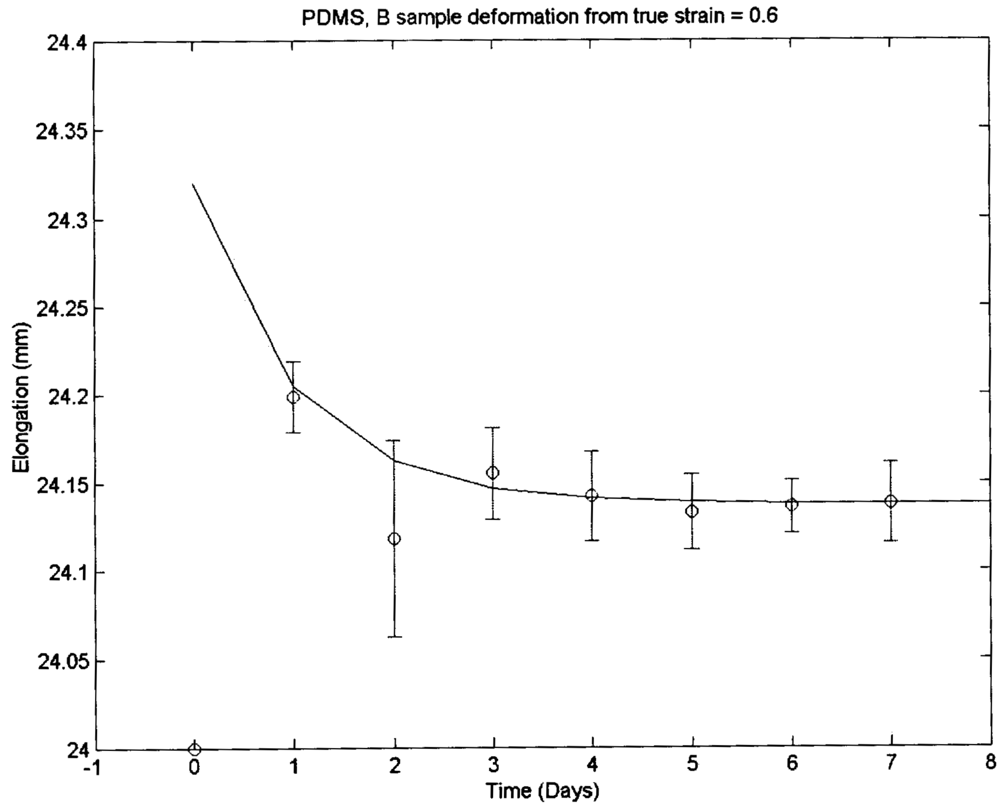

Fig. 3.10. - Plot of PDMS stress deformation at true strain = 60%

Decaying exponential curve fit: $Y = Y_0 \exp(-t/\tau)$, where $\tau = 7.1E4$ seconds

3.2 Membrane tests

Data from the circular and square membrane bulge test experiments for PDMS and LLDPE depict the characteristic curves of load–deflection mechanical response for these membranes. Fig. 3.11 and 3.12 display the experimental results for the circular and square membranes tested in the membrane block for the PDMS and LLDPE films. Three sets of membranes, circular and square, were tested for each material.

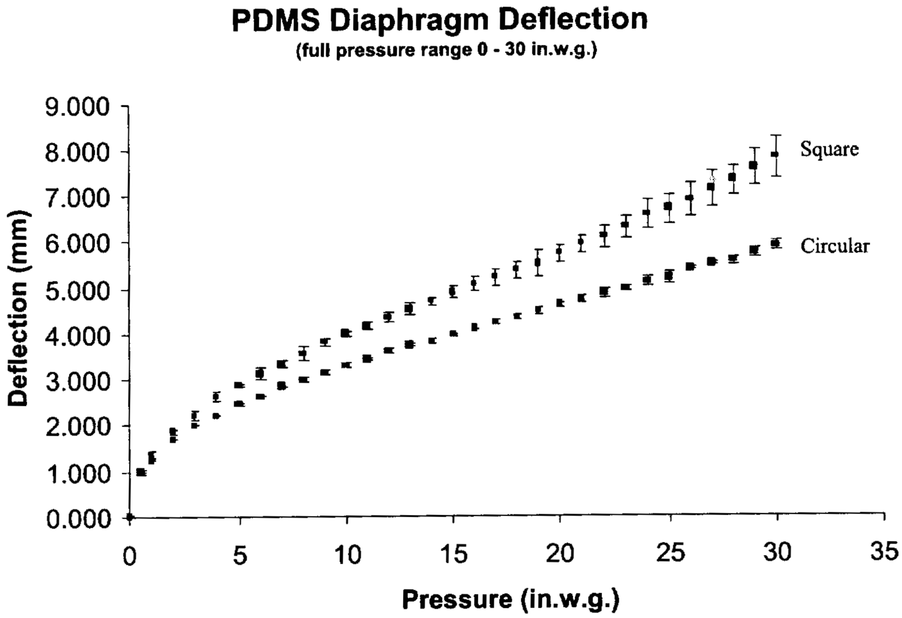

Fig. 3.11. - Plot of PMDS membrane load-deflection

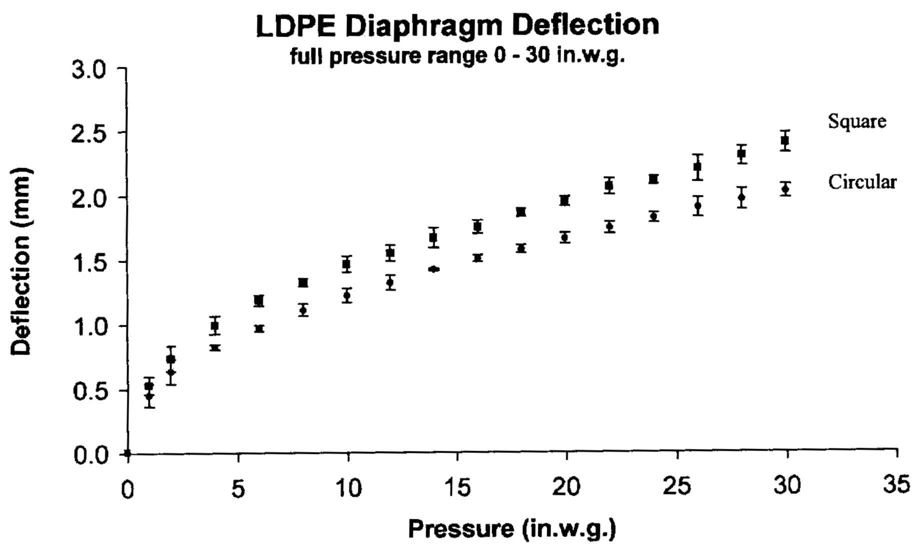

Fig. 3.12. - Plot of LLDPE membrane load-deflection

Fig. 3.11 and 3.12, display typical circular and square membrane load-deflection mechanical response of the membranes tested. The error bars indicate the standard deviation at each point. The square membranes have larger deflection uniformly throughout the loading range compared to the circular membranes, at the same pressure, due to dominating membrane tensile mechanics coupled with the greater area of the square membranes.

3.2.1 Membrane biaxial stress-strain

Circular membrane experimental data analyzed with large deflection membrane theory was used to develop biaxial stress-strain plots. Pressure and deflection values were converted to stress and strain by using the Almansi true strain definition and equations (1.3) and (1.30) respectively, as discussed in section 2.1.6. Fig. 3.13 and 3.14 are biaxial stress-strain plots for representative PDMS and LLDPE circular membrane samples. From these plots it is possible to determine the amount of residual stress in the membrane, added during loading of the film, and the biaxial modulus at the center deflection point of the membrane [70,91]. A standard linear curve fit with the equation of a line in the form of:

$$y = mx + b$$

yields m as the slope, or the biaxial modulus (M), and b the y-offset as the residual stress (σ_0).

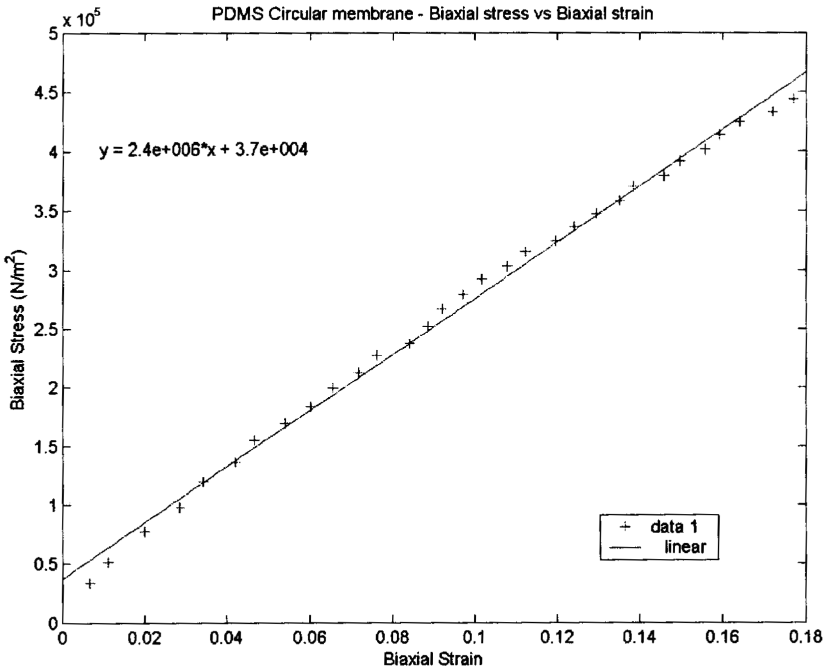

Fig. 3.13. - PDMS Biaxial stress-strain plot

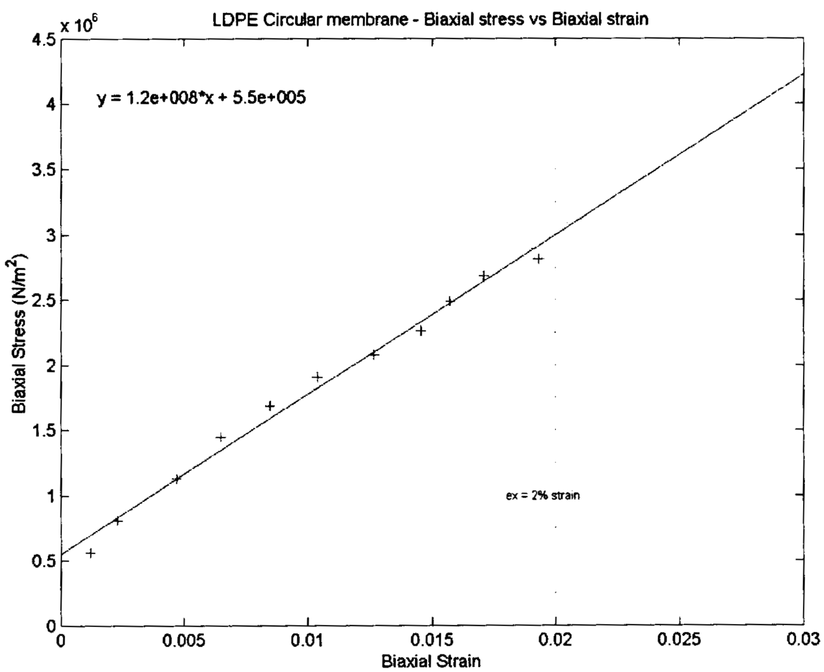

Fig. 3.14. - LLDPE biaxial stress-strain plot

Analyzing the experimental data in this manner allows the determination of the elastic modulus (E) from the biaxial modulus (M) utilizing equation (2.9). The elastic modulus (E) and the residual stress (σ_0) are useful input values for circular and square membrane analytical models. The plot for LLDPE was limited to 2% strain to remove the effects of plastic deformation in the determination of the membrane elastic modulus [94]. Table 3.4 contains biaxial stress-strain average elastic modulus and residual stress values for the PDMS and LLDPE circular membrane samples tested.

Table 3.4.: Circular membrane biaxial stress-strain results

Material	σ_{xxMax}	ε_{xxMax}	M	E	σ_0
PDMS	0.427 MPa	0.21	2.03 MPa	1.08 ±0.250 MPa	0.038 Mpa
LLDPE	2.75 MPa	0.020	127 MPa	76.0 ±6.110 MPa	0.427 Mpa

3.2.2 Membrane analytical Models

Circular and square membrane analytical model results were developed using Matlab, and were designed to simulate the experimental membrane tests. For circular membranes *The new spherical cap model* was used, while the Maier-Schneider *et al* model was used for square membranes. *The new spherical cap model* is designed for materials capable of large elongations, while the Maier-Schneider *et al* model is designed for more traditional linear elastic materials. Elastic modulus and residual stress data from the biaxial stress-strain tests was input to meet model material property and test condition requirements.

3.2.3 Circular membrane analytical models

Fig. 3.15 displays PDMS bulge test experimental results from a sample circular membrane and compares the results to a number of membrane analytical models.

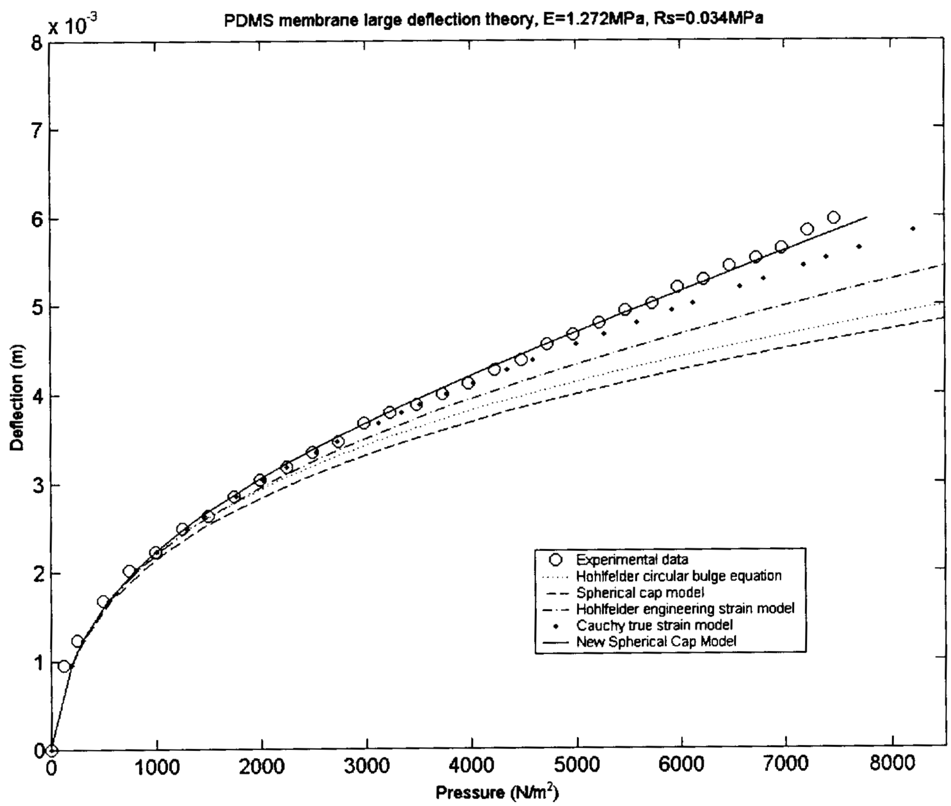

Fig. 3.15. - PDMS bulge test experiment simulated with different models

The new spherical cap model provides the best fit to the PDMS membrane experimental data compared to the other analytical models. The same comparison of experimental results and analytical models was done for an LLDPE membrane as shown in Fig. 3.16, with the same result.

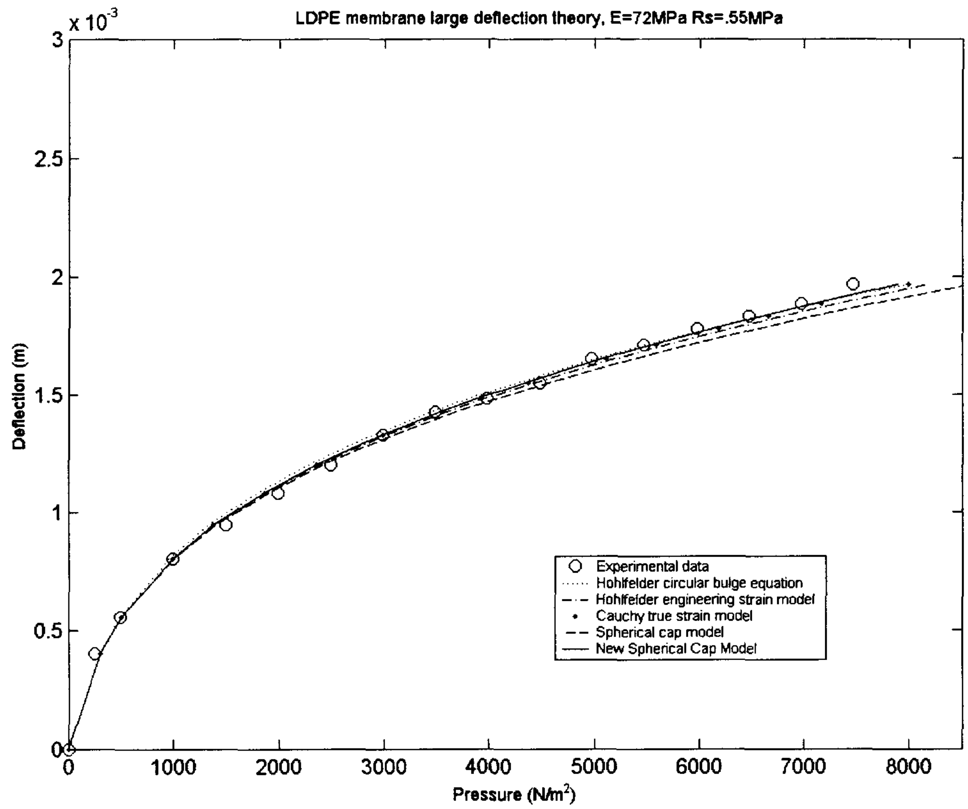

Fig. 3.16. - LLDPE bulge test experiment simulated with different models

While *the new spherical cap model* best represents the PDMS circular membrane of all models compared, with large differences clearly seen between the models, the same comparison for the LLDPE membrane yields less discrepancy between the models. The alignment of the models for the LLDPE membrane experimental results is due to the much reduced amount of strain in the LLDPE membrane, $\varepsilon_{xx} = 0.0275$,compared to, $\varepsilon_{xx} = 0.18$, for the PDMS membrane, see table 3.4. This substantiates the fact that initial membrane theory was developed for linear elastic materials, and that it is inadequate for simulating materials capable of large non-plastic elongations. Fig. 3.16 also shows the ability of *the new spherical cap model* to approximate more crystalline material model performance, thus providing a new circular membrane deflection model for potential use with all material types. Fig. 3.17 and 3.18 display the new circular membrane deflection analytical model fit to experimental data for PDMS and LLDPE circular membranes.

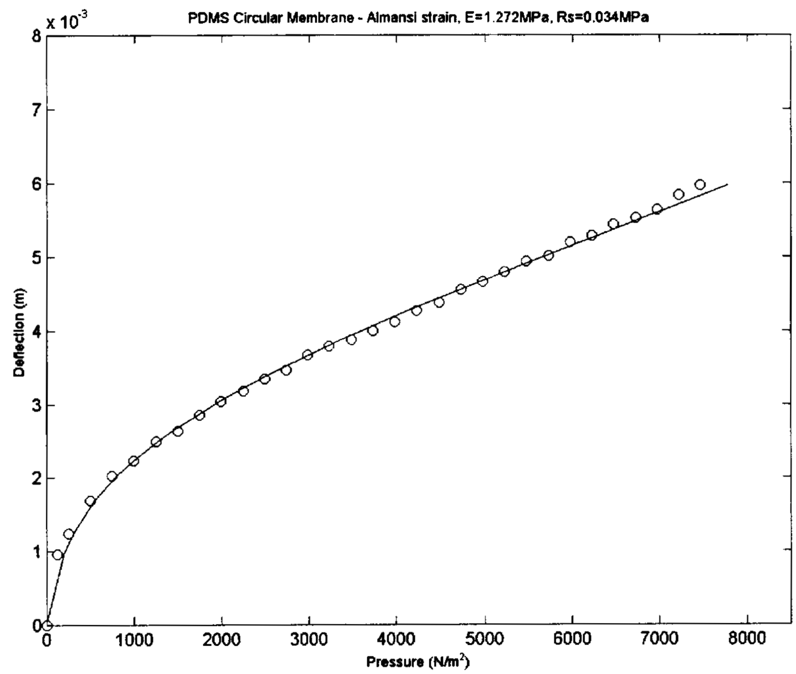

Fig. 3.17. - PDMS analytical model fit to circular membrane bulge test experimental results.

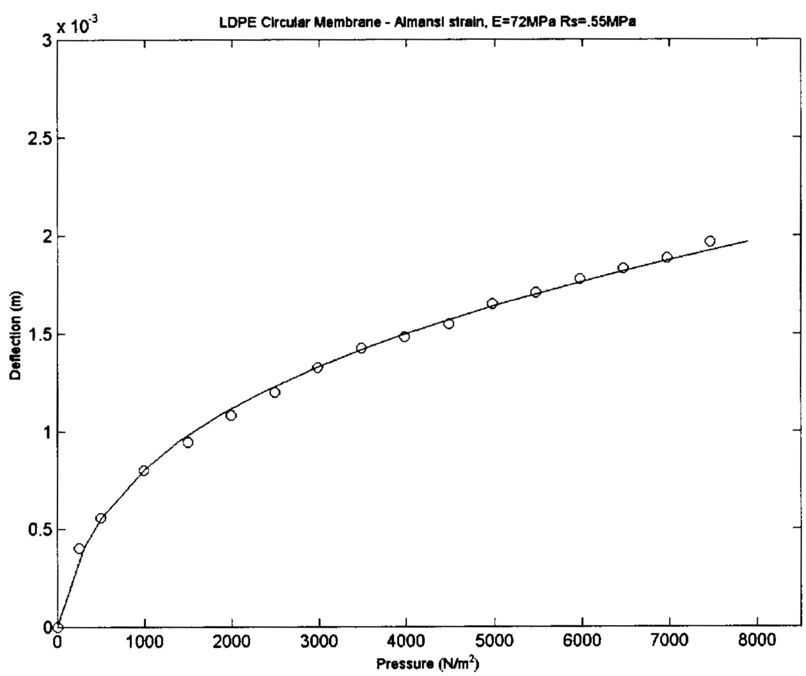

Fig. 3.18. - LLDPE analytical model fit to circular membrane bulge test experimental results.

The analytical results compared to the experimental bulge test data from PDMS and LLDPE circular membranes agree well for the systems investigated. However, the LLDPE circular membranes plastically deformed during the experiment as they were loose upon release of pressure, while the PDMS membranes remained taught, indicating no noticeable deformation.

3.2.4 Square membrane analytical model

The Maier-Schneider *et al* square membrane analytical model was used to produce analytical results for comparison to PDMS and LLDPE square membrane bulge test experimental data. This is the most accurate square membrane theory to date from the literature search conducted herein. Development of a new square membrane theory for elastomeric materials requires further research due to the complexity of the physical system. Elastic modulus (E) and residual stress (σ_0) values generated from the biaxial stress-strain tests were input to the square membrane analytical models for analysis. It was assumed that the residual stress was the same for both circular and square membranes as assembled in the membrane block. Fig. 3.19 and 3.20 display the theoretical results in comparison to the experimental data. The analytical model results for the PDMS square membrane do not agree well with the experimental data. This is most likely due to the theory having been developed for linear elastic materials, as opposed to elastomeric materials such as PDMS, which have the ability to achieve great elongations ~ 600% without plastically deforming. Fig. 3.19 most resembles the performance of the PDMS circular membrane results analyzed with the spherical cap analytical model as displayed in Fig. 3.15. Thus showing a similarity between the square analytical and original spherical cap models, and their inability to accurately simulate the experimental results.

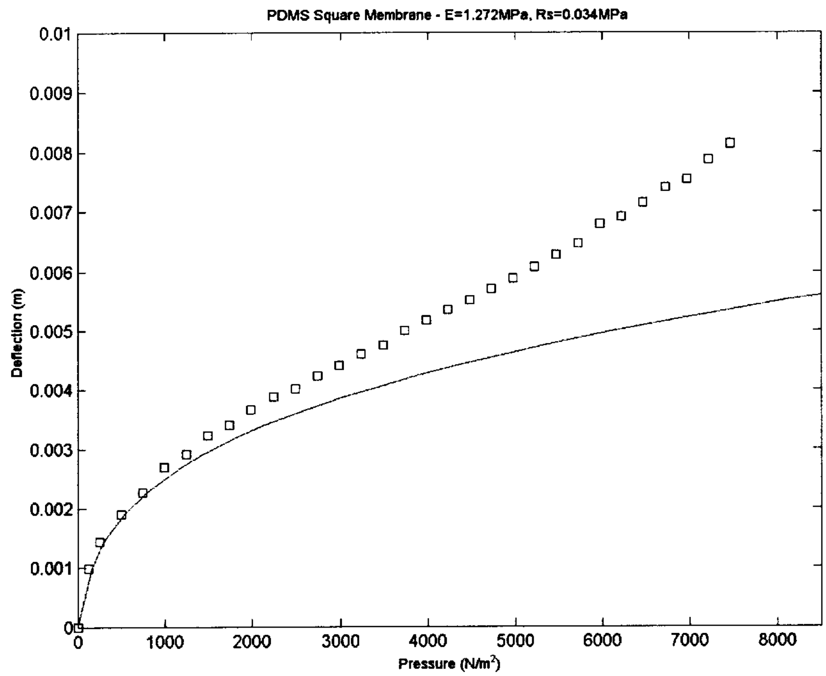

Fig. 3.19. - Square analytical model fit to PDMS square membrane bulge test experimental results.

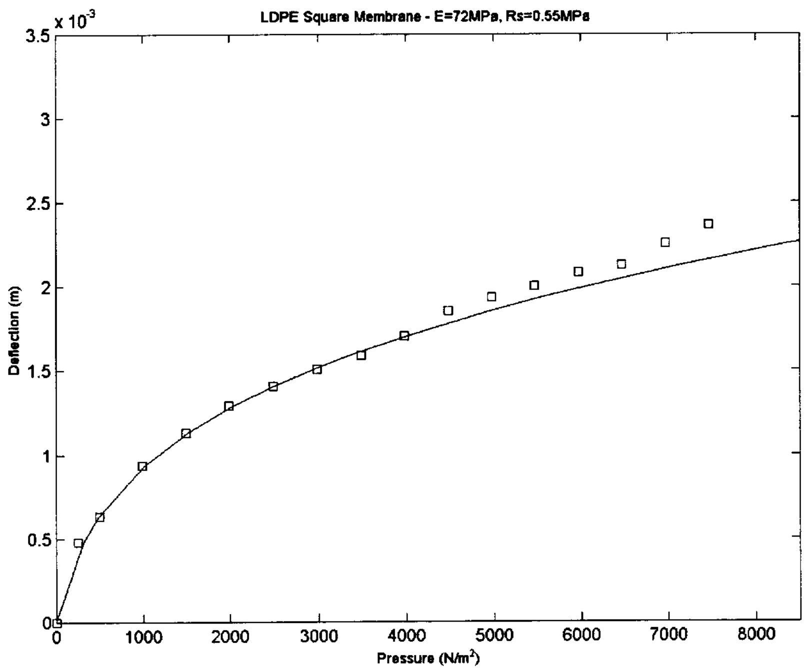

Fig. 3.20. - Square analytical model fit to LLDPE square membrane bulge test experimental results.

The Maier-Schneider *et al* analytical model agrees well with LLDPE membranes; a more linear elastic material with smaller elastic deflections, for the square membrane experimental data of this system, up to a pressure of ~ 6.5 KN/m^2, or a biaxial strain of $\varepsilon_{xx} = 0.0275$.

Chapter 4
Discussion

The main focus of this thesis was the investigation of the tensile mechanical properties of PDMS and large deflection membrane theory, in an effort to provide more accurate tensile mechanical material properties and analytical membrane models for MEMS application design with PDMS. The discussion is comprised of a comparison of data from the tensile and membrane tests, the experimental bulge test data, the analytical model results, and other researcher's published results. The areas of interest for the discussion are the tensile mechanical material properties; elastic modulus (E), tan δ, and Poisson's ratio (ν), for polydimethylsiloxane (PDMS) and linear low density polyethylene (LLDPE). The analytical membrane theories and how they describe the systems and materials tested is also discussed. Finally, a table is given summarizing the polydimethylsiloxane (PDMS) tensile mechanical properties from this work.

4.1 Comparison of data

4.1.1 Tensile test versus Membrane test

Tensile testing as a method of material characterization is well established in fields of science and engineering for materials with crystalline molecular structure, such as steel and aluminum. The material properties and stress-strain relationships for materials of this type are well documented, as many of these materials are used in engineering design, resulting in industrial application. Therefore, it is paramount that the material properties be well characterized for designers to properly select and accurately predict material performance for a given application. Numerous test methods have been developed and standardized to obtain accurate material property data for a variety of materials. The standard tensile test (ASTM E8) for determining the stress-strain relationship of steel is an industrial standard and a universally accepted test method [97]. A similar test method for tensile testing elastomers, standard (ASTM D 412-98a), was used herein to develop the tensile mechanical properties of PDMS and LLDPE, see section 2.1. Both tests make use of dumbbell specimen uniaxial tension elongation with end gripping. While these tensile methods are similar, there are inherent differences in the materials, which limit the usefulness of the elastomer stress-strain data. Due to the amorphous molecular structure of PDMS, grip end effects and test strain rate have a profound effect on the stress-strain relationship developed during testing. The main function of dumbbell specimen design is to focus the tensile load on the necked section of the dumbbell, away from the grips. For accurate results a contact or optical extensometer is commonly used in the necked section to provide localized strain measurements, therefore isolating grip end effects [102]. While the use of an extensometer is practical for crystalline materials, their use for testing elastomers is difficult due to the amorphous molecular structure, thus contributing to the difficulties of elastomer material characterization. Therefore, tensile elongation and strain were measured from grip end displacement. For PDMS elastomer specimens, as the elongation and strain increase during the tensile test, the ends of the dumbbell begin to deform. Deformation of this type is clearly evident in Fig. 2.5, as compared to the initial specimen shape as seen in Fig. 2.1 and 2.5. This phenomenon is a function of the dumbbell geometry, strain rate, and amount of tensile elongation. Fig. 4.1 below, depicts the typical stress-strain curve of a tested *B* type PDMS uniaxial tensile specimen.

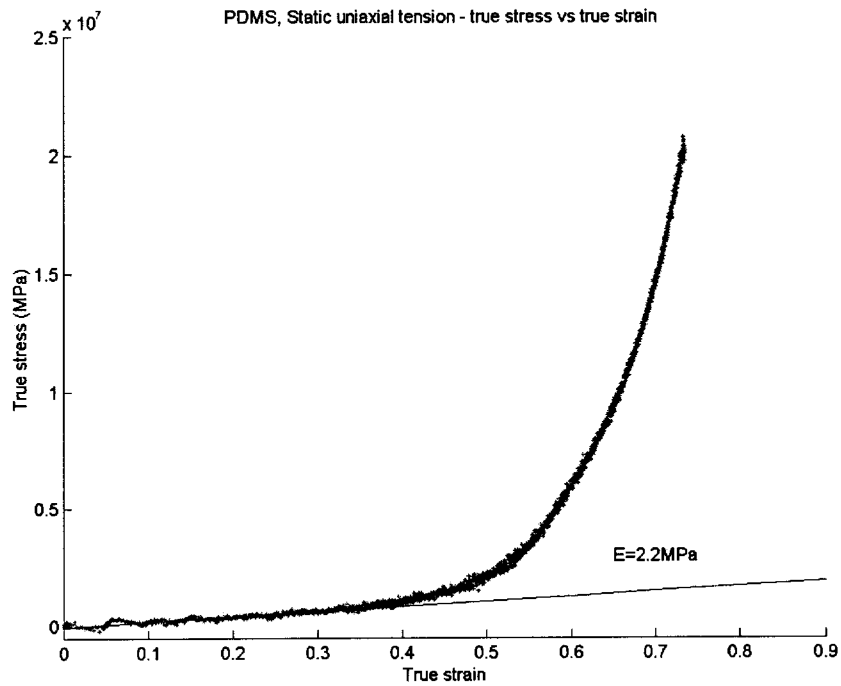

Fig. 4.1. - Stress-strain relationship and Elastic Modulus for PDMS tested in uniaxial tension. Non-linear curve fit: $Y = 5.1e8x^5-5.8e8x^4+2.6e8x^3-5.3e7x^2+5.7e6x+6.7e2$

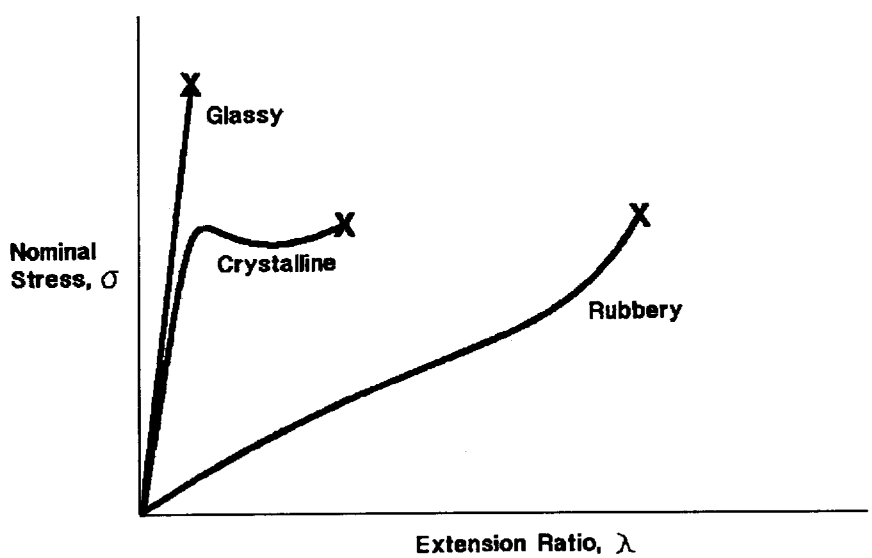

Fig. 4.2 - Stress-strain relationship of typical rubbery elastomers and different materials

This is a fairly characteristic curve for an elastomer material [82,90]. However, the PDMS curve appears to have distinct linear and non-linear regions, which is similar and yet different from the curve for rubbery elastomers shown in Fig. 4.2 [82]. This may be due to test specimen end effects, the gripping technique, or the test strain rate $\dot{\varepsilon}$ = 0.8/sec, but is most likely the inherent molecular structure elastic response specific to PDMS. The PDMS linear region tensile modulus, E = 2.18 MPa, generated from the static and dynamic uniaxial tensile tests performed. The PDMS loss factor, tan $\delta = 0.03$, and Poisson's ratio $\nu = 0.47$. Poisson's ratio is in close agreement with published results for PDMS of the same consistency, while the tan δ value is unique to this work, but acceptable for a material of this type [96]. In general, the results presented may be affected by the manual difficulties in performing these tests combined with test strain rate, and specimen end effects, respectively. This made clear the need for a comparative test with a different material.

The LLDPE tensile tests had a much different result. The specimen end effects were much less of a factor as specimen deformation occurred only in the necked region. This was most likely due to the more deformation resistant crystalline molecular structure of LLDPE [81]. The LLDPE linear region tensile modulus, E = 166 MPa, generated from the static uniaxial tensile tests performed. This result is within the published range of values E = 50 – 300 MPa for all Polyethylenes [104], and is appropriate for LLDPE within that range, thus giving more confidence in the static uniaxial testing results of both materials.

Membrane testing, or bulge testing, was conducted to investigate the load-deflection mechanical response of PDMS circular and square membranes for MEMS applications. Further research made clear the use of the bulge test to derive the elastic modulus and membrane residual stress from material films. This gave further elastic modulus comparison information. Bulge testing is an easy test to conduct, using sheet film materials and the specially fabricated membrane block, as discussed in section 2.1.6. Many of the difficulties and potential errors associated with elastomer uniaxial tensile testing previously mentioned are not encountered in the bulge test. The simplicity of the test combined with the ability to derive the test material elastic modulus and residual stress makes the bulge test a favored test method, and useful for result comparison. Biaxial stress-strain plots were made from PDMS and LLDPE circular membrane load-deflection experimental data, and the membrane elastic modulus and residual stress derived, see sections 2.2.6 and 3.2.1. Table 4.1 below compares the tensile and membrane test results.

Table 4.1: Comparison of tensile and membrane elastic modulus results

Material	Test	σ_{max}	ε_{max}	E
PDMS	Tensile	1.26 ±0.16 Mpa	0.342 ±0.026	2.18 ±0.184 MPa
	Membrane	0.45 ±0.03 MPa	0.180 ±0.060	1.08 ±0.250 MPa
LLDPE	Tensile	3.33 ±0.22 MPa	0.020 ±0.000	166 ±6.270 MPa
	Membrane	2.75 ±0.15 MPa	0.020 ±0.000	76.0 ±6.110 MPa

From table 4.1, there is a substantial amount of difference between the results of the tensile tests and the membrane tests conducted herein. However, considering the difficulties associated with polymer mechanical testing and the rather unsophisticated deflection measurement techniques employed, the results are not only within reason, but are very close to published elastic modulus values for these materials, see table 4.2. The elastic modulus values of the membrane and static uniaxial tensile tests have a similar variance in this comparison under the same test conditions for both materials. This is most likely due to the greater strain rate dependence of the uniaxial tensile tests. This problem is attributed to the amorphous molecular structure of both materials. The membrane tests are a more static test, reducing strain rate dependence, and providing a simple and more accurate elastic modulus testing method, for similar static applications of these materials. The differences in the elastic modulus results for the same material, display the varying "elastic" performance of these materials, due to their molecular structure.

4.1.2 Analytical results versus Experimental membrane results

Fig. 4.3, displays PDMS bulge test experimental results from a sample circular membrane and compares the results to a number of membrane analytical models. There is a large variation in the results produced by each model as compared to the experimental results, therefore underlining the need of the development of *the new spherical cap model.* The differences between these models is in the fundamental membrane strain definition and how it is applied as a function of the radius of curvature of the membrane load-deflection equation; as defined in the circular membrane mechanics section 1.2.1.2.

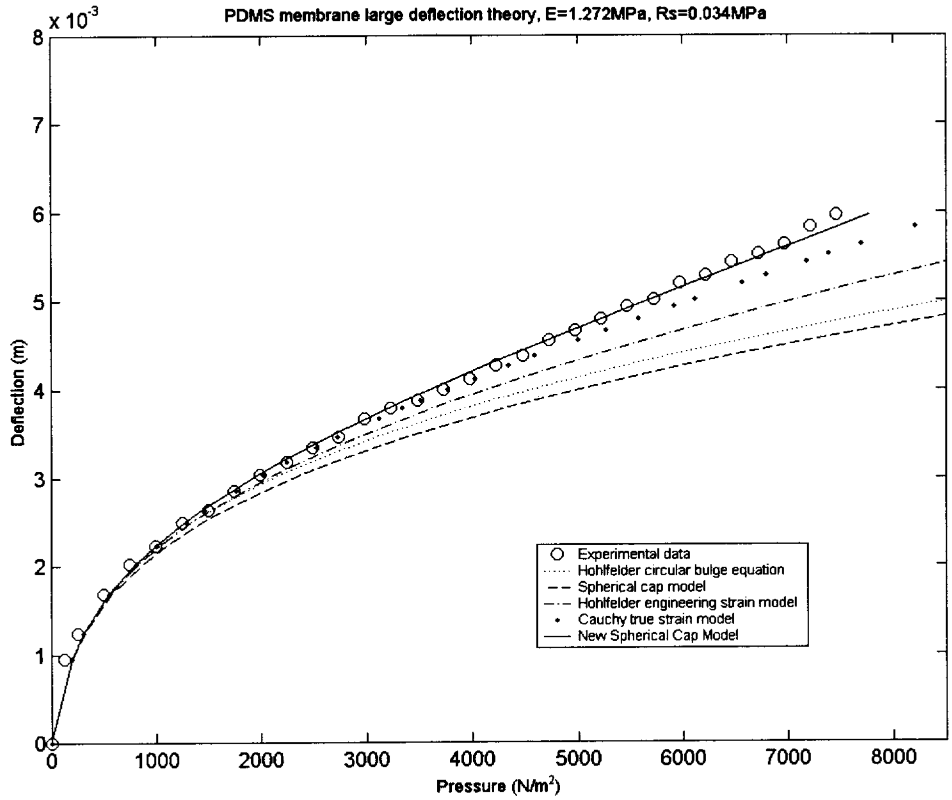

Fig. 4.3 - PDMS bulge test experiment simulated with different models

The new large deflection theory, *The new spherical cap model*, based upon the Almansi true strain definition is clearly the analytical model that best describes the load-deflection response of PDMS circular membranes as displayed by the experimental data, Fig. 4.4.

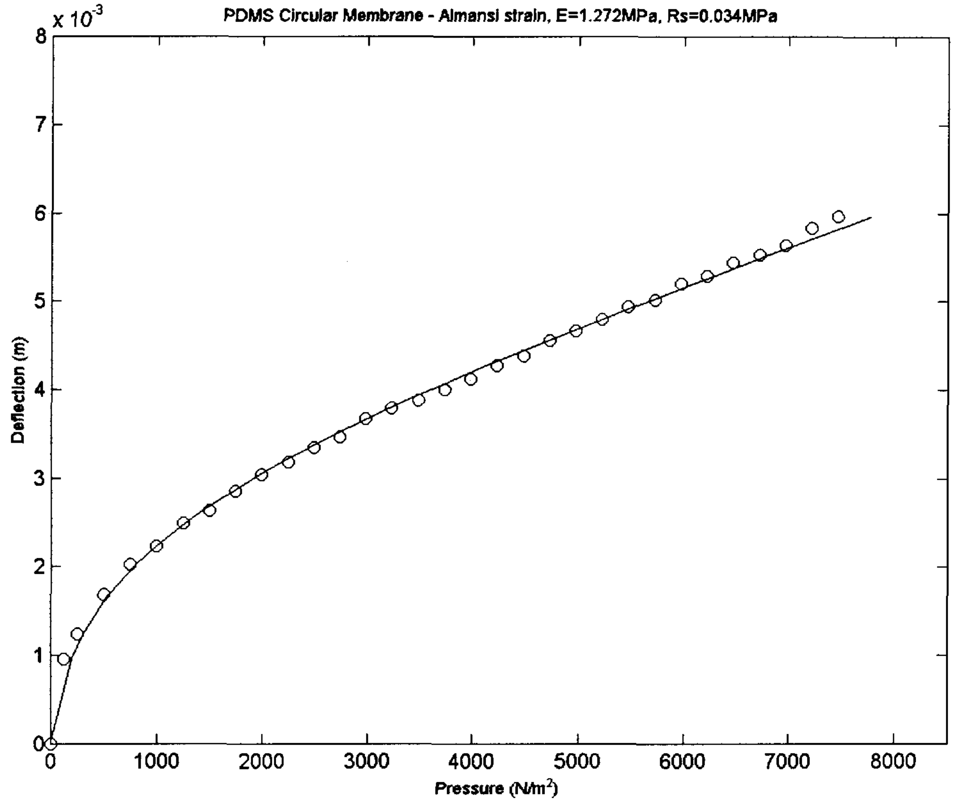

Fig. 4.4 - PDMS analytical model fit to circular membrane bulge test experimental results.

The same analytical model comparison of Fig. 4.4 was done with LLDPE membranes, Fig. 4.5. This comparison shows much less difference between the analytical models for LLDPE. This is most likely due to the smaller strain level in the LLDPE membrane compared to the PDMS membrane. There is good agreement with the analytical and experimental results for LLDPE. Given the apparent ability of *the new spherical cap model* to approximate both amorphous and semi-crystalline material bulge test performance, use with all material types is proposed as a new universal circular membrane deflection analytical model. Further testing and validation is needed to prove this proposed application.

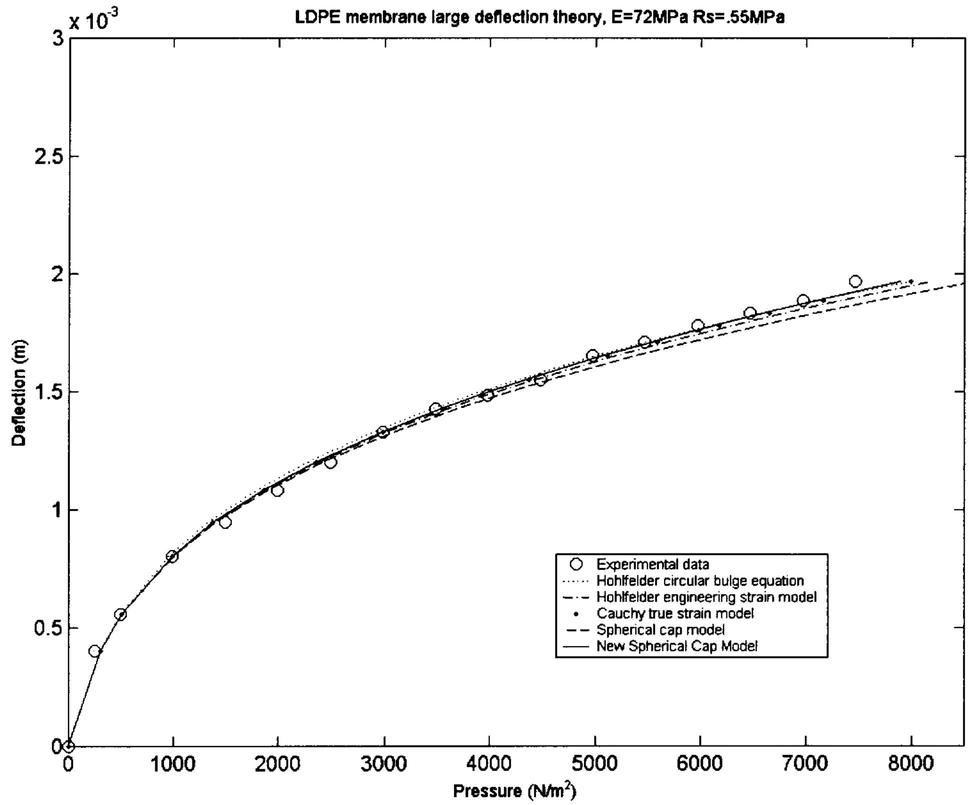

Fig. 4.5 - LLDPE bulge test experiment simulated with different models.

The analytical model results for the PDMS square membrane do not agree well with the experimental data, Fig. 3.19. This is most likely due to the theory having been developed for crystalline materials, instead of amorphous elastomeric materials such as PDMS, which have the ability to achieve great elongations ~600% without plastically deforming. There is better agreement between the analytical and experimental results for the LLDPE square membrane, Fig. 3.20, confirming the functional pairing of a correct strain model and material. Further research is needed to develop a square membrane large deflection model for elastomeric materials.

4.2 Comparison of PDMS results versus other researcher's results

Polydimethylsiloxane, silicone rubber, and other similar elastomers have seen increasing use in the field of MEMS [7-30]. The advantages polymers offer in processing flexibility and material property manipulation are main criteria for there selection. The use of polymers in MEMS micro fluidics and other MEMS membrane applications has prioritized the need to characterize elastomer material mechanical properties and resulting behavior in mechanical systems. Many groups have investigated characterizing the mechanical properties of PDMS, and have used PDMS for varied MEMS applications. Similar polymers, such as Parylene, low density polyethylene, and numerous commercially available RTV silicone rubbers have also been investigated. For these assorted polymers, each demonstrates very similar membrane load-deflection behavior from the results presented, which is characteristic for low modulus polymer materials, Fig. 3.15 [7,8,9,10]. However, no group has specifically investigated PDMS circular and square membrane load-deflection mechanics and the material properties derived. PDMS membranes are desirable for MEMS actuator applications for their large displacement capability due to the molecular structure of PDMS. Therefore it is required to have accurate material property data for a specific PDMS process to realistically simulate PDMS membrane actuator performance. For this investigation a common mixing ratio (10:1 base to activator), or cross-link polymerization ratio, and curing process was used. Varying batch polymerization results may be easily obtained from addition cure RTV polymers, due to the process dependent polymer cross-linking. It is this feature of elastomers that makes them very useful, as well as frequently ubiquitous from a mechanical property perspective. Table 7 displays PDMS material property results from this work and from other research groups [84,98,99,100]. Varied fabrication, testing, and analysis methods were used to obtain these contrasting results for PDMS.

Table 4.2 - PDMS Mechanical Property values from various Research groups

Research group	***E***	**Test type**	**Tan δ**	**ν**
Lotters *et al*, 1997	0.75 Mpa	Shear	<<0.001	-
Armani *et al*, 2003	0.75 Mpa	Beam bending	-	0.5
Yang *et al*, 1999	0.51 Mpa	Membrane	-	-
Hosokawa *et al*, 2001	2.20 Mpa	Tensile static	-	0.5
Qi *et al*, 2000	1.99 Mpa	Tensile static	-	0.49
This work, 2004	2.18 Mpa	Tensile static	0.03	0.47
	1.45 Mpa	Tensile dynamic	-	-
	1.04 Mpa	Membrane	-	-

Comparing these elastic modulus values for PDMS, there is confidence in the results generated from this work, given their close proximity and uniformity. The PDMS circular membrane test results have less dynamic components and strain rate dependence than the uniaxial static and dynamic tensile test results, and fewer testing difficulties. This may explain some of the variation in the tensile test results in table 4.2. The circular membrane test is a more accurate method for determining the elastic modulus of PDMS for static tensile applications, while the dynamic test values are more suited for applications similar to those tests. It is this strain dependent behavior that makes PDMS and other polymers perform differently in varying applications [94]. These phenomenon should be considered when designing applications for the use of PDMS and similar polymers. This work agrees closely with other published test techniques and their results.

Chapter 5
Conclusions

The elastomer polymer Polydimethylsiloxane (PDMS) is a material that has become very popular for MEMS applications due to its processing and material property flexibility, low cost, and availability. However, it is a ubiquitous material from processing, material property characterization, and performance perspectives.

Many PDMS processing techniques exist which ultimately influence the material properties and resulting application performance [84]. It is the relationship between the processing technique and the polymerization reaction that determines the amount of cross-linking and the resulting polymer material properties. Monomer base to catalyst activator ratio forms the basis of the amount of polymerization. For this work a common base to actuator ratio of 10 to 1 parts by weight was used. Variable polymerization is generally a good phenomenon, increasing application flexibility through customizing material properties, it may also add difficulty in the ability to reach or maintain consistent material properties and application performance. There may be variance in polymer material properties from batch processing, not only due to the process itself, but in the raw materials supplied; the two part monomer and catalyst components of the polymers themselves, and what manufacturer is being used. PDMS has a manufacturer recommended shelf life of approximately six months. This is due to the PDMS monomer base polymerizing over time with vibration, exposure to heat and oxygen [83]. Therefore, it is recommended that PDMS be stored in a sealed container in a cooled, stable environment. Once polymerized or fully cured, PDMS may be considered inert, changing only with exposure to extreme temperatures (-60° C to 300° C in air) and swelling with exposure to some solvents [80].

The polymerized molecular structure of PDMS is considered amorphous and changes with strain, going from amorphous to semi-crystallization, compounding the difficulties of material characterization and introducing strain rate dependence in testing. This change in structure occurs through alignment of the polymer chains in the loading direction [80]. It was found that this material behavior had numerous impacts upon tensile tests and results. Initial difficulties were encountered with specimen loading in the tester grips, while during testing specimen end effects and slippage may have contributed erroneously to the results. The molecular structure of PDMS also yielded distinct linear and non-linear stress-strain regions in uniaxial tensile test results. The linear region modulus of PDMS from static uniaxial tensile testing was, $E = 2.18$ MPa up to a true strain $\varepsilon = 0.342$, the stress-strain curve becoming non-linear after that point with significant strain crystallization, failure was not attained. The PDMS linear elastic modulus is a higher value than published results, most likely due to the strain rate of the test, and the true stress and true strain analysis used to simulate the material behavior. To obtain a more accurate uniaxial tensile modulus, static uniaxial testing should be done with extensometers. The results generated from the dynamic uniaxial tensile tests were an average, $E = 1.45$ Mpa for the A and B samples. This test gives a more realistic "in-situ" elastic modulus value for PDMS. The lower modulus value may be due to stress conditioning of the material during the cyclic testing [80]. This varying range of the PDMS elastic modulus displays the strain dependent behavior that makes PDMS and other polymers perform differently in varied applications [94]. These phenomenon should be considered when designing applications for the use of PDMS and similar polymers. The LLDPE tensile tests were also dependent upon strain rate and end effects. LLDPE yielded an elastic modulus of, $E \sim 166$ MPa, an acceptable value for LLDPE, thus validating the test procedure and confirming the PDMS results.

Heat was generated by the PDMS molecules sliding past each other during tensile testing, and was most significant in the dynamic uniaxial tensile tests as the specimens were cyclically strained, strain energy was lost in the form of heat. This energy loss was quantified by the loss factor or tan δ = 0.03 over a test frequency range of 0.5 Hz, 1.0 Hz, 2.0 Hz, 3.0 Hz, 4.0 Hz, and 5 Hz., which is an appropriate value for a low loss rubber up to 100 Hz [96]. Poisson's ratio using video dimensional analysis was found to be, ν = 0.47.

Bulge testing of PDMS circular and square membranes was performed to investigate their mechanical load-deflection performance for MEMS applications. The bulge test is a static mechanical test that is easy to perform and yields membrane elastic modulus and residual stress results. Through in depth investigation of circular membrane deflection theory and PDMS experimental results, a new circular membrane analysis and large deflection theory was developed; *The new spherical cap model.* Biaxial stress-strain analysis, as defined below as a function of membrane radius of curvature, enable the derivation of the elastic modulus and residual stress of circular membranes.

Membrane radius of curvature, $R = \dfrac{h}{2} + \dfrac{a^2}{2h}$ (1.5)

Circular membrane biaxial stress, $\sigma_{xx} = \sigma_{yy} = \dfrac{PR}{2t}$, from equation (1.3).

Circular membrane Almansi biaxial true strain, $\varepsilon_{xx} = \varepsilon_{yy} = \dfrac{\left[\left(R\sin^{-1}\dfrac{a}{R}\right)^2 - a^2\right]}{2\left(R\sin^{-1}\dfrac{a}{R}\right)^2}$ (1.30)

The elastic modulus and residual stress values for PDMS circular membranes were found to be, E = 1.08 MPa and σ_0 = 0.038 MPa, which agree with published results. These elastic constants may then be used in the new large deflection circular membrane theory.

The new spherical cap model:

$$P = \frac{\left[\frac{E}{1-v}\left(\frac{\left(R\sin^{-1}\frac{a}{R}\right)^2 - a^2}{2\left(R\sin^{-1}\frac{a}{R}\right)^2}\right) + \sigma_0\right]2t}{R} \tag{1.32}$$

The new spherical cap model provides an accurate elastomer circular membrane load-deflection analytical model. Application of this model to semi-crystalline material circular LLDPE membranes produced results indicating the use of this new theory for small and large deflecting materials. The square membrane theory of Maier-Schneider *et al* approximated the experimental results of LLDPE very well, but poorly for PDMS. MEMS applications that may benefit from this new theory are, aerodynamic control membrane actuators for jet aircraft, micro mirrors mounted on polymer membrane structures for optical coherence tomography applications, and in-situ semiconductor CMOS thin film material testing. Applications may also include the investigation of biological material properties, and nondestructive material testing.

Further research may include, the application of *The new spherical cap model* universally for all material types in the bulge test, and the development of the Almansi true strain definition for square membrane theory for use with elastomers.

Appendix A
Experimental data

A.1 Uniaxial tensile test data description

Tensile test data was collected in real time with the MTS data acquisition system and saved to data files, *specimen.dat*, for each sample tested. These files were then edited to remove headings to provide 3 columns of the collected experimental data; time, axial displacement, axial force, for analysis with Matlab. Typically these files contain data collected at 1 millisecond intervals. The data described was collected for the static and dynamic uniaxial tests, as well as the stress relaxation tests. Examples of the test data files and analysis files are shown in part below.

A.1.1 MTS specimen.dat test data file; example

```
MTS793|MPT|ENU|1|2|.|/|:|1|0|0|A
Data Acquisition                                   Time:  10.443115
Sec
Time    Axial Displacement    Axial Force
Sec      mm      N
0.16430664    -0.0033624831           -0.0083912509
0.17431641    -0.001680776  0.0041976348
0.18432617    -0.001680776  0.0041976348
0.19433594    0.030271659   0.02517911
0.2043457     0.43051797    0.0083939293
0.21435547    0.99557155    -0.0083912509
```

0.22436523	1.2865069	0.016786519
0.234375	1.446269	0.075534649
0.24438477	1.8162446	0.071338356
0.25439453	2.2770324	0.041964289
0.2644043	2.5763762	0.046160586
0.27441406	2.8000433	0.058749467
0.28442383	3.1532018	0.054553177
0.29443359	3.4962702	0.02517911
0.30444336	3.4004128	0.067142054
0.31445313	3.1498384	0.10071243
0.32446289	3.2137432	0.092319831
0.33447266	3.4155481	0.041964289
0.34448242	3.3785505	0.046160586
0.35449219	3.2053347	0.054553177
0.36450195	3.215425	0.071338356
0.37451172	3.3566883	0.062945768
0.38452148	3.3802323	0.075534649
0.39453125	3.2911017	0.083927236
0.40454102	3.2524226	0.067142054

A.1.2 Edited *specimen.dat* file for Matlab analysis; example

1.3674316	10.007325	2.6006777
1.3774414	10.00229	2.5922909
1.3874512	10.014039	2.5964844
1.3974609	10.03586	2.5964844
1.4074707	10.039217	2.5922909
1.4174805	10.03586	2.6132579
1.4274902	10.03586	2.6132579
1.4375	10.047609	2.6174512
1.4475098	10.05768	2.6174512
1.4575195	10.061037	2.6216447
1.4675293	10.054323	2.6342247
1.4775391	10.06943	2.6174512
1.4875488	10.074466	2.6132579
1.4975586	10.074466	2.6216447
1.5075684	10.079501	2.6132579
1.5175781	10.089572	2.6090646
1.5275879	10.087893	2.6174512
1.5375977	10.09125	2.6174512
1.5476074	10.101322	2.6174512
1.5576172	10.103001	2.6132579
1.567627	10.106358	2.6174512

1.5776367	10.116428	2.6132579
1.5876465	10.121464	2.6216447
1.5976563	10.121464	2.6258378
1.607666	10.128179	2.6216447
1.6176758	10.138249	2.6174512
1.6276855	10.136571	2.6258378
1.6376953	10.146642	2.6300311
1.6477051	10.149999	2.638418
1.6577148	10.153356	2.6258378
1.6677246	10.158392	2.6258378
1.6777344	10.168463	2.6258378
1.6877441	10.173498	2.6174512
1.6977539	10.178534	2.6342247
1.7077637	10.186926	2.638418
1.7177734	10.193641	2.6300311
1.7277832	10.195319	2.6216447

A.2 Poisson's ratio test data

Poisson's ratio testing of PDMS was done by collecting three sets of uniaxial displacement data. Video dimensional analysis was used to measure axial displacements as the samples were incrementally displaced. Data was recorded manually; cross head displacement, sample axial displacement, sample width displacement, and load. The notation *gl* stands for sample gauge length or original length.

Table. A.1 – PDMS Poisson's ratio data set A

Test A

gltx=19.45mmglx=4.33mm gly=8.45mm

gldis mm	X dis mm	Y dis mm	Force (N)
0	4.3	7.8	0.00
4	5.3	7.2	2.20
8	6.2	6.6	3.60
12	6.5	6.2	4.93
16	7.2	5.8	6.38
20	8.0	5.6	8.25
24	8.7	5.3	10.32
28	9.5	5.2	13.00
32	10.0	5.0	14.70
36	11.0	4.2	16.60
40	11.4	4.6	18.25
44	11.8	4.6	19.58
48	12.5	4.2	20.80

No failure in

Table. A.2 – PDMS Poisson's ratio data set B

Test B

gltx=19.25mm glx=5.42mm gly=7.80mm

gldis mm	X dis mm	Y dis mm	Force (N)
0	5.4	7.6	0.00
4	6.9	6.9	1.90
8	7.7	6.2	3.37
12	8.3	6.0	4.70
16	9.5	5.4	6.24
20	10.7	5.3	7.88
24	11.9	5.0	9.89
28	12.9	4.7	12.66
32	14.0	4.5	14.60
36	14.2	4.3	16.25
40	15.2	4.2	18.40
44	15.7	4.2	20.06
48	16.4	4.1	21.50

No failure in sample

Table. A.3 – PDMS Poisson's ratio data set C

Test C

gltx=19.40mm glx=4.33mm gly=7.65mm

gldis mm	X dis mm	Y dis mm	Force (N)
0	3.8	7.3	0.00
4	4.7	6.6	2.07
8	5.8	6.1	3.45
12	6.2	5.7	4.78
16	7.1	5.4	6.27
20	8.0	5.2	8.16
24	8.7	4.7	NA
28	9.8	4.6	12.26
32	10.4	4.5	14.60
36	11.0	4.2	17.50
40	11.3	4.1	18.70
44	11.5	3.9	20.60
48	11.8	3.9	NA

No failure in sample

A.3 Membrane deflection test data

Membrane deflection data was collected as circular and square PDMS and LLDPE membranes were incrementally pressurized. The tables below are comprised of an average of three deflection measurements for one deflection data point for each pressure level. A set of three membranes were tested for each material , data collection was done manually.

Table A.4 – PDMS membrane deflection data

PDMS membrane testing

Raw data - Full pressure range 0 - 30 in.w.g. (membrane thicknesses - t1 =.004, t2=.003, t3=.0035, **tavg=.0035**)

Square 1		Round 1		Square 2		Round 2		Square 3		Round 3	
Pressure	Deflection	Pressure	Deflection	Pressure	Deflection	Pressure	Deflection	Pressure	Deflection	Pressure	Deflection
inwg	mm	inwg	mm	inwg	mm	inwg	mm	inwg	mm	inwg	mm
0.0	0.0	0.0	0.0	0.0	0.0	0.0	0.0	0.0	0.0	0.0	0.0
0.5	0.9	0.5	1.0	0.5	1.1	0.5	1.1	0.5	1.0	0.5	1.0
1.0	1.3	1.0	1.3	1.0	1.6	1.0	1.5	1.0	1.4	1.0	1.2
2.0	1.8	2.0	1.7	2.0	2.1	2.0	2.0	2.0	1.9	2.0	1.7
3.0	2.1	3.0	2.0	3.0	2.5	3.0	2.4	3.0	2.3	3.0	2.0
4.0	2.6	4.0	2.2	4.0	2.9	4.0	2.7	4.0	2.7	4.0	2.2
5.0	2.9	5.0	2.5	5.0	3.2	5.0	3.0	5.0	2.9	5.0	2.5
6.0	3.0	6.0	2.6	6.0	3.5	6.0	3.2	6.0	3.2	6.0	2.6
7.0	3.3	7.0	2.9	7.0	3.8	7.0	3.4	7.0	3.4	7.0	2.9
8.0	3.4	8.0	3.0	8.0	4.0	8.0	3.6	8.0	3.7	8.0	3.0
9.0	3.8	9.0	3.1	9.0	4.4	9.0	3.9	9.0	3.9	9.0	3.2
10.0	4.0	10.0	3.3	10.0	4.6	10.0	4.1	10.0	4.0	10.0	3.3
11.0	4.1	11.0	3.4	11.0	4.9	11.0	4.3	11.0	4.2	11.0	3.5
12.0	4.3	12.0	3.6	12.0	5.1	12.0	4.6	12.0	4.4	12.0	3.7
13.0	4.4	13.0	3.7	13.0	5.4	13.0	4.7	13.0	4.6	13.0	3.8
14.0	4.7	14.0	3.8	14.0	5.6	14.0	5.0	14.0	4.8	14.0	3.9
15.0	4.8	15.0	4.0	15.0	5.9	15.0	5.2	15.0	5.0	15.0	4.0
16.0	5.0	16.0	4.1	16.0	6.1	16.0	5.4	16.0	5.2	16.0	4.1
17.0	5.1	17.0	4.2	17.0	6.4	17.0	5.6	17.0	5.4	17.0	4.3
18.0	5.3	18.0	4.3	18.0	6.5	18.0	5.8	18.0	5.5	18.0	4.4
19.0	5.3	19.0	4.4	19.0	6.8	19.0	6.0	19.0	5.7	19.0	4.6
20.0	5.6	20.0	4.6	20.0	7.2	20.0	6.3	20.0	5.9	20.0	4.7
21.0	5.8	21.0	4.7	21.0	7.5	21.0	6.4	21.0	6.1	21.0	4.8
22.0	5.9	22.0	4.8	22.0	7.7	22.0	6.8	22.0	6.3	22.0	4.9
23.0	6.2	23.0	4.9	23.0	8.1	23.0	7.0	23.0	6.5	23.0	5.0
24.0	6.4	24.0	5.1	24.0	8.2	24.0	7.2	24.0	6.8	24.0	5.2
25.0	6.5	25.0	5.1	25.0	8.6	25.0	7.5	25.0	6.9	25.0	5.3
26.0	6.6	26.0	5.4	26.0	9.0	26.0	7.7	26.0	7.2	26.0	5.4
27.0	6.8	27.0	5.5	27.0	9.3	27.0	7.9	27.0	7.4	27.0	5.5
28.0	7.1	28.0	5.5	28.0	9.6	28.0	8.2	28.0	7.6	28.0	5.6
29.0	7.3	29.0	5.7	29.0	9.9	29.0	8.6	29.0	7.9	29.0	5.8
30.0	7.5	30.0	5.8	30.0	10.3	30.0	8.9	30.0	8.1	30.0	6.0

Table. A.5 – LLDPE membrane deflection data

LDPE membrane testing

Full pressure range 0 - 30 in.w.g. LDPE film thickness tavg=.001in, made by Glad.

Square 1		Round 1		Square 2		Round 2		Square 3		Round 3	
Pressure	Deflection	Pressure	Deflection	Pressure	Deflection	Pressure	Deflection	Pressure	Deflection	Pressure	Deflection
inwg	mm	inwg	mm	inwg	mm	inwg	mm	inwg	mm	inwg	mm
0.0	0.0	0.0	0.0	0.0	0.0	0.0	0.0	0.0	0.0	0.0	0.0
1.0	0.5	1.0	0.4	1.0	0.6	1.0	0.5	1.0	0.5	1.0	0.4
2.0	0.8	2.0	0.6	2.0	0.7	2.0	0.7	2.0	0.6	2.0	0.6
4.0	1.0	4.0	0.8	4.0	1.1	4.0	0.8	4.0	0.9	4.0	0.8
6.0	1.2	6.0	1.0	6.0	1.2	6.0	1.0	6.0	1.1	6.0	0.9
8.0	1.3	8.0	1.1	8.0	1.4	8.0	1.2	8.0	1.3	8.0	1.1
10.0	1.5	10.0	1.2	10.0	1.4	10.0	1.3	10.0	1.4	10.0	1.2
12.0	1.6	12.0	1.3	12.0	1.5	12.0	1.4	12.0	1.5	12.0	1.3
14.0	1.7	14.0	1.4	14.0	1.7	14.0	1.4	14.0	1.6	14.0	1.4
16.0	1.8	16.0	1.5	16.0	1.7	16.0	1.5	16.0	1.7	16.0	1.5
18.0	1.9	18.0	1.6	18.0	1.8	18.0	1.6	18.0	1.9	18.0	1.6
20.0	2.0	20.0	1.7	20.0	1.9	20.0	1.6	20.0	1.9	20.0	1.7
22.0	2.1	22.0	1.8	22.0	2.1	22.0	1.7	22.0	2.0	22.0	1.7
24.0	2.1	24.0	1.9	24.0	2.1	24.0	1.8	24.0	2.1	24.0	1.8
26.0	2.3	26.0	2.0	26.0	2.2	26.0	1.9	26.0	2.1	26.0	1.8
28.0	2.4	28.0	2.0	28.0	2.3	28.0	2.0	28.0	2.3	28.0	1.9
30.0	2.5	30.0	2.1	30.0	2.3	30.0	2.0	30.0	2.4	30.0	2.0

A.4 PDMS stress deformation test data

Stress deformation data was generated by measuring the overall length of samples strained for one minute at 60% true strain, and then released. Manual dial calipers were used to measure the samples over a period of one week.

Table. A.6 – PDMS stress deformation test data

PDMS stress deformation data

B sample pre test length = 24mm

Sample	Day 0	Day 1	Day 2	Day 3	Day 4	Day 5	Day 6	Day 7
	Lo (mm)	L (mm)	L (mm)	L (mm)	L (mm)	L (mm)	L (mm)	L (mm)
1	24	24.22	24.02	24.18	24.18	24.13	24.13	24.13
2	24	24.19	24.08	24.13	24.13	24.15	24.13	24.10
3	24	24.18	24.18	24.13	24.10	24.10	24.18	24.15
4	24	24.22	24.13	24.13	24.13	24.13	24.13	24.13
5	24	24.21	24.10	24.18	24.15	24.13	24.15	24.13
6	24	24.16	24.13	24.18	24.13	24.13	24.13	24.13
7	24	24.20	24.13	24.18	24.13	24.18	24.13	24.18
8	24	24.21	24.05	24.13	24.13	24.13	24.13	24.18
9	24	24.18	24.18	24.18	24.13	24.15	24.13	24.13
10	24	24.23	24.20	24.18	24.18	24.13	24.13	24.13
11	24	24.19	24.07	24.13	24.13	24.13	24.13	24.13
12	24	24.20	24.15	24.13	24.18	24.10	24.13	24.13

Appendix B
Data analysis programs

B.1 Matlab programs

All experimental data analysis programs were written using Matlab. Matlab is a high-performance programming language for technical computing that utilizes data and computation arrays which enable the building of sophisticated analysis models in familiar mathematical notation [88]. Tensile specimen data was imported from specimen test files created during experimentation, while membrane data was made a part of the analysis programs.

B.1.1 Static uniaxial tensile test analysis programs

B.1.1.1 PDMS Static uniaxial tension analysis program

```
%Program for plotting Cauchy true stress vs true strain of viscoelastic materials
%(polymers).
% Filename:  [PDMS_staticauchy_true.m]  Patrick Roman 11/13/03
%++++++++++++++++++++++++++++++++++++++++++++++++++
%Plot MTS data (Time, Stroke, Load)
%Reset Matlab
clear all
close all
%Sample dimensions
W=2e-3;
T=.08e-3; %input('Input thickness of specimen in meters>'); %Specimen thickness
Gauge=18.1;
%Calculating xsect area
X_section = W*T; %Cross-sectional area of test specimen
%Opening data file.txt
```

```
fid=fopen('C:\WINDOWS\Desktop\Thesis3\Matlab
programs\Static_UTT\TpdmsII_data\Tpdmsf.txt');
d = fscanf(fid,'%g %g %g',[3,inf]);
fclose(fid);
d=d';
jsize=size(d);
Time=d(:,1);
Displacement=d(:,2);
Load=d(:,3);
%Calculating stress and true strain (Cauchy)
Stress_C=Load/X_section;
Strain_Eng=(Displacement)./(Gauge);
Straintrue_Cauchy=(Displacement)./(Gauge+Displacement);
%L=Gauge+Displacement;
%Lo=Gauge;
%AlmansiStrain=(L.^2-Lo.^2)./(2*L.^2);
AlmansiStrain=(((Gauge+Displacement).^2)-Gauge.^2)./(2*((Gauge+Displacement).^2));
%==========================================================
%Calculating true Stress (Euler)
%Assumes constant volume and that strainyy/strainxx=strainzz/strainxx
%Stresstrue=stretch ratio(lambda)*Engineering Stress;
lambda=(Gauge+Displacement)./Gauge;
Stresstrue_Euler=(lambda).*Stress_C;
%=============================================================
%Plotting stress vs strain
%figure(1);plot(Strain_Eng,Stress_C,'g.','markersize',.25);legend('Tpdmsf');title('PDM
%S in Uniaxial Tension - Stress vs Strain ');
%hold on
%plot(Strain_Eng,Stresstrue_Euler,'r.','markersize',.25);legend('Tpdmsf%');title('PDMS
%in Uniaxial Tension - Stress vs Strain ');
hold on
plot(Straintrue_Cauchy,Stresstrue_Euler,'r+','markersize',2);
title('PDMS, Static uniaxial tension - true stress vs true strain ');
legend('Tpdmsf')
hold on
%plot(Straintrue_Cauchy,Stress_C,'m.','markersize',.25);legend('Tpdmsf');
title('PDMS in Uniaxial Tension - Stress vs Strain ');
hold on
%plot(AlmansiStrain,Stresstrue_Euler,'b.','markersize',.25);legend('Tpd%msf2');title('
PDMS in Uniaxial Tension - Stress vs Strain ');
%Axis labels
xlabel('True strain');ylabel('True stress (MPa)')
%Setting plot range
axis([0 .9 -.5e6 2.5e7])
%fitting straight line
x=[0:.1:.9];
m=2.2e6;
b=-.05e6;
y=m*x+b;
%adding fit to plot
figure(1)
hold on
plot (x,y,'k')
%adding label
text(.65,.3e7,'E=2.2MPa')
```

B.1.1.2 LLDPE Static uniaxial tension analysis program

```
%________________________________LLDPE________________________________
_%Program for plotting Cauchy true stress vs true strain of
viscoelastic %materials (polymers).
%Patrick Roman 02/05/02
%Plot MTS static data (Time, Stroke, Load)
%Reset Matlab
clear all
close all
%Sample dimensions
W=2e-3;
T=.025E-3;%input('Input thickness of specimen in meters>'); %Specimen
thickness
Gauge=18.5;
%Calculating xsect area
X_section = W*T; %Cross-sectional area of test specimen
%Opening data file.txt
%C:\PATRICK\Masters\Thesis general\Materials Researcha\Test
data_all\Patrick\P_E\pe4
fid = fopen('C:\directory\Matlabprograms\Static_UTT\PE_data\pe13.txt');
d = fscanf(fid,'%g %g %g',[3,inf]);
fclose(fid);
d=d'
jsize=size(d);
Time=d(:,1);
Displacement=d(:,2);
Load=d(:,3);
%Calculating Engineering stress
Stress=Load/X_section;
%=======================================================
%Calculating true Stress (Euler)
%Assumes constant volume and that strainyy/strainxx=strainzz/strainxx
%Stresstrue=stretch ratio(lambda)*Engineering Stress;
lambda=(Gauge+Displacement)./Gauge;
Stresstrue_Euler=(lambda).*Stress;
%==========================================================
%Calculating true Strain (Cauchy)
True_Strain=(Displacement)./(Gauge+Displacement);
%cnt=0;
%for i=1:length(Strain)
%if Strain(i)>0
%cnt=cnt+1;
%Strain_s(cnt)=Strain(i);
%Stress_s(cnt)=Stress(i);
%end
%end
%Plotting True stress vs True strain
plot(True_Strain,Stresstrue_Euler,'r+');
legend('Tpdmsd');
title('PDMS in Uniaxial Tension - Stress vs Strain ');
%Setting plot range
axis([-0.1 .5 0e6 35e6])
%Axis labels
```

```
xlabel('Strain');
ylabel('Stress (MPa)');
%fitting straight line
x=[0:.02:.35];
m=165e6;
b=0e5;
y=m*x+b;
%adding fit to plot
figure(1)
hold on
plot (x,y,'bl')
%adding label
text(.3,3.25e7,'E=165MPa')
%plotting 2% strain limit
x1=.02;
y1=[0:.5e6:.75e7];
plot (x1,y1,'k-','markersize',12)
text(.03,.15e7,'2% strain','fontsize',7)
```

B.1.2 PDMS dynamic uniaxial tension analysis programs

B.1.2.1 Phasediff1bb.m

```
%Plot dynamic data (Time, Stroke, Load) and calculate phase difference
and tan delta for
%selected cycles
%Also calculates True Stress (in terms of Cauchy) and True Strain
%This program should be run with Box.m in the same directory
%DO NOT USE IF EXTENSOMETER DATA COLLECTED.  USE PHASEDIFF2.M FOR THAT
%USE THIS SCRIPT ONLY FOR DATA THAT WAS GENERATED UNDER STROKE CONTROL
%SJ Kirkpatrick 03/12/01
%
%User called functions - Box
close all
clear all
%Modifiy below before each run
fprintf (1,'\ttest\n'); %Sample name
fprintf (1,' \tOPERATOR - Patrick Roman 6 Nov 2001\n');
fid = fopen('C:\PATRICK\Masters\Materials Research\PDMS research\PDMS
tests\Dpdms1\DPDMSDAR1\pdmst_3d.txt');
d = fscanf(fid,'%g %g %g',[3,inf]);
fclose(fid);
d=d';
leng1=size(d);
leng=round((leng1(1))/10);
W=6e-3%input('Input width of specimen in meters>'); %Specimen width
T=input('Input thickness of specimen in meters>'); %Specimen thickness
Gauge=48%input ('Input gauge length in mm>'); %Gauge length
X_section = W*T; %Cross-sectional area of test specimen
Time=d(:,1);
```

```
Time(1,:)=[];
Displacement=d(:,2);Displacement(1,:)=[];
Load=d(:,3);Load(1,:)=[];
figure(1);plot(Displacement,Load,'r');
xlabel('Displacement (mm)');ylabel('Load (N)');
%print
Strain = (Displacement./Gauge);
Stress = Load./X_section;
%filtering of stress & Strain
Stress=filtfilt(ones(1,4),4,Stress);
Strain=filtfilt(ones(1,4),4,Strain);
figure(2);
plot(Strain,Stress);
title('Stress-Strain Plot of Polydimethylsilioxane (PDMS)');
xlabel('Strain ');
ylabel('Stress (N/m^2)');
grid on
%print
%grid on
figure(3);
plot(Time,Strain,'g-');
title('Strain as function of time');
xlabel('Time, (s)');
ylabel('Strain');
figure(4);
plot(Time,Stress,'g-');
title('Stress as function of time');
xlabel('Time, (s)');
ylabel('Stress');
figure(5);
plotyy(Time,Strain,Time,Stress);
grid on
xlabel('Time, s');
ylabel('Strain');
grid on
Strainnorm=Strain./max(Strain);
Stressnorm=Stress./max(Stress);
figure(6);
plotyy(Time,Strainnorm,Time,Stressnorm);
grid on
xlabel('Time, s');ylabel('Strain');
%Calculate E as a function of strain
for ii = 1:leng-1
i= 10*(ii-1) + 1;
j=i+10;
sigma=Stress(i:j);
deltastress(ii,1)=max(sigma)-min(sigma);
meanstress(ii,1)=mean(sigma);
end;
for ii = 1:leng-1
i= 10*(ii-1) + 1;
```

```
j=i+10;
sigma=Strain(i:j);
deltastrain(ii,1)=max(sigma)-min(sigma);
meanstrain(ii,1) = mean(sigma);
end;
for ii = 1:leng-1
i= 10*(ii-1) + 1;
j=i+10;
sigma=Time(i:j);
deltatime(ii,1)=max(sigma)-min(sigma);
end
Strain_rate=deltastrain./deltatime;
E = deltastress./deltastrain;
E(1,:)=[];
meanstrain(1,:)=[];
meanstress(1,:)=[];
Strain_rate(1,:)=[];
figure(7);
plot(meanstrain,E,'ro');
xlabel('Strain');
ylabel('E(\epsilon)');
grid off;%print
Em=mean(E);
StandardDeviation=std(E,1);
figure(8);
plot(meanstrain,Strain_rate,'ro');
xlabel('Strain');
ylabel('Strain rate, \epsilon/s');%print
%figure(9);
plot(Strain_rate,E,'r-');
axis([0 0.7 0.4e6 2.5e6]);
xlabel('Strain rate, \epsilon/s');
%ylabel('E(\epsilon)')
len = length(Time);
relmax = max(Strainnorm) / max(Stressnorm);
if (abs(relmax)>2)
refscale = 2^(( relmax < (2.^(-10:10)) ).* ...
( 2*relmax > (2.^(-10:10)) )*((1:21))'-12);
else
refscale = 1;
end;
% define the initial axis scaling vector
axisvec = [0 Time(len) min([Stressnorm; Strainnorm/refscale])*1.1 ...
max([Stressnorm; Strainnorm/refscale])*1.1];
done=0;
while (~done)
figure(10);
subplot(2,1,1);
plot(Time, Stressnorm,'b');
hold on
plot(Time, Strainnorm/refscale,'r');
```

```
plot([0 max(Time)], [0 0], ':m')
xlabel ('time (seconds)');
ylabel (['Strain',' (red) and Stress (blue)']);
axis(axisvec)
%  axis([0 max(Time) min(Strainnorm/refscale)+.5
max(Strainnorm/refscale)])
[stime, spos] = ginput (1);
plot([stime stime], [min([Stressnorm; Strainnorm/refscale]),
max([Stressnorm; Strainnorm/refscale])], ':k*')
%fprintf (1, 'Click to the right of the test cycles \n\n');
[ftime, fpos] = ginput (1);
plot([ftime ftime], [min([Stressnorm; Strainnorm/refscale]),
max([Stressnorm; Strainnorm/refscale])], ':k*')
% check that these are in the right order
if (ftime<stime)
tmptime = ftime;
ftime = stime;
stime = tmptime;
clear tmptime;
end;
axisvec = [stime-0.1*ftime ftime*1.1 ...
min([Stressnorm; Strainnorm/refscale])*1.1 max([Stressnorm;
Strainnorm/refscale])*1.1];
axis(axisvec)
hold off
%fprintf (1, 'Check that selected data is at the same vertical
...level\n');
subplot (2,1,2)
box ([15 0], 20,'k')
axis off
axis ([0 90 -20 20])
hold on
box ([15 0], 15, 'y')
box ([45 0], 20, 'k')
box ([45 0], 15, 'y')
box ([75 0], 20, 'k')
box ([75 0], 15, 'y')
hold off
text (30, 16, '... then click below to ');
text (10, -16, 'reselect');
text (30, -16, 'zoom out, then reselect');
text (65, -16, 'accept selection');
[x, y] = ginput(1);
if ( (x>=30) & (x<60) ) % zoom out
axisvec = [0 Time(len) min([Stressnorm;Strainnorm/refscale])*1.1
...max([Stressnorm; Strainnorm/refscale])*1.1];
end;
if ( (x>=60) )           % done
done = 1;
axisvec = [0 Time(len) min([Stressnorm; Strainnorm/refscale])*1.1
...max([Stressnorm; Strainnorm/refscale])*1.1];
```

```
subplot (2,1,1)
%title (['Total Data Set: ',fname]);
axis(axisvec);          % put the whole data set back up
end
end;
%fprintf (1, 'calculating ... \n');
% find where in the data the user clicked
s_ind = 1;
while (Time(s_ind)<stime)
s_ind = s_ind+1;
end;
f_ind = 1;
while (Time(f_ind)<ftime)
f_ind = f_ind+1;
end;
% define the allowable offset from zero as a fraction of the max value
dev = 0.001;
totrefshift = 0;
totposshift = 0;
done = 0;
while (~done)
refavg = mean(Strainnorm);
posavg = mean(Stressnorm);
% now find the crossing times
refcrossind = [];
poscrossind = [];
tposcross = [];
trefcross = [];
upcross = 0
downcross = 0;
i=s_ind;
while (i<f_ind-1) % find reference crossings
if ( (Strainnorm(i)>refavg) & (Strainnorm(i+1)<=refavg) &
....(~upcross) )  % a downward crossing
trefcross = [trefcross interp1([Strainnorm(i:i+1)], [Time(i:i+1)],
....refavg)];
refcrossind = [refcrossind i];
downcross = 1 & (~upcross);    % do only downward crossings
end;
if ( (Strainnorm(i)<refavg) & (Strainnorm(i+1)>=refavg) &
...(~downcross) )% an upward crossing
trefcross = [trefcross interp1([Strainnorm(i:i+1)],
...[Time(i:i+1)], refavg)];
refcrossind = [refcrossind i];
upcross = 1 & (~downcross);    % do only upward crossings
end;
i = i + 1;
end;
i=refcrossind(1);
while (i<f_ind-1) % find position crossings
if ( downcross & ( (Stressnorm(i)>posavg) &
```

```
(Stressnorm(i+1)<=posavg) ) ) % a downward crossing
tposcross = [tposcross interp1([Stressnorm(i:i+1)], ...[Time(i:i+1)],
posavg)];
poscrossind = [poscrossind i];
end;
if ( upcross & ( (Stressnorm(i)<posavg) & (Stressnorm(i+1)>=posavg) )
% an upward crossing
tposcross = [tposcross interp1([Stressnorm(i:i+1)], ...[Time(i:i+1)],
posavg)];
poscrossind = [poscrossind i]
end;
i = i + 1;
end;
numcycles = length(refcrossind);%instead of floor(length
...(poscrossind)/2)-1;  % this is really 1 + the number of cycles
refcrossind = refcrossind(1:numcycles);    % keep no more ref than pos
%cycles
trefcross = trefcross(1:numcycles);
tposcross = tposcross(1:numcycles);
% examine averages to see if data needs to be centered about zero
refavg = sum(Strainnorm(refcrossind(1):refcrossind(numcycles))) / ...
(refcrossind(numcycles)-refcrossind(1));
posavg = sum(Stressnorm(poscrossind(1):poscrossind(numcycles))) / ...
(poscrossind(numcycles)-poscrossind(1));
refavgdev=
abs(refavg)/max(Strainnorm(refcrossind(1):refcrossind(numcycles)));
posavgdev =
abs(posavg) / max(Stressnorm(poscrossind(1):poscrossind(numcycles)));
done = ( (refavgdev<dev) & (posavgdev<dev) );
% try and center the data about zero
if (~done)
% fprintf(1, ['Selected data not centered about ' ...
% '(within %.2f percent of) zero.\n'], dev*100);
% fprintf(1, ['\t(reference average=%.4f = %.2f percent, \n' ...
% '\t position average=%.4f = %.2f percent)\n'], ...
% refavg, refavgdev*100, posavg, posavgdev*100);
% fprintf(1, 'Centering data...\n');
Strainnorm = Strainnorm - refavg;
Stressnorm = Stressnorm - posavg;
totrefshift = totrefshift + refavg;
totposshift = totposshift + posavg;
end;
end;
% announce how much fudging we've done
fprintf (1, ['To center selected data about zero, ', ...
'\n\t%.3f was added to Stress and \n' ...
'\t%.3f was added to Strain\n'],totposshift, totrefshift);
% using all selected cycles, averaged, find the gain and phase
tphase = 0;
tperiod = 0;
for i=1:numcycles-1
```

```
tphase = tphase + tposcross(i)-trefcross(i);
tperiod = tperiod + trefcross(i+1)-trefcross(i);
end;
tphase = tphase / (numcycles-1);
tperiod = tperiod / (numcycles-1);
magnitude = (max(Stressnorm(poscrossind(1):poscrossind(numcycles))) -
...min(Stressnorm(poscrossind(1):poscrossind(numcycles)))) / ...
(max(Strainnorm(refcrossind(1):refcrossind(numcycles))) - ...
min(Strainnorm(refcrossind(1):refcrossind(numcycles))));
phase = 360 * tphase / tperiod;
tandelta=tan(phase*0.017453);
Estore=E.*cos(phase*0.017453);
Estorem=abs(mean(Estore));
Estoresd=std(Estore,1);
Eloss=E.*sin(phase*0.017453);
Elossm=abs(mean(Eloss));
Elosssd=std(Eloss,1);
% plot the final range of data to be used
subplot (2,1,2)
plot(Time(refcrossind(1):poscrossind(numcycles)+1), ...
Stressnorm(refcrossind(1):poscrossind(numcycles)+1), 'b.');
hold on
plot (Time(refcrossind(1):poscrossind(numcycles)+1), ...
Strainnorm(refcrossind(1):poscrossind(numcycles)+1)/refscale,'r');
plot([Time(refcrossind(1))-tperiod*0.1 ...
Time(poscrossind(numcycles)+1)+tperiod*0.1],[0 0], ':k')
plot (trefcross, zeros(1,numcycles), '+k');
plot (tposcross, zeros(1,numcycles), 'ok');
axisvec2 = [trefcross(1)-tperiod*0.1 tposcross(numcycles)+tperiod*0.1
...min([Strainnorm(refcrossind(1):poscrossind(numcycles))/refscale; ...
Stressnorm(refcrossind(1):poscrossind(numcycles))])*1.1 ...
max([Strainnorm(refcrossind(1):poscrossind(numcycles))/refscale; ...
Stressnorm(refcrossind(1):poscrossind(numcycles))])*1.1];
axis(axisvec2);
title ([num2str(numcycles-1),' cycles selected, ', ...'centered and
scaled, crossing points shown'])
xlabel ('time (seconds)');
ylabel (['Strain',' (red) and Stress (blue)']);%print
text((0.05*axisvec2(2)+0.95*axisvec2(1)),(0.25*axisvec2(4)+1.25*axisvec
2(3)),['f = ',num2str(1/tperiod),'Hz   Mag ratio = ...
',num2str(magnitude),...'phase diff = ',num2str(phase),' deg']);
hold off
fprintf (1, 'From an average over %d complete cycles:\n', numcycles-1);
fprintf (1, '\tThe frequency is %.2f Hz\n', 1/tperiod);
fprintf (1, '\tMagnitude ratio is %6.4f \n', magnitude);
fprintf (1, '\tPhase difference is %6.4f degrees\n', phase);
fprintf (1, '\tTan delta is %.4f\n', tandelta);
disp(sprintf('Modulus (mean +/- SD) = %5.3e +/- %5.3e Nm^-2 (average
slope as function of strain)', Em, StandardDeviation))
disp(sprintf('\tMaximum Slope = %5.3e  Nm^-2', max(E)))
disp(sprintf('\tMinimum Slope = %5.3e  Nm^-2', min(E)))
```

```
disp(sprintf('Storage modulus (mean +/- SD) = %5.3e +/- %5.3e Nm^-2',
Estorem, Estoresd))
disp(sprintf('Loss modulus (mean +/- SD) = %5.3e +/- %5.3e Nm^-2',
Elossm, Elosssd))
disp(sprintf('Maximum Engineering Stress = %5.3e Nm^-2',max(Stress)))
disp(sprintf('Minimum Engineering Stress = %5.3e Nm^-2',min(Stress)))
disp(sprintf('Maximum Percent Engineering Strain = %5.3e
%',max(Strain)*100))
disp(sprintf('Minimum Percent Engineering Strain = %5.3e
%',min(Strain)*100))
%Routine for true stress and true strain
%Calculate true Strain
for i=1:1008;
Gaugetrue=(Gauge+Displacement);
Straintrue=(Displacement./Gaugetrue);
end
%
%Calculate true Stress
%Assumes constant volume and that strainyy/strainxx=strainzz/strainxx
%Stresstrue=stretch ratio(lambda)*Engineering Stress;
lambda=Gaugetrue./Gauge;
for i=1:1008;
Stresstrue=lambda.*Stress;
end
figure(11);plot(Straintrue,Stresstrue,'r+');legend ('True, -
Engineering');
hold on
plot(Strain,Stress,'b-');%title('Stress-Strain Plot');
xlabel('Strain ');ylabel('Stress (N/m^2)');%print
disp(sprintf('Maximum True Stress = %5.3e Nm^-2',max(Stresstrue)))
disp(sprintf('Minimum True Stress = %5.3e Nm^-2',min(Stresstrue)))
disp(sprintf('Maximum Percent True Strain = %5.3e
%',max(Straintrue)*100))
disp(sprintf('Minimum Percent True Strain = %5.3e
%',min(Straintrue)*100))
figure(12);plot(meanstress,E,'ro');
xlabel('Stress');ylabel('E(\sigma)');
```

B.1.2.2 Box.m

```
%  This program should reside in the main program and data file
directory
function box(center, size, color)
% (c) 1997 M. E. Brokowski
% BOX(CENTER, SIZE, COLOR)
% Draws a filled square in the current graph window.  The square
% is centered at CENTER, which is an x,y pair.  SIZE is the side
% length and COLOR is specifyable as it is in FILL.
% [ll ul ur lr]
fill ([center(1)-size/2 center(1)-size/2 center(1)+size/2 ...
center(1)+size/2],[center(2)-size/2 center(2)+size/2 ...
center(2)+size/2 center(2)-size/2], color);
```

B.1.3 Stress relaxation program

```
%  PDMS stress relaxation program -----------  Patrick Roman 01.24.04
clear all
close all
fid = fopen('C:\WINDOWS\Desktop\pdms_sr_data\pdms_sr002.txt');
d = fscanf(fid,'%g %g %g',[3,inf]);
fclose(fid);
d=d';
jsize=size(d);
Time=d(:,1);
Displacement=d(:,2);
Load=d(:,3);
%Sample dimensions
W=2e-3;
T=.11E-3;%input('Input thickness of specimen in meters>'); %Specimen
thickness
Gauge=18.5;
%Calculating xsect area
X_section = W*T; %Cross-sectional area of test specimen
%Calculating ENGR stress and ENGR strain
Stress=Load/X_section;
%=========================================================
%Calculating true Stress (Euler)
%Assumes constant volume and that strainyy/strainxx=strainzz/strainxx
%Stresstrue=stretch ratio(lambda)*Engineering Stress;
lambda=(Gauge+Displacement)./Gauge;
Stresstrue_Euler=(lambda).*Stress;
%==========================================================
figure(1);plot(Time,Stresstrue_Euler,'r+');title('PDMS, B sample stress
relaxation at true strain = 0.6');
%;legend('PDMS SR001')
%Setting plot range
%axis([0 65 0 2.5E6])
%Axis labels
xlabel('Time (sec)');ylabel('True stress (N/m^2)')
hold on
```

```
%Curve fitting decaying exponential
x=(0:63);
y=6.5e6*exp(-.1275*x-2)+4.9e6;
plot(x,y,'k')
axis([0 65 0e6 8e6])
```

B.1.4 Stress deformation program

```
%Plastic deformation of PDMS: stress relaxation curve fitting
%with a decaying exponential
close all
clear all
%data set
dataA=[
    0 24
    1 24.199
    2 24.118
    3 24.155
    4 24.142
    5 24.133
    6 24.136
    7 24.138];

std1=[0
0.020207259
0.055732043
0.026111648
0.025524795
0.021373305
0.01505042
0.022613351];

day = dataA(:,1)
Elongation = dataA(:,2)
%Plotting data (you don't need this stuff
% errorbar will plot the data AND the errorbars
%plot(day,Elongation,'ro')
%axis([0 8 24.4 24.5])
%hold on
%Curve fit
errorbar(day,Elongation,std1,'ro')
hold on
x=(0:8);
y=24.1375+exp(-x-1.7);
plot(x,y);title('PDMS, B sample deformation from true strain = 0.6');
%Axis labels
xlabel('Time (Days)');ylabel('Elongation (mm)')
%  Comparing SR to deformation test---------------------------------
%dataB=[
%10     24.0485
%15     24.0475
%20     24.0465
%25     24.046
```

```
%30     24.046
%35     24.0455
%40     24.045
%45     24.045
%50     24.045
%55     24.045
%60     24.045];
%Time = dataB(:,1)
%ElongationB = dataB(:,2)

%figure(2);plot(Time,ElongationB,'ro');
%axis([-10 70 24.042 24.054])
%hold on
%std1B=[0.0005
%0.0005
%0.0005
%0.0005
%0.0005
%0.0005
%0.0005
%0.0005
%0.0005
%0.0005
%0.0005
%0.0005];
%Curve fit
%errorbar(Time,ElongationB,std1B,'ro')
%hold on
%xB=(0:65);
%yB=.006*exp(-.07*xB-.004)+24.045;
%yB=24.0455+exp(-xB-1)
%plot(xB,yB);
%title('PDMS, B sample elongation at true strain = 0.6');
%Axis labels
%xlabel('Time (sec)');ylabel('Elongation (mm)')
```

B.1.5 Membrane analysis programs

B.1.5.1 PDMS circular membrane biaxial stress-strain program

```
%This program analyzes circular bulge test data for visoelastic
materials
%
%Patrick Roman 07/08/03
%Bulge test data for circular membrane
close all
clear all
%Copied PDMS data from experiment (Circular)
data=[
0.0     0.000
0.5     0.957
1.0     1.244
2.0     1.683
```

```
3.0      2.024
4.0      2.232
5.0      2.489
6.0      2.635
7.0      2.857
8.0      3.035
9.0      3.180
10.0     3.348
11.0     3.464
12.0     3.675
13.0     3.789
14.0     3.875
15.0     4.000
16.0     4.120
17.0     4.270
18.0     4.380
19.0     4.560
20.0     4.670
21.0     4.800
22.0     4.939
23.0     5.020
24.0     5.200
25.0     5.292
26.0     5.440
27.0     5.524
28.0     5.642
29.0     5.839
30.0     5.967];
%Experimental data plot
Deflection = data(:,2)*1e-3; %converts to meters
Pressure = data(:,1)*248.84; %converts inwg to N/m^2
figure(1)
plot(Deflection,Pressure,'ro')
title('PDMS Circular membrane experimental - Pressure vs Deflection');
ylabel('Pressure (N/m^2)')
xlabel('Deflection (m)')
%System geometries and variables
a=9.52e-3 %average membrane radius (mm)
%P=(0:100:7465); %Pressure load (Pa or N/M^2)
t=.089e-3; %Membrane thickness
v=.47; %Poisson's ratio
%defining R
R=((Deflection/2)+(a^2./(2*Deflection)));
%Defining Biaxial stress
Bstress=((Pressure.*R)/(2*t));
%Defining Biaxial strain
test=(((R.*asin(a./R)).^2)-(a^2))./(((R.*asin(a./R)).^2)*2);
figure(4)
s=length(Bstress);
plot(test(2:s),Bstress(2:s),'r+')
title('PDMS Circular membrane - Biaxial stress vs Biaxial strain');
ylabel('Biaxial Stress (N/m^2)')
xlabel('Biaxial Strain')
```

B.1.5.2 LLDPE circular membrane biaxial stress-strain program

```
%This program analyzes circular bulge test data for visoelastic
materials
%
%Patrick Roman 07/08/03
%Bulge test data for circular membrane
close all
clear all
%Copied LLDPE data from experiment (Circular)
data=[
0.0     0.000
1.0     0.549
2.0     0.739
4.0     0.848
6.0     0.992
8.0     1.163
10.0    1.282
12.0    1.371
14.0    1.408
16.0    1.492
18.0    1.571
20.0    1.625]; %------------ data cut here for 2% strain analysis
%22.0   1.709
%24.0   1.778
%26.0   1.830
%28.0   1.884
%30.0   1.966];
%Experimental data plot
Deflection = data(:,2)*1e-3; %converts to meters
Pressure = data(:,1)*248.84; %converts inwg to N/m^2
figure(1)
plot(Deflection,Pressure,'ro')
title('PDMS Circular membrane experimental - Pressure vs Deflection');
ylabel('Pressure (N/m^2)')
xlabel('Deflection (m)')
%System geometries and variables
a=9.52e-3 %average membrane radius (mm)
%P=(0:100:7465); %Pressure load (Pa or N/M^2)
t=.025e-3; %Membrane thickness
v=.4; %Poisson's ratio
%defining R
R=((Deflection/2)+(a^2./(2*Deflection)));
%Defining Biaxial stress
Bstress=((Pressure.*R)/(2*t));
%Defining Biaxial strain Almansi
test=(((R.*asin(a./R)).^2)-(a^2))./(((R.*asin(a./R)).^2)*2); %almansi
figure(4)
s=length(Bstress);
plot(test(2:s),Bstress(2:s),'r+')
%Setting plot range
axis([0 .03 0e6 4.5e6])
title('LLDPE Circular membrane - Biaxial stress vs Biaxial strain');
ylabel('Biaxial Stress (N/m^2)')
```

```
xlabel('Biaxial Strain')
%adding straight line fit
x=[0:.0025:.03];
m=120e6;
b=.61e6;
y=m*x+b;
%adding fit to plot
%hold on
%plot (x,y,'bl')
%adding label
text(.3,3.25e7,'E=165MPa')
%plotting 2% strain limit
x1=.02;
y1=[0:.25e6:3.5e6];
hold on
plot (x1,y1,'k-','markersize',12)
text(.018,1e6,'ex = 2% strain','fontsize',7)
```

B.1.5.3 PDMS circular membrane program

```
%Membrane analysis program (Circular)
%Better fitting program using varying
%radius of curvature and more accurate strain definitions.
%Patrick Roman 07.13.03
%This program fits experimental load - deflection data for bulge tests
%of silicone membranes.  Material elastic modulus and residual stress
%are determined.  Circular membranes are analyzed.
%SI units only
close all
clear all
%  Membrane geometry and constants
a=9.52e-3 %average membrane radius (mm)
P=(0:100:7465); %Pressure load (Pa or N/M^2)
t=0.089e-3; %Membrane thickness
v=0.47; %Poisson's ratio
%Copied PDMS data from experiment (Circular) - data set #3
data=[
0.0     0.000
0.5     0.957
1.0     1.244
2.0     1.683
3.0     2.024
4.0     2.232
5.0     2.489
6.0     2.635
7.0     2.857
8.0     3.035
9.0     3.180
10.0    3.348
11.0    3.464
12.0    3.675
13.0    3.789
14.0    3.875
```

```
15.0    4.000
16.0    4.120
17.0    4.270
18.0    4.380
19.0    4.560
20.0    4.670
21.0    4.800
22.0    4.939
23.0    5.020
24.0    5.200
25.0    5.292
26.0    5.440
27.0    5.524
28.0    5.642
29.0    5.839
30.0    5.967];
CPressure=data(:,1)*248.84;
CDeflection=data(:,2)*1e-3;
%=============== Hohlfelder Spherical cap Model =================
%========membrane constants
C1c=4
C2c=((8/3)/(1-v))
%Fitting Circular membrane experimental data to spherical cap bulge
%eqn.
CRc = 3.7e4;
Ec  = 1.272e6 %Circular membrane Elastic modulus
Cscap=( ( 4*CRc*t*CDeflection)/a^2+(C2c*Ec*t*CDeflection.^3)/a^4);
%=============== Hohlfelder Circular membrane theory =================
% ENGINEERING STRAIN with constant radius of curvature
%Constant calculation (Circular membrane)
C1c=4
C2c=(8/3)*(1.015-.247*v)/(1-v)
%Fitting Circular membrane experimental data to Hohlfelder circular
%bulge eqn.
CRc = 3.7e4;
Ec  = 1.272e6 %Circular membrane Elastic modulus
CPressurefit=( (
4*CRc*t*CDeflection)/a^2+(C2c*Ec*t*CDeflection.^3)/a^4);
%=============== Hohlfelder Circular membrane theory (Non
%linear)===============
%         ENGINEERING STRAIN....... with varying radius of curvature
%Radius of curvature varying with deflection (strain Eng)
%Strain Eng=((R.*asin(a./R)/a)-1);    %Hohlfelder non linear strain
%definition
R=CDeflection/2+(a^2)./(2*CDeflection); %Radius of curvature
R(1)=0;
%Fitting Hohlfelder Non linear circular bulge Eqn to Circular membrane
%experimental data #3
CRce = 3.7e4;%Residual stress
Ece  = 1.272e6 %Circular membrane Elastic modulus
%Peng=(( (Ece/(1-v) )*(  R.*asin(a./R)/a -1 )+CRce)*2*t )./R;
AA=Ece/(1-v);
BB=R.*asin(a./R)/a;
Peng=(AA*(BB-1)+CRce)*2*t./R;
%=============== Modified Hohlfelder Circular membrane theory (Non
```

```
%linear)==============
%          TRUE STRAIN....... with varying radius of curvature
%Radius of curvature varying with deflection (strain True)
%Strain True=(1-(a./(R.*asin(a./R))));    %Roman non linear strain
%definition
%R=(((CDeflection./2)+(a^2))/((2*CDeflection))); %Radius of curvature
%Fitting Hohlfelder Non linear circular bulge Eqn to Circular membrane
%experimental data #3
CRct = 3.7e4;%Residual stress
Ect  = 1.272e6 %Circular membrane Elastic modulus
Ptrue= (( (Ect/(1-v) )*   (1-(a./(R.*asin(a./R))))  +CRct)*2*t)./R;
%+++++++++++++++++++++++++++++++++++++++++++++++++++++++++++++++++++++
%     More      TRUE STRAIN....... with varying radius of curvature
%+++++++++++++++++++++++++++++++++++++++++++++++++++++++++++++++++++++
%Almansi true strain     %;
CRctA = 3.7e4;%Residual stress
EctA  = 1.272e6 %Circular membrane Elastic modulus
A1=(R.*asin(a./R)).^2;
A=(A1-a^2)./(2*A1);
B=EctA/(1-v);
PtrueA=(B*A+CRctA)*2*t./R;
%Green true strain     %;
CRctG = 3.7e4;%Residual stress
EctG  = 1.272e6 %Circular membrane Elastic modulus
A1=(R.*asin(a./R)).^2;
A=(A1-a^2)./(2*a^2);
B=Ect/(1-v);
PtrueG=(B*A+CRct)*2*t./R;%
%------------------------------Plotting
figure(1)
plot(data(:,1)*248.84,data(:,2)*1e-3,'bo')% experimental data
hold on
plot(CPressurefit,CDeflection,'k-')%;
legend('Theory')
title('PDMS Circular Membrane - E=1.272MPa, Rs=0.034MPa','fontsize',8);
xlabel('Pressure (N/m^2)','fontsize',8)
ylabel('Deflection (m)','fontsize',8)
axis([0 8500 0 8e-3])
figure(2)
plot(data(:,1)*248.84,data(:,2)*1e-3, 'bo')% experimental data
hold on
plot(CPressurefit,CDeflection,'k-')%;legend('Theory')
hold on
plot(Cscap,CDeflection,'m-')%;legend('Theory')
hold on
Peng(1)=0 %forces first point to 0 ,infinitive is due to h=0 division
plot(Peng,CDeflection,'g-')
title('PDMS Circular Membrane - E=1.272MPa, Rs=0.034MPa','fontsize',8);
xlabel('Pressure (N/m^2)','fontsize',8)
ylabel('Deflection (m)','fontsize',8)
axis([0 8500 0 8e-3])
figure(3)
plot(data(:,1)*248.84,data(:,2)*1e-3, 'bo')% experimental data
hold on
plot(CPressurefit,CDeflection,'k:')%;legend('Theory')
```

```
hold on
plot(Cscap,CDeflection,'k--')%;legend('Theory')
hold on
Peng(1)=0 %forces first point to 0 ,infinitive is due to h=0 division
plot(Peng,CDeflection,'k-.')
hold on
Ptrue(1)=0
plot(Ptrue,CDeflection,'k.','markersize',4')
hold on
%plot(PtrueA,CDeflection,'r-')
hold on
PtrueA(1)=0 %forces first point to 0 ,infinitive is due to h=0 division
plot(PtrueA,CDeflection,'k-')
%plot(PtrueG,CDeflection,'c-')

%plot(Ptrue,CDeflection,'r-')
title('PDMS membrane large deflection theory, E=1.272MPa,
Rs=0.034MPa','fontsize',8);
xlabel('Pressure (N/m^2)','fontsize',8)
axis([0 8500 0 8e-3])
ylabel('Deflection (m)','fontsize',8)
figure(4)
plot(data(:,1)*248.84,data(:,2)*1e-3, 'bo')% experimental data
hold on
plot(PtrueA,CDeflection,'k-')
%plot(Ptrue,CDeflection,'g-')
title('PDMS Circular Membrane - Almansi strain, E=1.272MPa,
Rs=0.034MPa','fontsize',8);
xlabel('Pressure (N/m^2)','fontsize',8)
axis([0 8500 0 8e-3])
ylabel('Deflection (m)','fontsize',8)
```

B.1.5.4 LLDPE circular membrane program

```
%Membrane analysis program (Circular)
%Better fitting program using varying
%radius of curvature and more accurate strain definitions.
%Patrick Roman 07.13.03
%This program fits experimental load - deflection data for bulge tests
%of silicone membranes.  Material elastic modulus and residual stress
%are determined.  Circular membranes are analyzed.
%SI units only
close all
clear all
%  Membrane geometry and constants
a=9.52e-3 %average membrane radius (mm)
P=(0:100:7465); %Pressure load (Pa or N/M^2)
t=0.025e-3; %Membrane thickness
v=0.4; %Poisson's ratio
%Copied LLDPE data from experiment (Circular) - data set #3
data=[
0.0     0.000
1.0     0.404
```

```
2.0      0.560
4.0      0.806
6.0      0.946
8.0      1.083
10.0     1.200
12.0     1.327
14.0     1.426
16.0     1.483
18.0     1.550
20.0     1.650
22.0     1.709
24.0     1.778
26.0     1.830
28.0     1.884
30.0     1.966];
CPressure=data(:,1)*248.84;
CDeflection=data(:,2)*1e-3;
%=============== Hohlfelder Spherical cap Model =================
%========membrane constants
C1c=4
C2c=((8/3)/(1-v))
%Fitting Circular membrane experimental data to spherical cap bulge
%eqn.
CRc = .55e6;
Ec  = 72e6 %Circular membrane Elastic modulus
Cscap=( ( 4*CRc*t*CDeflection)/a^2+(C2c*Ec*t*CDeflection.^3)/a^4);
%=============== Hohlfelder circular bulge equation =================
%         ENGINEERING STRAIN........with constant radius of curvature
%Constant calculation (Circular membrane)
C1c=4
C2c=(8/3)*(1.015-.247*v)/(1-v)
%Fitting Circular membrane experimental data to Hohlfelder circular
%bulge eqn.
CRc = .55e6;
Ec  = 72e6 %Circular membrane Elastic modulus
CPressurefit=( ( 4*CRc*t*CDeflection)/a^2+...
(C2c*Ec*t*CDeflection.^3)/a^4);
%==== Hohlfelder Circular membrane theory (Non %linear)===============
%         ENGINEERING STRAIN....... with varying radius of curvature
%Radius of curvature varying with deflection (strain Eng)
%Strain Eng=((R.*asin(a./R)/a)-1);    %Hohlfelder non linear strain
%definition
R=CDeflection/2+(a^2)./(2*CDeflection); %Radius of curvature
R(1)=0;
%Fitting Hohlfelder Non linear circular bulge Eqn to Circular membrane
%experimental data #3
CRce = .55e6;%Residual stress
Ece  = 72e6 %Circular membrane Elastic modulus
%Peng=(( (Ece/(1-v) )*(  R.*asin(a./R)/a -1 )+CRce)*2*t )./R;
AA=Ece/(1-v);
BB=R.*asin(a./R)/a;
Peng=(AA*(BB-1)+CRce)*2*t./R;
%= Modified Hohlfelder Circular membrane theory (Nonlinear)========
%          TRUE STRAIN....... with varying radius of curvature
%Radius of curvature varying with deflection (strain True)
```

```
%Strain True=(1-(a./(R.*asin(a./R))));%Roman non linear strain
%definition
%R=(((CDeflection./2)+(a^2))/((2*CDeflection))); %Radius of curvature
%Fitting Hohlfelder Non linear circular bulge Eqn to Circular membrane
%experimental data #3
CRct = .55e6;%Residual stress
Ect  = 72e6 %Circular membrane Elastic modulus
Ptrue= (( (Ect/(1-v) )*   (1-(a./(R.*asin(a./R))))  +CRct)*2*t)./R;
%++++++++++++++++++++++++++++++++++++++++++++++++++++++++++++++++++++++
%     More      TRUE STRAIN....... with varying radius of curvature
%++++++++++++++++++++++++++++++++++++++++++++++++++++++++++++++++++++++
%Cauchy true strain     %;
%Almansi true strain     %;
CRctA =  .55e6;%Residual stress
EctA  =  72e6 %Circular membrane Elastic modulus
A1=(R.*asin(a./R)).^2;
A=(A1-a^2)./(2*A1);
B=EctA/(1-v);
PtrueA=(B*A+CRctA)*2*t./R;
%Green true strain     %;
CRctG = .55e6;%Residual stress
EctG  = 72e6 %Circular membrane Elastic modulus
A1=(R.*asin(a./R)).^2;
A=(A1-a^2)./(2*a^2);
B=Ect/(1-v);
PtrueG=(B*A+CRct)*2*t./R;%
%-----------------------------Plotting
figure(1)
plot(data(:,1)*248.84,data(:,2)*1e-3, 'bo')% experimental data
hold on
plot(CPressurefit,CDeflection,'k-')%;legend('Theory')
title('LLDPE Circular Membrane - E=72MPa Rs=.55MPa','fontsize',8);
xlabel('Pressure (N/m^2)','fontsize',8)
ylabel('Deflection (m)','fontsize',8)
axis([0 8500 0 3e-3])
figure(2)
plot(data(:,1)*248.84,data(:,2)*1e-3, 'bo')% experimental data
hold on
plot(CPressurefit,CDeflection,'k-')%;legend('Theory')
hold on
Peng(1)=0 %forces first point to 0 ,infinitive is due to h=0 division
plot(Peng,CDeflection,'g-')
title('LLDPE Circular Membrane - E=72MPa Rs=.55MPa','fontsize',8);
xlabel('Pressure (N/m^2)','fontsize',8)
ylabel('Deflection (m)','fontsize',8)
axis([0 8500 0 3e-3])
figure(3)
plot(data(:,1)*248.84,data(:,2)*1e-3, 'bo')% experimental data
hold on
plot(CPressurefit,CDeflection,'k:')%;legend('Theory')
hold on
Peng(1)=0 %forces first point to 0 ,infinitive is due to h=0 division
plot(Peng,CDeflection,'k-.')
hold on
Ptrue(1)=0
```

```
plot(Ptrue,CDeflection,'k.')
hold on
plot(Cscap,CDeflection,'k--')
hold on
PtrueA(1)=0 %forces first point to 0 ,infinitive is due to h=0 division
plot(PtrueA,CDeflection,'k-')
%plot(PtrueG,CDeflection,'c-')
%plot(Ptrue,CDeflection,'r-')
title('  LLDPE membrane large deflection theory, E=72MPa
Rs=.55MPa','fontsize',8);
xlabel('Pressure (N/m^2)','fontsize',8)
axis([0 8500 0 3e-3])
ylabel('Deflection (m)','fontsize',8)
figure(4)
plot(data(:,1)*248.84,data(:,2)*1e-3, 'bo')% experimental data

hold on
plot(PtrueA,CDeflection,'k-')
%plot(Ptrue,CDeflection,'g-')
title('LLDPE Circular Membrane - Almansi strain, E=72MPa
Rs=.55MPa','fontsize',8);
xlabel('Pressure (N/m^2)','fontsize',8)
axis([0 8500 0 3e-3])
ylabel('Deflection (m)','fontsize',8)
```

B.1.5.5 PDMS square membrane program

```
%Membrane analysis program (Square)
%Patrick Roman 07.13.03
%This program fits experimental load - deflection data for bulge tests
%of silicone membranes.  Material elastic modulus and residual stress
%are determined.  Square membranes are analyzed.
%SI units only
close all
clear all
%  Variables
a=9.52e-3 %average membrane radius (mm)
%P=(0:100:7465); %Pressure load (Pa or N/M^2)
%E1=1.45e6; %Elastic Modulus of PDMS material
t=.089e-3; %Membrane thickness
v=.47; %Poisson's ratio
%Es= 1.04e6  %Square membrane elastic modulus
%SRs= 3.8e4  %Square membrane residual stress
%Deiter et al - Square membrane Bulge equation
%Constant C2 calculation (SQUARE membrane)
C2s=1.994*(1-.271*v)/(1-v)
%C2s=4.3
%(Square membrane) Deflection calculation
%hs=((P*a^4)./(C2s*E1*t)).^(1/3);
%elastic modulus (square)
%Est=((P*a^4)./(C2s*t*hs.^3));
%Copied data PDMS from experiment (Square)
data=[
```

```
0.0     0.000
0.5     0.987
1.0     1.433
2.0     1.908
3.0     2.276
4.0     2.700
5.0     2.912
6.0     3.228
7.0     3.400
8.0     3.667
9.0     3.875
10.0    4.023
11.0    4.230
12.0    4.409
13.0    4.611
14.0    4.755
15.0    5.000
16.0    5.180
17.0    5.361
18.0    5.512
19.0    5.715
20.0    5.880
21.0    6.077
22.0    6.286
23.0    6.468
24.0    6.794
25.0    6.920
26.0    7.154
27.0    7.419
28.0    7.557
29.0    7.875
30.0    8.139];

SPressure=data(:,1)*248.84; %converts inwg to N/m^2
SDeflection=data(:,2)*1e-3; %converts to meters
%figure(1)
%plot(SPressure,SDeflection, 'bs') %experimental data plot
%hold on
%plot(P,hs,'rs') %analytical theory plot
%title('PDMS 3 Square Membrane - Pressure vs Deflection');
%xlabel('Pressure (N/m^2)')
%ylabel('Deflection (m)')
%Square bulge equation
zz=(1:25);
a  = 9.52e-3 %average membrane radius (mm)
P  = (0:7465); %Pressure load (Pa or N/M^2)
%E1 = 0.0001e6; %Elastic Modulus of PDMS material
t  = 0.09e-3; %Membrane thickness
v  = 0.47; %Poisson_'s ratio
Es  = 1.272e6;  %Square membrane elastic modulus
SRs = 0.034e6;%Square membrane residual stress
C2s = 1.94*(1-.271*v)/(1-v)
%global data
%start=[SRs Es];
%results=fmins('ftting',start);
```

```
%Es  = results(2);
%SRs = results(1);
SPressurefit=( ( 3.45*SRs*t*SDeflection)/a^2+....
(C2s*Es*t*SDeflection.^3)/a^4);
figure(2)
plot(data(:,1)*248.84,data(:,2)*1e-3, 'bs')% experimental data
hold on
plot(SPressurefit,SDeflection,'r-')%;legend('Theory')
%title(sprintf('SRs=%5.5f Es=%5.5f',SRs,Es))
title('PDMS Square Membrane - E=1.272MPa, Rs=0.034MPa','fontsize',8);
xlabel('Pressure (N/m^2)','fontsize',8)
ylabel('Deflection (m)','fontsize',8)
axis([0 8500 0 10e-3])
```

B.1.5.6 LLDPE square membrane program

```
%  POLYETHYLENE LLDPE
%Membrane analysis program (Square)
%Patrick Roman 04.14.03
%This program plots the load deflection of Square membranes.
%Fitting is possible to determine E and the residual stress of LLDPE.
%experimental data set 3 was used for LLDPE at t=.001" or .025e-3 M
%SI units only
close all
clear all
%  Variables
a=9.52e-3 %average membrane radius (mm)
P=(0:100:7465); %Pressure load (Pa or N/M^2)
E1=1.45e6; %Elastic Modulus of PDMS material
t=.025e-3; %Membrane thickness
v=.4; %Poisson's ratio
%Constant C2 calculation (Circular membrane)
C2c=(8/3)*(1.015-.247*v)/(1-v)
%C2c=6.1
%(Circular membrane) Deflection calculation
hc=((P*a^4)./(C2c*E1*t)).^(1/3);
%elastic modulus (circular)
Ec=((P*a^4)./(C2c*t*hc.^3));
%Copied PDMS data from experiment (Square)
data=[
0.0     0.000
1.0     0.478
2.0     0.631
4.0     0.940
6.0     1.133
8.0     1.292
10.0    1.408
12.0    1.507
14.0    1.586
16.0    1.704
18.0    1.850
20.0    1.930
22.0    2.000
```

```
24.0    2.081
26.0    2.123
28.0    2.250
30.0    2.360];
SPressure=data(:,1)*248.84;
SDeflection=data(:,2)*1e-3;
%Square bulge equation
%zz=(1:25);
a  = 9.52e-3 %average membrane radius (mm)
%P  = (0:7465); %Pressure load (Pa or N/M^2)
%E1 = 0.0001e6; %Elastic Modulus of PDMS material
t  = 0.025e-3; %Membrane thickness
v  = 0.4; %Poisson_'s ratio
C2s = 1.94*(1-.271*v)/(1-v)
Es  = 72e6;  %Square membrane elastic modulus
SRs = .55e6;%Square membrane residual stress
%global data
%start=[SRs Es];
%results=fmins('ftting',start);
%Es  = results(2);
%SRs = results(1);
SPressurefit=( ( 3.45*SRs*t*SDeflection)/a^2+...
(C2s*Es*t*SDeflection.^3)/a^4);
figure(2)
plot(data(:,1)*248.84,data(:,2)*1e-3,'bs')% experimental data
hold on
plot(SPressurefit,SDeflection,'k-')%;legend('Theory')
%title(sprintf('SRs=%5.5f Es=%5.5f',SRs,Es))
title('LLDPE Square Membrane - E=72MPa, Rs=0.55MPa','fontsize',8);
xlabel('Pressure (N/m^2)','fontsize',8)
ylabel('Deflection (m)','fontsize',8)
axis([0 8500 0 3.5e-3])
```

Appendix C
Analysis program results

C.1 Data analysis results

Data analysis results generated by the Matlab analysis programs in appendix B were expressed in numeric and graphical forms. This appendix contains program numerical output values and example graphical results for the analysis performed.

C.1.1 Dynamic uniaxial tension *A* sample numeric results

The results below were generated by the Matlab program (Phasediff1bb.m). This program was designed to analyze dynamic uniaxial tension test data. The results are listed for each *A* sample run and correspond to the text data file name and dynamic frequency at which the samples were tested. For example, the result below of `Pdmst_025.txt` corresponds to the sample tested at 0.25Hz of the "*A*" group of samples. The next result `Pdmst_05.txt` corresponds to the sample tested at 0.5Hz of the "*A*" group of samples, and so on increasing in test frequency. There are five groups of samples, one group for each of the five samples tested per frequency.

PDMS Dynamic uniaxial tension analysis – Matlab results
Matlab program (phasediff1bb.m)
A samples – [Group A]

Pdmst_025.txt

```
OPERATOR - Patrick Roman 20 Aug 2001
To center selected data about zero,
        0.873 was added to Stress and
        0.909 was added to Strain
From an average over 1 complete cycles:
        The frequency is 0.25 Hz
        Magnitude ratio is 1.0327
        Phase difference is 358.2839 degrees
        Tan delta is -0.0301
Modulus (mean +/- SD) = 2.377e+006 +/- 6.060e+006 Nm^-2 (average slope as function of strain)
        Maximum Slope = 9.650e+007  Nm^-2
        Minimum Slope = 3.501e+005  Nm^-2
Storage modulus (mean +/- SD) = 2.376e+006 +/- 6.057e+006 Nm^-2
Loss modulus (mean +/- SD) = 7.144e+004 +/- 1.821e+005 Nm^-2
Maximum Engineering Stress = 2.608e+005 Nm^-2
Minimum Engineering Stress = 2.027e+005 Nm^-2
Maximum Percent Engineering Strain = 2.292e+001
Minimum Percent Engineering Strain = 1.874e+001
Maximum True Stress = 3.205e+005 Nm^-2
Minimum True Stress = 2.407e+005 Nm^-2
Maximum Percent True Strain = 1.865e+001
Minimum Percent True Strain = 1.578e+001
```

Pdmst_05.txt

```
        OPERATOR - Patrick Roman 20 Aug 2001
Input width of specimen in meters>6e-3
Input thickness of specimen in meters>1.15e-3
Input gauge length in mm>48
To center selected data about zero,
        0.902 was added to Stress and
        0.909 was added to Strain
From an average over 3 complete cycles:
        The frequency is 0.50 Hz
        Magnitude ratio is 1.0240
        Phase difference is 356.1869 degrees
        Tan delta is -0.0668
Modulus (mean +/- SD) = 1.806e+006 +/- 1.411e+006 Nm^-2 (average slope as function of strain)
        Maximum Slope = 1.516e+007  Nm^-2
        Minimum Slope = 4.542e+005  Nm^-2
Storage modulus (mean +/- SD) = 1.802e+006 +/- 1.408e+006 Nm^-2
Loss modulus (mean +/- SD) = 1.203e+005 +/- 9.396e+004 Nm^-2
Maximum Engineering Stress = 3.430e+005 Nm^-2
Minimum Engineering Stress = 2.773e+005 Nm^-2
Maximum Percent Engineering Strain = 2.292e+001
Minimum Percent Engineering Strain = 1.874e+001
Maximum True Stress = 4.216e+005 Nm^-2
Minimum True Stress = 3.293e+005 Nm^-2
Maximum Percent True Strain = 1.865e+001
Minimum Percent True Strain = 1.578e+001
```

Pdmst_1.txt

```
OPERATOR - Patrick Roman 20 Aug 2001
Input width of specimen in meters>6e-3
Input thickness of specimen in meters>1.54e-3
Input gauge length in mm>48
To center selected data about zero,
        0.901 was added to Stress and
        0.909 was added to Strain
From an average over 4 complete cycles:
        The frequency is 1.00 Hz
        Magnitude ratio is 1.0728
        Phase difference is 355.3822 degrees
        Tan delta is -0.0809
Modulus (mean +/- SD) = 1.598e+006 +/- 3.401e+005 Nm^-2 (average slope as function of strain)
        Maximum Slope = 3.951e+006  Nm^-2
        Minimum Slope = 6.718e+005  Nm^-2
Storage modulus (mean +/- SD) = 1.593e+006 +/- 3.390e+005 Nm^-2
Loss modulus (mean +/- SD) = 1.288e+005 +/- 2.741e+004 Nm^-2
Maximum Engineering Stress = 3.343e+005 Nm^-2
Minimum Engineering Stress = 2.679e+005 Nm^-2
Maximum Percent Engineering Strain = 2.293e+001
Minimum Percent Engineering Strain = 1.873e+001
Maximum True Stress = 4.110e+005 Nm^-2
Minimum True Stress = 3.181e+005 Nm^-2
Maximum Percent True Strain = 1.866e+001
Minimum Percent True Strain = 1.577e+001
```

Pdmst_2.txt

```
OPERATOR - Patrick Roman 20 Aug 2001
Input width of specimen in meters>6e-3
Input thickness of specimen in meters>1.4e-3
Input gauge length in mm>48
To center selected data about zero,
        0.786 was added to Stress and
        0.908 was added to Strain
From an average over 3 complete cycles:
        The frequency is 2.00 Hz
        Magnitude ratio is 1.8897
        Phase difference is -2.7011 degrees
        Tan delta is -0.0472
Modulus (mean +/- SD) = 1.244e+006 +/- 1.453e+005 Nm^-2 (average slope as function of strain)
        Maximum Slope = 1.612e+006  Nm^-2
        Minimum Slope = 8.304e+005  Nm^-2
Storage modulus (mean +/- SD) = 1.243e+006 +/- 1.451e+005 Nm^-2
Loss modulus (mean +/- SD) = 5.863e+004 +/- 6.845e+003 Nm^-2
Maximum Engineering Stress = 1.540e+005 Nm^-2
Minimum Engineering Stress = 9.436e+004 Nm^-2
Maximum Percent Engineering Strain = 2.295e+001
Minimum Percent Engineering Strain = 1.873e+001
Maximum True Stress = 1.892e+005 Nm^-2
Minimum True Stress = 1.121e+005 Nm^-2
Maximum Percent True Strain = 1.871e+001
Minimum Percent True Strain = 1.573e+001
```

Pdmst_3.txt

```
OPERATOR - Patrick Roman 20 Aug 2001
Input width of specimen in meters>6e-3
Input thickness of specimen in meters>1.29e-3
Input gauge length in mm>48
To center selected data about zero,
        0.793 was added to Stress and
        0.910 was added to Strain
From an average over 3 complete cycles:
        The frequency is 3.00 Hz
        Magnitude ratio is 2.0004
        Phase difference is -3.2299 degrees
        Tan delta is -0.0564
Modulus (mean +/- SD) = 1.227e+006 +/- 1.057e+005 Nm^-2 (average slope as function of strain)
        Maximum Slope = 1.517e+006  Nm^-2
        Minimum Slope = 1.036e+006  Nm^-2
Storage modulus (mean +/- SD) = 1.225e+006 +/- 1.055e+005 Nm^-2
Loss modulus (mean +/- SD) = 6.913e+004 +/- 5.954e+003 Nm^-2
Maximum Engineering Stress = 1.392e+005 Nm^-2
Minimum Engineering Stress = 8.236e+004 Nm^-2
Maximum Percent Engineering Strain = 2.296e+001
Minimum Percent Engineering Strain = 1.875e+001
Maximum True Stress = 1.712e+005 Nm^-2
Minimum True Stress = 9.780e+004 Nm^-2
Maximum Percent True Strain = 1.873e+001
Minimum Percent True Strain = 1.564e+001
```

Pdmst_4.txt

```
        OPERATOR - Patrick Roman 20 Aug 2001
Input width of specimen in meters>6e-3
Input thickness of specimen in meters>1.14e-3
Input gauge length in mm>48
To center selected data about zero,
        0.779 was added to Stress and
        0.909 was added to Strain
From an average over 2 complete cycles:
        The frequency is 4.00 Hz
        Magnitude ratio is 2.0630
        Phase difference is -2.1375 degrees
        Tan delta is -0.0373
Modulus (mean +/- SD) = 1.405e+006 +/- 9.337e+004 Nm^-2 (average slope as function of strain)
        Maximum Slope = 1.600e+006  Nm^-2
        Minimum Slope = 1.214e+006  Nm^-2
Storage modulus (mean +/- SD) = 1.404e+006 +/- 9.330e+004 Nm^-2
Loss modulus (mean +/- SD) = 5.242e+004 +/- 3.482e+003 Nm^-2
Maximum Engineering Stress = 1.592e+005 Nm^-2
Minimum Engineering Stress = 9.319e+004 Nm^-2
Maximum Percent Engineering Strain = 2.289e+001
Minimum Percent Engineering Strain = 1.876e+001
Maximum True Stress = 1.957e+005 Nm^-2
Minimum True Stress = 1.108e+005 Nm^-2
Maximum Percent True Strain = 1.886e+001
Minimum Percent True Strain = 1.556e+001
```

Pdmst_5.txt

```
OPERATOR - Patrick Roman 20 Aug 2001
Input width of specimen in meters>6e-3
Input thickness of specimen in meters>1.68e-3
Input gauge length in mm>48
To center selected data about zero,
        0.602 was added to Stress and
        0.903 was added to Strain
From an average over 2 complete cycles:
        The frequency is 5.00 Hz
        Magnitude ratio is 4.3662
        Phase difference is 351.4361 degrees
        Tan delta is -0.1507
Modulus (mean +/- SD) = 8.415e+005 +/- 1.150e+004 Nm^-2 (average slope as function of strain)
        Maximum Slope = 8.659e+005  Nm^-2
        Minimum Slope = 8.102e+005  Nm^-2
Storage modulus (mean +/- SD) = 8.321e+005 +/- 1.138e+004 Nm^-2
Loss modulus (mean +/- SD) = 1.254e+005 +/- 1.714e+003 Nm^-2
Maximum Engineering Stress = 4.618e+004 Nm^-2
Minimum Engineering Stress = -1.374e+004 Nm^-2
Maximum Percent Engineering Strain = 2.307e+001
Minimum Percent Engineering Strain = 1.745e+001
Maximum True Stress = 5.683e+004 Nm^-2
Minimum True Stress = -1.613e+004 Nm^-2
Maximum Percent True Strain = 1.885e+001
Minimum Percent True Strain = 1.485e+001
```

A samples - [Group B]

Pdmst_025b.txt

```
OPERATOR - Patrick Roman 27 Aug 2001
Input width of specimen in meters>6e-3
Input thickness of specimen in meters>1.36e-3
Input gauge length in mm>48
To center selected data about zero,
        0.859 was added to Stress and
        0.909 was added to Strain
From an average over 3 complete cycles:
        The frequency is 0.25 Hz
        Magnitude ratio is 1.1307
        Phase difference is 358.2384 degrees
        Tan delta is -0.0309
Modulus (mean +/- SD) = 2.328e+006 +/- 7.008e+006 Nm^-2 (average slope as function of strain)
        Maximum Slope = 9.403e+007  Nm^-2
        Minimum Slope = 1.293e+005  Nm^-2
Storage modulus (mean +/- SD) = 2.327e+006 +/- 7.005e+006 Nm^-2
Loss modulus (mean +/- SD) = 7.181e+004 +/- 2.162e+005 Nm^-2
Maximum Engineering Stress = 1.653e+005 Nm^-2
Minimum Engineering Stress = 1.239e+005 Nm^-2
Maximum Percent Engineering Strain = 2.292e+001
Minimum Percent Engineering Strain = 1.874e+001
Maximum True Stress = 2.032e+005 Nm^-2
Minimum True Stress = 1.472e+005 Nm^-2
Maximum Percent True Strain = 1.865e+001
Minimum Percent True Strain = 1.578e+001
```

Pdmst_05.txt

```
        OPERATOR - Patrick Roman 27 Aug 2001
Input width of specimen in meters>6e-3
Input thickness of specimen in meters>1.22e-3
Input gauge length in mm>48
To center selected data about zero,
        0.885 was added to Stress and
        0.909 was added to Strain
From an average over 4 complete cycles:
        The frequency is 0.50 Hz
        Magnitude ratio is 0.9510
        Phase difference is -0.0009 degrees
        Tan delta is -0.0000
Modulus (mean +/- SD) = 1.808e+006 +/- 1.582e+006 Nm^-2 (average slope as function of strain)
        Maximum Slope = 2.100e+007  Nm^-2
        Minimum Slope = 4.642e+005  Nm^-2
Storage modulus (mean +/- SD) = 1.808e+006 +/- 1.582e+006 Nm^-2
Loss modulus (mean +/- SD) = 2.772e+001 +/- 2.426e+001 Nm^-2
Maximum Engineering Stress = 3.583e+005 Nm^-2
Minimum Engineering Stress = 2.837e+005 Nm^-2
Maximum Percent Engineering Strain = 2.293e+001
Minimum Percent Engineering Strain = 1.874e+001
Maximum True Stress = 4.404e+005 Nm^-2
Minimum True Stress = 3.368e+005 Nm^-2
Maximum Percent True Strain = 1.865e+001
Minimum Percent True Strain = 1.578e+001
```

Pdmst_1.txt

```
OPERATOR - Patrick Roman 27 Aug 2001
Input width of specimen in meters>6e-3
Input thickness of specimen in meters>1.48e-3
Input gauge length in mm>48
To center selected data about zero,
        0.875 was added to Stress and
        0.908 was added to Strain
From an average over 2 complete cycles:
        The frequency is 1.00 Hz
        Magnitude ratio is 1.0106
        Phase difference is 0.2422 degrees
        Tan delta is 0.0042
Modulus (mean +/- SD) = 1.503e+006 +/- 3.310e+005 Nm^-2 (average slope as function of strain)
        Maximum Slope = 3.850e+006  Nm^-2
        Minimum Slope = 6.774e+005  Nm^-2
Storage modulus (mean +/- SD) = 1.503e+006 +/- 3.310e+005 Nm^-2
Loss modulus (mean +/- SD) = 6.354e+003 +/- 1.399e+003 Nm^-2
Maximum Engineering Stress = 3.329e+005 Nm^-2
Minimum Engineering Stress = 2.589e+005 Nm^-2
Maximum Percent Engineering Strain = 2.293e+001
Minimum Percent Engineering Strain = 1.873e+001
Maximum True Stress = 4.092e+005 Nm^-2
Minimum True Stress = 3.074e+005 Nm^-2
Maximum Percent True Strain = 1.866e+001
Minimum Percent True Strain = 1.577e+001
```

Pdmst_2.txt

```
OPERATOR - Patrick Roman 27 Aug 2001
Input width of specimen in meters>6e-3
Input thickness of specimen in meters>1.17e-3
Input gauge length in mm>48
To center selected data about zero,
        0.769 was added to Stress and
        0.908 was added to Strain
From an average over 1 complete cycles:
        The frequency is 2.00 Hz
        Magnitude ratio is 2.0530
        Phase difference is -3.0966 degrees
        Tan delta is -0.0541
Modulus (mean +/- SD) = 1.367e+006 +/- 1.640e+005 Nm^-2 (average slope as function of strain)
        Maximum Slope = 1.977e+006  Nm^-2
        Minimum Slope = 9.652e+005  Nm^-2
Storage modulus (mean +/- SD) = 1.365e+006 +/- 1.637e+005 Nm^-2
Loss modulus (mean +/- SD) = 7.382e+004 +/- 8.858e+003 Nm^-2
Maximum Engineering Stress = 1.501e+005 Nm^-2
Minimum Engineering Stress = 8.636e+004 Nm^-2
Maximum Percent Engineering Strain = 2.295e+001
Minimum Percent Engineering Strain = 1.873e+001
Maximum True Stress = 1.845e+005 Nm^-2
Minimum True Stress = 1.025e+005 Nm^-2
Maximum Percent True Strain = 1.870e+001
Minimum Percent True Strain = 1.573e+001
```

Pdmst_3.txt

```
OPERATOR - Patrick Roman 27 Aug 2001
Input width of specimen in meters>6e-3
Input thickness of specimen in meters>1.23e-3
Input gauge length in mm>48
To center selected data about zero,
        0.787 was added to Stress and
        0.910 was added to Strain
From an average over 2 complete cycles:
        The frequency is 3.00 Hz
        Magnitude ratio is 2.0042
        Phase difference is -2.5072 degrees
        Tan delta is -0.0438
Modulus (mean +/- SD) = 1.350e+006 +/- 1.298e+005 Nm^-2 (average slope as function of strain)
        Maximum Slope = 1.671e+006  Nm^-2
        Minimum Slope = 1.002e+006  Nm^-2
Storage modulus (mean +/- SD) = 1.349e+006 +/- 1.297e+005 Nm^-2
Loss modulus (mean +/- SD) = 5.907e+004 +/- 5.677e+003 Nm^-2
Maximum Engineering Stress = 1.540e+005 Nm^-2
Minimum Engineering Stress = 9.333e+004 Nm^-2
Maximum Percent Engineering Strain = 2.295e+001
Minimum Percent Engineering Strain = 1.874e+001
Maximum True Stress = 1.893e+005 Nm^-2
Minimum True Stress = 1.108e+005 Nm^-2
Maximum Percent True Strain = 1.875e+001
Minimum Percent True Strain = 1.564e+001
```

Pdmst_4.txt

```
OPERATOR - Patrick Roman 27 Aug 2001
Input width of specimen in meters>6e-3
Input thickness of specimen in meters>1.2e-3
Input gauge length in mm>48
To center selected data about zero,
        0.782 was added to Stress and
        0.910 was added to Strain
From an average over 3 complete cycles:
        The frequency is 4.00 Hz
        Magnitude ratio is 2.0980
        Phase difference is -2.4435 degrees
        Tan delta is -0.0427
Modulus (mean +/- SD) = 1.305e+006 +/- 9.352e+004 Nm^-2 (average slope as function of strain)
        Maximum Slope = 1.514e+006  Nm^-2
        Minimum Slope = 1.118e+006  Nm^-2
Storage modulus (mean +/- SD) = 1.304e+006 +/- 9.343e+004 Nm^-2
Loss modulus (mean +/- SD) = 5.565e+004 +/- 3.987e+003 Nm^-2
Maximum Engineering Stress = 1.439e+005 Nm^-2
Minimum Engineering Stress = 8.213e+004 Nm^-2
Maximum Percent Engineering Strain = 2.289e+001
Minimum Percent Engineering Strain = 1.876e+001
Maximum True Stress = 1.770e+005 Nm^-2
Minimum True Stress = 9.761e+004 Nm^-2
Maximum Percent True Strain = 1.885e+001
Minimum Percent True Strain = 1.556e+001
```

Pdmst_5.txt

```
OPERATOR - Patrick Roman 27 Aug 2001
Input width of specimen in meters>6e-3
Input thickness of specimen in meters>1.45e-3
Input gauge length in mm>48
To center selected data about zero,
        0.842 was added to Stress and
        0.910 was added to Strain
From an average over 3 complete cycles:
        The frequency is 5.00 Hz
        Magnitude ratio is 1.4333
        Phase difference is -2.0229 degrees
        Tan delta is -0.0353
Modulus (mean +/- SD) = 1.608e+006 +/- 1.036e+005 Nm^-2 (average slope as function of strain)
        Maximum Slope = 1.794e+006  Nm^-2
        Minimum Slope = 1.476e+006  Nm^-2
Storage modulus (mean +/- SD) = 1.607e+006 +/- 1.035e+005 Nm^-2
Loss modulus (mean +/- SD) = 5.677e+004 +/- 3.657e+003 Nm^-2
Maximum Engineering Stress = 2.592e+005 Nm^-2
Minimum Engineering Stress = 1.845e+005 Nm^-2
Maximum Percent Engineering Strain = 2.289e+001
Minimum Percent Engineering Strain = 1.874e+001
Maximum True Stress = 3.190e+005 Nm^-2
Minimum True Stress = 2.192e+005 Nm^-2
Maximum Percent True Strain = 1.886e+001
Minimum Percent True Strain = 1.554e+001
```

A samples - [Group C]

Pdmst_025c.txt

```
OPERATOR - Patrick Roman 27 Aug 2001
Input width of specimen in meters>6e-3
Input thickness of specimen in meters>1.53e-3
Input gauge length in mm>48
To center selected data about zero,
        0.857 was added to Stress and
        0.909 was added to Strain
From an average over 1 complete cycles:
        The frequency is 0.25 Hz
        Magnitude ratio is 1.0514
        Phase difference is 0.2303 degrees
        Tan delta is 0.0040
Modulus (mean +/- SD) = 2.136e+006 +/- 5.911e+006 Nm^-2 (average slope as function of strain)
        Maximum Slope = 8.491e+007  Nm^-2
        Minimum Slope = 1.303e+005  Nm^-2
Storage modulus (mean +/- SD) = 2.136e+006 +/- 5.911e+006 Nm^-2
Loss modulus (mean +/- SD) = 8.587e+003 +/- 2.376e+004 Nm^-2
Maximum Engineering Stress = 1.726e+005 Nm^-2
Minimum Engineering Stress = 1.308e+005 Nm^-2
Maximum Percent Engineering Strain = 2.292e+001
Minimum Percent Engineering Strain = 1.875e+001
Maximum True Stress = 2.121e+005 Nm^-2
Minimum True Stress = 1.553e+005 Nm^-2
Maximum Percent True Strain = 1.865e+001
Minimum Percent True Strain = 1.578e+001
```

Pdmst_05.txt

```
OPERATOR - Patrick Roman 27 Aug 2001
Input width of specimen in meters>6e-3
Input thickness of specimen in meters>1.20e-3
Input gauge length in mm>48
To center selected data about zero,
        0.878 was added to Stress and
        0.909 was added to Strain
From an average over 1 complete cycles:
        The frequency is 0.50 Hz
        Magnitude ratio is 1.0213
        Phase difference is 359.5977 degrees
        Tan delta is -0.0071
Modulus (mean +/- SD) = 1.896e+006 +/- 1.716e+006 Nm^-2 (average slope as function of strain)
        Maximum Slope = 2.683e+007  Nm^-2
        Minimum Slope = 4.981e+005  Nm^-2
Storage modulus (mean +/- SD) = 1.896e+006 +/- 1.716e+006 Nm^-2
Loss modulus (mean +/- SD) = 1.351e+004 +/- 1.223e+004 Nm^-2
Maximum Engineering Stress = 3.490e+005 Nm^-2
Minimum Engineering Stress = 2.733e+005 Nm^-2
Maximum Percent Engineering Strain = 2.292e+001
Minimum Percent Engineering Strain = 1.874e+001
Maximum True Stress = 4.290e+005 Nm^-2
Minimum True Stress = 3.245e+005 Nm^-2
Maximum Percent True Strain = 1.865e+001
Minimum Percent True Strain = 1.578e+001
```

Pdmst_1.txt

```
OPERATOR - Patrick Roman 27 Aug 2001
Input width of specimen in meters>6e-3
Input thickness of specimen in meters>1.38e-3
Input gauge length in mm>48
To center selected data about zero,
        0.880 was added to Stress and
        0.908 was added to Strain
From an average over 2 complete cycles:
        The frequency is 1.00 Hz
        Magnitude ratio is 0.9622
        Phase difference is 0.6369 degrees
        Tan delta is 0.0111
Modulus (mean +/- SD) = 1.515e+006 +/- 2.269e+005 Nm^-2 (average slope as function of strain)
        Maximum Slope = 2.370e+006  Nm^-2
        Minimum Slope = 7.241e+005  Nm^-2
Storage modulus (mean +/- SD) = 1.515e+006 +/- 2.269e+005 Nm^-2
Loss modulus (mean +/- SD) = 1.684e+004 +/- 2.522e+003 Nm^-2
Maximum Engineering Stress = 3.604e+005 Nm^-2
Minimum Engineering Stress = 2.850e+005 Nm^-2
Maximum Percent Engineering Strain = 2.293e+001
Minimum Percent Engineering Strain = 1.873e+001
Maximum True Stress = 4.431e+005 Nm^-2
Minimum True Stress = 3.384e+005 Nm^-2
Maximum Percent True Strain = 1.866e+001
Minimum Percent True Strain = 1.577e+001
```

Pdmst_2.txt

```
OPERATOR - Patrick Roman 27 Aug 2001
Input width of specimen in meters>6e-3
Input thickness of specimen in meters>1.42e-3
Input gauge length in mm>48
To center selected data about zero,
        0.786 was added to Stress and
        0.908 was added to Strain
From an average over 1 complete cycles:
        The frequency is 2.00 Hz
        Magnitude ratio is 1.9266
        Phase difference is -2.0905 degrees
        Tan delta is -0.0365
Modulus (mean +/- SD) = 1.246e+006 +/- 1.412e+005 Nm^-2 (average slope as function of strain)
        Maximum Slope = 1.546e+006  Nm^-2
        Minimum Slope = 8.540e+005  Nm^-2
Storage modulus (mean +/- SD) = 1.245e+006 +/- 1.411e+005 Nm^-2
Loss modulus (mean +/- SD) = 4.545e+004 +/- 5.149e+003 Nm^-2
Maximum Engineering Stress = 1.491e+005 Nm^-2
Minimum Engineering Stress = 9.023e+004 Nm^-2
Maximum Percent Engineering Strain = 2.295e+001
Minimum Percent Engineering Strain = 1.873e+001
Maximum True Stress = 1.833e+005 Nm^-2
Minimum True Stress = 1.072e+005 Nm^-2
Maximum Percent True Strain = 1.870e+001
Minimum Percent True Strain = 1.571e+001
```

Pdmst_3.txt

```
OPERATOR - Patrick Roman 27 Aug 2001
Input width of specimen in meters>6e-3
Input thickness of specimen in meters>1.21e-3
Input gauge length in mm>48
To center selected data about zero,
        0.774 was added to Stress and
        0.910 was added to Strain
From an average over 1 complete cycles:
        The frequency is 3.00 Hz
        Magnitude ratio is 2.1212
        Phase difference is -1.2756 degrees
        Tan delta is -0.0223
Modulus (mean +/- SD) = 1.320e+006 +/- 1.276e+005 Nm^-2 (average slope as function of strain)
        Maximum Slope = 1.687e+006  Nm^-2
        Minimum Slope = 1.092e+006  Nm^-2
Storage modulus (mean +/- SD) = 1.320e+006 +/- 1.276e+005 Nm^-2
Loss modulus (mean +/- SD) = 2.939e+004 +/- 2.841e+003 Nm^-2
Maximum Engineering Stress = 1.418e+005 Nm^-2
Minimum Engineering Stress = 8.145e+004 Nm^-2
Maximum Percent Engineering Strain = 2.295e+001
Minimum Percent Engineering Strain = 1.869e+001
Maximum True Stress = 1.743e+005 Nm^-2
Minimum True Stress = 9.667e+004 Nm^-2
Maximum Percent True Strain = 1.873e+001
Minimum Percent True Strain = 1.566e+001
```

Pdmst_4.txt

```
OPERATOR - Patrick Roman 27 Aug 2001
Input width of specimen in meters>6e-3
Input thickness of specimen in meters>1.18e-3
Input gauge length in mm>48
To center selected data about zero,
        0.799 was added to Stress and
        0.911 was added to Strain
From an average over 3 complete cycles:
        The frequency is 4.00 Hz
        Magnitude ratio is 1.8677
        Phase difference is -2.4176 degrees
        Tan delta is -0.0422
Modulus (mean +/- SD) = 1.387e+006 +/- 9.710e+004 Nm^-2 (average slope as function of strain)
        Maximum Slope = 1.594e+006  Nm^-2
        Minimum Slope = 1.189e+006  Nm^-2
Storage modulus (mean +/- SD) = 1.385e+006 +/- 9.701e+004 Nm^-2
Loss modulus (mean +/- SD) = 5.848e+004 +/- 4.096e+003 Nm^-2
Maximum Engineering Stress = 1.741e+005 Nm^-2
Minimum Engineering Stress = 1.060e+005 Nm^-2
Maximum Percent Engineering Strain = 2.288e+001
Minimum Percent Engineering Strain = 1.877e+001
Maximum True Stress = 2.141e+005 Nm^-2
Minimum True Stress = 1.260e+005 Nm^-2
Maximum Percent True Strain = 1.886e+001
Minimum Percent True Strain = 1.555e+001
```

Pdmst_5.txt

```
OPERATOR - Patrick Roman 27 Aug 2001
Input width of specimen in meters>6e-3
Input thickness of specimen in meters>1.37e-3
Input gauge length in mm>48
To center selected data about zero,
        0.828 was added to Stress and
        0.910 was added to Strain
From an average over 2 complete cycles:
        The frequency is 5.00 Hz
        Magnitude ratio is 1.6587
        Phase difference is 357.9089 degrees
        Tan delta is -0.0366
Modulus (mean +/- SD) = 1.700e+006 +/- 2.435e+004 Nm^-2 (average slope as function of strain)
        Maximum Slope = 1.773e+006  Nm^-2
        Minimum Slope = 1.643e+006  Nm^-2
Storage modulus (mean +/- SD) = 1.699e+006 +/- 2.434e+004 Nm^-2
Loss modulus (mean +/- SD) = 6.222e+004 +/- 8.912e+002 Nm^-2
Maximum Engineering Stress = 2.214e+005 Nm^-2
Minimum Engineering Stress = 1.474e+005 Nm^-2
Maximum Percent Engineering Strain = 2.290e+001
Minimum Percent Engineering Strain = 1.867e+001
Maximum True Stress = 2.725e+005 Nm^-2
Minimum True Stress = 1.750e+005 Nm^-2
Maximum Percent True Strain = 1.882e+001
Minimum Percent True Strain = 1.559e+001
```

A samples - [Group D]

Pdmst_025d.txt

```
OPERATOR - Patrick Roman 27 Aug 2001
Input width of specimen in meters>6e-3
Input thickness of specimen in meters>1.51e-3
Input gauge length in mm>48
To center selected data about zero,
        0.874 was added to Stress and
        0.909 was added to Strain
From an average over 2 complete cycles:
        The frequency is 0.25 Hz
        Magnitude ratio is 1.0800
        Phase difference is 0.7833 degrees
        Tan delta is 0.0137
Modulus (mean +/- SD) = 2.364e+006 +/- 9.119e+006 Nm^-2 (average slope as function of strain)
        Maximum Slope = 1.943e+008  Nm^-2
        Minimum Slope = 1.522e+005  Nm^-2
Storage modulus (mean +/- SD) = 2.363e+006 +/- 9.118e+006 Nm^-2
Loss modulus (mean +/- SD) = 3.231e+004 +/- 1.247e+005 Nm^-2
Maximum Engineering Stress = 1.438e+005 Nm^-2
Minimum Engineering Stress = 1.075e+005 Nm^-2
Maximum Percent Engineering Strain = 2.292e+001
Minimum Percent Engineering Strain = 1.875e+001
Maximum True Stress = 1.767e+005 Nm^-2
Minimum True Stress = 1.276e+005 Nm^-2
Maximum Percent True Strain = 1.865e+001
Minimum Percent True Strain = 1.578e+001
```

Pdmst_05.txt

```
OPERATOR - Patrick Roman 27 Aug 2001
Input width of specimen in meters>6e-3
Input thickness of specimen in meters>1.73e-3
Input gauge length in mm>48
To center selected data about zero,
        0.876 was added to Stress and
        0.909 was added to Strain
From an average over 1 complete cycles:
        The frequency is 0.50 Hz
        Magnitude ratio is 0.9739
        Phase difference is 360.0956 degrees
        Tan delta is 0.0016
Modulus (mean +/- SD) = 1.401e+006 +/- 1.183e+006 Nm^-2 (average slope as function of strain)
        Maximum Slope = 2.091e+007  Nm^-2
        Minimum Slope = 3.863e+005  Nm^-2
Storage modulus (mean +/- SD) = 1.401e+006 +/- 1.183e+006 Nm^-2
Loss modulus (mean +/- SD) = 2.190e+003 +/- 1.848e+003 Nm^-2
Maximum Engineering Stress = 2.782e+005 Nm^-2
Minimum Engineering Stress = 2.183e+005 Nm^-2
Maximum Percent Engineering Strain = 2.292e+001
Minimum Percent Engineering Strain = 1.874e+001
Maximum True Stress = 3.419e+005 Nm^-2
Minimum True Stress = 2.593e+005 Nm^-2
Maximum Percent True Strain = 1.865e+001
Minimum Percent True Strain = 1.578e+00
```

Pdmst_1.txt

```
OPERATOR - Patrick Roman 27 Aug 2001
Input width of specimen in meters>6e-3
Input thickness of specimen in meters>1.48e-3
Input gauge length in mm>48
To center selected data about zero,
        0.881 was added to Stress and
        0.909 was added to Strain
From an average over 1 complete cycles:
        The frequency is 1.00 Hz
        Magnitude ratio is 0.9810
        Phase difference is -1.7521 degrees
        Tan delta is -0.0306
Modulus (mean +/- SD) = 1.545e+006 +/- 3.909e+005 Nm^-2 (average slope as function of strain)
        Maximum Slope = 4.042e+006  Nm^-2
        Minimum Slope = 7.627e+005  Nm^-2
Storage modulus (mean +/- SD) = 1.544e+006 +/- 3.907e+005 Nm^-2
Loss modulus (mean +/- SD) = 4.724e+004 +/- 1.195e+004 Nm^-2
Maximum Engineering Stress = 3.412e+005 Nm^-2
Minimum Engineering Stress = 2.697e+005 Nm^-2
Maximum Percent Engineering Strain = 2.293e+001
Minimum Percent Engineering Strain = 1.874e+001
Maximum True Stress = 4.193e+005 Nm^-2
Minimum True Stress = 3.203e+005 Nm^-2
Maximum Percent True Strain = 1.865e+001
Minimum Percent True Strain = 1.578e+00
```

Pdmst_2.txt

```
OPERATOR - Patrick Roman 27 Aug 2001
Input width of specimen in meters>6e-3
Input thickness of specimen in meters>1.25e-3
Input gauge length in mm>48
To center selected data about zero,
        0.764 was added to Stress and
        0.908 was added to Strain
From an average over 1 complete cycles:
        The frequency is 2.00 Hz
        Magnitude ratio is 2.0295
        Phase difference is -0.1312 degrees
        Tan delta is -0.0023
Modulus (mean +/- SD) = 1.317e+006 +/- 1.510e+005 Nm^-2 (average slope as function of strain)
        Maximum Slope = 1.753e+006  Nm^-2
        Minimum Slope = 7.924e+005  Nm^-2
Storage modulus (mean +/- SD) = 1.317e+006 +/- 1.510e+005 Nm^-2
Loss modulus (mean +/- SD) = 3.017e+003 +/- 3.457e+002 Nm^-2
Maximum Engineering Stress = 1.483e+005 Nm^-2
Minimum Engineering Stress = 8.545e+004 Nm^-2
Maximum Percent Engineering Strain = 2.296e+001
Minimum Percent Engineering Strain = 1.873e+001
Maximum True Stress = 1.823e+005 Nm^-2
Minimum True Stress = 1.016e+005 Nm^-2
Maximum Percent True Strain = 1.870e+001
Minimum Percent True Strain = 1.573e+001
```

Pdmst_3.txt

```
OPERATOR - Patrick Roman 27 Aug 2001
Input width of specimen in meters>6e-3
Input thickness of specimen in meters>1.55e-3
Input gauge length in mm>48
To center selected data about zero,
        0.813 was added to Stress and
        0.909 was added to Strain
From an average over 2 complete cycles:
        The frequency is 3.00 Hz
        Magnitude ratio is 1.7123
        Phase difference is -2.2899 degrees
        Tan delta is -0.0400
Modulus (mean +/- SD) = 1.303e+006 +/- 1.179e+005 Nm^-2 (average slope as function of strain)
        Maximum Slope = 1.619e+006  Nm^-2
        Minimum Slope = 1.095e+006  Nm^-2
Storage modulus (mean +/- SD) = 1.302e+006 +/- 1.179e+005 Nm^-2
Loss modulus (mean +/- SD) = 5.207e+004 +/- 4.713e+003 Nm^-2
Maximum Engineering Stress = 1.712e+005 Nm^-2
Minimum Engineering Stress = 1.105e+005 Nm^-2
Maximum Percent Engineering Strain = 2.296e+001
Minimum Percent Engineering Strain = 1.870e+001
Maximum True Stress = 2.105e+005 Nm^-2
Minimum True Stress = 1.311e+005 Nm^-2
Maximum Percent True Strain = 1.876e+001
Minimum Percent True Strain = 1.566e+001
```

Pdmst_4.txt

```
OPERATOR - Patrick Roman 27 Aug 2001
Input width of specimen in meters>6e-3
Input thickness of specimen in meters>1.08e-3
Input gauge length in mm>48
To center selected data about zero,
        0.692 was added to Stress and
        0.910 was added to Strain
From an average over 2 complete cycles:
        The frequency is 4.00 Hz
        Magnitude ratio is 3.0725
        Phase difference is 356.2377 degrees
        Tan delta is -0.0659
Modulus (mean +/- SD) = 1.288e+006 +/- 9.848e+004 Nm^-2 (average slope as function of strain)
        Maximum Slope = 1.528e+006  Nm^-2
        Minimum Slope = 1.106e+006  Nm^-2
Storage modulus (mean +/- SD) = 1.285e+006 +/- 9.826e+004 Nm^-2
Loss modulus (mean +/- SD) = 8.464e+004 +/- 6.472e+003 Nm^-2
Maximum Engineering Stress = 9.732e+004 Nm^-2
Minimum Engineering Stress = 4.057e+004 Nm^-2
Maximum Percent Engineering Strain = 2.289e+001
Minimum Percent Engineering Strain = 1.844e+001
Maximum True Stress = 1.199e+005 Nm^-2
Minimum True Stress = 4.815e+004 Nm^-2
Maximum Percent True Strain = 1.884e+001
Minimum Percent True Strain = 1.557e+001
```

Pdmst_5.txt

```
OPERATOR - Patrick Roman 27 Aug 2001
Input width of specimen in meters>6e-3
Input thickness of specimen in meters>1.60e-3
Input gauge length in mm>48
To center selected data about zero,
       0.834 was added to Stress and
       0.910 was added to Strain
From an average over 3 complete cycles:
       The frequency is 5.00 Hz
       Magnitude ratio is 1.5177
       Phase difference is -2.4947 degrees
       Tan delta is -0.0436
Modulus (mean +/- SD) = 1.652e+006 +/- 7.861e+004 Nm^-2 (average slope as
function of strain)
       Maximum Slope = 1.739e+006  Nm^-2
       Minimum Slope = 1.421e+006  Nm^-2
Storage modulus (mean +/- SD) = 1.650e+006 +/- 7.854e+004 Nm^-2
Loss modulus (mean +/- SD) = 7.190e+004 +/- 3.422e+003 Nm^-2
Maximum Engineering Stress = 2.376e+005 Nm^-2
Minimum Engineering Stress = 1.651e+005 Nm^-2
Maximum Percent Engineering Strain = 2.289e+001
Minimum Percent Engineering Strain = 1.878e+001
Maximum True Stress = 2.929e+005 Nm^-2
Minimum True Stress = 1.961e+005 Nm^-2
Maximum Percent True Strain = 1.886e+001
Minimum Percent True Strain = 1.555e+001
```

A samples – [Group E]

Pdmst_025e.txt

```
OPERATOR - Patrick Roman 27 Aug 2001
Input width of specimen in meters>6e-3
Input thickness of specimen in meters>1.65e-3
Input gauge length in mm>48
To center selected data about zero,
        0.860 was added to Stress and
        0.909 was added to Strain
From an average over 1 complete cycles:
        The frequency is 0.25 Hz
        Magnitude ratio is 1.0976
        Phase difference is 360.4245 degrees
        Tan delta is 0.0073
Modulus (mean +/- SD) = 1.847e+006 +/- 4.985e+006 Nm^-2 (average slope as function of strain)
        Maximum Slope = 1.090e+008  Nm^-2
        Minimum Slope = 1.737e+005  Nm^-2
Storage modulus (mean +/- SD) = 1.847e+006 +/- 4.985e+006 Nm^-2
Loss modulus (mean +/- SD) = 1.349e+004 +/- 3.641e+004 Nm^-2
Maximum Engineering Stress = 1.602e+005 Nm^-2
Minimum Engineering Stress = 1.210e+005 Nm^-2
Maximum Percent Engineering Strain = 2.293e+001
Minimum Percent Engineering Strain = 1.874e+001
Maximum True Stress = 1.969e+005 Nm^-2
Minimum True Stress = 1.437e+005 Nm^-2
Maximum Percent True Strain = 1.865e+001
Minimum Percent True Strain = 1.578e+001
```

Pdmst_05.txt

```
OPERATOR - Patrick Roman 27 Aug 2001
Input width of specimen in meters>6e-3
Input thickness of specimen in meters>1.72e-3
Input gauge length in mm>48
To center selected data about zero,
        0.876 was added to Stress and
        0.909 was added to Strain
From an average over 1 complete cycles:
        The frequency is 0.50 Hz
        Magnitude ratio is 0.9706
        Phase difference is 358.9593 degrees
        Tan delta is -0.0183
Modulus (mean +/- SD) = 1.518e+006 +/- 1.491e+006 Nm^-2 (average slope as function of strain)
        Maximum Slope = 2.281e+007  Nm^-2
        Minimum Slope = 1.913e+005  Nm^-2
Storage modulus (mean +/- SD) = 1.518e+006 +/- 1.491e+006 Nm^-2
Loss modulus (mean +/- SD) = 2.773e+004 +/- 2.723e+004 Nm^-2
Maximum Engineering Stress = 2.895e+005 Nm^-2
Minimum Engineering Stress = 2.272e+005 Nm^-2
Maximum Percent Engineering Strain = 2.292e+001
Minimum Percent Engineering Strain = 1.874e+001
Maximum True Stress = 3.557e+005 Nm^-2
Minimum True Stress = 2.698e+005 Nm^-2
Maximum Percent True Strain = 1.865e+001
Minimum Percent True Strain = 1.578e+001
```

Pdmst_1.txt

```
OPERATOR - Patrick Roman 27 Aug 2001
Input width of specimen in meters>6e-3
Input thickness of specimen in meters>1.26e-3
Input gauge length in mm>48
To center selected data about zero,
        0.875 was added to Stress and
        0.909 was added to Strain
From an average over 2 complete cycles:
        The frequency is 1.00 Hz
        Magnitude ratio is 1.0094
        Phase difference is -1.2587 degrees
        Tan delta is -0.0220
Modulus (mean +/- SD) = 1.407e+006 +/- 2.966e+005 Nm^-2 (average slope as function of strain)
        Maximum Slope = 3.407e+006  Nm^-2
        Minimum Slope = 3.842e+005  Nm^-2
Storage modulus (mean +/- SD) = 1.407e+006 +/- 2.965e+005 Nm^-2
Loss modulus (mean +/- SD) = 3.091e+004 +/- 6.515e+003 Nm^-2
Maximum Engineering Stress = 3.157e+005 Nm^-2
Minimum Engineering Stress = 2.465e+005 Nm^-2
Maximum Percent Engineering Strain = 2.293e+001
Minimum Percent Engineering Strain = 1.874e+001
Maximum True Stress = 3.879e+005 Nm^-2
Minimum True Stress = 2.927e+005 Nm^-2
Maximum Percent True Strain = 1.865e+001
Minimum Percent True Strain = 1.578e+001
```

Pdmst_2.txt

```
OPERATOR - Patrick Roman 27 Aug 2001
Input width of specimen in meters>6e-3
Input thickness of specimen in meters>1.19e-3
Input gauge length in mm>48
To center selected data about zero,
        0.694 was added to Stress and
        0.690 was added to Strain
From an average over 4 complete cycles:
        The frequency is 2.00 Hz
        Magnitude ratio is 1.2324
        Phase difference is 357.3667 degrees
        Tan delta is -0.0461
Modulus (mean +/- SD) = 1.355e+006 +/- 3.114e+005 Nm^-2 (average slope as function of strain)
        Maximum Slope = 3.805e+006  Nm^-2
        Minimum Slope = 5.504e+005  Nm^-2
Storage modulus (mean +/- SD) = 1.354e+006 +/- 3.111e+005 Nm^-2
Loss modulus (mean +/- SD) = 6.239e+004 +/- 1.434e+004 Nm^-2
Maximum Engineering Stress = 3.629e+005 Nm^-2
Minimum Engineering Stress = 4.408e+003 Nm^-2
Maximum Percent Engineering Strain = 3.033e+001
Minimum Percent Engineering Strain = 2.704e+000
Maximum True Stress = 4.731e+005 Nm^-2
Minimum True Stress = 4.522e+003 Nm^-2
Maximum Percent True Strain = 2.338e+001
Minimum Percent True Strain = 2.512e+000
```

Pdmst_3.txt

```
OPERATOR - Patrick Roman 27 Aug 2001
Input width of specimen in meters>6e-3
Input thickness of specimen in meters>1.44e-3
Input gauge length in mm>48
To center selected data about zero,
        0.799 was added to Stress and
        0.909 was added to Strain
From an average over 2 complete cycles:
        The frequency is 3.00 Hz
        Magnitude ratio is 1.8010
        Phase difference is -1.3640 degrees
        Tan delta is -0.0238
Modulus (mean +/- SD) = 1.319e+006 +/- 1.187e+005 Nm^-2 (average slope as function of strain)
        Maximum Slope = 1.659e+006  Nm^-2
        Minimum Slope = 1.090e+006  Nm^-2
Storage modulus (mean +/- SD) = 1.319e+006 +/- 1.187e+005 Nm^-2
Loss modulus (mean +/- SD) = 3.140e+004 +/- 2.826e+003 Nm^-2
Maximum Engineering Stress = 1.672e+005 Nm^-2
Minimum Engineering Stress = 1.048e+005 Nm^-2
Maximum Percent Engineering Strain = 2.296e+001
Minimum Percent Engineering Strain = 1.872e+001
Maximum True Stress = 2.056e+005 Nm^-2
Minimum True Stress = 1.245e+005 Nm^-2
Maximum Percent True Strain = 1.876e+001
Minimum Percent True Strain = 1.567e+00
```

Pdmst_4.txt

```
OPERATOR - Patrick Roman 27 Aug 2001
Input width of specimen in meters>6e-3
Input thickness of specimen in meters>1.21e-3
Input gauge length in mm>48
To center selected data about zero,
        0.766 was added to Stress and
        0.910 was added to Strain
From an average over 3 complete cycles:
        The frequency is 4.00 Hz
        Magnitude ratio is 2.2043
        Phase difference is -1.7998 degrees
        Tan delta is -0.0314
Modulus (mean +/- SD) = 1.285e+006 +/- 8.885e+004 Nm^-2 (average slope as function of strain)
        Maximum Slope = 1.475e+006  Nm^-2
        Minimum Slope = 1.017e+006  Nm^-2
Storage modulus (mean +/- SD) = 1.284e+006 +/- 8.881e+004 Nm^-2
Loss modulus (mean +/- SD) = 4.035e+004 +/- 2.791e+003 Nm^-2
Maximum Engineering Stress = 1.344e+005 Nm^-2
Minimum Engineering Stress = 7.278e+004 Nm^-2
Maximum Percent Engineering Strain = 2.288e+001
Minimum Percent Engineering Strain = 1.856e+001
Maximum True Stress = 1.655e+005 Nm^-2
Minimum True Stress = 8.629e+004 Nm^-2
Maximum Percent True Strain = 1.886e+001
Minimum Percent True Strain = 1.556e+001
```

Pdmst_5.txt

```
OPERATOR - Patrick Roman 27 Aug 2001
Input width of specimen in meters>6e-3
Input thickness of specimen in meters>1.21e-3
Input gauge length in mm>48
To center selected data about zero,
       0.787 was added to Stress and
       0.910 was added to Strain
From an average over 3 complete cycles:
       The frequency is 5.00 Hz
       Magnitude ratio is 1.9784
       Phase difference is -3.7930 degrees
       Tan delta is -0.0663
Modulus (mean +/- SD) = 1.289e+006 +/- 2.781e+004 Nm^-2 (average slope as
function of strain)
       Maximum Slope = 1.352e+006  Nm^-2
       Minimum Slope = 1.223e+006  Nm^-2
Storage modulus (mean +/- SD) = 1.286e+006 +/- 2.775e+004 Nm^-2
Loss modulus (mean +/- SD) = 8.526e+004 +/- 1.840e+003 Nm^-2
Maximum Engineering Stress = 1.635e+005 Nm^-2
Minimum Engineering Stress = 9.935e+004 Nm^-2
Maximum Percent Engineering Strain = 2.289e+001
Minimum Percent Engineering Strain = 1.873e+001
Maximum True Stress = 2.014e+005 Nm^-2
Minimum True Stress = 1.180e+005 Nm^-2
Maximum Percent True Strain = 1.885e+001
Minimum Percent True Strain = 1.557e+001
```

C.1.2 Dynamic uniaxial tension *B* sample numeric results

The results below were generated by the Matlab program (Phasediff1bb.m). This program was designed to analyze dynamic uniaxial tension test data. The results are listed for each *B* sample run and correspond to the text data file name and dynamic frequency at which the samples were tested. For example, the result below of `Dpdms_1A.txt` corresponds to the first "*A*" sample tested at 0.1Hz. Five samples were tested, A through E for each frequency. The next result set `Dpdms_1B.txt` corresponds to the next sample of the 0.1Hz group tested at 0.1Hz, and so on increasing in test frequency. There are six groups of samples with five sample per group per test frequency.

PDMS Dynamic uniaxial tension analysis – Matlab results
Matlab program (phasediff1bb.m)

B samples – [0.1Hz]

Dpdms Test2 Analysis log Roman – 11/18/01

Dpdms_1A

```
To center selected data about zero,
        0.545 was added to Stress and
        0.666 was added to Strain
From an average over 9 complete cycles:
        The frequency is 0.10 Hz
        Magnitude ratio is 1.0578
        Phase difference is -1099.0397 degrees
        Tan delta is -0.3447
Modulus (mean +/- SD) = 1.813e+007 +/- 8.003e+007 Nm^-2 (average slope as function of strain)
        Maximum Slope = 1.006e+009  Nm^-2
        Minimum Slope = 3.450e+005  Nm^-2
Storage modulus (mean +/- SD) = 1.714e+007 +/- 7.566e+007 Nm^-2
Loss modulus (mean +/- SD) = 5.909e+006 +/- 2.608e+007 Nm^-2
Maximum Engineering Stress = 1.099e+006 Nm^-2
Minimum Engineering Stress = 2.506e+005 Nm^-2
Maximum Percent Engineering Strain = 9.097e+001
Minimum Percent Engineering Strain = 3.030e+001
Maximum True Stress = 2.086e+006 Nm^-2
Minimum True Stress = 3.268e+005 Nm^-2
Maximum Percent True Strain = 4.764e+001
Minimum Percent True Strain = 2.325e+001
```

Dpdms_1B

```
W =0.0020
Input thickness of specimen in meters>.1e-3
Gauge =16.5000

To center selected data about zero,
        0.598 was added to Stress and
        0.667 was added to Strain
From an average over 11 complete cycles:
        The frequency is 0.10 Hz
        Magnitude ratio is 1.0601
        Phase difference is -1119.8915 degrees
        Tan delta is -0.8353
Modulus (mean +/- SD) = 1.676e+007 +/- 7.964e+007 Nm^-2 (average slope as function of strain)
        Maximum Slope = 1.441e+009  Nm^-2
        Minimum Slope = 2.354e+005  Nm^-2
Storage modulus (mean +/- SD) = 1.287e+007 +/- 6.112e+007 Nm^-2
Loss modulus (mean +/- SD) = 1.075e+007 +/- 5.106e+007 Nm^-2
Maximum Engineering Stress = 1.001e+006 Nm^-2
Minimum Engineering Stress = 2.374e+005 Nm^-2
Maximum Percent Engineering Strain = 9.088e+001
Minimum Percent Engineering Strain = 3.031e+001
Maximum True Stress = 1.909e+006 Nm^-2
Minimum True Stress = 3.110e+005 Nm^-2
Maximum Percent True Strain = 4.761e+001
Minimum Percent True Strain = 2.326e+001
```

Dpdms_1C

W =0.0020
Input thickness of specimen in meters>.1e-3
Gauge =16.5000

To center selected data about zero,
    0.542 was added to Stress and
    0.667 was added to Strain
From an average over 14 complete cycles:
    The frequency is 0.10 Hz
    Magnitude ratio is 1.0794
    Phase difference is -1522.1041 degrees
    Tan delta is -7.1869
Modulus (mean +/- SD) = 1.746e+007 +/- 8.404e+007 Nm^-2 (average slope as function of strain)
    Maximum Slope = 1.646e+009 Nm^-2
    Minimum Slope = 3.457e+005 Nm^-2
Storage modulus (mean +/- SD) = 2.406e+006 +/- 1.158e+007 Nm^-2
Loss modulus (mean +/- SD) = 1.729e+007 +/- 8.324e+007 Nm^-2
Maximum Engineering Stress = 1.046e+006 Nm^-2
Minimum Engineering Stress = 2.059e+005 Nm^-2
Maximum Percent Engineering Strain = 9.088e+001
Minimum Percent Engineering Strain = 3.032e+001
Maximum True Stress = 1.995e+006 Nm^-2
Minimum True Stress = 2.683e+005 Nm^-2
Maximum Percent True Strain = 4.761e+001
Minimum Percent True Strain = 2.325e+001

Dpdms_1D

W = 0.0020
Input thickness of specimen in meters>.1e-3
Gauge =16.5000

To center selected data about zero,
    0.581 was added to Stress and
    0.666 was added to Strain
From an average over 18 complete cycles:
    The frequency is 0.10 Hz
    Magnitude ratio is 1.0643
    Phase difference is -2002.1848 degrees
    Tan delta is -0.4071
Modulus (mean +/- SD) = 1.594e+007 +/- 7.114e+007 Nm^-2 (average slope as function of strain)
    Maximum Slope = 1.389e+009 Nm^-2
    Minimum Slope = 3.683e+005 Nm^-2
Storage modulus (mean +/- SD) = 1.476e+007 +/- 6.589e+007 Nm^-2
Loss modulus (mean +/- SD) = 6.009e+006 +/- 2.682e+007 Nm^-2
Maximum Engineering Stress = 9.901e+005 Nm^-2
Minimum Engineering Stress = 2.583e+005 Nm^-2
Maximum Percent Engineering Strain = 9.096e+001
Minimum Percent Engineering Strain = 3.030e+001
Maximum True Stress = 1.889e+006 Nm^-2
Minimum True Stress = 3.384e+005 Nm^-2
Maximum Percent True Strain = 4.764e+001
Minimum Percent True Strain = 2.325e+001

Dpdms_1E

```
W =0.0020
Input thickness of specimen in meters>.09e-3
Gauge =16.5000

To center selected data about zero,
        0.595 was added to Stress and
        0.667 was added to Strain
From an average over 14 complete cycles:
        The frequency is 0.10 Hz
        Magnitude ratio is 1.0543
        Phase difference is -1701.2881 degrees
        Tan delta is -6.5043
Modulus (mean +/- SD) = 2.011e+007 +/- 1.023e+008 Nm^-2 (average slope as function of strain)
        Maximum Slope = 1.658e+009  Nm^-2
        Minimum Slope = 3.929e+005  Nm^-2
Storage modulus (mean +/- SD) = 3.055e+006 +/- 1.555e+007 Nm^-2
Loss modulus (mean +/- SD) = 1.987e+007 +/- 1.011e+008 Nm^-2
Maximum Engineering Stress = 9.063e+005 Nm^-2
Minimum Engineering Stress = 2.054e+005 Nm^-2
Maximum Percent Engineering Strain = 9.088e+001
Minimum Percent Engineering Strain = 3.032e+001
Maximum True Stress = 1.729e+006 Nm^-2
Minimum True Stress = 2.690e+005 Nm^-2
Maximum Percent True Strain = 4.761e+001
Minimum Percent True Strain = 2.326e+001
```

B samples – [0.25Hz]

Dpdms_25A

```
W = 0.0020
Input thickness of specimen in meters>.09e-3
Gauge =16.5000

To center selected data about zero,
        0.545 was added to Stress and
        0.667 was added to Strain
From an average over 25 complete cycles:
        The frequency is 0.25 Hz
        Magnitude ratio is 1.0789
        Phase difference is -959.9286 degrees
        Tan delta is -1.7260
Modulus (mean +/- SD) = 3.810e+006 +/- 1.069e+007 Nm^-2 (average slope as function of strain)
        Maximum Slope = 1.682e+008  Nm^-2
        Minimum Slope = 1.445e+005  Nm^-2
Storage modulus (mean +/- SD) = 1.910e+006 +/- 5.360e+006 Nm^-2
Loss modulus (mean +/- SD) = 3.297e+006 +/- 9.250e+006 Nm^-2
Maximum Engineering Stress = 1.072e+006 Nm^-2
Minimum Engineering Stress = 2.550e+005 Nm^-2
Maximum Percent Engineering Strain = 9.096e+001
Minimum Percent Engineering Strain = 3.030e+001
Maximum True Stress = 2.041e+006 Nm^-2
Minimum True Stress = 3.324e+005 Nm^-2
Maximum Percent True Strain = 4.763e+001
Minimum Percent True Strain = 2.325e+001
```

Dpdms_25B

```
W =0.0020
Input thickness of specimen in meters>.11e-3
Gauge =16.5000

To center selected data about zero,
        0.557 was added to Stress and
        0.667 was added to Strain
From an average over 23 complete cycles:
        The frequency is 0.25 Hz
        Magnitude ratio is 1.0329
        Phase difference is -839.9265 degrees
        Tan delta is 1.7382
Modulus (mean +/- SD) = 3.278e+006 +/- 8.594e+006 Nm^-2 (average slope as function of strain)
        Maximum Slope = 1.300e+008  Nm^-2
        Minimum Slope = 1.449e+005  Nm^-2
Storage modulus (mean +/- SD) = 1.635e+006 +/- 4.286e+006 Nm^-2
Loss modulus (mean +/- SD) = 2.841e+006 +/- 7.449e+006 Nm^-2
Maximum Engineering Stress = 1.078e+006 Nm^-2
Minimum Engineering Stress = 2.682e+005 Nm^-2
Maximum Percent Engineering Strain = 9.094e+001
Minimum Percent Engineering Strain = 3.030e+001
Maximum True Stress = 2.055e+006 Nm^-2
Minimum True Stress = 3.516e+005 Nm^-2
Maximum Percent True Strain = 4.763e+001
Minimum Percent True Strain = 2.325e+001
```

Dpmds_25C

```
W =0.0020
Input thickness of specimen in meters>.11e-3
Gauge =16.5000

To center selected data about zero,
        0.537 was added to Stress and
        0.667 was added to Strain
From an average over 26 complete cycles:
        The frequency is 0.25 Hz
        Magnitude ratio is 0.9929
        Phase difference is -1525.1990 degrees
        Tan delta is -11.8428
Modulus (mean +/- SD) = 3.276e+006 +/- 8.562e+006 Nm^-2 (average slope as function of strain)
        Maximum Slope = 1.352e+008  Nm^-2
        Minimum Slope = 1.767e+005  Nm^-2
Storage modulus (mean +/- SD) = 2.757e+005 +/- 7.204e+005 Nm^-2
Loss modulus (mean +/- SD) = 3.265e+006 +/- 8.531e+006 Nm^-2
Maximum Engineering Stress = 1.075e+006 Nm^-2
Minimum Engineering Stress = 2.658e+005 Nm^-2
Maximum Percent Engineering Strain = 9.090e+001
Minimum Percent Engineering Strain = 3.031e+001
Maximum True Stress = 2.051e+006 Nm^-2
Minimum True Stress = 3.465e+005 Nm^-2
Maximum Percent True Strain = 4.762e+001
Minimum Percent True Strain = 2.325e+001
```

Dpmds_25D

W =0.0020
Input thickness of specimen in meters>.1e-3
Gauge = 16.5000

To center selected data about zero,
    0.595 was added to Stress and
    0.667 was added to Strain
From an average over 21 complete cycles:
    The frequency is 0.25 Hz
    Magnitude ratio is 1.0244
    Phase difference is -1252.6172 degrees
    Tan delta is 0.1299
Modulus (mean +/- SD) = 3.581e+006 +/- 9.040e+006 Nm^-2 (average slope as function of strain)
    Maximum Slope = 1.195e+008 Nm^-2
    Minimum Slope = 1.410e+005 Nm^-2
Storage modulus (mean +/- SD) = 3.552e+006 +/- 8.965e+006 Nm^-2
Loss modulus (mean +/- SD) = 4.615e+005 +/- 1.165e+006 Nm^-2
Maximum Engineering Stress = 1.141e+006 Nm^-2
Minimum Engineering Stress = 3.226e+005 Nm^-2
Maximum Percent Engineering Strain = 9.091e+001
Minimum Percent Engineering Strain = 3.030e+001
Maximum True Stress = 2.178e+006 Nm^-2
Minimum True Stress = 4.222e+005 Nm^-2
Maximum Percent True Strain = 4.762e+001
Minimum Percent True Strain = 2.325e+001

Dpmds_25E

W =0.0020
Input thickness of specimen in meters>.1e-3
Gauge =16.5000
To center selected data about zero,
    0.550 was added to Stress and
    0.667 was added to Strain
From an average over 24 complete cycles:
    The frequency is 0.25 Hz
    Magnitude ratio is 1.0389
    Phase difference is -287.8758 degrees
    Tan delta is 3.1014
Modulus (mean +/- SD) = 3.726e+006 +/- 1.141e+007 Nm^-2 (average slope as function of strain)
    Maximum Slope = 2.279e+008 Nm^-2
    Minimum Slope = 1.958e+005 Nm^-2
Storage modulus (mean +/- SD) = 1.144e+006 +/- 3.501e+006 Nm^-2
Loss modulus (mean +/- SD) = 3.547e+006 +/- 1.086e+007 Nm^-2
Maximum Engineering Stress = 1.134e+006 Nm^-2
Minimum Engineering Stress = 2.898e+005 Nm^-2
Maximum Percent Engineering Strain = 9.090e+001
Minimum Percent Engineering Strain = 3.031e+001
Maximum True Stress = 2.165e+006 Nm^-2
Minimum True Stress = 3.796e+005 Nm^-2
Maximum Percent True Strain = 4.762e+001
Minimum Percent True Strain = 2.325e+001

B samples – [0.5Hz]

Dpmds_5A

W =0.0020
Input thickness of specimen in meters>.1e-3
Gauge =16.5000

To center selected data about zero,
    0.565 was added to Stress and
    0.667 was added to Strain
From an average over 25 complete cycles:
    The frequency is 0.50 Hz
    Magnitude ratio is 1.0788
    Phase difference is 305.6008 degrees
    Tan delta is -1.3970
Modulus (mean +/- SD) = 1.631e+006 +/- 1.559e+006 Nm^-2 (average slope as function of strain)
    Maximum Slope = 1.296e+007 Nm^-2
    Minimum Slope = 8.915e+004 Nm^-2
Storage modulus (mean +/- SD) = 9.491e+005 +/- 9.074e+005 Nm^-2
Loss modulus (mean +/- SD) = 1.326e+006 +/- 1.268e+006 Nm^-2
Maximum Engineering Stress = 1.003e+006 Nm^-2
Minimum Engineering Stress = 2.439e+005 Nm^-2
Maximum Percent Engineering Strain = 9.089e+001
Minimum Percent Engineering Strain = 3.031e+001
Maximum True Stress = 1.915e+006 Nm^-2
Minimum True Stress = 3.182e+005 Nm^-2
Maximum Percent True Strain = 4.762e+001
Minimum Percent True Strain = 2.325e+001

Dpmds_5B

W =0.0020
Input thickness of specimen in meters>.1e-3
Gauge =16.5000

To center selected data about zero,
    0.544 was added to Stress and
    0.667 was added to Strain
From an average over 27 complete cycles:
    The frequency is 0.50 Hz
    Magnitude ratio is 1.0904
    Phase difference is -152.4884 degrees
    Tan delta is 0.5209
Modulus (mean +/- SD) = 1.636e+006 +/- 1.660e+006 Nm^-2 (average slope as function of strain)
    Maximum Slope = 1.563e+007 Nm^-2
    Minimum Slope = 2.034e+005 Nm^-2
Storage modulus (mean +/- SD) = 1.451e+006 +/- 1.472e+006 Nm^-2
Loss modulus (mean +/- SD) = 7.560e+005 +/- 7.670e+005 Nm^-2
Maximum Engineering Stress = 9.678e+005 Nm^-2
Minimum Engineering Stress = 2.098e+005 Nm^-2
Maximum Percent Engineering Strain = 9.095e+001
Minimum Percent Engineering Strain = 3.031e+001
Maximum True Stress = 1.843e+006 Nm^-2
Minimum True Stress = 2.734e+005 Nm^-2
Maximum Percent True Strain = 4.763e+001
Minimum Percent True Strain = 2.325e+001

Dpmds_5C

```
W =0.0020
Input thickness of specimen in meters>.1e-3
Gauge =16.5000

To center selected data about zero,
        0.545 was added to Stress and
        0.667 was added to Strain
From an average over 21 complete cycles:
        The frequency is 0.50 Hz
        Magnitude ratio is 1.0611
        Phase difference is -133.8088 degrees
        Tan delta is 1.0426
Modulus (mean +/- SD) = 1.641e+006 +/- 1.741e+006 Nm^-2 (average slope as function of strain)
        Maximum Slope = 2.227e+007  Nm^-2
        Minimum Slope = 1.752e+005  Nm^-2
Storage modulus (mean +/- SD) = 1.136e+006 +/- 1.205e+006 Nm^-2
Loss modulus (mean +/- SD) = 1.185e+006 +/- 1.256e+006 Nm^-2
Maximum Engineering Stress = 1.043e+006 Nm^-2
Minimum Engineering Stress = 2.505e+005 Nm^-2
Maximum Percent Engineering Strain = 9.094e+001
Minimum Percent Engineering Strain = 3.031e+001
Maximum True Stress = 1.970e+006 Nm^-2
Minimum True Stress = 3.264e+005 Nm^-2
Maximum Percent True Strain = 4.763e+001
Minimum Percent True Strain = 2.325e+001
```

Dpmds_5D

```
W =0.0020
Input thickness of specimen in meters>8e-5
Gauge =16.5000

To center selected data about zero,
        0.528 was added to Stress and
        0.667 was added to Strain
From an average over 20 complete cycles:
        The frequency is 0.50 Hz
        Magnitude ratio is 1.0464
        Phase difference is -76.4929 degrees
        Tan delta is -4.1626
Modulus (mean +/- SD) = 1.844e+006 +/- 1.978e+006 Nm^-2 (average slope as function of strain)
        Maximum Slope = 2.102e+007  Nm^-2
        Minimum Slope = 1.697e+005  Nm^-2
Storage modulus (mean +/- SD) = 4.307e+005 +/- 4.621e+005 Nm^-2
Loss modulus (mean +/- SD) = 1.793e+006 +/- 1.924e+006 Nm^-2
Maximum Engineering Stress = 1.103e+006 Nm^-2
Minimum Engineering Stress = 2.459e+005 Nm^-2
Maximum Percent Engineering Strain = 9.095e+001
Minimum Percent Engineering Strain = 3.031e+001
Maximum True Stress = 2.092e+006 Nm^-2
Minimum True Stress = 3.205e+005 Nm^-2
Maximum Percent True Strain = 4.763e+001
Minimum Percent True Strain = 2.325e+001
```

Dpmds_5E

```
W =0.0020
Input thickness of specimen in meters>8e-5
Gauge =16.5000

To center selected data about zero,
        0.567 was added to Stress and
        0.666 was added to Strain
From an average over 20 complete cycles:
        The frequency is 0.50 Hz
        Magnitude ratio is 1.1001
        Phase difference is -189.3712 degrees
        Tan delta is -0.1650
Modulus (mean +/- SD) = 1.777e+006 +/- 2.184e+006 Nm^-2 (average slope as function of strain)
        Maximum Slope = 2.503e+007  Nm^-2
        Minimum Slope = 1.930e+005  Nm^-2
Storage modulus (mean +/- SD) = 1.753e+006 +/- 2.155e+006 Nm^-2
Loss modulus (mean +/- SD) = 2.892e+005 +/- 3.555e+005 Nm^-2
Maximum Engineering Stress = 9.130e+005 Nm^-2
Minimum Engineering Stress = 2.082e+005 Nm^-2
Maximum Percent Engineering Strain = 9.098e+001
Minimum Percent Engineering Strain = 3.031e+001
Maximum True Stress = 1.743e+006 Nm^-2
Minimum True Stress = 2.714e+005 Nm^-2
Maximum Percent True Strain = 4.764e+001
Minimum Percent True Strain = 2.325e+001
```

B samples – [1.0Hz]

Dpmds1A

```
W =0.0020
Input thickness of specimen in meters>7e-5
Gauge =16.5000

To center selected data about zero,
        0.562 was added to Stress and
        0.667 was added to Strain
From an average over 44 complete cycles:
        The frequency is 1.00 Hz
        Magnitude ratio is 1.1669
        Phase difference is 319.3805 degrees
        Tan delta is -0.8579
Modulus (mean +/- SD) = 1.308e+006 +/- 8.234e+005 Nm^-2 (average slope as function of strain)
        Maximum Slope = 6.212e+006  Nm^-2
        Minimum Slope = 1.999e+005  Nm^-2
Storage modulus (mean +/- SD) = 9.927e+005 +/- 6.250e+005 Nm^-2
Loss modulus (mean +/- SD) = 8.516e+005 +/- 5.361e+005 Nm^-2
Maximum Engineering Stress = 9.704e+005 Nm^-2
Minimum Engineering Stress = 2.136e+005 Nm^-2
Maximum Percent Engineering Strain = 9.085e+001
Minimum Percent Engineering Strain = 3.032e+001
Maximum True Stress = 1.853e+006 Nm^-2
Minimum True Stress = 2.783e+005 Nm^-2
Maximum Percent True Strain = 4.763e+001
Minimum Percent True Strain = 2.325e+001
```

Dpmds1B

W = 0.0020
Input thickness of specimen in meters>7e-5
Gauge = 16.5000

To center selected data about zero,
        0.504 was added to Stress and
        0.667 was added to Strain
From an average over 32 complete cycles:
        The frequency is 1.00 Hz
        Magnitude ratio is 1.2210
        Phase difference is 302.1076 degrees
        Tan delta is -1.5940
Modulus (mean +/- SD) = 1.296e+006 +/- 7.701e+005 Nm^-2 (average slope as function of strain)
        Maximum Slope = 4.999e+006 Nm^-2
        Minimum Slope = 1.686e+005 Nm^-2
Storage modulus (mean +/- SD) = 6.887e+005 +/- 4.093e+005 Nm^-2
Loss modulus (mean +/- SD) = 1.098e+006 +/- 6.524e+005 Nm^-2
Maximum Engineering Stress = 9.835e+005 Nm^-2
Minimum Engineering Stress = 1.667e+005 Nm^-2
Maximum Percent Engineering Strain = 9.091e+001
Minimum Percent Engineering Strain = 3.030e+001
Maximum True Stress = 1.876e+006 Nm^-2
Minimum True Stress = 2.176e+005 Nm^-2
Maximum Percent True Strain = 4.765e+001
Minimum Percent True Strain = 2.325e+001

Dpmds1C

To center selected data about zero,
        0.608 was added to Stress and
        0.667 was added to Strain
From an average over 14 complete cycles:
        The frequency is 1.00 Hz
        Magnitude ratio is 1.0525
        Phase difference is 0.6419 degrees
        Tan delta is 0.0112
Modulus (mean +/- SD) = 8.429e+005 +/- 3.947e+005 Nm^-2 (average slope as function of strain)
        Maximum Slope = 3.871e+006 Nm^-2
        Minimum Slope = 2.426e+005 Nm^-2
Storage modulus (mean +/- SD) = 8.429e+005 +/- 3.947e+005 Nm^-2
Loss modulus (mean +/- SD) = 9.443e+003 +/- 4.422e+003 Nm^-2
Maximum Engineering Stress = 7.100e+005 Nm^-2
Minimum Engineering Stress = 1.855e+005 Nm^-2
Maximum Percent Engineering Strain = 9.094e+001
Minimum Percent Engineering Strain = 3.030e+001
Maximum True Stress = 1.355e+006 Nm^-2
Minimum True Stress = 2.417e+005 Nm^-2
Maximum Percent True Strain = 4.765e+001
Minimum Percent True Strain = 2.325e+001

Dpmds1D

```
To center selected data about zero,
        0.554 was added to Stress and
        0.666 was added to Strain
From an average over 35 complete cycles:
        The frequency is 1.00 Hz
        Magnitude ratio is 1.0660
        Phase difference is 6.7234 degrees
        Tan delta is 0.1179
Modulus (mean +/- SD) = 1.203e+006 +/- 5.767e+005 Nm^-2 (average slope as function of strain)
        Maximum Slope = 3.862e+006  Nm^-2
        Minimum Slope = 2.026e+005  Nm^-2
Storage modulus (mean +/- SD) = 1.195e+006 +/- 5.727e+005 Nm^-2
Loss modulus (mean +/- SD) = 1.408e+005 +/- 6.752e+004 Nm^-2
Maximum Engineering Stress = 9.685e+005 Nm^-2
Minimum Engineering Stress = 2.351e+005 Nm^-2
Maximum Percent Engineering Strain = 9.098e+001
Minimum Percent Engineering Strain = 3.030e+001
Maximum True Stress = 1.850e+006 Nm^-2
Minimum True Stress = 3.066e+005 Nm^-2
Maximum Percent True Strain = 4.767e+001
Minimum Percent True Strain = 2.325e+001
```

Dpmds1E

```
To center selected data about zero,
        0.556 was added to Stress and
        0.667 was added to Strain
From an average over 24 complete cycles:
        The frequency is 1.00 Hz
        Magnitude ratio is 1.0486
        Phase difference is 6.5156 degrees
        Tan delta is 0.1142
Modulus (mean +/- SD) = 1.403e+006 +/- 6.728e+005 Nm^-2 (average slope as function of strain)
        Maximum Slope = 4.505e+006  Nm^-2
        Minimum Slope = 2.363e+005  Nm^-2
Storage modulus (mean +/- SD) = 1.394e+006 +/- 6.685e+005 Nm^-2
Loss modulus (mean +/- SD) = 1.592e+005 +/- 7.635e+004 Nm^-2
Maximum Engineering Stress = 1.130e+006 Nm^-2
Minimum Engineering Stress = 2.743e+005 Nm^-2
Maximum Percent Engineering Strain = 9.098e+001
Minimum Percent Engineering Strain = 3.030e+001
Maximum True Stress = 2.158e+006 Nm^-2
Minimum True Stress = 3.577e+005 Nm^-2
Maximum Percent True Strain = 4.767e+001
Minimum Percent True Strain = 2.325e+001
```

B samples – [3.0Hz]

Dpmds3A

```
To center selected data about zero,
        0.555 was added to Stress and
        0.666 was added to Strain
From an average over 39 complete cycles:
        The frequency is 1.00 Hz
        Magnitude ratio is 1.0719
        Phase difference is 6.6163 degrees
        Tan delta is 0.1160
Modulus (mean +/- SD) = 1.531e+006 +/- 7.340e+005 Nm^-2 (average slope as function of strain)
        Maximum Slope = 4.915e+006  Nm^-2
        Minimum Slope = 2.578e+005  Nm^-2
Storage modulus (mean +/- SD) = 1.521e+006 +/- 7.291e+005 Nm^-2
Loss modulus (mean +/- SD) = 1.764e+005 +/- 8.457e+004 Nm^-2
Maximum Engineering Stress = 1.233e+006 Nm^-2
Minimum Engineering Stress = 2.992e+005 Nm^-2
Maximum Percent Engineering Strain = 9.098e+001
Minimum Percent Engineering Strain = 3.030e+001
Maximum True Stress = 2.355e+006 Nm^-2
Minimum True Stress = 3.902e+005 Nm^-2
Maximum Percent True Strain = 4.767e+001
Minimum Percent True Strain = 2.325e+001
```

Dpmds3B

```
To center selected data about zero,
        0.554 was added to Stress and
        0.667 was added to Strain
From an average over 30 complete cycles:
        The frequency is 1.00 Hz
        Magnitude ratio is 1.0660
        Phase difference is 6.8553 degrees
        Tan delta is 0.1202
Modulus (mean +/- SD) = 1.295e+006 +/- 6.211e+005 Nm^-2 (average slope as function of strain)
        Maximum Slope = 4.159e+006  Nm^-2
        Minimum Slope = 2.182e+005  Nm^-2
Storage modulus (mean +/- SD) = 1.286e+006 +/- 6.166e+005 Nm^-2
Loss modulus (mean +/- SD) = 1.546e+005 +/- 7.413e+004 Nm^-2
Maximum Engineering Stress = 1.043e+006 Nm^-2
Minimum Engineering Stress = 2.532e+005 Nm^-2
Maximum Percent Engineering Strain = 9.098e+001
Minimum Percent Engineering Strain = 3.030e+001
Maximum True Stress = 1.992e+006 Nm^-2
Minimum True Stress = 3.302e+005 Nm^-2
Maximum Percent True Strain = 4.767e+001
Minimum Percent True Strain = 2.325e+001
```

Dpmds3C

```
To center selected data about zero,
        0.525 was added to Stress and
        0.672 was added to Strain
From an average over 35 complete cycles:
        The frequency is 3.00 Hz
        Magnitude ratio is 1.0613
        Phase difference is 12.1010 degrees
        Tan delta is 0.2144
Modulus (mean +/- SD) = 9.850e+005 +/- 2.611e+005 Nm^-2 (average slope as function of strain)
        Maximum Slope = 1.834e+006  Nm^-2
        Minimum Slope = 4.400e+005  Nm^-2
Storage modulus (mean +/- SD) = 9.632e+005 +/- 2.553e+005 Nm^-2
Loss modulus (mean +/- SD) = 2.065e+005 +/- 5.473e+004 Nm^-2
Maximum Engineering Stress = 8.887e+005 Nm^-2
Minimum Engineering Stress = 1.130e+005 Nm^-2
Maximum Percent Engineering Strain = 9.013e+001
Minimum Percent Engineering Strain = 3.022e+001
Maximum True Stress = 1.699e+006 Nm^-2
Minimum True Stress = 1.471e+005 Nm^-2
Maximum Percent True Strain = 4.776e+001
Minimum Percent True Strain = 2.312e+001
```

Dpmds3D

```
W = 0.0020
Input thickness of specimen in meters>1.3e-4
Gauge = 16.5000
To center selected data about zero,
        0.568 was added to Stress and
        0.673 was added to Strain
From an average over 52 complete cycles:
        The frequency is 3.00 Hz
        Magnitude ratio is 1.0883
        Phase difference is -11.2737 degrees
        Tan delta is -0.1993
Modulus (mean +/- SD) = 9.039e+005 +/- 2.123e+005 Nm^-2 (average slope as function of strain)
        Maximum Slope = 1.632e+006  Nm^-2
        Minimum Slope = 4.053e+005  Nm^-2
Storage modulus (mean +/- SD) = 8.865e+005 +/- 2.082e+005 Nm^-2
Loss modulus (mean +/- SD) = 1.767e+005 +/- 4.150e+004 Nm^-2
Maximum Engineering Stress = 8.443e+005 Nm^-2
Minimum Engineering Stress = 2.088e+005 Nm^-2
Maximum Percent Engineering Strain = 9.002e+001
Minimum Percent Engineering Strain = 3.021e+001
Maximum True Stress = 1.614e+006 Nm^-2
Minimum True Stress = 2.719e+005 Nm^-2
Maximum Percent True Strain = 4.773e+001
Minimum Percent True Strain = 2.307e+001
```

Dpmds3E

To center selected data about zero,
        0.565 was added to Stress and
        0.673 was added to Strain
From an average over 42 complete cycles:
        The frequency is 3.00 Hz
        Magnitude ratio is 1.0717
        Phase difference is 5.7864 degrees
        Tan delta is 0.1013
Modulus (mean +/- SD) = 1.068e+006 +/- 2.509e+005 Nm^-2 (average slope as function of strain)
        Maximum Slope = 1.929e+006 Nm^-2
        Minimum Slope = 4.790e+005 Nm^-2
Storage modulus (mean +/- SD) = 1.063e+006 +/- 2.496e+005 Nm^-2
Loss modulus (mean +/- SD) = 1.077e+005 +/- 2.530e+004 Nm^-2
Maximum Engineering Stress = 9.978e+005 Nm^-2
Minimum Engineering Stress = 2.468e+005 Nm^-2
Maximum Percent Engineering Strain = 9.002e+001
Minimum Percent Engineering Strain = 3.021e+001
Maximum True Stress = 1.908e+006 Nm^-2
Minimum True Stress = 3.213e+005 Nm^-2
Maximum Percent True Strain = 4.773e+001
Minimum Percent True Strain = 2.307e+001

B samples – [5.0Hz]

Dpmds5A

To center selected data about zero,
        0.564 was added to Stress and
        0.673 was added to Strain
From an average over 35 complete cycles:
        The frequency is 3.00 Hz
        Magnitude ratio is 1.0717
        Phase difference is 6.1333 degrees
        Tan delta is 0.1075
Modulus (mean +/- SD) = 1.068e+006 +/- 2.509e+005 Nm^-2 (average slope as function of strain)
        Maximum Slope = 1.929e+006 Nm^-2
        Minimum Slope = 4.790e+005 Nm^-2
Storage modulus (mean +/- SD) = 1.062e+006 +/- 2.495e+005 Nm^-2
Loss modulus (mean +/- SD) = 1.141e+005 +/- 2.681e+004 Nm^-2
Maximum Engineering Stress = 9.978e+005 Nm^-2
Minimum Engineering Stress = 2.468e+005 Nm^-2
Maximum Percent Engineering Strain = 9.002e+001
Minimum Percent Engineering Strain = 3.021e+001
Maximum True Stress = 1.908e+006 Nm^-2
Minimum True Stress = 3.213e+005 Nm^-2
Maximum Percent True Strain = 4.773e+001
Minimum Percent True Strain = 2.307e+001

Dpmds5B

```
To center selected data about zero,
        0.601 was added to Stress and
        0.688 was added to Strain
From an average over 73 complete cycles:
        The frequency is 5.00 Hz
        Magnitude ratio is 1.0616
        Phase difference is 2.4670 degrees
        Tan delta is 0.0431
Modulus (mean +/- SD) = 8.679e+005 +/- 1.412e+005 Nm^-2 (average slope as function of strain)
        Maximum Slope = 1.323e+006  Nm^-2
        Minimum Slope = 5.488e+005  Nm^-2
Storage modulus (mean +/- SD) = 8.671e+005 +/- 1.410e+005 Nm^-2
Loss modulus (mean +/- SD) = 3.736e+004 +/- 6.076e+003 Nm^-2
Maximum Engineering Stress = 8.083e+005 Nm^-2
Minimum Engineering Stress = 2.463e+005 Nm^-2
Maximum Percent Engineering Strain = 8.827e+001
Minimum Percent Engineering Strain = 3.045e+001
Maximum True Stress = 1.549e+006 Nm^-2
Minimum True Stress = 3.211e+005 Nm^-2
Maximum Percent True Strain = 4.786e+001
Minimum Percent True Strain = 2.253e+001
```

Dpmds5C

```
W = 0.0020
Input thickness of specimen in meters>1.2e-4
Gauge = 16.5000

To center selected data about zero,
        0.608 was added to Stress and
        0.688 was added to Strain
From an average over 75 complete cycles:
        The frequency is 5.00 Hz
        Magnitude ratio is 1.0842
        Phase difference is -10.9709 degrees
        Tan delta is -0.1939
Modulus (mean +/- SD) = 8.948e+005 +/- 1.009e+005 Nm^-2 (average slope as function of strain)
        Maximum Slope = 1.135e+006  Nm^-2
        Minimum Slope = 5.724e+005  Nm^-2
Storage modulus (mean +/- SD) = 8.784e+005 +/- 9.909e+004 Nm^-2
Loss modulus (mean +/- SD) = 1.703e+005 +/- 1.921e+004 Nm^-2
Maximum Engineering Stress = 8.753e+005 Nm^-2
Minimum Engineering Stress = -1.748e+004 Nm^-2
Maximum Percent Engineering Strain = 8.829e+001
Minimum Percent Engineering Strain = 3.011e+001
Maximum True Stress = 1.679e+006 Nm^-2
Minimum True Stress = -2.278e+004 Nm^-2
Maximum Percent True Strain = 4.787e+001
Minimum Percent True Strain = 2.258e+001
```

Dpmds5D

```
To center selected data about zero,
        0.623 was added to Stress and
        0.690 was added to Strain
From an average over 83 complete cycles:
        The frequency is 5.00 Hz
        Magnitude ratio is 1.0663
        Phase difference is 0.9755 degrees
        Tan delta is 0.0170
Modulus (mean +/- SD) = 9.418e+005 +/- 6.357e+004 Nm^-2 (average slope as function of strain)
        Maximum Slope = 1.184e+006  Nm^-2
        Minimum Slope = 7.777e+005  Nm^-2
Storage modulus (mean +/- SD) = 9.416e+005 +/- 6.356e+004 Nm^-2
Loss modulus (mean +/- SD) = 1.603e+004 +/- 1.082e+003 Nm^-2
Maximum Engineering Stress = 9.212e+005 Nm^-2
Minimum Engineering Stress = 1.923e+005 Nm^-2
Maximum Percent Engineering Strain = 8.807e+001
Minimum Percent Engineering Strain = 3.030e+001
Maximum True Stress = 1.765e+006 Nm^-2
Minimum True Stress = 2.506e+005 Nm^-2
Maximum Percent True Strain = 4.782e+001
Minimum Percent True Strain = 2.267e+001
```

Dpmds5E

```
To center selected data about zero,
        0.623 was added to Stress and
        0.690 was added to Strain
From an average over 83 complete cycles:
        The frequency is 5.00 Hz
        Magnitude ratio is 1.0663
        Phase difference is 0.9755 degrees
        Tan delta is 0.0170
Modulus (mean +/- SD) = 9.418e+005 +/- 6.357e+004 Nm^-2 (average slope as function of strain)
        Maximum Slope = 1.184e+006  Nm^-2
        Minimum Slope = 7.777e+005  Nm^-2
Storage modulus (mean +/- SD) = 9.416e+005 +/- 6.356e+004 Nm^-2
Loss modulus (mean +/- SD) = 1.603e+004 +/- 1.082e+003 Nm^-2
Maximum Engineering Stress = 9.212e+005 Nm^-2
Minimum Engineering Stress = 1.923e+005 Nm^-2
Maximum Percent Engineering Strain = 8.807e+001
Minimum Percent Engineering Strain = 3.030e+001
Maximum True Stress = 1.765e+006 Nm^-2
Minimum True Stress = 2.506e+005 Nm^-2
Maximum Percent True Strain = 4.782e+001
Minimum Percent True Strain = 2.267e+001
```

C.1.3 Dynamic uniaxial tension graphical results

The graphical results below were generated by the Matlab programs (Phasediff1bb.m) and (Box.m). The results shown below are examples of plots for samples run.

C.1.3.1 Dynamic uniaxial tension *A* sample graphical results

A sample, **`Pdmst_025d.txt`** plots.

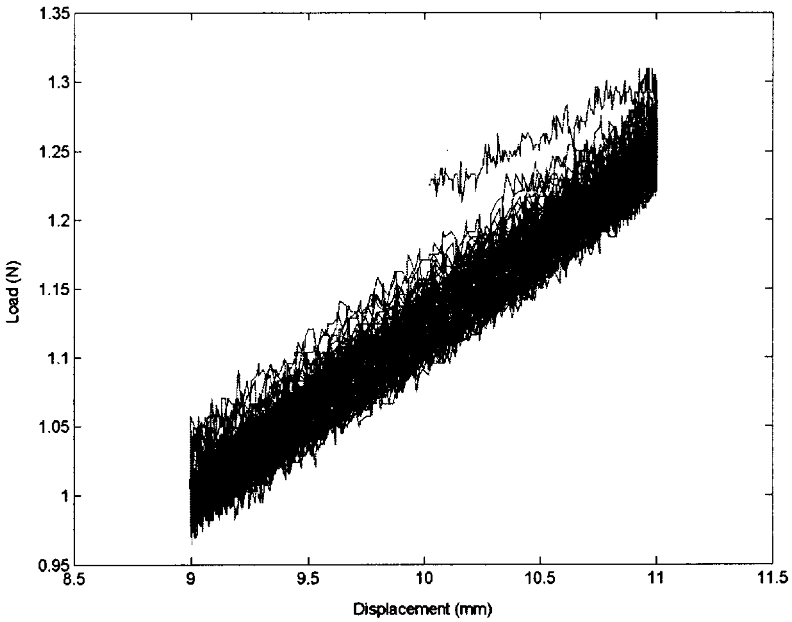

Fig. C.1 – PDMS *A* sample – Load vs Displacement

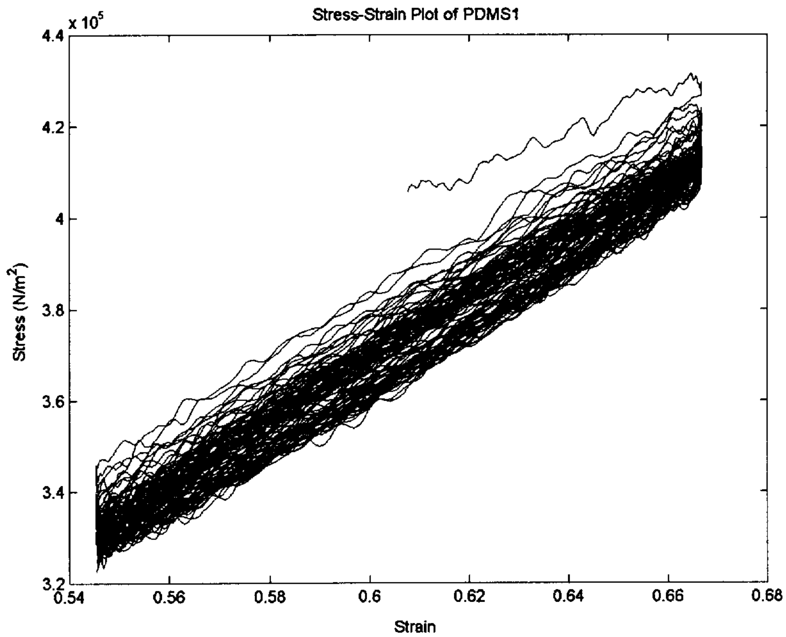

Fig. C.2 – PDMS *A* sample - Stress vs Strain (Engineering)

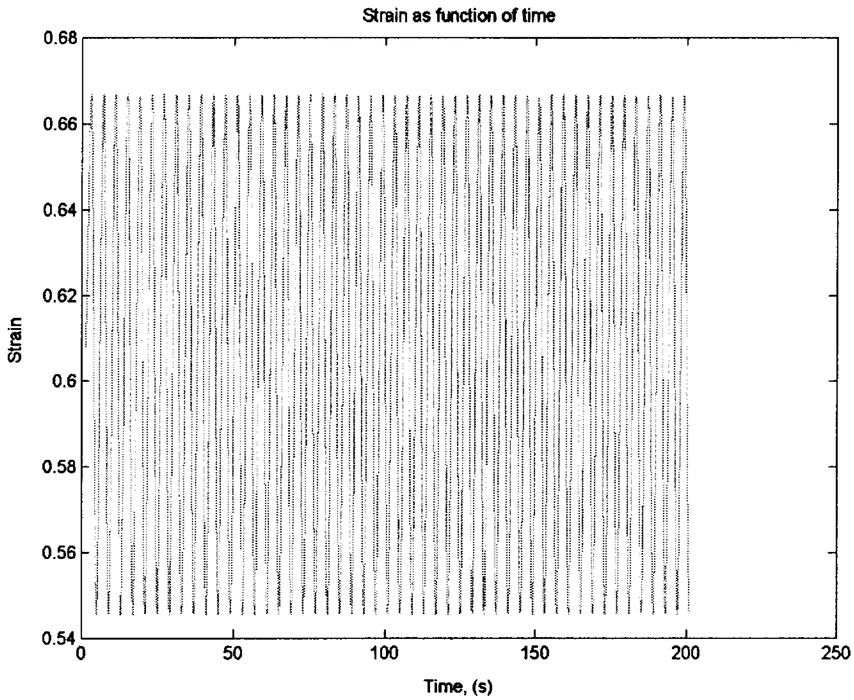

Fig. C.3 – PDMS *A* sample - Strain vs Time

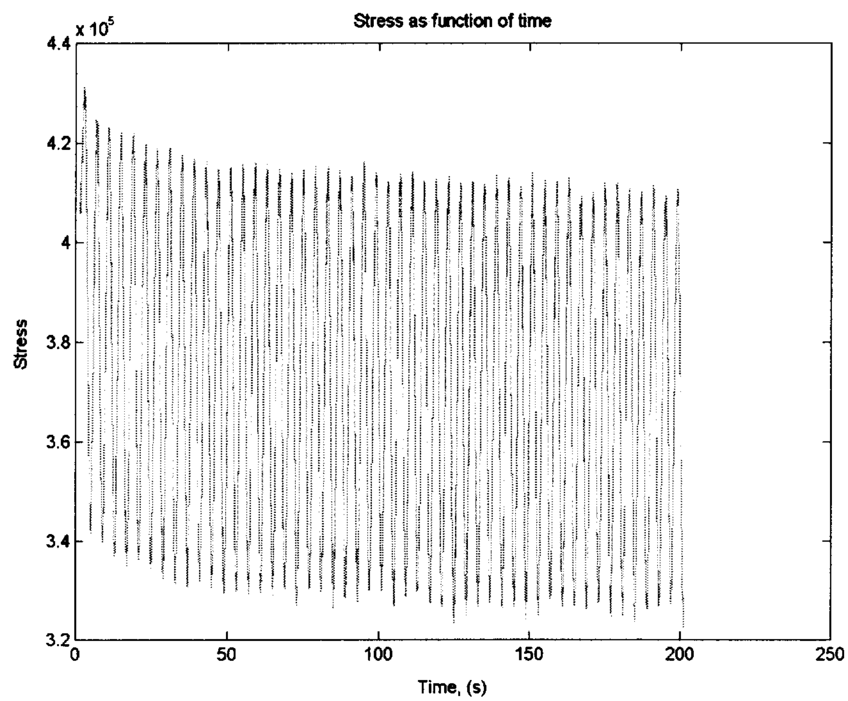

Fig. C.4 – PDMS *A* sample - Stress vs Time

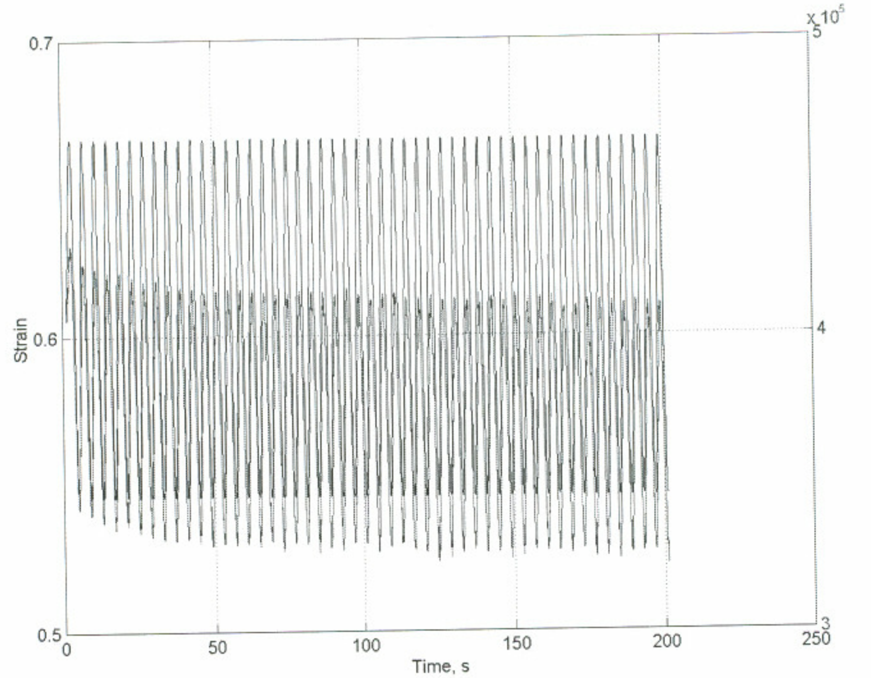

Fig. C.5 – PDMS Poisson's *A* sample - Strain vs Time

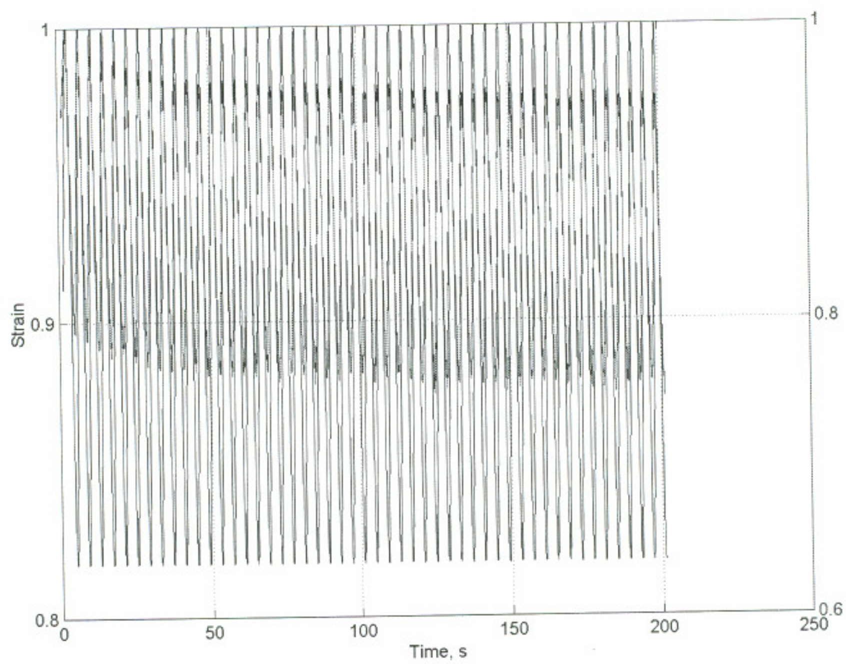

Fig. C.6 – PDMS *A* sample - Strain vs Time

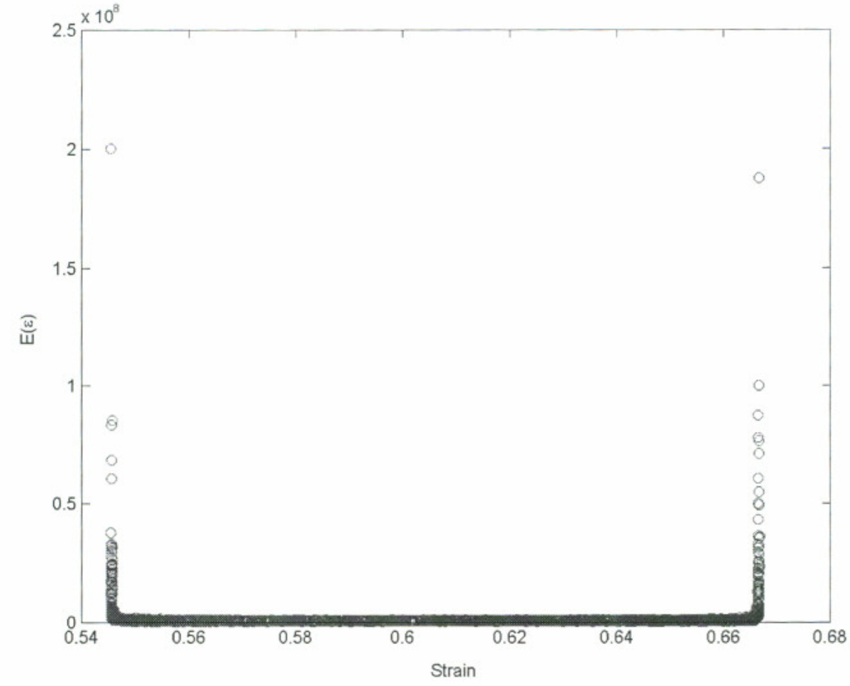

Fig. C.7 – PDMS *A* sample - E vs Strain

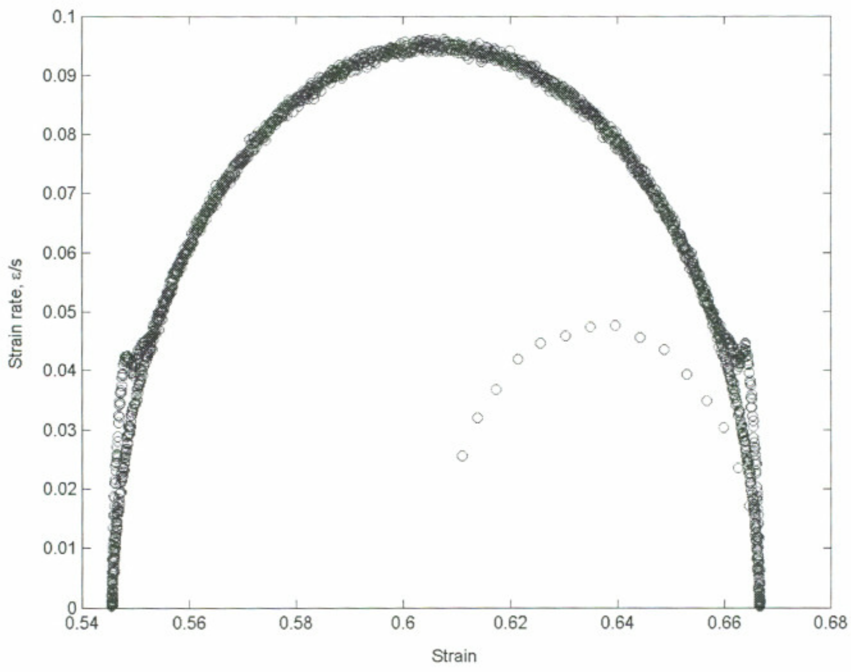

Fig. C.8 – PDMS *A* sample - Strain rate vs Strain

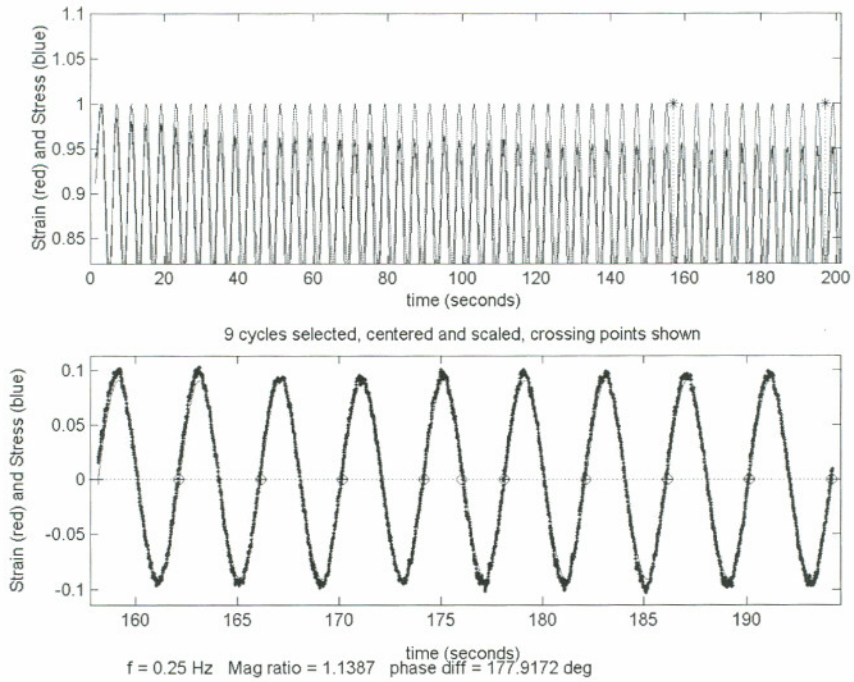

Fig. C.9 – PDMS *A* sample – Stress and Strain vs Time

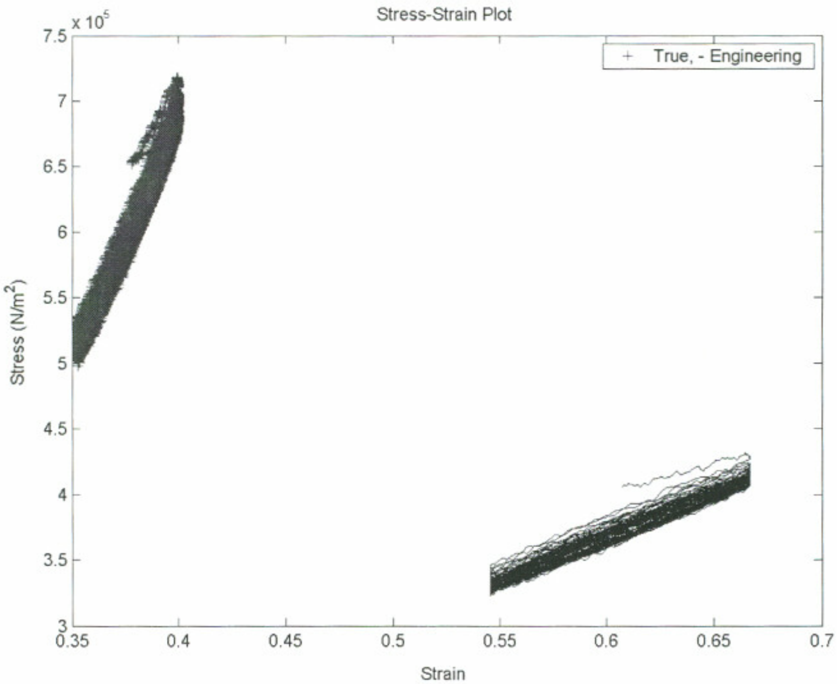

Fig. C.10 – PDMS *A* sample - Stress vs Strain (True and Engineering)

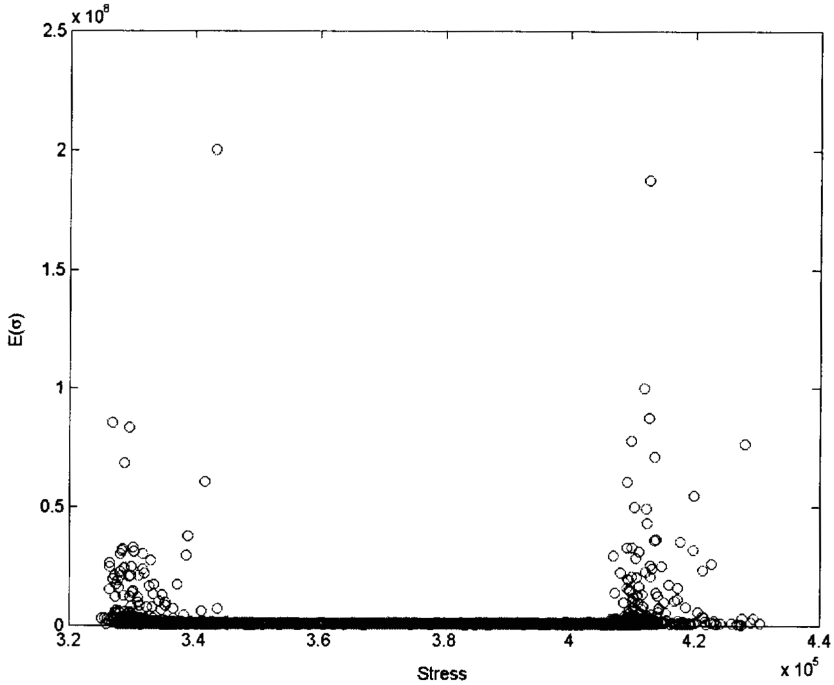

Fig. C.11 – PDMS *A* sample - E vs Stress

C.1.3.2 Dynamic uniaxial tension *B* sample graphical results

B sample, **Dpdms_25d.txt** plots.

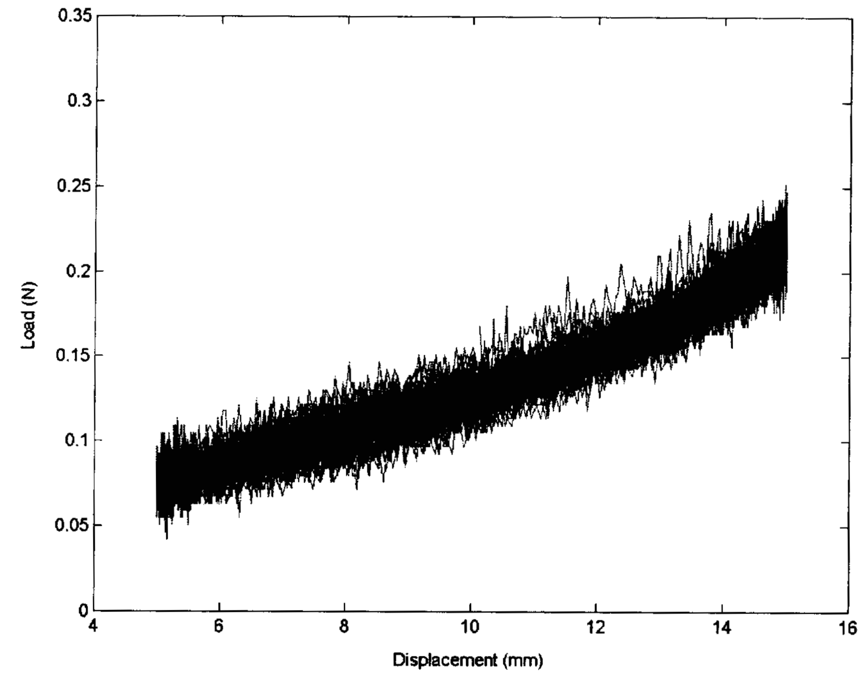

Fig. C.12 – PDMS *B* sample - Load vs Displacement

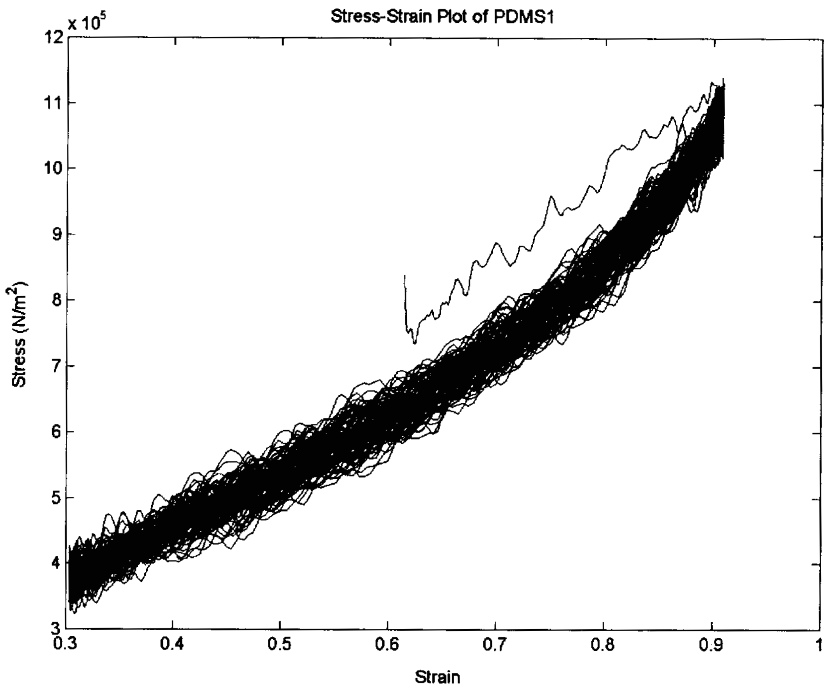

Fig. C.13 – PDMS *B* sample – Stress vs Strain

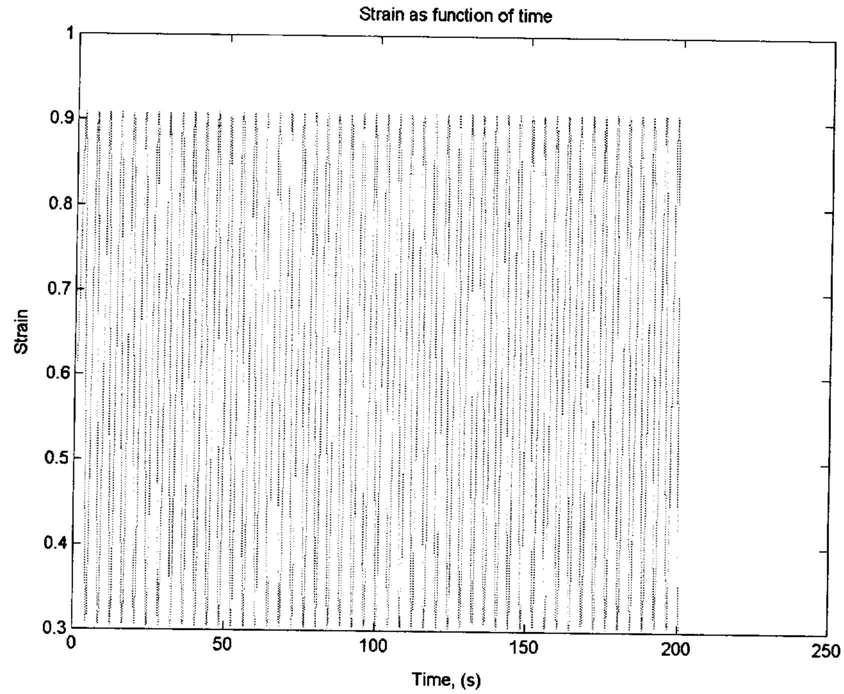

Fig. C.14 – PDMS *B* sample - Strain vs Time

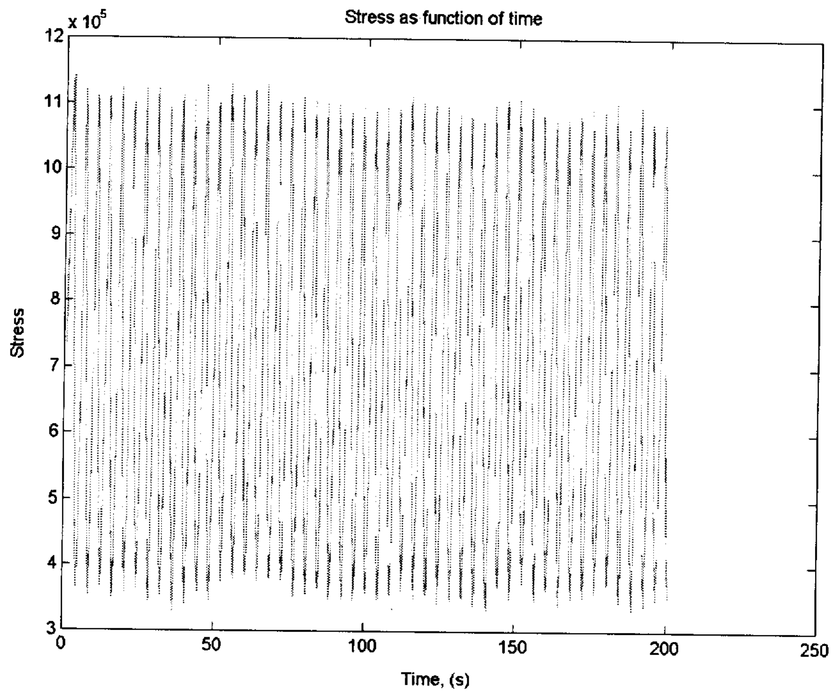

Fig. C.15 – PDMS *B* sample - Stress vs Time

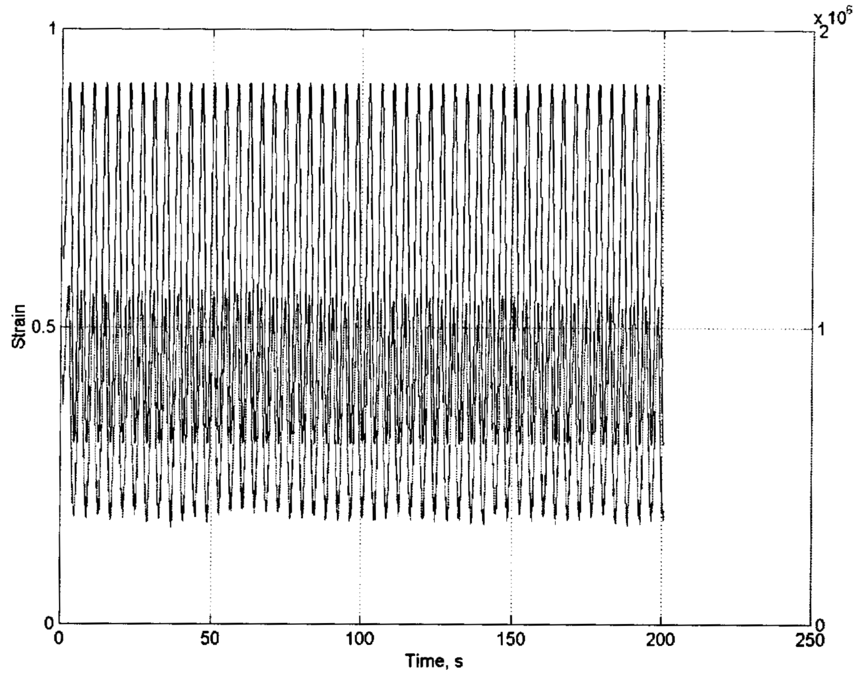

Fig. C.16 – PDMS *B* sample - Strain vs Time

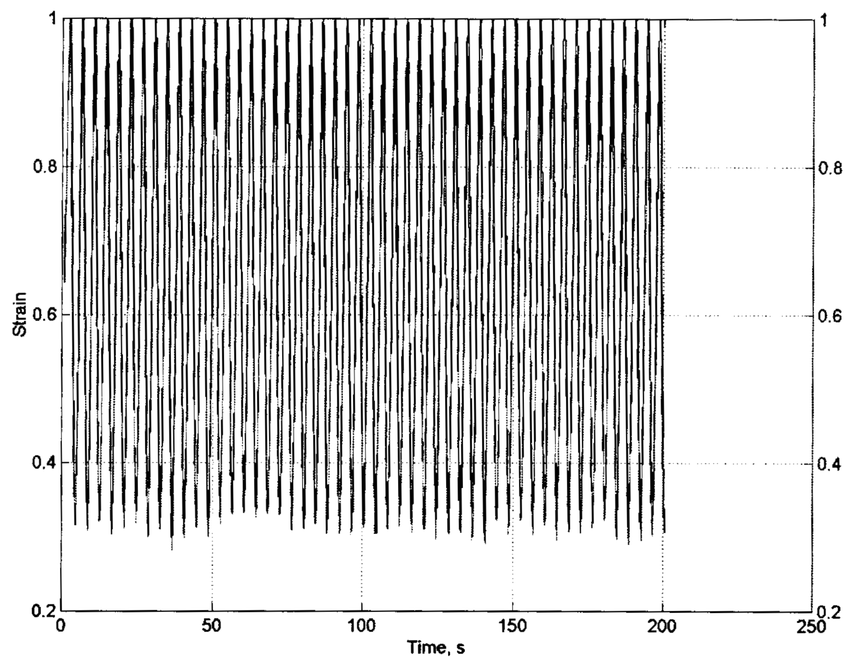

Fig. C.17 – PDMS *B* sample - Strain vs Time

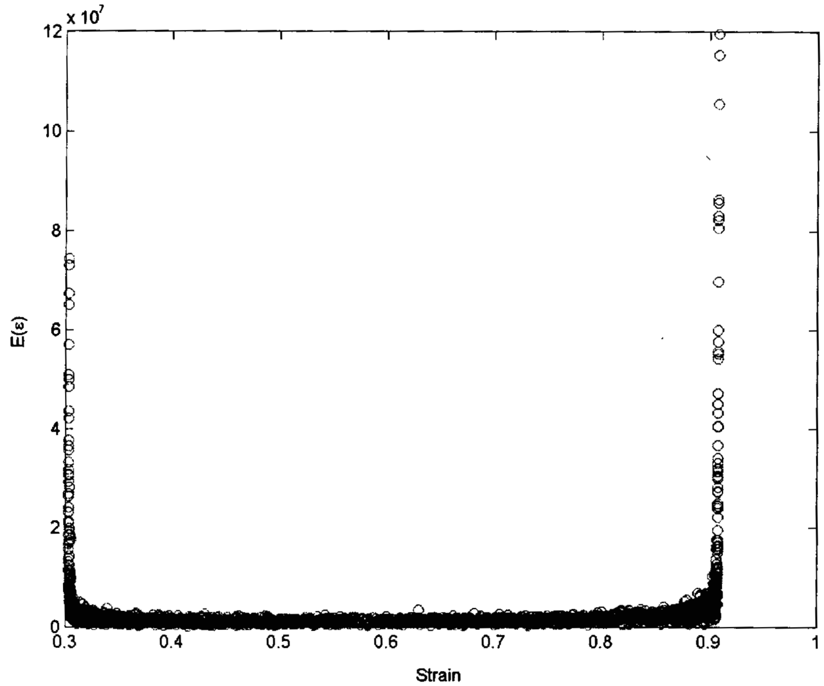

Fig. C.18 – PDMS *B* sample - E vs Strain

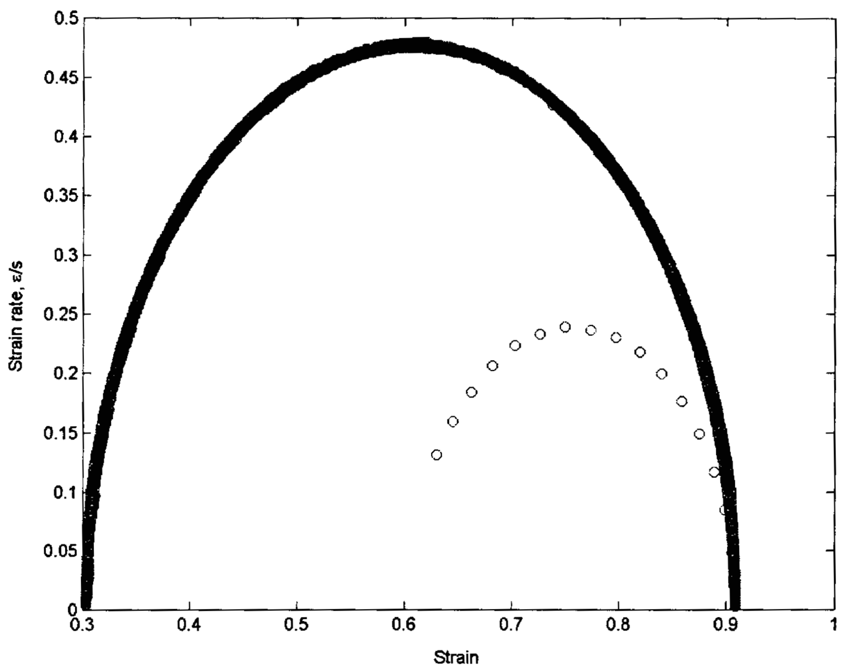

Fig. C.19 – PDMS *B* sample - Stress rate vs Strain

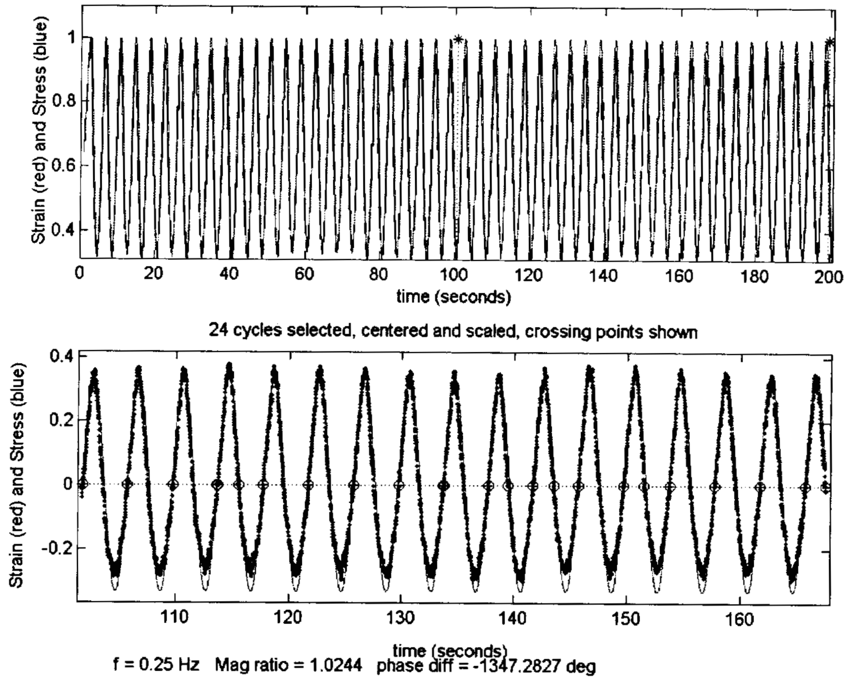

Fig. C.20 – PDMS *B* sample - Strain vs Time

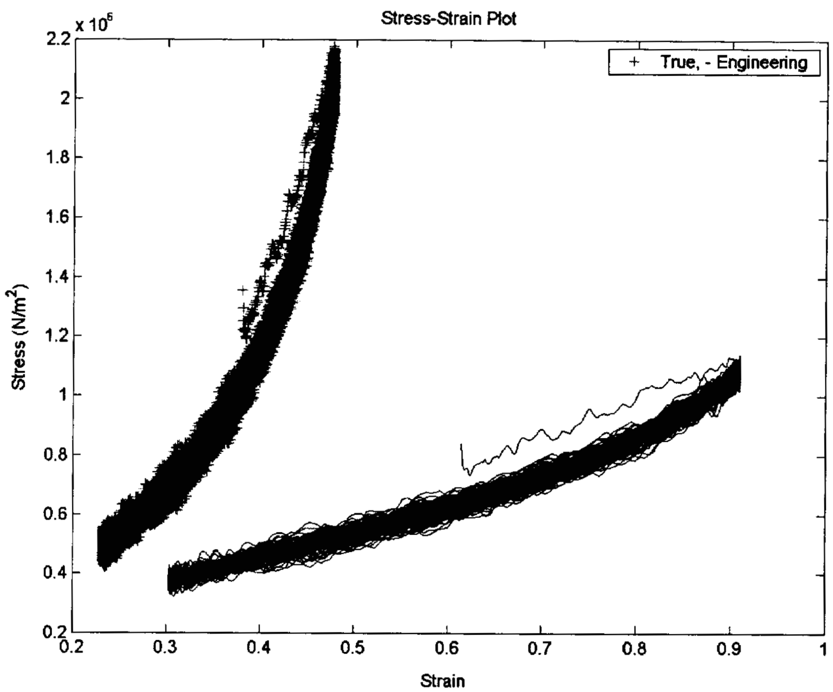

Fig. C.21 – PDMS *B* sample – Stress vs Strain

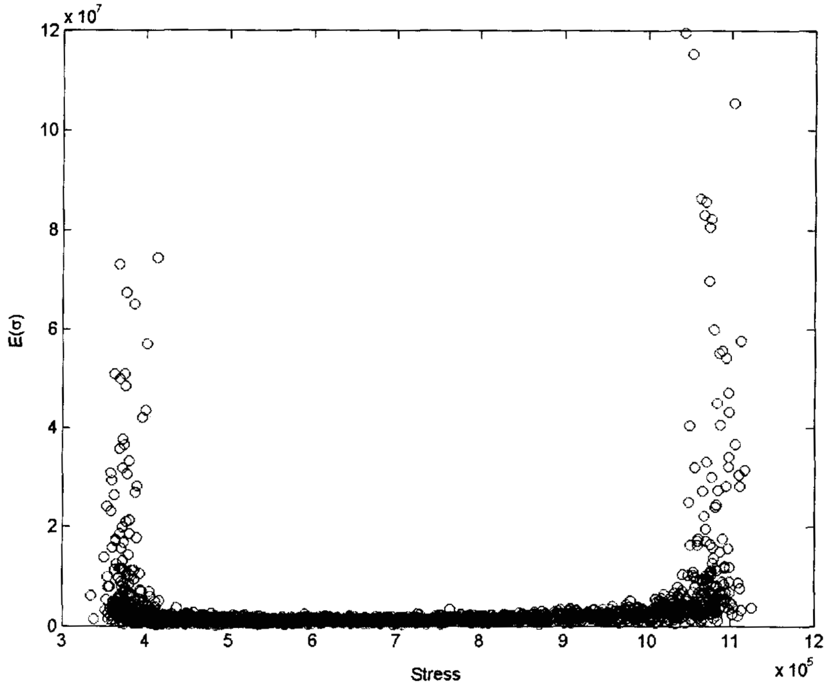

Fig. C.22 – PDMS *B* sample – E vs Stress

C.1.4 Static uniaxial tension graphical results

The graphical results below were generated by the Matlab programs (PDMS_staticauchy_true.m) and (PE_staticauchy_true.m). The results shown below are the plots for the *B* samples tested.

C.1.4.1 PDMS static uniaxial tension *B* sample graphical results

b sample, **`Tpdmsa.txt`** through **`Tpdmsf.txt`** data file example plots.

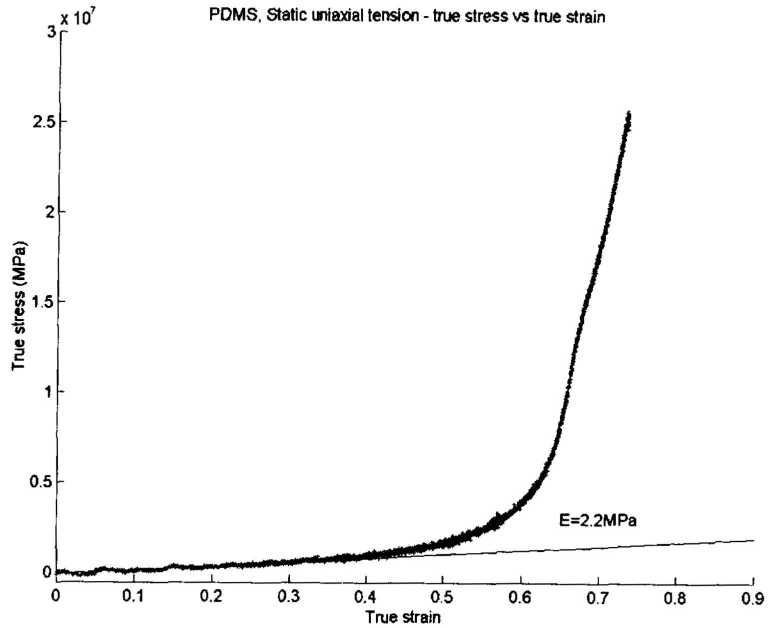

Fig. C.23 – PDMS *B* sample, (Tpdmsa.txt) - True stress vs True strain

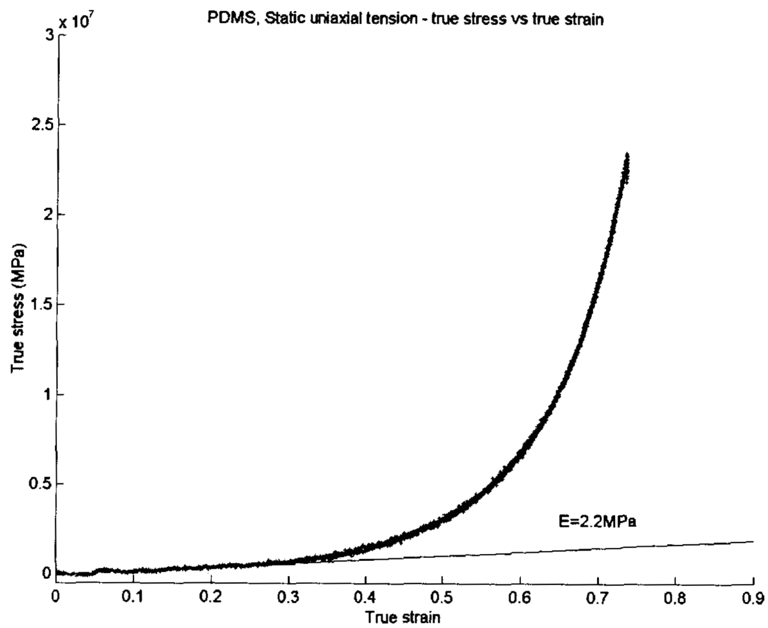

Fig. C.24 – PDMS *B* sample, (Tpdmsb.txt) - True stress vs True strain

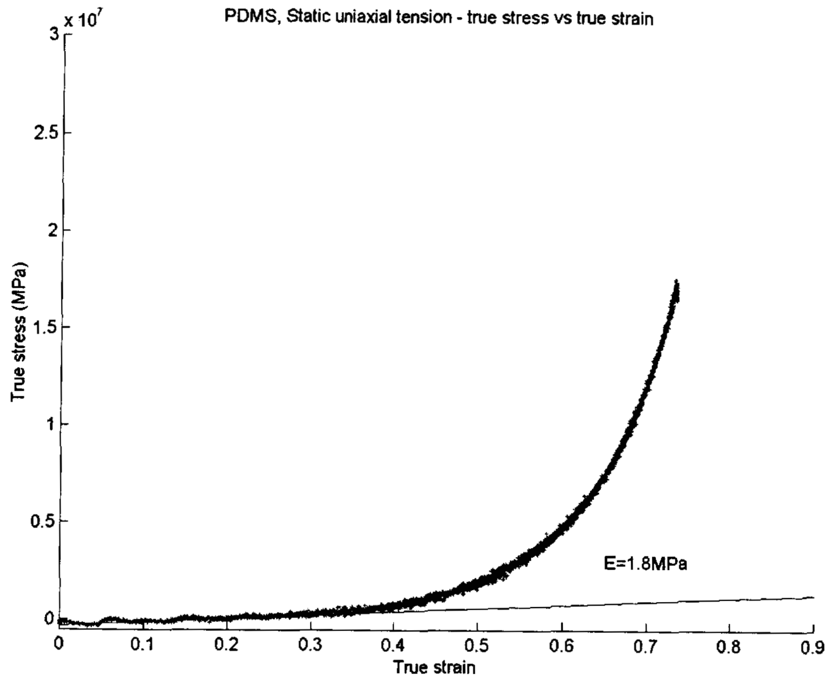

Fig. C.25 – PDMS *B* sample, (Tpdmsc.txt) - True stress vs True strain

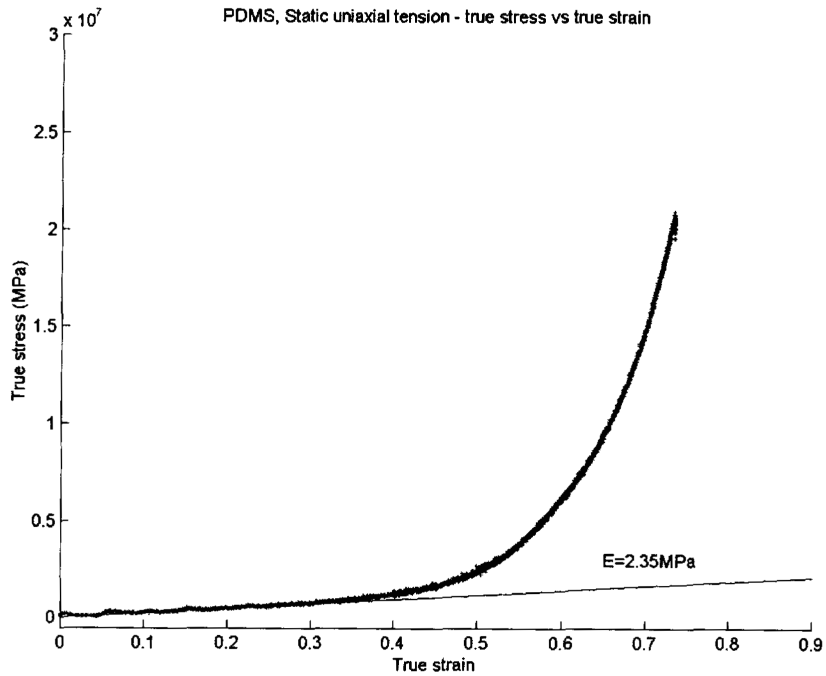

Fig. C.26 – PDMS *B* sample, (Tpdmsd.txt) - True stress vs True strain

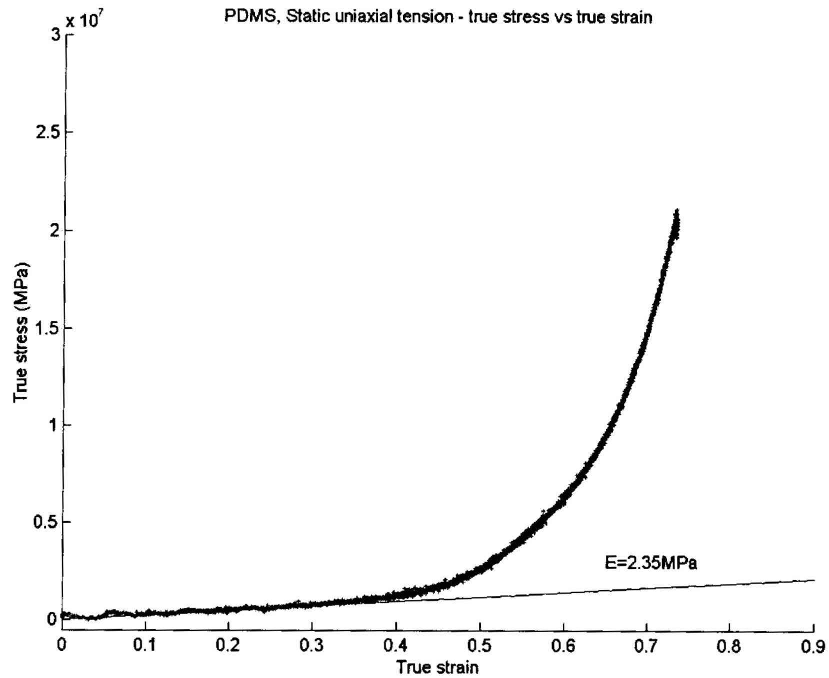

Fig. C.27 – PDMS *B* sample, (Tpdmse.txt) - True stress vs True strain

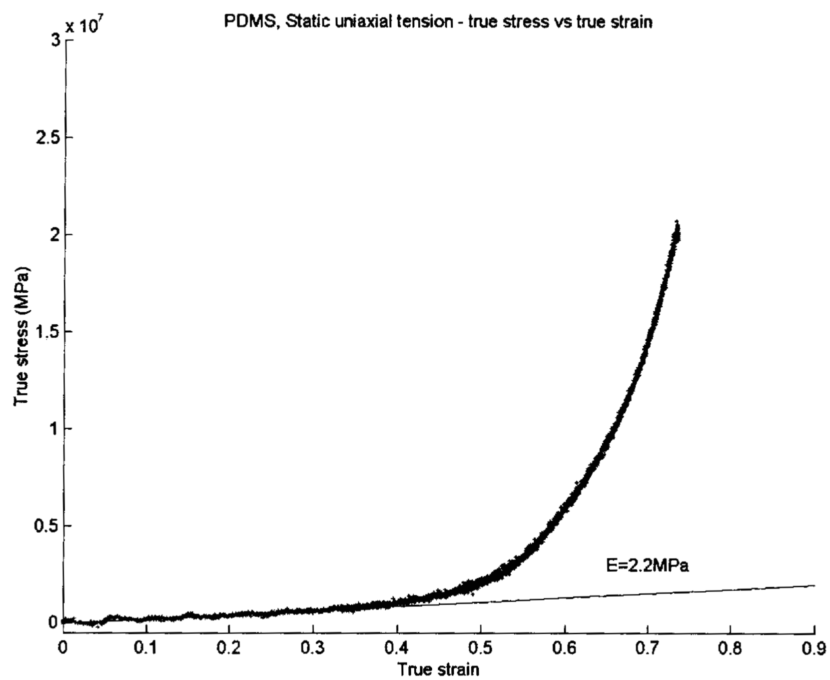

Fig. C.28 – PDMS *B* sample, (Tpdmsf.txt) - True stress vs True strain

C.1.4.2 LLDPE static uniaxial tension *B* sample graphical results

LLDPE *B* sample, **pe2.txt** through **pe15.txt** selected data file example plots. Uniaxial stress-strain elastic modulus taken at 2% strain to minimize effects of plastic deformation in modulus results [94].

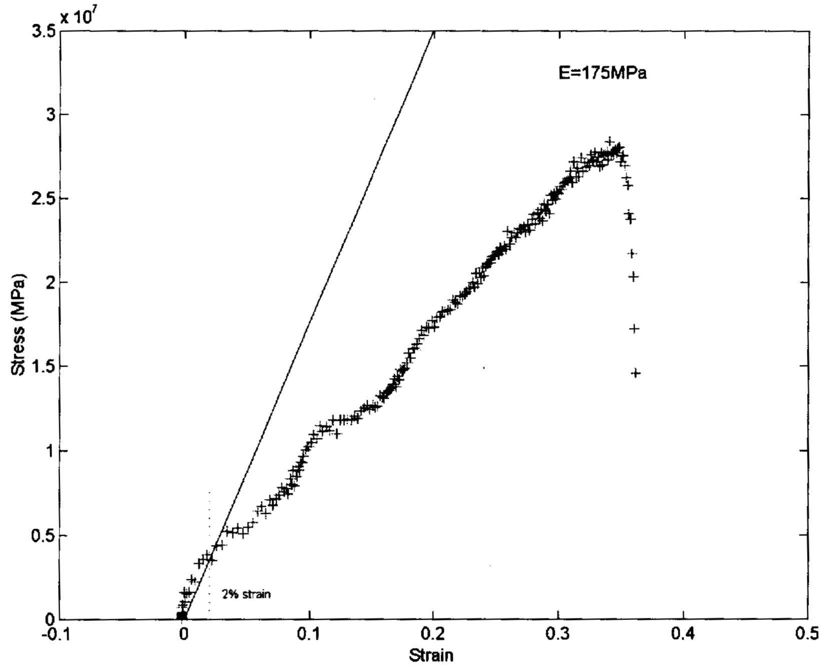

Fig. C.29 – LLDPE *B* sample, (pe2.txt) - True stress vs True strain

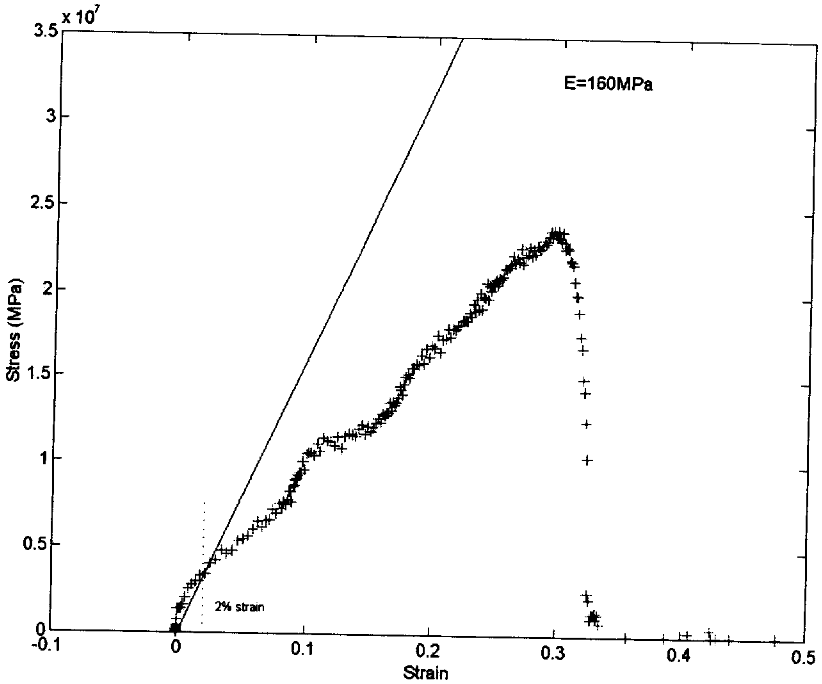

Fig. C.30 – LLDPE *B* sample, (pe4.txt) - True stress vs True strain

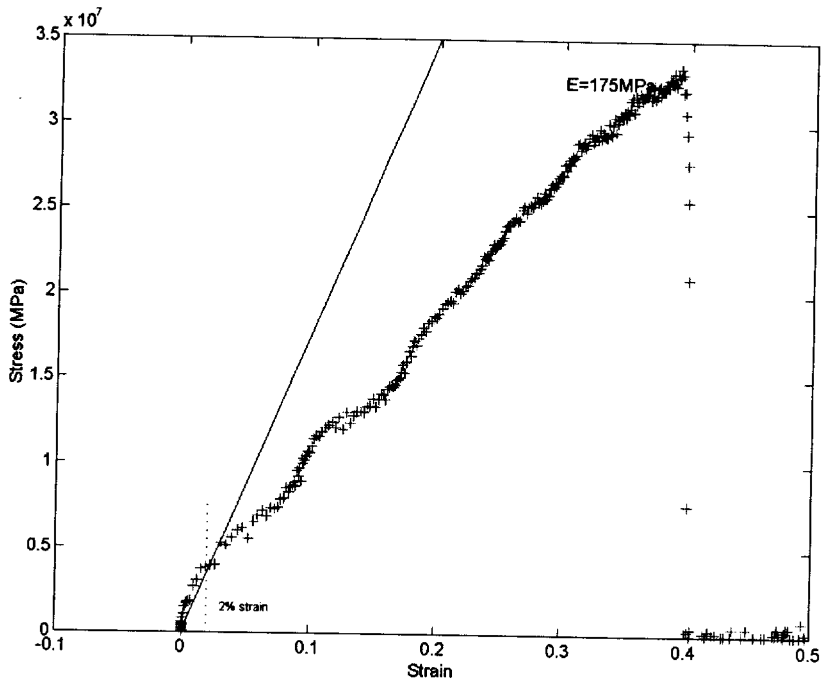

Fig. C.31 – LLDPE *B* sample, (pe9.txt) - True stress vs True strain

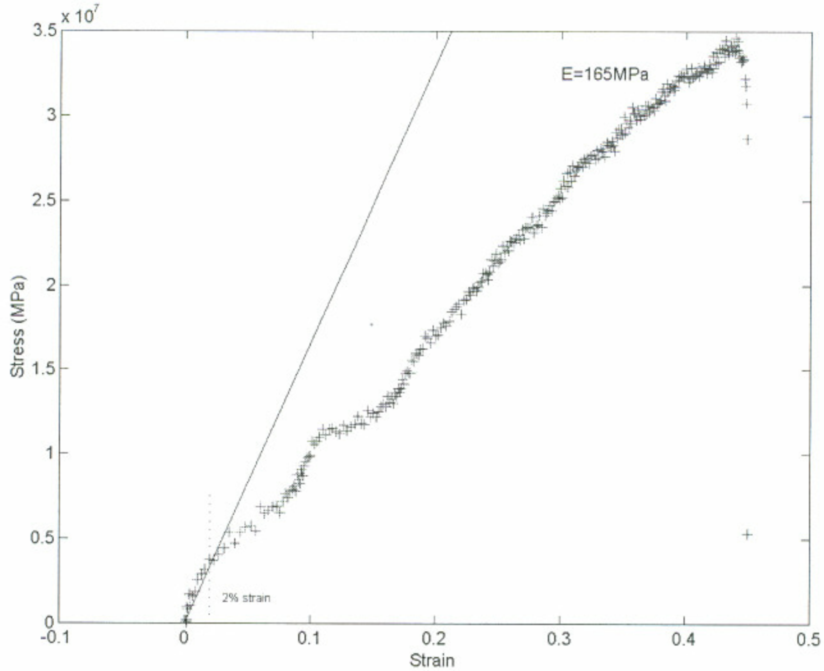

Fig. C.32 – LLDPE *B* sample, (pe12.txt) - True stress vs True strain

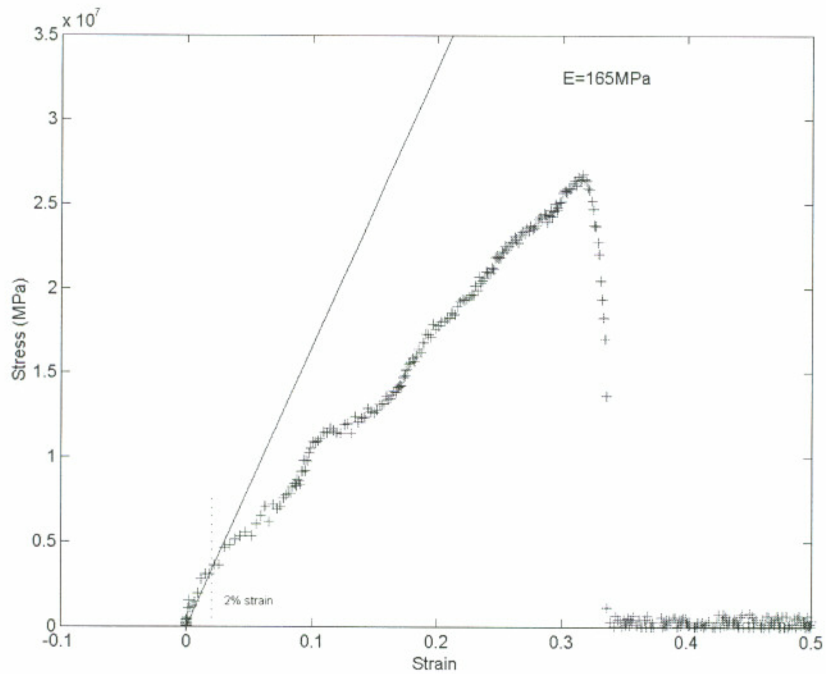

Fig. C.33 – LLDPE *B* sample, (pe13.txt) - True stress vs True strain

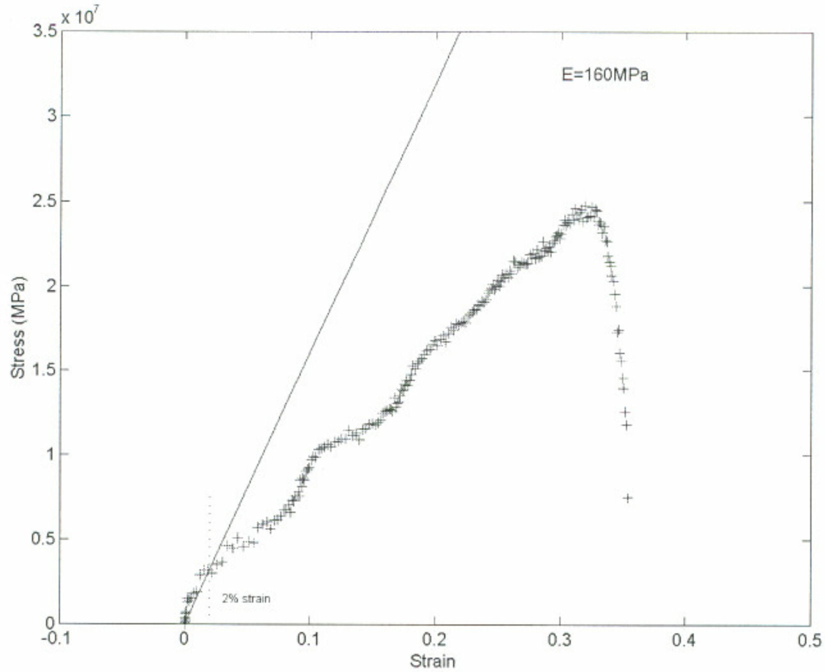

Fig. C.34 – LLDPE *B* sample, (pe14.txt) - True stress vs True strain

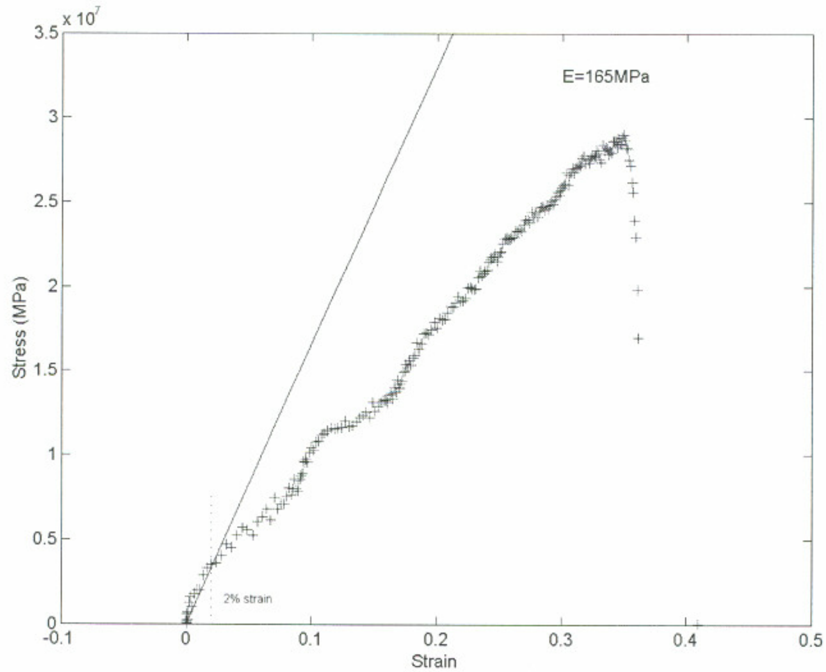

Fig. C.35 – LLDPE *B* sample, (pe15.txt) - True stress vs True strain

C.1.4.3 PDMS *B* sample stress relaxation graphical results

B sample, **`pdms_sr_01.txt`** through **`pdms_sr03.txt`**, and **`pdms_sr001.txt`** through **`pdms_sr003.txt`** data file result plots.

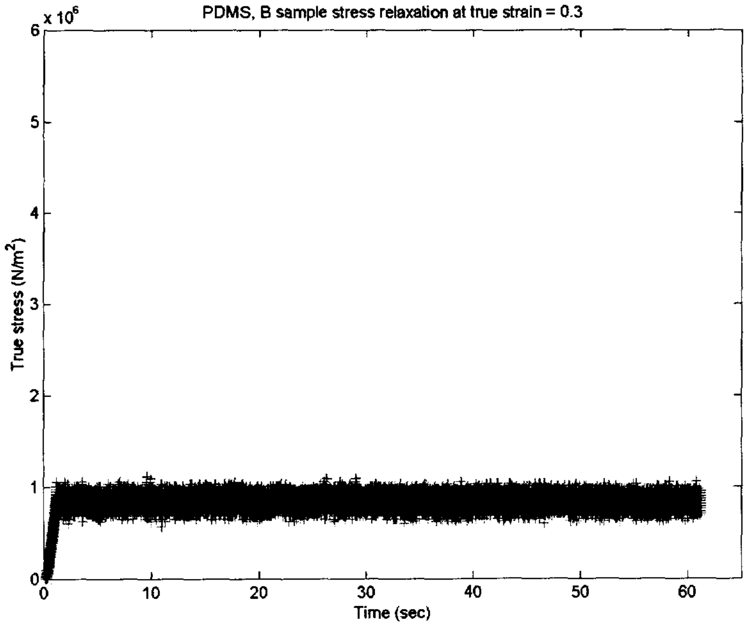

Fig. C.36 – Stress relaxation plot at true strain = 0.3 - PDMS *B* sample, (pdms_sr01.txt)

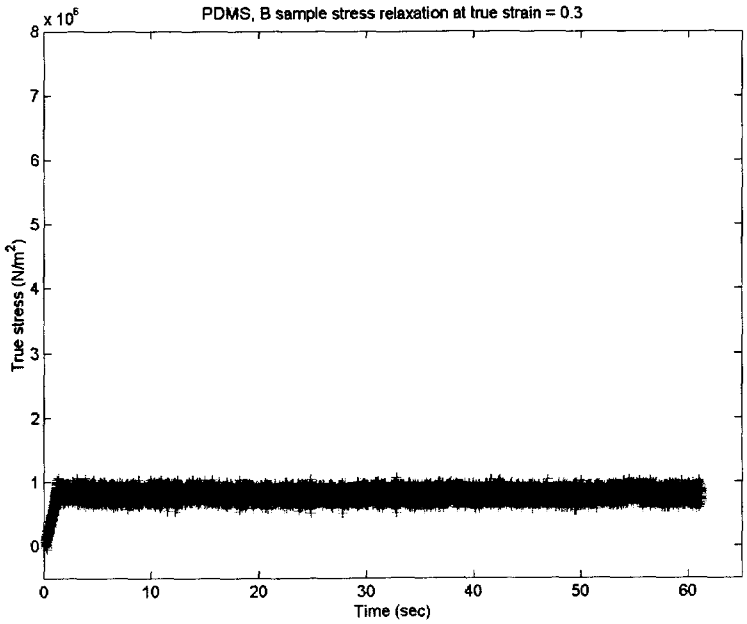

Fig. C.37 – Stress relaxation plot at true strain = 0.3 - PDMS *B* sample, (pdms_sr02.txt)

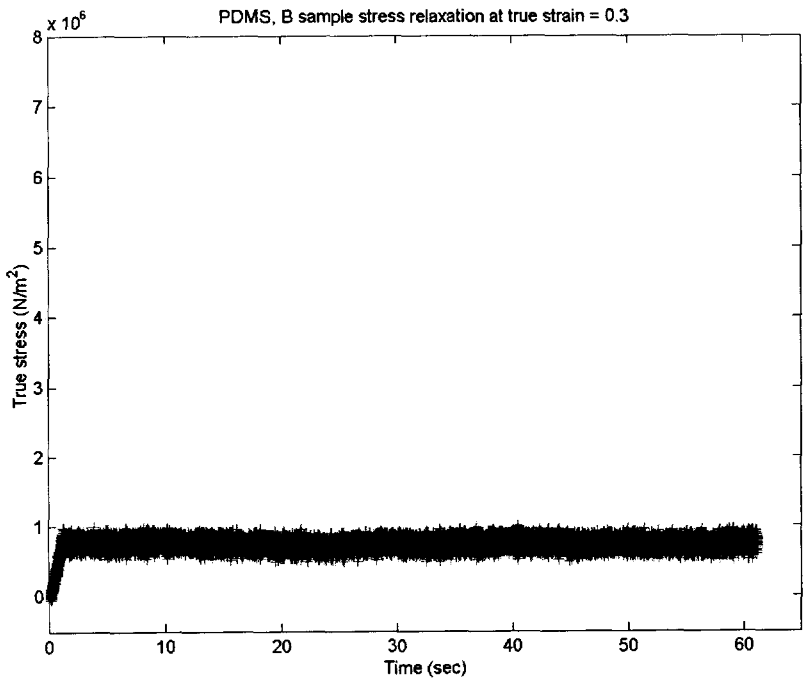

Fig. C.38 – Stress relaxation plot at true strain = 0.3 - PDMS *B* sample, (pdms_sr03.txt)

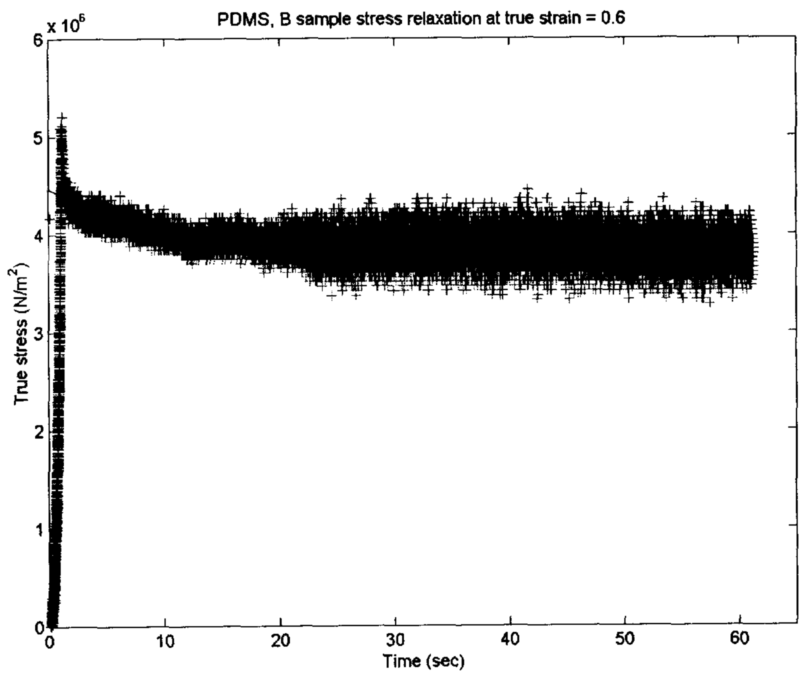

Fig. C.39– Stress relaxation plot at true strain = 0.6 - PDMS *B* sample, (pdms_sr001.txt)

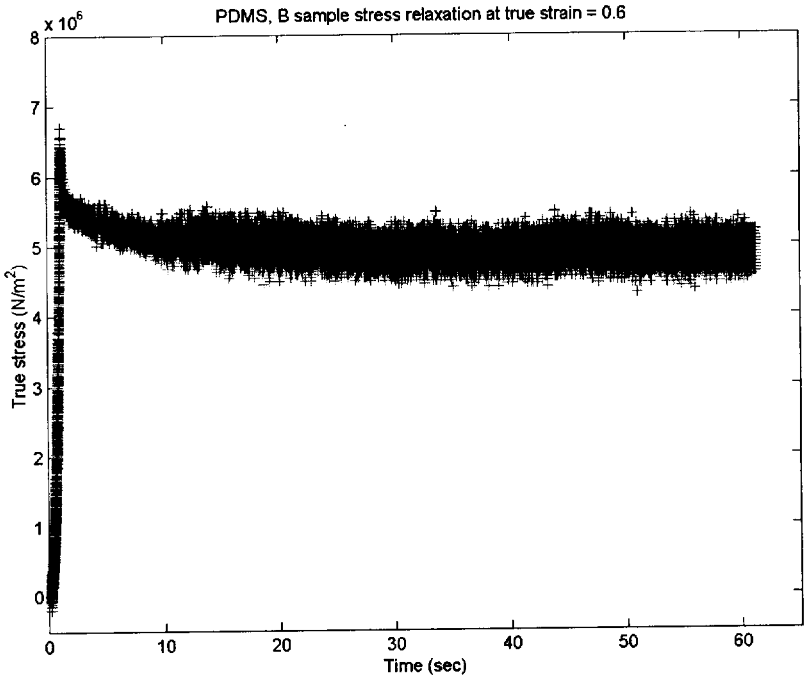

Fig. C.40 – Stress relaxation plot at true strain = 0.6 - PDMS *B* sample, (pdms_sr002.txt)

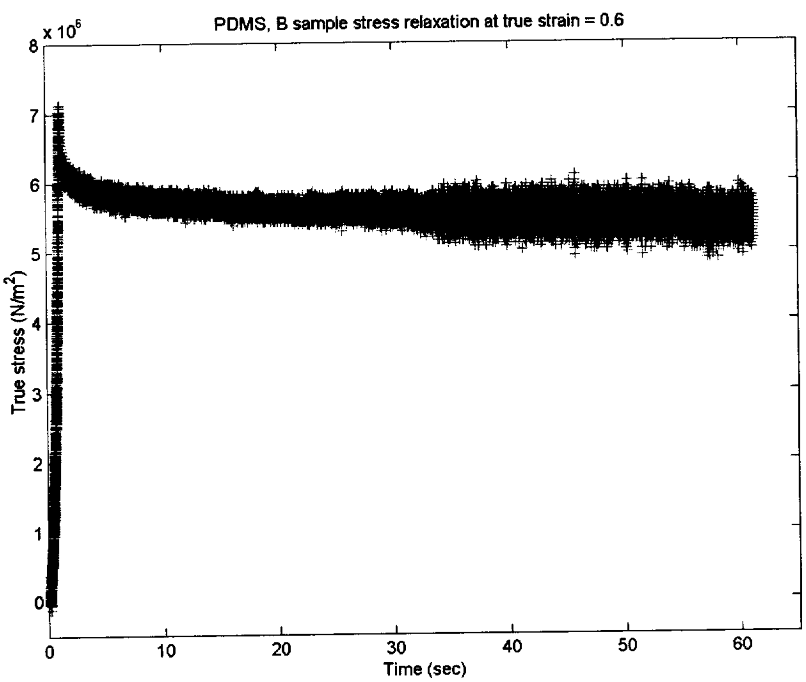

Fig. C.41 – Stress relaxation plot at true strain = 0.6 - PDMS *B* sample, (pdms_sr003.txt)

C.1.4.4 PDMS *B* sample stress deformation graphical result

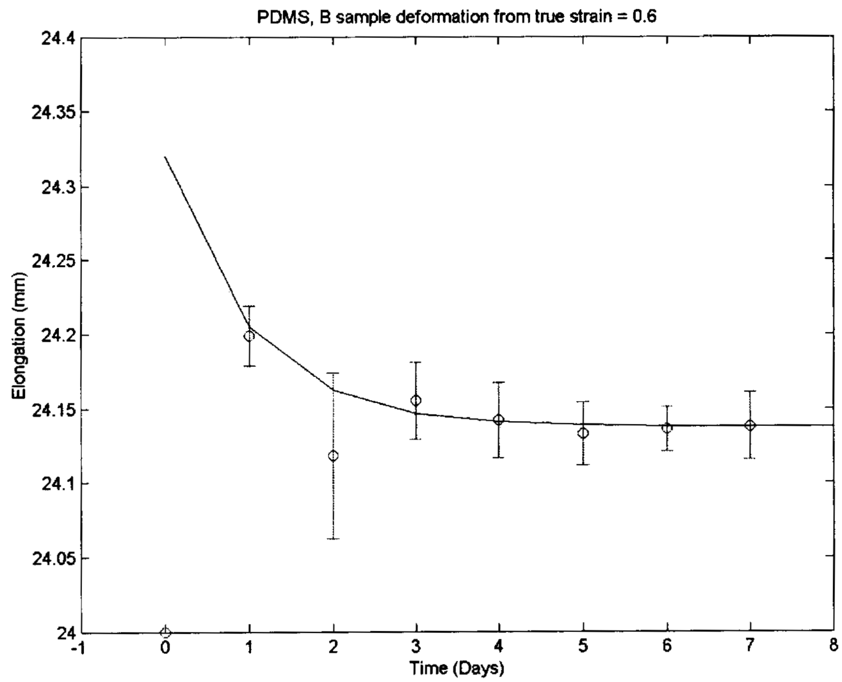

Fig. C.42 – Stress deformation plot at true strain = 0.6 - PDMS *B* samples

C.1.5 Circular membrane biaxial stress-strain graphical results

Biaxial stress-strain and biaxial modulus results for PDMS and LLDPE membranes, generated from membrane deflection data incorporated into Matlab programs.

C.1.6 PDMS circular membrane biaxial stress-strain result plots

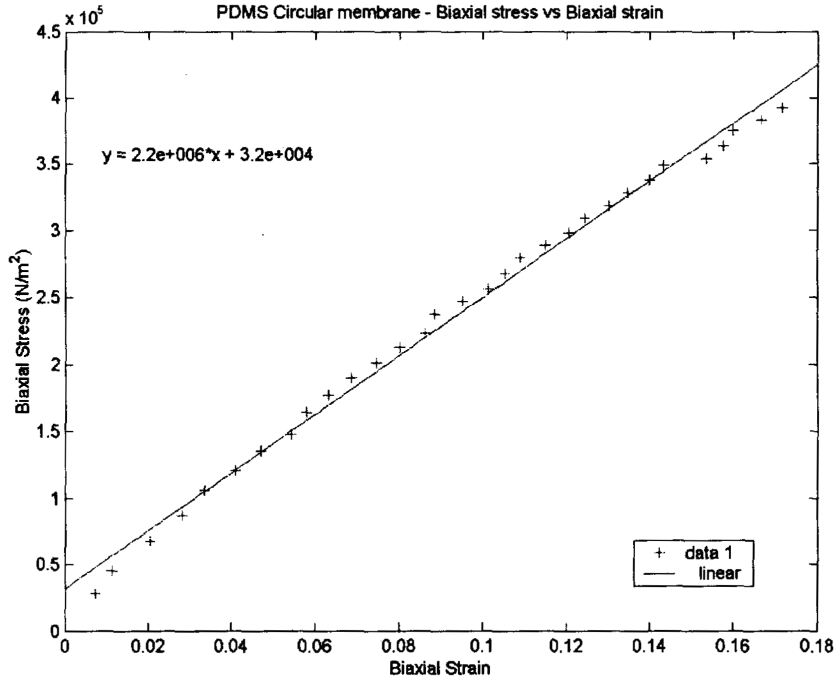

Fig. C.43 – PDMS circular membrane biaxial stress-strain results, membrane sample 1

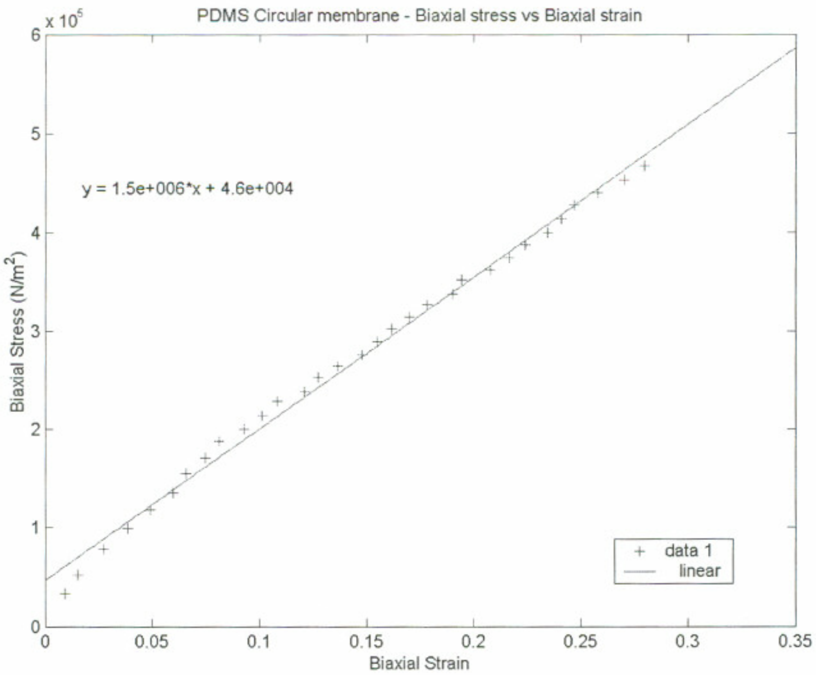

Fig. C.44 – PDMS circular membrane biaxial stress-strain results, membrane sample 2

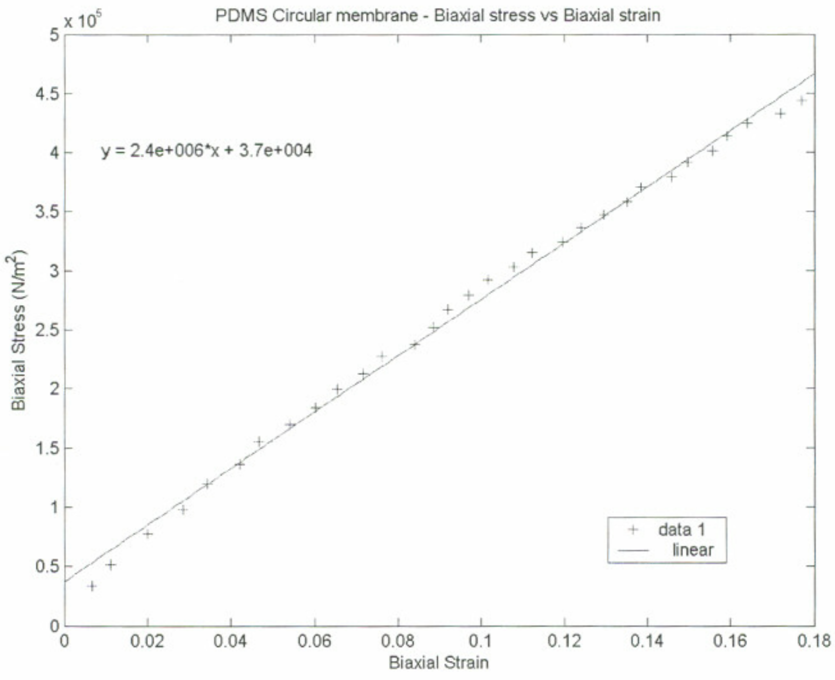

Fig. C.45 – PDMS circular membrane biaxial stress-strain results, membrane sample 3

C.1.7 LLDPE circular membrane biaxial stress-strain graphical results

LLDPE biaxial stress-strain plots limited to 2% strain to minimize effects of plastic deformation in modulus results [94].

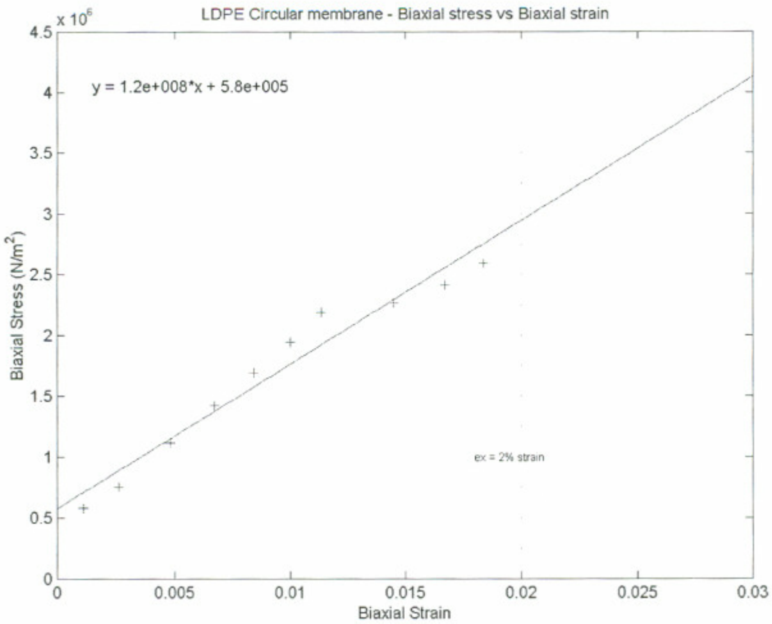

Fig. C.46 – LLDPE circular membrane biaxial stress-strain results, membrane sample 1

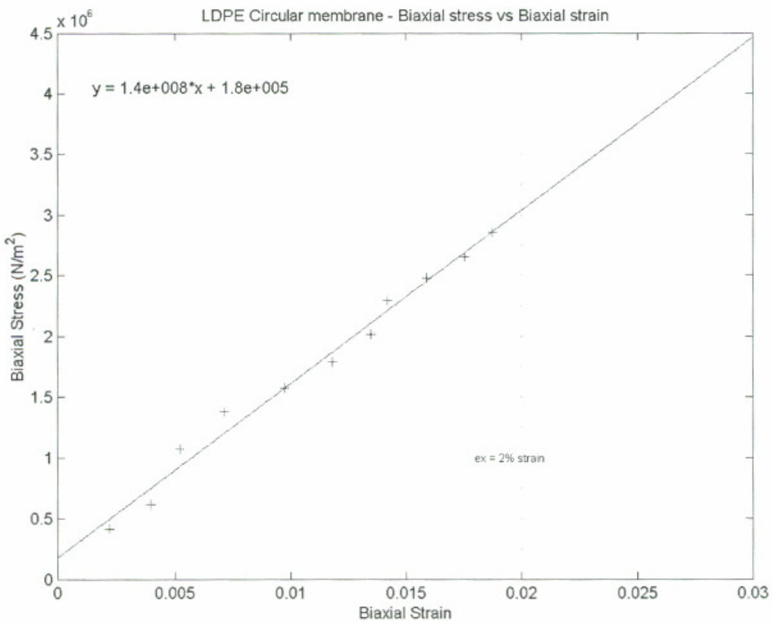

Fig. C.47 – LLDPE circular membrane biaxial stress-strain results, membrane sample 2

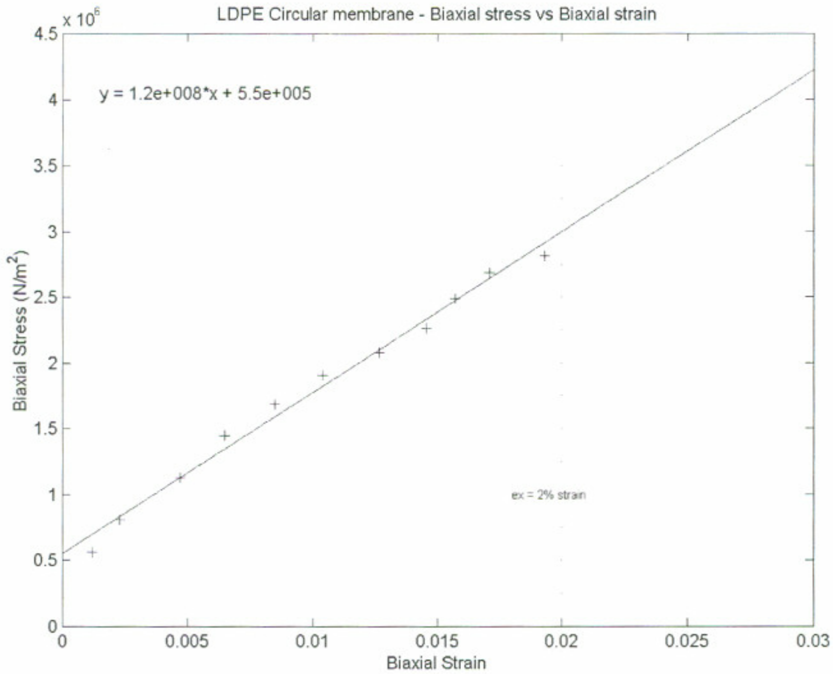

Fig. C.48 – LLDPE circular membrane biaxial stress-strain results, membrane sample 3

C.1.8 Membrane deflection program graphical results

PDMS and LLDPE membrane deflection graphical results from matlab membrane theory comparison programs. Results for circular and square membranes.

C.1.8.1 PDMS circular membrane deflection program graphical results

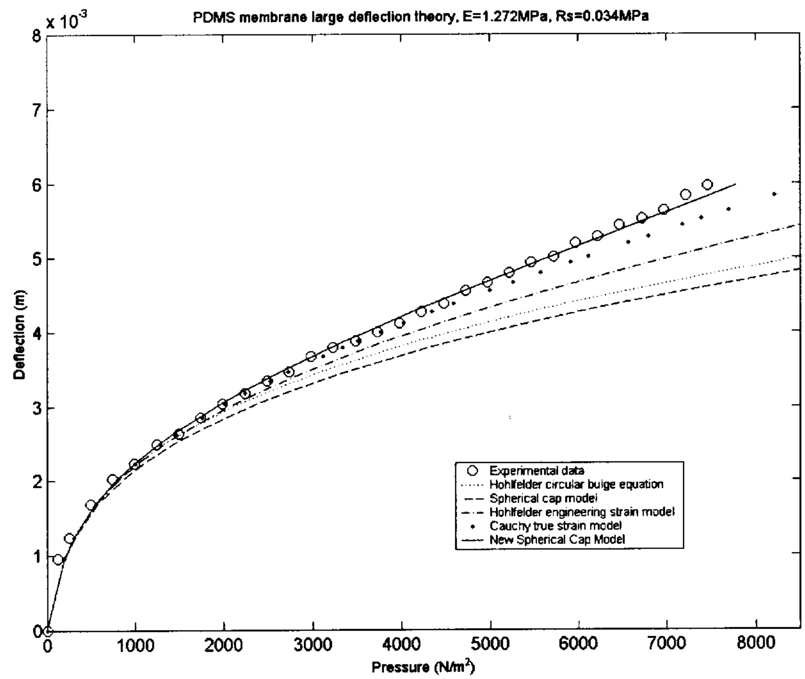

Fig. C.49 – PDMS circular membrane theory comparison – PDMS membrane sample 3

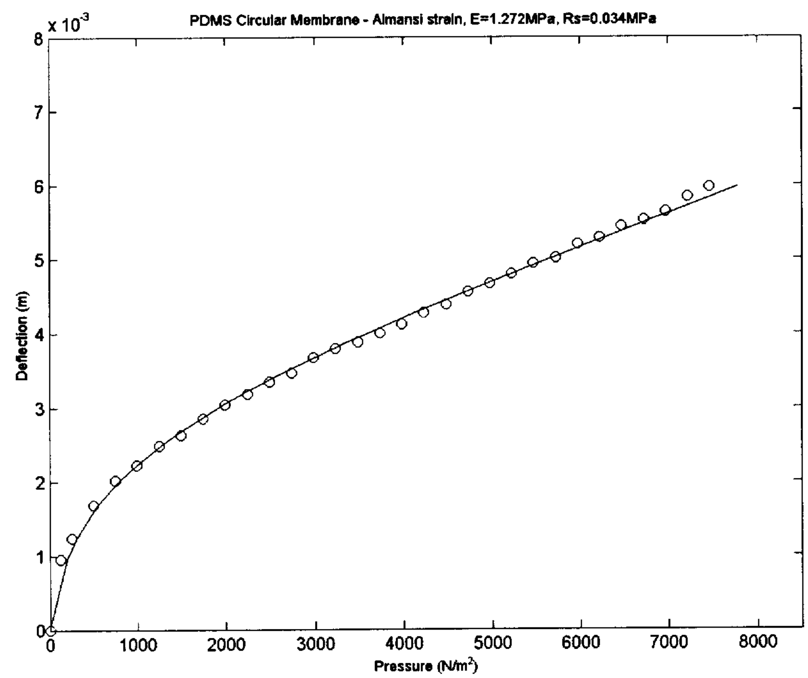

Fig. C.50 – New Spherical Cap Model results for PDMS membrane sample 3

C.1.8.2 PDMS square membrane deflection program graphical results

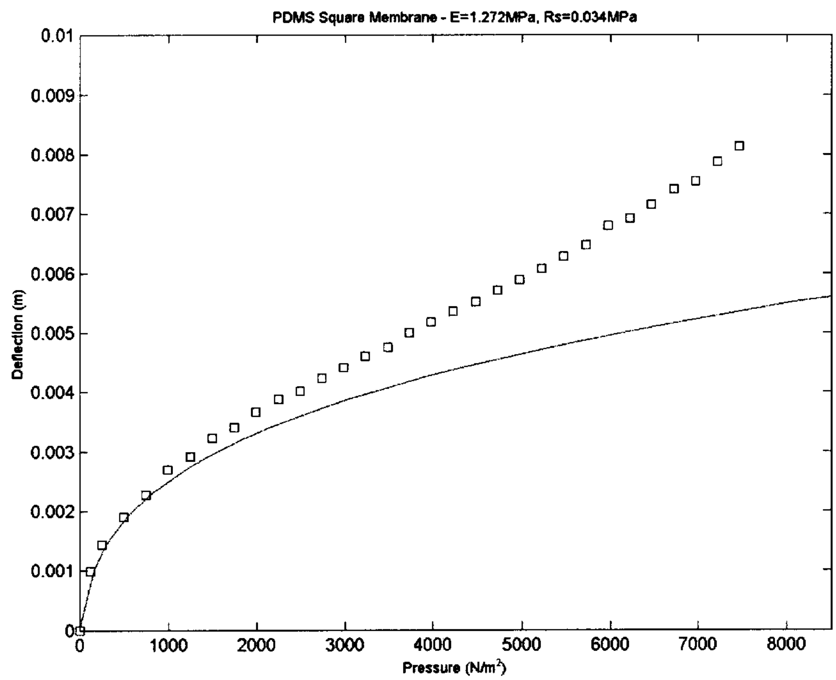

Fig. C.51 – Square membrane theory and PDMS experimental result comparison - membrane sample 3

C.1.8.3 LDPE circular membrane deflection program graphical results

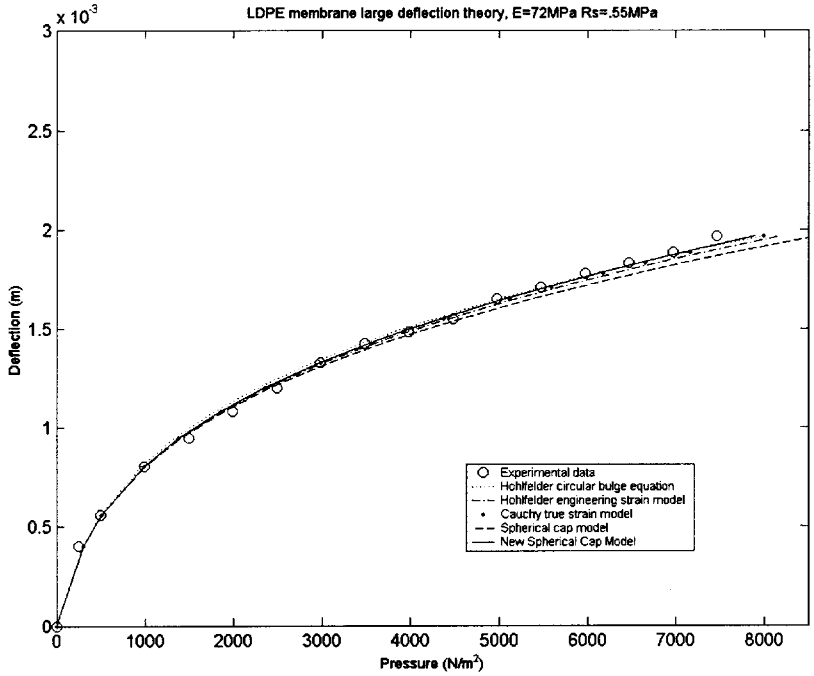

Fig. C.52 – LLDPE circular membrane theory comparison – LLDPE membrane sample 3

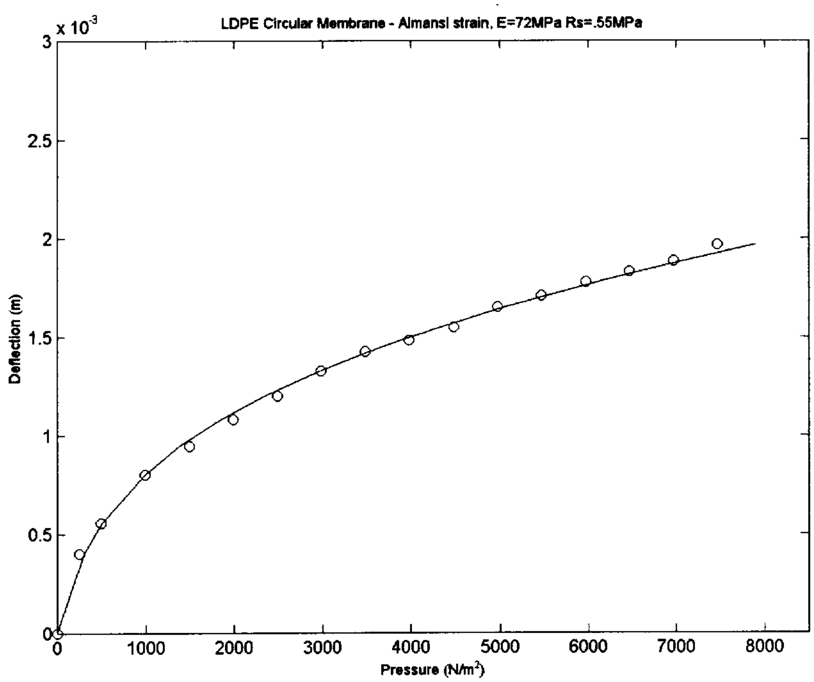

Fig. C.53 – New Spherical Cap Model results for LLDPE membrane sample 3

C.1.8.4 LLDPE square membrane deflection program graphical results

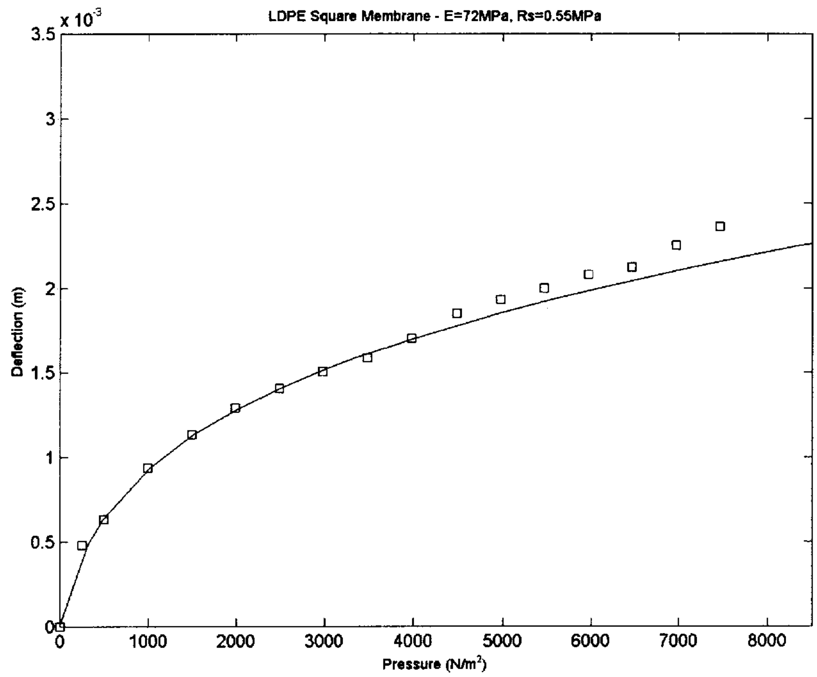

Fig. C.54 – Square membrane theory and LLDPE experimental result comparison - membrane sample 3

REFERENCES

[1] Grace R.H., *The Growing Presence of MEMS and MST in Automotive Applications,* Sensors Express. revised 1999. Available: http://www.sensorsmag.com/articles/0999/89/main.shtml, [Viewed: February 20, 2004].

[2] Judy J., "Microelectromechanical systems (MEMS): fabrication, design and applications," *Smart Materials and Structures,* vol. 10, pp. 1115-1134, 2001.

[3] Xia Y., Whitesides G.M., "Soft Lithography," *Annu. Rev. Mater. Sci.,* vol. 28, pp. 153-184, 1998.

[4] Wolffenbuttel R.F., *Silicon Sensors and Circuits: On-chip compatibility,* Chapman & Hall, London, 2001.

[5] Hsu T.R., *MEMS & Microsystems Design and Manufacture,* McGraw-Hill, New York, 2002.

[6] Maluf N., *An Introduction to Microelectromechanical Systems Engineering,* Artech House, Inc., Boston, 2000.

[7] Sim W., Kim D., Kim K., Kwon K., Kim B., Choi B., Yang S., Park J., "Fabrication, Test and Simulation of a Parylene Diaphragm", Korean Institute of Science and Technology Intelligent Microsystem Center, Seoul, Korea. Available: http://microbot.kist.re.kr/publication/4B1.08P.pdf, [Viewed: February 20, 2004].

[8] Yang X., Grosjean C., Tai Y.-C., "Design, Fabrication and Testing of Micromachined Silicone Rubber Membrane Valves," *Journal of Microelectromechanical Systems,* vol. 8, pp. 393-402, 1999.

[9] Yang X., Grosjean C., Tai Y.-C., Ho C.-M., "A MEMS Theropneumatic Silicone Membrane Valve," *Proc. IEEE (MEMS'97) Workshop,* pp. 114-118, 1997.

[10] Sim W., Kim B., Choi B., Park J., "Theoretical and Experimental studies on the Parylene Diaphragms", Korean Institute of Science and Technology Intelligent Microsystem Center, Seoul, Korea. Available: http://microbot.kist.re.kr/publication/Wonchul%20Sim%20et%20al.pdf, [Viewed: February 20, 2004].

[11] Grosjean C., Yang X., Tai Y.-C., "A Practical Thermopneumatic Valve," Caltech Micromachining Lab, Pasadena, Ca., USA. Available: http://touch.caltech.edu/publications/charlesg/mems99/mems99.pdf, [Viewed: February 20, 2004].

[12] X. Yang, C. Grosjean and Y.C. Tai, A Low Power MEMS Silicone/parylene Valve, Technical Digest, Solid State Sensor and actuator Workshop (**SSAW98**), Hilton Head Island, South Carolina, pp. 316-319, June 1998.

[13] T. Harder, T.J. Yao, Q. He, C.Y. Shih and Y.C. Tai," Residual Stress in thin-film Parylene-C *,Fifteenth IEEE International Conference on Micro Electro Mechanical Systems (* ***MEMS*** *'02),* Las Vegas, USA, Jan. 20-24, pp. 435-438, (2002).

[14] X.Q. Wang and Y.C. Tai, A Parylene Micro Check Valve, Proceedings, IEEE 12th International Micro Electro Mechanical Systems Conference (**MEMS99**), Orlando, Florida, pp. 177-182, Jan 17-21, 1999.

[15] Vieider C., Ohman O., Elderstig H., "A pneumatically Actuated Valve with a Silicone Rubber Membrane for Integration with Fluid-Handling Systems," *The 8th International Conference on Solid-State Sensors and Actuators, and Eurosensors IX,* Stockholm Sweden, June 25-29, pp.284-286, 1995.

[16] E. Meng, X.Q. Wang, H. Mak, and Y.C. Tai,"A Check-Valved Silicone Diaphragm Pump," Thirteenth IEEE International Conference on Micro Electro Mechanical Systems (**MEMS '00**), Miyazaki, Japan, pp. 62-67, Jan. 23-27 (2000).

[17] Hosokawa K., Maeda R., "A pneumatically-actuated three-way microvalve fabricated with polydimethylsiloxane using the membrane transfer technique," *Journal of Micromechanics and Microengineering,* vol. 10, pp. 415-420, 2000.

[18] Duffy D., Schueller O.J.A., Brittain S.T., Whitesides G.M., "Rapid prototyping of microfluidic switches in poly(dimethyl siloxane) and their actuation by electro-osmotic flow," *Journal of Micromechanics and Microengineering,* vol. 9, pp. 211-217, 1999.

[19] Jeong O.C., Yang S.S., "Fabrication and test of a thermopneumatic micropump with a corrugated p+ diaphragm," *Sensors and Actuators,* vol. 83, pp. 249-255, 2000.

[20] Li H.Q., Roberts D.C., Steyn J.L., Turner K.T., Carretero J.A., Yaglioglu O., Su Y.H., Saggere L., Hagwood N.W., Spearing S.M., Schmidt M.A., "A High Frequency High Flow Rate Piezoelectrically Driven MEMS Micropump," *Proceedings IEEE Solid State Sensors and Actuators Workshop,* Hilton Head, North Carolina, June, 2000.

[21] Morris C.J., Forster F.K., "Optimization of a Piezoelectric Bimorph for a Micropump Driver," *Journal of Micromechanics and Microengineering,* vol. 10, pp. 459-465, 2000.

[22] Khoo M., Liu C., *"Development of A Novel Micromachined Magnetostatic Membrane Actuator,"* The 58th Annual IEEE Device Research Conference, pp. 109-110, Denver, CO, 2000.

[23] M. Khoo, C. Liu, *"A Novel Micromachined Magnetic Membrane Microfluid Pump,"* 22nd Annual International Conference of the IEEE Engineering in Medicine and Biology Society, Chicago, IL, 2000.

[24] Yun K.-S., Cho I.-J., Bu J.-U., Kim G.-H., Jeon Y.-S., Kim C.-J., Yoon E., "A Micropump Driven by Continuous Electrowetting Actuation for Low Voltage and Low Power Operations," *IEEE Conf. Micro Electro Mechanical Systems (MEMS '01)*, Interlaken, Switzerland, Jan. 2001, pp. 487-490.

[25] Liu R.H., Yu Q., Beebe D.J., "Fabrication and Characterization of Hydrogel-Based Microvalves," *Journal of Microelectromechanical Systems,* vol. 11, pp. 45-53, 2002.

[26] Henning A.K., "Microfluidic MEMS for Semiconductor Processing," *Proceedings for IEEE Conference on Integrated Systems in Silicon,* pp. 340-349, 1997.

[27] Gerlach T., Schuenemann M., Wurmus H., "A new micropump principle of the reciprocating type using pyramidic micro flowchannels as passive valves," *Journal of Micromechanics and Microengineering,* vol. 5, pp. 199-201, 1995.

[28] Bohm S., Olthius W., Bergveld P., "A plastic micropump constructed with conventional techniques and materials," *Sensors and Actuators,* vol, 77, pp. 223-228, 1999.

[29] Unger M.A., Chou H.-P., Thorsen T., Scherer A., Quake S.R, "Monolithic Microfabricated Valves and Pumps by Multilayer Soft Lithography," *Science,* vol. 288, pp. 113-116, 2000.

[30] Tamanaha C.R., Whitman L.J., Colton R.J., "Hybrid macro-micro fluidics system for a chip-based biosensor," *Journal of Micromechanics and Microengineering,* vol. 12, pp. 7-17, 2002.

[31] Xu Y., Jiang F., Tai Y.-C., Donzier E., Loomis W., Liberman A., "A Surface Micromachined Nitride-Diaphragm High-Pressure Sensor for Oil Well Application," ASME International Mechanical Engineering Congress and Exposition, Orlando, Florida, 2000.

[32] Hosokawa K., Maeda R., "In-line pressure monitoring for microfluidic devices using a deformable diffraction grating," *Proceedings IEEE,* pp. 174-177, 2001.

[33] Ziaie B., Wu T.-W., Kocaman N., Najafi K., Anderson D.J., *An implantable pressure sensor cuff for tonometric blood pressure measurement,* (CICS), University of Michigan, Ann Arbor, Michigan, USA, 1997.

[34] Stanford University Mechanical Engineering Lectures, Stanford University, Berkley, Califronia, USA. Available: http://design.stanford.edu/courses/me220/lectures/lect07/lect_7.html, [Viewed: February 20, 2004].

[35] University of Southhampton Institute of Transducer Technology, *Micromachined Silicon Capactive Sensors,* revised 2002. Available: http://www.usitt.ecs.soton.ac.uk, [Viewed: February 20, 2004].

[36] Endevco Corp., *Silicon MEMS Pressure Sensor,* revised 2003. Available: www.endevco.com, [Viewed: February 20, 2004].

[37] Han J., Neikirk D.P., *Deflection behavior of Fabry-Perot pressure sensors having planar and corrugated diaphragms,* Microelectronics Research Center, University of Texas, Austin, Texas, USA, revised February 4, 1997. Available: http://weewave.mer.utexas.edu/med_files/med_research/F_P_sensor_folder/, [Viewed: February 06, 2001].

[38] Smith R.L., Collins P.I., Collins S.D., Howard D.L., *A Micromachined Silicon Transducer for the Simultaneous Measurement of Pressure and Temperature of Gas in the Compressed Natrual Gas (CNG) Tank,* University of Calilfornia, Davis, California, USA, revised 1998, Available: www.ucop.edu/research/micro/97_98/97_164.pdf, [Viewed: February 20, 2004].

[39] Scheeper P.R., Olthuis W., Bergveld P., "The Design, Fabrication, and Testing of Corrugated Silicon Nitride Diaphragms," *Journal of Microelectromechanical Systems,* vol. 3, pp. 36-42, 1994.

[40] Han C.-H., "Corrugated Circular Diaphragm for Microphone and Microspeaker Applications," [Online]. Available: http://www-ee.eng.hawaii.edu/~cheol/class/ee626/corrugated.html, [Viewed: February 22, 2001]

[41] Khoo M., Liu C., "Micro magnetice silicone elastomer membrane actuator," *Sensors and Actuators,* vol. 89, pp. 259-266, 2000.

[42] Grosjean C., Lee G., Hong W., Tai Y.C., Ho C.M., Micro Balloon Actuators for Aerodynamic Control, *Proceedings 1998 IEEE Micro Electro Mechanical Systems Workshop* (**MEMS '98**), Heidelberg, Germany, pp. 166-171, Jan. 25-29 (1998).

[43] T. N. Pornsin-Sisirak, H. Nassef, Y.C. Tai, and C.M. Ho," Flexible Parylene Actuator for Micro Adaptive Flow Control, *Fourteenth IEEE International Conference on Micro Electro Mechanical Systems (**MEMS '01**),* Interlaken, Switzerland, Jan. 21-24, pp. 510-513, (2001).

[44] X. Yang, Y.C. Tai, and C.M. Ho, "Micro Bellow Actuators," Technical Digest, 1997 International Conference on Solid State Sensors and Actuators (**TRANSDUCERS97**), Chicago, IL, Vol. 1, pp. 45-48, Jun. 16-19 (1997).

[45] Kim K.H., Yang S.S, "Fabrication and Test of an Electromagnetic Micro Actuator with a Planar Coil on a Parylene Diaphragm," *Micro-Electro-Mechanical Systems (MEMS), ASME,* vol. 2, pp. 281-286, 2000.

[46] van Drieenhuizen B.P., Goosen J.F.L., French P.J., Wolffenbuttel R.F., "Comparison of techmiques for measuring both compressive and tensile stress in thin films," *Sensors and Actuators A,* vol. 37-38, pp. 756-765, 1993.

[47] Tabata O., Kawahata K., Sugiyama S., Igarashi I., "Mechanical Property Measurements of Thin Films Using Load-Deflection of Composite Rectangular Membranes," *Sensors and Actuators,* vol. 20, pp.135-141, 1989.

[48] Maier-Schneider D., Maibach J., Obermeier E., "A New Analytical Solution for the Load-Deflection of Square Membranes," *Journal of Microelectromechanical Systems,* vol. 4, pp. 238-241, 1995.

[49] Pan J.Y., Lin P., Maseeh F., Senturia S.D., "Verification of FEM Analysis of Load-Deflection Methods for Measuring Mechanical Properties of Thin Films," *Proceedings IEEE,* September, 1990.

[50] Ziebart V., Paul O., Munch U., Schwizer J., Baltes H., "Mechanical Properties of Thin Films from Load Deflection of Long Clamped Plates," *Journal of Microelectromechanical Systems,* vol. 7, pp. 320-327, 1998.

[51] Sheplak M., Dugundji J., *Large Deflections of Clamped Plates Under Initial Tension and Transitions to Membrane Behavior,* MIT, Cambridge, Massachusetts, USA, 1998.

[52] Zhang Y., Wise K.D., "Performance of Non-Planar Silicon Diaphragms under Large Deflections," *Journal of Microelectromechanical Systems,* vol. 3, pp. 59-68, 1994.

[53] Espinosa H.D., Prorok B.C., "A Novel Chip Level Test to Identify Elasticity, Plasticity, and Fracture of Thin Films and MEMS Materials," *Journal of Mechanics and Physics of Solids,* September, 2001.

[54] Tayebati P., Wang P.D., Vakshoori D., Sacks R.N., "Widely Tunable Fabry-Perot Filter Using Ga(Al)As-AlOx Deformable Mirrors," *IEEE Photonics Technology Letters,* vol. 10, pp. 394-396, 1998.

[55] *Technology of silicon-based liquid crystal wavefront correctors,* Delft Technical University, Optical Microsystems Group of Electronic Instrumentation Laboratory. Available: http://guernsey.et.tudelft.nl/group/project_loktev.html, [Viewed: February 20, 2004].

[56] Perreault J.A., Bifano T.G., Levine B.M., Horenstein M.N., "Adaptive optic correction using microelectromechanical deformable mirrors," *Optical Engineering,* vol. 41, pp. 561-566, 2002.

[57] Vdovin G., "Micromachined adaptive mirrors," Delft Technical University, revised December 12, 1996. Available: http://guernsey.et.tudelft.nl/tyson4/, [Viewed: February 20, 2004].

[58] *MMDM-Micro Machined Deformable Mirrors,* Flexible Optical b.v., Delft, Holland, revised 2003. Available: http://www.okotech.com/mirrors/small, [Viewed: February 20, 2004].

[59] *Deformable Mirror,* MEMS Optical Inc., Huntsville, Al, USA, revised 2002. Available: http://www.memsoptical.com/prodserv/products/def_mirrors.htm, [Viewed: February 20, 2004].

[60] Patterson C., "Membrane Mirrors and Adaptive Optics," Imperial College, London, revised February 19, 2004. Available: http://op.ph.ic.ac.uk/membrane/membrane.html, [Viewed: February 20, 2004].

[61] *Micro-Optics*, WaveFrontSciences, Albuquerque, New Mexico, USA. Available: http://www.wavefrontsciences.com/micro-optics/microoptics.html, [Viewed: February 20, 2004].

[62] Peter Y.-A., *Micro-optical fiber switch for a large number of interconnects,* PhD dissertation, University of Neuchatel, Neuchatel, France, 2001.

[63] Sheplak M., Chandrasekaran V., Cain A., Nishida T., Cattafesta L.N., "Characterization of a Silicon-Micromachined Thermal Shear-Stress Sensor," *AIAA Journal,* vol. 40, pp. 1099-1104, June, 2002.

[64] Fenner R.L., Padilla W., *HMX2000 – A Shear/Stress MEMS Hygrometer,* Hygrometrix, Inc., Alpine, California, USA. Available: www.fennerassociates.com/DETROIT.pdf, [Viewed: February 20, 2004].

[65] Makel D.B., "Low-Cost Chemical Composition and Mass Flow Sensor System for Compression-Ignition Engines Using MEMS-Based Sensor Technology," Makel Engineering, Inc, Chico, California, USA. Available: http://www.ipd.anl.gov/carat/1999projects/makel_results.htm, [Viewed: February 20, 2004].

[66] Di Giovanni M., *Flat and Corrugated DiaphragmDesign Handbook,* Marcel Dekker, New York, 1982.

[67] Roark R.J., Young W.C., *Formulas for Stress and Strain,* McGraw-Hill Book Company, New York, 1959.

[68] Ugural, A.C., *Stresses in Plates and Shells,* McGraw-Hill Book Company, Inc., New York, 1981.

[69] Timoshenko S., Winowsky-Krieger S., *Theory of Plates and Shells,* McGraw-Hill Book Company, Inc., New York, 1959.

[70] Hohlfelder R.J., *Bulge and Blister Testing of Thin Films and their Interfaces,* PhD dissertation, Stanford University, Palo Alto, California, USA, 1999.

[71] Vlassak J.J., *New Experimental Techniques and Analysis Methods for the Study of the Mechanical Properties of Materials in Small Volumes,* PhD dissertation, Stanford University, Palo Alto, California, USA, 1994.

[72] Nix W.D., *Mechanical Properties of Thin Films,* Class notes, Stanford University, Palo Alto, California, USA, 1999.

[73] Beer F.P., Johnston Jr. E.R., *Mechanics of Materials,* McGraw-Hill, Inc., New York, 1992.

[74] Kirkpatrick S.J., Oregon Graduate Institute of Science & Technology at Oregon Health & Science University, personal communication, (2002).

[75] Hohlfelder, R.J., Sandia National Laboratory, personal communication, (2003).

[76] Scholl M., *Introduction to Micro-Electrical Mechanical Systems (MEMS),* Class notes, Oregon Graduate Institute of Science & Technology at Oregon Health & Science University, Portland, Oregon, USA, 2001.

[77] Park J.B., *Biomaterials Science and Engineering,* Plenum Press, New York, 1990.

[78] Reed-Hill R.E., *Physical Metallurgy,* D. Van Nostrand Company, Inc., Princeton, New Jersey, 1964.

[79] Beiser A., *Modern Technical Physics,* Addison-Wesley Publishing Company, Inc., Reading, Massachusetts, 1987.

[80] Nagdi K., *Rubber as an Engineering Material: Guideline for Users,* Hanser Publishers, Munich, 1993.

[81] Kresser T.O.J., *Polyolefin Plastics,* Van Nostrand Reinhold Company, New York, 1969.

[82] Gent A.N., *Engineering with Rubber,* Hanser Publishers, Munich, 1992.

[83] *RTV-2 Silicone Rubber P-125,* Silicones, Inc., High Point, North Carollina, USA. Available: http://www.silicones-inc.com, [Viewed: February 20, 2004].

[84] Armani D., Liu C., Aluru N., "Re-Configurable Fluid Circuits by PDMS Elastomer Micromachining," University of Illinois at Urbana-Champaign, USA, revised 2004. Available: http://galaxy.micro.uiuc.edu/publications/papers/26.pdf, [Viewed: February 20, 2004].

[85] *Glad plastic wrap,* Glad products of Australia, Padstow, NSW, Australia, revised 2000. Available: http://www.glad.com.au/content/GLAD_Australian_Student_Pack.pdf, [Viewed: February 20, 2004].

[86] ASTM D 412-98a, *Standard Test Methods for Vulcanized Rubber and Thermoplastic Elastomers-Tension,* American National Standards Institute, 1998.

[87] Mackin T.J., Vernon P.J., Begley M.R., "Fatigue Testing of Polymer Membranes," University of Virginia-Charlottesville, Virginia, USA. Available: http://www.people.virginia.edu/~mrb3h/papers/p3.pdf, [Viewed: February 20, 2004].

[88] Etter D.M., *Introduction to Matlab for Engineers and Scientists,* Prentice Hall, Upper Saddle River, New Jersey, 1996.

[89] Higdon A., Ohlson E.H., Stiles W.B., *Mechanics of Materials,* John Wiley & Sons, Inc., New York, 1960.

[90] Young R.J., Lovell P.A., *Introduction to Polymers,* Chapman & Hall, London, 1996.

[91] Mal A.K., Zheng D.W., Tu K.N., Wang X., Korkmaz Y., "Nondestructive characterization of the properties of thin diaphragms," *in Advanced Nondestructive Evaluation for Structural and Biological Health Monitoring,* Kundu T., *Proceedings SPIE*, vol. 4335, pp. 210-220, 2001.

[92] Shojaei O.R., Kruml T., Karimi A., Martin J.L., "Mechanical Properties of TiN Thin Films Investigated using Biaxial Tensile Testing," *Surface Engineering,* vol. 14, pp. 240-245, 1998.

[93] Billmeyer F., *Textbook of Polymer Science,* John Wiley & Sons, New York, 1971.

[94] *Engineering Properties of Polyethylene,* Plastic Pipe Institute, Washington, D.C., revised 2003. Available: http://www.plasticpipe.org/applications/ppihandbook03_8_4.php, [Viewed: February 20, 2004].

[95] Wang P., Guo J., Wunder S., "Surface stress of Polydimethylsiloxane Networks," *Journal of Polymer Science: Part B: Polymer Physics,* vol. 35, pp. 2391-2396, 1997.

[96] Lakes R.S., *Viscoelastic Solids,* CRC Press, Boca Raton, Florida, 1998.

[97] ASTM E 8, *Standard Test Methods for Tension Testing of Metallic Materials,* American National Standards Institute, Washington, D.C., 1999.

[98] Qi J., *Measurement of Surface and Interfacial Energies between Solid Materials Using and Elastica Loop,* Masters thesis, Virginia Polytechnic Institute and State University, Blacksburg, Virginia, 2000.

[99] Lotters J.C., Olthius W., Veltnik P.H., Bergveld P., "The Mechanical Properties of the rubber elastic polymer polydimethylsiloxane for sensor applications," *Journal of Micromechanics and Microengineering,* vol. 7, pp. 145-147, 1997.

[100] Hosokawa K., Hanada K., Maeda R., "A Polydimethylsiloxane (PDMS) deformable diffraction grating for monitoring of local pressure in microfluidic devices," *Journal of Micromechanics and Microengineering,* vol. 12, pp. 1-6, 2001.

[101] Boban T., Dunning, D., *Deformation of Polymers,* The University of Liverpool, England, revised October 23, 2001. Available: http://www.matter.org.uk/matscicdrom/manual/pm.html, [Viewed: February 20, 2004].

[102] Han P., *Tensile Testing,* ASM International, Materials Park, Ohio, 1996.

[103] Fung Y.C., *Biomechanics*, Springer-Verlag, New York, 1996.

[104] *Polyethylene*, Eastpoint Oltean Company, revised February 20, 2004. Available: http://www.plasticsusa.com/pe.html, [Viewed: February 20, 2004].

Biographical Sketch

Patrick Roman was born on February 10, 1969 in New Hartford, New York. A suburb of Utica, New York, approximately 200 miles northwest of New York City. Throughout his childhood he lived on either coast of the USA with his family as his father was a US Naval Officer. His adolescence and young adulthood were spent in Ithaca and upstate New York where he lived and attended engineering schools. Patrick earned an Associates of Applied Science degree in Mechanical Engineering Technology from SUNY Morrisville in 1993. He then went on to earn a Bachelor of Technology degree in Mechanical Engineering Technology at SUNY Buffalo in 1995. Upon graduating from his undergraduate program Patrick moved to Portland, Oregon where he found employment in the semiconductor industry as a field service engineer. This position took him throughout his country and to Europe where he met his wife. He then lived in Milan, Italy for 1.5 years and traveled to various semiconductor fabs throughout Europe to work. In 1997 he returned to Portland, Oregon and worked as a cleanroom processing research and development engineer for three years. In late 2000 he volunteered some of his time to help in the building of a MEMS and sensors research laboratory at the Oregon Graduate Institute of Science and Technology. Through this experience he chose to pursue a Masters degree in electrical engineering in 2001, researching MEMS, sensors, and actuators. Patrick currently lives in Washington D.C. with his wife and two cats, and is employed as a MEMS research and development engineer at NASA Goddard Space Flight Center in Greenbelt, Maryland, USA.